

## Durham E-Theses

---

# *Syntheses and ROMP of norbornene-functionalised polyesters and polyurethanes and evaluation of their products*

ATTER, KIERAN,TIMOTHY

### How to cite:

---

ATTER, KIERAN,TIMOTHY (2018) *Syntheses and ROMP of norbornene-functionalised polyesters and polyurethanes and evaluation of their products* , Durham theses, Durham University. Available at Durham E-Theses Online: <http://etheses.dur.ac.uk/12612/>

### Use policy

---

The full-text may be used and/or reproduced, and given to third parties in any format or medium, without prior permission or charge, for personal research or study, educational, or not-for-profit purposes provided that:

- a full bibliographic reference is made to the original source
- a [link](#) is made to the metadata record in Durham E-Theses
- the full-text is not changed in any way

The full-text must not be sold in any format or medium without the formal permission of the copyright holders.

Please consult the [full Durham E-Theses policy](#) for further details.

---

Academic Support Office, Durham University, University Office, Old Elvet, Durham DH1 3HP  
e-mail: [e-theses.admin@dur.ac.uk](mailto:e-theses.admin@dur.ac.uk) Tel: +44 0191 334 6107  
<http://etheses.dur.ac.uk>

# **Syntheses and ROMP of norbornene- functionalised polyesters and polyurethanes and evaluation of their products**

A thesis submitted for the degree of

Doctor of Philosophy

by

**Kieran Timothy Atter**



Department of Chemistry

Durham University

United Kingdom

**2018**

## Abstract

The aim of this project is to develop a polymer system which: 1) incorporates one or more norbornene rings in the pre-polymer; 2) can be polymerised using ROMP to yield linear or cross-linked polymers; 3) utilises little, or no, styrene; 4) produces products with comparable properties to current unsaturated polyester resins; 5) can polymerise in solvent, or in the presence of a reactive diluent; 6) is as environmentally friendly as possible; and 7) is as cost-effective as possible.

Chapter 1 contains a history of olefin metathesis, ROMP, and ROMP catalysts. Using ROMP to polymerise norbornene-containing monomers is also included, as well as the synthesis of random and block-copolymers using ROMP.

In Chapter 2, norbornene-containing polyesters – synthesised at Scott Bader – are characterised using  $^1\text{H}$  and  $^{13}\text{C}$  NMR spectroscopy, and SEC. The syntheses of hexamethylene-1,6-bis(5-norbornene-2-methoxy tetraethylene glycol carbamate) (DFM1); 2-hydroxyethyl-5-norbornene-2-carboxylate (HE-NBE-CO<sub>2</sub>); hexamethylene-1,6-bis(5-norbornene-2-carboxylate-2-ethoxy carbamate) (DFM2); and 2-hydroxyethyl-5-norbornene-2-carboxylate butyl carbamate (MFM) are all reported, and confirmed by characterisation using  $^1\text{H}$  and  $^{13}\text{C}$  NMR spectroscopy and ASAP mass spectrometry.

Chapter 3 details the polymerisation of *N*-2-ethylhexyl norbornene dicarboximide (EHNBEDC) using Grubbs 1<sup>st</sup> generation (G1); 2<sup>nd</sup> generation (G2); and modified 2<sup>nd</sup> generation (MG2) catalysts; and analyses thereof. As well as this, Polyesters 1 and 2 are shown to undergo ROMP with all three catalysts and cross-link to form a gelled polymer. The gel contents and gel time of which was measured. Finally, Polyesters 1 and 2 are copolymerised with EHNBEDC using the three catalysts and shown to increase the gel contents with increasing concentration of the polyester.

In Chapter 4, styrene is added to the reaction mixture for the ROMP of Polyesters 1 and 2. Increasing the level of styrene up to 2 equivalents with respect to the initiator is shown to have no effect on the gel contents with any of G1, G2 or MG2. However, the gel time can be increased by increasing the styrene up to 5 equivalents with respect to G1 or G2; though there is no increase in gel time observed when using styrene with MG2.

Chapter 5 shows that MFM, DFM1 and DFM2 can be polymerised using ROMP with G1, G2 and MG2. The ROMP of MFM produces a linear polymer which can be characterised using  $^1\text{H}$  and  $^{13}\text{C}$  NMR, as well as SEC. DFM1 and DFM2 produce cross-linked polymers when they undergo ROMP. MFM can produce a block copolymer with EHNBEDC when using G1 as the initiator. Random and block copolymers of HE-NBE-CO<sub>2</sub> and MFM are also formed using varying levels of each monomer.

Some of the copolymer systems are tested using Dynamic Mechanical and Thermal Analysis (DMTA): measuring their  $T_g$ 's and storage moduli. In-mould bulk copolymers, using MG2 as the initiator, are achievable in several copolymer systems. Any trends in the  $T_g$ , or storage modulus, are investigated for each system.

Finally, Chapter 6 offers conclusions to the work undertaken and some possible future work to further understand the polyesters and polyurethanes and their ROMP products, as well as the possibility of increasing the library of polyesters and polyurethanes using differing starting materials.



### **Acknowledgements**

I would firstly like to thank my supervisor, Dr Ezat Khosravi, for affording me the opportunity to undertake this PhD, as well as offering to share with me his expertise on ROMP and other polymer systems. I would also like to thank everyone at Scott Bader, Wollaston for supporting me with this project: particularly Dr Steven Brown and Clive Williams for their help with ideas within the project; and Keith Cheasman, who synthesised the norbornene-functionalised polyesters as well as gave advice on their handling and usage.

I would also like to thank the mass spectrometry and NMR services at Durham University for their handling of samples, and advice on which techniques would be suitable for my work. For help with SEC, I would like to thank Prof Lian Hutchings and Dr Cat Blackwell.

Thanks also to Doug Carswell for his help with TGA of monomers and the thermal analysis of polymers, as well as being a friendly face who would visit in the lab occasionally – especially during Radio 2's Popmaster. The help that Prof Richard Thompson and Dr Stephen Boothroyd gave me when using thermal analysis was also indispensable.

Thanks must also go to all the members of the Khosravi research group (Drs David Cole, Peter King, Cat Blackwell, Andrew Longstaff, Russell Balster, Shenghui Hou, and Rose Simnett) for their help and support in both the desk room and for making the lab an enjoyable place to work. I must also thank everyone else in CG156 for providing a friendly working environment. Specifically, I would also like to thank Dr Hannah Bolt for her help with proofreading and Caitlin Mooney for helping me relax from time to time by going running with me.

Away from Durham University, I would like to thank my mum, dad, Uncle John, brother – Calum, my dear and supportive friend – Jules, and my partner – Scott, for their ongoing support throughout my PhD and especially during the write-up. I would finally like to thank my friends at Cambridge University for their support during my PGCE whilst I was finishing off editing my thesis.

### **Memorandum**

The work reported in this thesis was carried out in the Department of Chemistry, Durham University, between November 2012 and June 2016. This work has not been submitted for any other degree in Durham and is the original work of the author except where acknowledged by means of appropriate reference.

Signed:

A handwritten signature in black ink, consisting of several overlapping loops and a long horizontal stroke extending to the right.

Date: 16/05/2018

### **Statement of Copyright**

The copyright of this thesis rests with the author. No quotation from it should be published without their prior written consent and information derived from it should be acknowledged.

### **Financial Support**

I would like to acknowledge Scott Bader Company Ltd. for their funding of this research.

## Contents

Abstract.....	i
Acknowledgements.....	ii
Memorandum.....	iii
Statement of Copyright.....	iii
Financial Support.....	iii
Contents .....	iv
Abbreviations .....	xi
Chapter 1. General Introduction.....	1
1.1 Background.....	2
1.2 Olefin metathesis .....	2
1.2.1 Discovery of olefin metathesis .....	2
1.2.2 Mechanism of olefin metathesis.....	3
1.2.3 Ring Opening Metathesis Polymerisation (ROMP).....	5
1.2.4 Schrock and Fischer carbenes.....	6
1.2.5 ROMP of multifunctional monomers .....	7
1.2.6 ROM copolymerisation .....	9
1.2.6.1 Homopolymers .....	9
1.2.6.2 Random Copolymers .....	10
1.2.6.3 Block Copolymers .....	11
1.3 ROMP initiators.....	12
1.3.1 Early ROMP initiators .....	12
1.3.2 Katz initiator.....	13
1.3.3 Titanium-based ROMP initiators .....	13
1.3.4 Tantalum-based ROMP initiators .....	14
1.3.5 Tungsten-based ROMP initiators .....	14
1.3.6 Molybdenum-based ROMP initiators .....	15
1.3.7 Ruthenium-based ROMP initiators.....	16
1.3.7.1 Mechanism of ruthenium-catalysed ROMP .....	19
1.3.8 Alternative metal initiators .....	21
1.4 Living polymerisations .....	21
1.5 Grubbs' classification of alkenes .....	23
1.6 Dicyclopentadiene .....	24
1.6.1 Current uses of DCPD .....	25
1.6.2 Synthesis of norbornene-based monomers .....	26
1.7 Green Chemistry.....	27

1.7.1	E-factor .....	28
1.8	Mechanical properties of polymers.....	29
1.9	Thesis aims and objectives .....	30
1.10	Summary .....	31
1.11	References .....	33
Chapter 2.	Synthesis of Norbornene-Functionalised Monomers and Pre-Polymers .....	38
2.1	Introduction .....	39
2.2	Experimental.....	40
2.2.1	Materials for all work .....	40
2.2.1.1	Purification of 2-hydroxyethyl acrylate .....	40
2.2.2	Instrumentation.....	41
2.2.3	Synthesis of <i>N</i> -(2-ethylhexyl)-5-norbornene-2,3-dicarboximide (EHNBEDC) .....	42
2.2.4	Characterisation of norbornene dicarboxylate diethylene glycol phthalic acid polyester (Polyester 1).....	42
2.2.5	Characterisation of norbornene dicarboxylate propylene glycol polyester (Polyester 2)..	43
2.2.6	Synthesis of hexamethylene-1,6-bis(5-norbornene-2-methoxy tetraethylene glycol carbamate) (DFM1).....	43
2.2.7	Synthesis of 2-hydroxyethyl-5-norbornene-2-carboxylate (HE-NBE-CO <sub>2</sub> ) .....	44
2.2.8	Synthesis of hexamethylene-1,6-bis(5-norbornene-2-carboxylate-2-ethoxy carbamate) (DFM2) .....	44
2.2.9	Synthesis of 2-hydroxyethyl-5-norbornene-2-carboxylate butyl carbamate (MFM) .....	45
2.3	Results and Discussion .....	45
2.3.1	Synthesis of <i>N</i> -(2-Ethylhexyl)-5-norbornene-2,3-dicarboximide .....	45
2.3.2	Characterisation of norbornene dicarboxylate diethylene glycol phthalic acid polyester (Polyester 1).....	47
2.3.3	Characterisation of norbornene dicarboxylate propylene glycol polyester (Polyester 2)..	50
2.3.4	Correlation Spectroscopy of Norbornene-Functionalised Polyesters 1 and 2 .....	52
2.3.5	Structural confirmation of 5-norbornene-2-methoxy tetraethylene glycol .....	56
2.3.6	Synthesis of hexamethylene-1,6-bis(5-norbornene-2-methoxy tetraethylene glycol carbamate) (DFM1).....	57
2.3.7	Synthesis of 2-Hydroxyethyl-5-norbornene-2-carboxylate (HE-NBE-CO <sub>2</sub> ).....	62
2.3.8	Synthesis of hexamethylene-1,6-bis(5-norbornene-2-carboxylate-2-ethoxy carbamate) (DFM2) .....	67
2.3.9	Synthesis of 2-Hydroxyethyl-5-norbornene-2-carboxylate butyl carbamate (MFM) .....	75
2.3.10	E-factors .....	82
2.4	Conclusions .....	82
2.5	References .....	83
Chapter 3.	ROMP of Norbornene-Functionalised Polyesters .....	85

3.1	Introduction .....	86
3.2	Experimental.....	87
3.2.1	Instrumentation.....	87
3.2.2	Synthesis of pyridine-modified Grubbs 2 <sup>nd</sup> generation ruthenium initiator (MG2) .....	88
3.2.3	ROMP of <i>N</i> -(2-ethylhexyl)-5-norbornene-2,3-dicarboximide (EHNBEDC) .....	88
3.2.3.1	ROMP of EHNBEDC with G1.....	88
3.2.3.2	ROMP of EHNBEDC with G2.....	88
3.2.3.3	ROMP of EHNBEDC with MG2.....	89
3.2.4	ROMP of norbornene dicarboxylate diethylene glycol phthalic acid polyester (Polyester 1) .....	89
3.2.4.1	ROMP of Polyester 1 with G1 .....	89
3.2.4.2	ROMP of Polyester 1 with G2 .....	89
3.2.4.3	ROMP of Polyester 1 with MG2 .....	89
3.2.5	ROMP of norbornene dicarboxylate propylene glycol polyester (Polyester 2) .....	90
3.2.5.1	ROMP of Polyester 2 with G1 .....	90
3.2.5.2	ROMP of Polyester 2 with G2 .....	90
3.2.5.3	ROMP of Polyester 2 with MG2 .....	90
3.2.6	ROM copolymerisation of norbornene dicarboxylate diethylene glycol phthalic acid polyester (Polyester 1) with <i>N</i> -(2-ethylhexyl)-5-norbornene-2,3-dicarboximide (EHNBEDC) .....	90
3.2.7	ROM copolymerisation of norbornene dicarboxylate propylene glycol polyester (Polyester 2) with <i>N</i> -(2-ethylhexyl)-5-norbornene-2,3-dicarboximide (EHNBEDC) .....	91
3.2.8	In-mould bulk ROM copolymerisation of <i>N</i> -(2-ethylhexyl)-5-norbornene-2,3-dicarboximide (EHNBEDC) and norbornene dicarboxylate diethylene glycol phthalic acid polyester (Polyester 1) for DMTA testing .....	91
3.2.9	In-mould bulk ROM copolymerisation of <i>N</i> -(2-ethylhexyl)-5-norbornene-2,3-dicarboximide (EHNBEDC) and norbornene dicarboxylate propylene glycol polyester (Polyester 2) for DMTA testing .....	91
3.3	Results and Discussion .....	92
3.3.1	Synthesis of pyridine-modified Grubbs 2 <sup>nd</sup> generation ruthenium initiator (MG2) .....	92
3.3.2	ROMP of <i>N</i> -(2-ethylhexyl)-5-norbornene-2,3-dicarboximide (EHNBEDC) .....	93
3.3.3	ROMP of norbornene dicarboxylate diethylene glycol phthalic acid polyester (Polyester 1) .....	100
3.3.4	ROMP of norbornene dicarboxylate propylene glycol polyester (Polyester 2) .....	102
3.3.5	ROM copolymerisation of norbornene dicarboxylate diethylene glycol phthalic acid polyester (Polyester 1) and <i>N</i> -(2-ethylhexyl)-5-norbornene-2,3-dicarboximide (EHNBEDC).....	104
3.3.6	ROM copolymerisation of norbornene dicarboxylate propylene glycol polyester (Polyester 2) and <i>N</i> -(2-ethylhexyl)-5-norbornene-2,3-dicarboximide (EHNBEDC) .....	106
3.3.7	Comparing poly(norbornene dicarboxylate diethylene glycol phthalic acid polyester) and poly(norbornene dicarboxylate propylene glycol polyester).....	108

3.3.7.1	Homopolymerisations.....	108
3.3.7.2	Copolymerisations.....	110
3.3.8	Mechanical Testing .....	111
3.3.8.1	Equivalents of monomers for DMTA.....	111
3.3.8.2	Choice of Initiator .....	112
3.3.8.3	In-mould bulk ROM copolymerisation of <i>N</i> -(2-ethylhexyl)-5-norbornene-2,3-dicarboximide (EHNBEDC) and norbornene dicarboxylate diethylene glycol phthalic acid polyester (Polyester 1) .....	113
3.3.8.4	In-mould bulk ROM copolymerisation of <i>N</i> -(2-ethylhexyl)-5-norbornene-2,3-dicarboximide (EHNBEDC) and norbornene dicarboxylate propylene glycol polyester (Polyester 2).....	116
3.3.9	Evaluation of Green Chemistry aspects.....	118
3.3.9.1	E-factor.....	118
3.3.9.2	Compostable polymers .....	119
3.4	Conclusions .....	119
3.5	References .....	120
Chapter 4.	Gelation Control by the Addition of Styrene in ROMP of Norbornene-Functionalised Polyesters .....	123
4.1	Introduction .....	124
4.2	Experimental.....	125
4.2.1	Gel Content Investigations in the presence of styrene .....	125
4.2.1.1	ROMP of norbornene dicarboxylate diethylene glycol phthalic acid polyester (Polyester 1) with G1.....	125
4.2.1.2	ROMP of norbornene dicarboxylate propylene glycol polyester (Polyester 2) with G1 .....	125
4.2.1.3	ROMP of Polyester 1 with G2 .....	125
4.2.1.4	ROMP of Polyester 2 with G2 .....	125
4.2.1.5	ROMP of Polyester 1 with MG2 .....	126
4.2.1.6	ROMP of Polyester 2 with MG2 .....	126
4.2.2	Gel Time Investigations in the presence of styrene.....	126
4.2.2.1	ROMP of Polyester 1 with G1 .....	126
4.2.2.2	ROMP of Polyester 2 with G1 .....	126
4.2.2.3	ROMP of Polyester 1 with G2 .....	126
4.2.2.4	ROMP of Polyester 2 with G2 .....	127
4.2.2.5	ROMP of Polyester 1 with MG2 .....	127

4.2.2.6	ROMP of Polyester 2 with MG2 .....	127
4.3	Results and Discussion .....	127
4.3.1	Calculation of Error.....	127
4.3.2	Gel Content Investigations in the presence of styrene .....	128
4.3.2.1	ROMP of Polyester 1 .....	128
4.3.2.2	ROMP of Polyester 2 .....	130
4.3.3	Gel Time Investigations in the Presence of Styrene .....	133
4.3.3.1	ROMP of Polyester 1 with G1 .....	133
4.3.3.2	ROMP of Polyester 2 with G1 .....	135
4.3.3.3	ROMP of Polyester 1 with G2 .....	137
4.3.3.4	ROMP of Polyester 2 with G2 .....	138
4.3.3.5	ROMP Polyesters 1 and 2 using MG2 .....	140
4.4	Conclusions .....	141
4.5	References .....	142
Chapter 5.	ROMP of Norbornene-Functionalised Urethanes .....	143
5.1	Introduction .....	144
5.2	Experimental.....	146
5.2.1	ROMP of hexamethylene-1,6-bis(5-norbornene-2-methoxy tetraethylene glycol carbamate) (DFM1).....	146
5.2.1.1	ROMP of DFM1 with G1 .....	146
5.2.1.2	ROMP of DFM1 with G2 .....	146
5.2.1.3	ROMP of DFM1 with MG2 .....	146
5.2.2	ROMP of hexamethylene-1,6-bis(5-norbornene-2-carboxylate-2-ethoxy carbamate) (DFM2) .....	147
5.2.2.1	ROMP of DFM2 with G1 .....	147
5.2.2.2	ROMP of DFM2 with G2 .....	147
5.2.2.3	ROMP of DFM2 with MG2 .....	147
5.2.3	ROMP of 2-hydroxyethyl-5-norbornene-2-carboxylate butyl carbamate (MFM).....	147
5.2.3.1	ROMP of MFM with G1 .....	147
5.2.3.2	ROMP of MFM with G2 .....	148
5.2.3.3	ROMP of MFM with MG2 .....	148
5.2.4	ROM copolymerisations of 2-hydroxyethyl-5-norbornene-2-carboxylate butyl carbamate (MFM) and <i>N</i> -2-ethylhexyl norbornene dicarboximide (EHNBEDC) .....	148
5.2.4.1	Random ROM copolymerisation of MFM and EHNBEDC with G1 .....	148
5.2.4.2	Random ROM copolymerisation of MFM and EHNBEDC with MG2.....	149

5.2.4.3	Block ROM copolymerisations of MFM and EHNBEDC with G1 .....	149
5.2.4.4	Block ROM copolymerisations of MFM and EHNBEDC with MG2 .....	149
5.2.5	ROM copolymerisations of 2-hydroxyethyl-5-norbornene-2-carboxylate (HE-NBE-CO <sub>2</sub> ) and 2-hydroxyethyl-5-norbornene-2-carboxylate butyl carbamate (MFM).....	149
5.2.5.1	Random ROM copolymerisation of HE-NBE-CO <sub>2</sub> and MFM with G1 .....	149
5.2.5.2	Random ROM copolymerisation of HE-NBE-CO <sub>2</sub> and MFM with MG2 .....	150
5.2.5.3	Block ROM copolymerisation of MFM then HE-NBE-CO <sub>2</sub> with MG2.....	150
5.2.5.4	Block ROM copolymerisation of HE-NBE-CO <sub>2</sub> then MFM with MG2.....	150
5.2.6	In-bulk ROM copolymerisation of 2-hydroxyethyl-5-norbornene-2-carboxylate butyl carbamate (MFM) and hexamethylene-1,6-bis(5-norbornene-2-carboxylate-2-ethoxy carbamate) (DFM2) .....	151
5.2.7	In-mould bulk ROM copolymerisation of 2-hydroxyethyl-5-norbornene-2-carboxylate butyl carbamate (MFM) and hexamethylene-1,6-bis(5-norbornene-2-carboxylate-2-ethoxy carbamate) (DFM2) for DMTA testing.....	151
5.2.7.1	In-mould bulk ROM copolymerisation of MFM and DFM2 with G1.....	151
5.2.7.2	In-mould bulk ROM copolymerisation of MFM and DFM2 with MG2.....	151
5.2.8	In-mould bulk ROM copolymerisation of 2-hydroxyethyl-5-norbornene-2-carboxylate butyl carbamate (MFM) and 2-hydroxyethyl-5-norbornene-2-carboxylate (HE-NBE-CO <sub>2</sub> ) for DMTA testing.....	152
5.3	Results and Discussion .....	152
5.3.1	ROMP of hexamethylene-1,6-bis(5-norbornene-2-methoxy tetraethylene glycol carbamate) (DFM1).....	152
5.3.2	ROMP of hexamethylene-1,6-bis(5-norbornene-2-carboxylate-2-ethoxy carbamate) (DFM2) .....	155
5.3.3	ROMP of 2-hydroxyethyl-5-norbornene-2-carboxylate butyl carbamate (MFM).....	156
5.3.4	Random ROM copolymerisation of MFM and EHNBEDC .....	164
5.3.5	Block ROM copolymerisation of EHNBEDC and MFM .....	168
5.3.6	ROMP of 2-hydroxyethyl-5-norbornene-2-carboxylate (HE-NBE-CO <sub>2</sub> ) .....	171
5.3.7	Random ROM copolymerisations of HE-NBE-CO <sub>2</sub> and MFM .....	171
5.3.8	Block ROM copolymerisations of HE-NBE-CO <sub>2</sub> and MFM .....	174
5.3.9	In-bulk ROM copolymerisation of 2-hydroxyethyl-5-norbornene-2-carboxylate butyl carbamate and hexamethylene-1,6-bis(5-norbornene-2-carboxylate-2-ethoxy carbamate) .....	177
5.3.10	Mechanical Testing .....	179
5.3.10.1	In-mould bulk ROM copolymerisation of MFM and DFM2 for DMTA testing.....	179
5.3.10.2	In-mould bulk ROM copolymerisation of HE-NBE-CO <sub>2</sub> and MFM for DMTA testing ....	182
5.4	Conclusions .....	185
5.5	References .....	187
Chapter 6.	Conclusions and Future Work.....	188



6.1	Conclusions .....	189
6.2	Future Work .....	191
6.2.1	Use of latent initiators.....	191
6.2.2	Use of different polyesters .....	191
6.2.3	Use of different polyurethanes .....	192
6.2.4	Different methods of mechanical testing .....	193
6.2.5	Green Chemistry .....	194
6.3	References .....	194

## Abbreviations

**ASAP** = Atmospheric Solids Analysis Probe

**AV** = Acid Value

**CM** = cross metathesis

**COSY** = Correlation Spectroscopy

**Cy** = cyclohexyl group

**D** = Polymer molecular weight dispersity

**dn/dc** = differential index of refraction

**DCM** = dichloromethane

**DCPD** = dicyclopentadiene

**DEG** = diethylene glycol

**DEPT** = Distortionless Enhancement by Polarisation Transfer

**DFM1** = hexamethylene-1,6-bis(5-norbornene-2-methoxy tetraethylene glycol carbamate)

**DFM2** = hexamethylene-1,6-bis(5-norbornene-2-carboxylate-2-ethoxy carbamate)

**DMF** = *N,N*-dimethylformamide

**DMTA** = Dynamic Mechanical and Thermal Analysis

**EHNBEDC** = *N*-(2-ethylhexyl)-5-norbornene-2,3-dicarboximide

**FT-IR** = Fourier Transform Infrared (Spectroscopy)

**G1** = Grubbs' 1<sup>st</sup> generation ruthenium catalyst

**G2** = Grubbs' 2<sup>nd</sup> generation ruthenium catalyst

**HDI** = hexamethylene diisocyanate

**HEA** = 2-hydroxyethyl acrylate

**HE-NBE-CO<sub>2</sub>** = 2-hydroxyethyl-5-norbornene-2-carboxylate

**HSQC** = Heteronuclear Single-Quantum Correlation Spectroscopy

**Mes** = mesityl group

**MFM** = 2-hydroxyethyl-5-norbornene-2-carboxylate butyl carbamate

**MG2** = Modified Grubbs 2<sup>nd</sup> generation ruthenium catalyst

**M<sub>n</sub>** = Number-averaged molecular weight

**M<sub>w</sub>** = Weight-averaged molecular weight

**NBE** = norbornene

**NHC** = *N*-heterocyclic carbene

**NMR** = Nuclear Magnetic Resonance

**rDA** = retro-Diels–Alder

**PNBE** = polynorbornene

**Polyester 1 / PE1** = norbornene dicarboxylate diethylene glycol phthalic acid polyester

**Polyester 2 / PE2** = norbornene dicarboxylate propylene glycol polyester

**ppm** = parts per million

**PS** = polystyrene

**P.T.** = proton transfer

**ROMP** = Ring Opening Metathesis Polymerisation

**SEC** = Size Exclusion Chromatography

**TCPD** = tricyclopentadiene

**TeCPD** = tetracyclopentadiene

**TGA** = Thermogravimetric Analysis

**THF** = tetrahydrofuran

**T<sub>rDA</sub>** = retro Diels Alder temperature

**UPR** = unsaturated polyester resin

## **Chapter 1. General Introduction**

## 1.1 Background

Unsaturated polyester resins (UPRs) are commonly used, once cross-linked, to make plastics and gel coats. These are used in a wide range of applications including, but not limited to: boats,<sup>1-2</sup> pipes,<sup>3</sup> and storage vessels<sup>3-4</sup> due to their high chemical resistance. UPRs are usually dissolved in styrene,<sup>5</sup> but also can be provided in other media.

In the UK, styrene is classified as “hazardous” in case of eye contact, skin contact, ingestion and inhalation.<sup>6</sup> In 1995 work was carried out in Denmark by Kolstad *et al.* studying styrene’s use in industry and the incidence of cancers in the workplace.<sup>7</sup> They concluded that there was a possible link between exposure in the plastics industry (particularly to styrene) and degenerative diseases of the nervous system and pancreatic cancer, which required attention. Despite this, in 2011, the Danish Environmental Protection Agency (EPA) announced<sup>8</sup> that styrene would be classified neither as carcinogenic, nor as mutagenic. The United States EPA also conducted studies on styrene<sup>9</sup> and decided not to reclassify it as carcinogenic. Notwithstanding all these studies and findings, the International Agency for Research on Chemistry (IARC) continues to classify styrene as “possibly carcinogenic to humans.”<sup>10</sup> Current developments in the field of UPRs are focussed towards the development of cross-linking agents with improved toxicity profiles whilst trying to maintain the simplicity and keep down the cost as much as possible.

Due to these pressures to reduce levels of styrene across different markets, other methods of polymerisation must also be considered, which is where this work focuses. Ring-Opening Metathesis Polymerisation, or ROMP, can eliminate the need to introduce styrene into the reaction mixture. It can also proffer the opportunity to tailor a polymer system to each individual situation with a wide range of monomers and initiators available.

## 1.2 Olefin metathesis

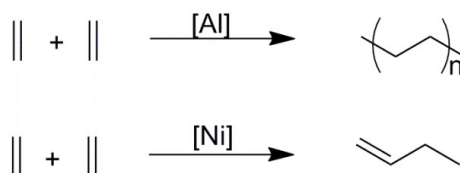
### 1.2.1 Discovery of olefin metathesis

The word olefin comes from the Latin words *oleum*<sup>11</sup> meaning oil, and *facere* meaning to make – stemming from the fact many olefins are obtained from crude oil, and are often extremely useful in chemical synthesis of a wide variety of products, e.g. polyethylene, polypropene.

As defined by International Union of Pure and Applied Chemistry (IUPAC),<sup>12</sup> metathesis is: “the exchange of bonds in a bimolecular reaction between similar interacting species so that the bonding affiliations in the product are identical (or similar) to those in the reactants”. The word metathesis comes from the Greek *metatithenai*<sup>13</sup> meaning to transpose – as the double bonds are rearranged during metathesis reactions.

The first view of olefin metathesis in action was seen in the 1950s (although the term ‘olefin metathesis’ was not used until 1967, when the term was coined by Calderon of Goodyear)<sup>14</sup> when Karl Ziegler attempted to form high molecular weight polyethylene from ethylene in the presence of an aluminium catalyst.<sup>15</sup> Instead, he achieved the formation of almost exclusively 1-butene. This was

found to be due to the presence of nickel salts in the autoclave used for the reaction, which were catalysing the cross metathesis reaction – shown in Scheme 1.1 – rather than the polymerisation.

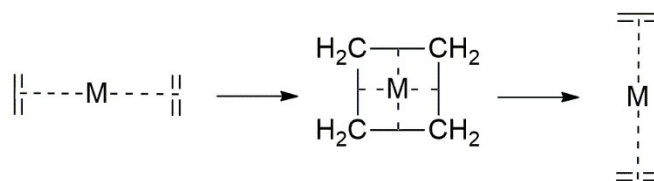


**Scheme 1.1:** The polymerisation (top) and cross metathesis (bottom) of ethylene

Ziegler realised that if one metal could promote the cross metathesis, then perhaps another could promote the polymerisation – and so it was necessary for the mechanism of olefin metathesis to be investigated.

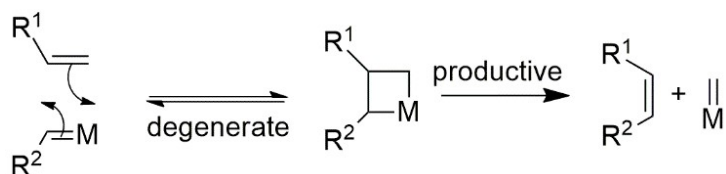
### 1.2.2 Mechanism of olefin metathesis

Notable work, by Rowland Pettit, Robert Grubbs and Yves Chauvin, made significant steps towards the elucidation of a mechanism for olefin metathesis. In 1971, Pettit *et al.* published a paper proposing a ‘quasicyclobutane’ mechanism – a phrase previously coined by Bradshaw *et al.*<sup>16</sup> – in which the metal (tungsten, tantalum, titanium, molybdenum or ruthenium) is at the centre of a four membered ring in the transition state complex.<sup>17</sup> They reasoned that the orbitals on the carbons and on the metal must influence the transition state. Pettit suggested that cyclobutane must also be produced if the intermediate is the aforementioned quasicyclobutane-metal complex. The production of cyclobutane is indeed seen, but at very low yields (<0.1 %). Disproportionation products of ethylene are the main product if ethylene is added to the metal complexes – which Pettit attributes to activation energy barriers of the two reactions. The mechanism which Pettit and Lewandos theorised is shown in Scheme 1.2.



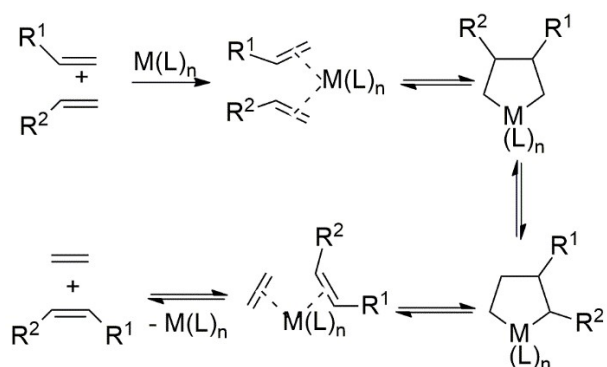
**Scheme 1.2:** Proposed Pettit and Lewandos mechanism for olefin metathesis

In 1971, Yves Chauvin devised an alternative mechanism,<sup>18</sup> which was also based upon a metallocyclobutane mechanism, where the metal forms part of the four-membered cycle as shown in Scheme 1.3. This mechanism also shows the importance of a metal carbene species in the reaction; unlike Pettit’s mechanism, the metal is actually bound to the olefin rather than solely coordinated to it. This avoids the kinetically unfavourable formation of the cyclobutane which has a very high activation energy barrier. The first step of the Chauvin mechanism is reversible since the metallocyclobutane can break both productively and degenerately, as highlighted in Scheme 1.3.



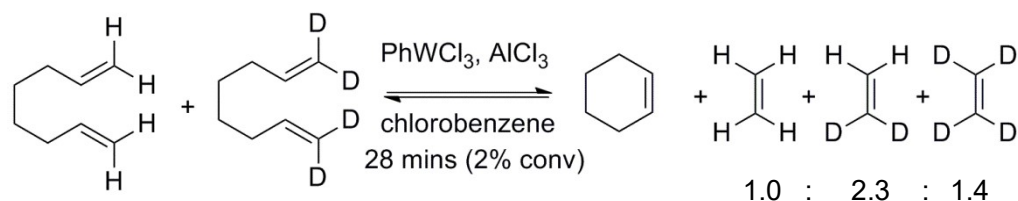
**Scheme 1.3:** Yves Chauvin's proposed mechanism for olefin metathesis

In 1972, Robert Grubbs proposed a third alternative mechanism,<sup>19</sup> detailed in Scheme 1.4. This mechanism involves a five-membered cyclic intermediate with the metal in the ring. Grubbs was able to confirm that the intermediate was indeed a metallocycle but could not confirm if his mechanism was correct.



**Scheme 1.4:** Robert Grubbs' proposed olefin metathesis mechanism, involving a five-membered metallocycle

Later, in 1975, Grubbs *et al.* confirmed that Chauvin's carbene mechanism was indeed correct,<sup>20</sup> thus discounting his own proposed mechanism in the process. Grubbs used the metathesis of 1,7-octadiene-1,1,8,8-d<sub>4</sub> and 1,7-octadiene (Equation 1.1) utilising a tungsten initiator, yielding cyclohexene and ethylene as the main products from the reaction. If Grubbs' or Pettit's mechanism was to be proven correct, then [C<sub>2</sub>H<sub>4</sub>] : [C<sub>2</sub>D<sub>2</sub>H<sub>2</sub>] : [C<sub>2</sub>D<sub>4</sub>] was calculated by Grubbs to be 1 : 1.76 : 1.61, whereas using Chauvin's carbene mechanism, he predicted this ratio to be 1 : 2 : 1 in non-equilibrating conditions.

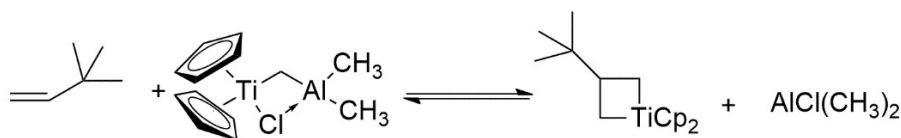


**Equation 1.1:** Reaction carried out by Grubbs *et al.* to confirm the mechanism of olefin metathesis

The experiment performed by Grubbs achieved a ratio of 1 : 2.3 : 1.4, analysed by mass spectroscopy after collection using SEC, when using equal concentrations of the deuterated and non-deuterated starting materials. Grubbs claimed this supported the Chauvin mechanism as it was closer to the predicted ratio – though he also stated that this was further “obscured by monohydride exchange” which meant that ethylene-d<sub>1</sub> and ethylene-d<sub>3</sub> were also produced. Furthermore, in 1976,

Grubbs published another paper<sup>21</sup> which varied the relative concentrations of the octadiene starting materials – and he claimed the ethylene “produced on metathesis of the deuterated mixture under non-equilibrating conditions gave results which were most consistent with the carbene scheme.”

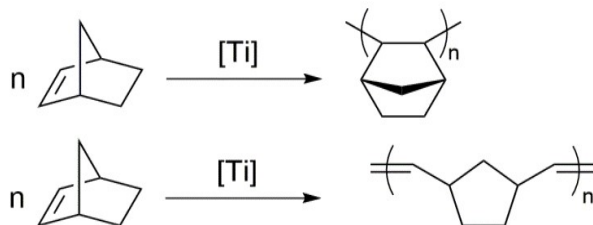
In 1980, Howard *et al.* went one step further<sup>22</sup> and definitively proved the presence of the metallocyclobutane intermediate, by isolating a titanocyclobutane when a titanium-aluminium initiator was reacted with an alkene – detailed in Equation 1.2. This confirmed that Chauvin’s mechanism was indeed the correct mechanism and is now widely accepted.



**Equation 1.2:** Reaction carried out by Howard *et al.* to form the isolable metallocycle

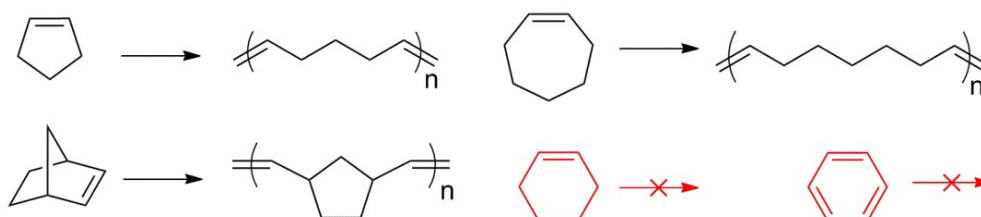
### 1.2.3 Ring Opening Metathesis Polymerisation (ROMP)

In common with olefin metathesis previously, Ring Opening Metathesis Polymerisation (ROMP) was discovered serendipitously. In 1955, chemists at DuPont aimed to polymerise norbornene *via* vinyl polymerisation (Scheme 1.5, top) to form a linear, saturated polymer. Instead of this, an unsaturated polymer with some of the rings opened<sup>23</sup> was retrieved as the major reaction product – as shown in the bottom equation of Scheme 1.5. Interestingly, in 1987, BF Goodrich found that one could polymerise norbornene (and norbornene-related molecules) to form the linear polymer which DuPont were after in the 1950s by using a nickel and palladium catalyst.<sup>24-25</sup> In other words, by tailoring the metal initiator, two different types of polymerisation are easily accessible.



**Scheme 1.5:** Vinyl polymerisation of norbornene expected by DuPont (top), and ring-opened polymeric major product (bottom)

ROMP is generally applicable to unsaturated strained rings (Scheme 1.6); bicyclic and fused rings, *e.g.* norbornenes, are among the most strained, and are therefore inherently easy to perform ROMP. For rings with solely olefin functionality, only cyclohexene cannot undergo ROMP at room temperature, although the polymerisation of cycloheptene and cyclopentene are very slow due to their low ring strain.<sup>26</sup> Aromatic rings are more or less impossible to polymerise in this manner.



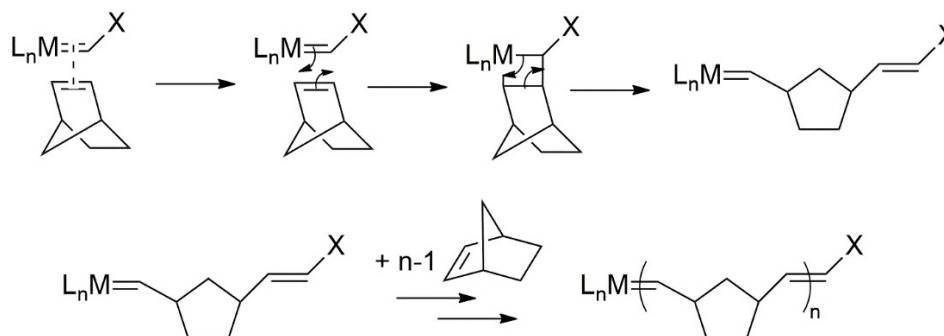
**Scheme 1.6:** Examples of olefinic monomers that can, and cannot, undergo ROMP

Some rings with low ring strain, such as cyclopentene, are hard to polymerise – and are sometimes only possible to polymerise by ROMP at lower temperatures. This is due to the fact that the change in entropy could actually be negative, and to make Gibbs free energy negative (where a process becomes favourable) one must decrease the positivity of the  $-T\Delta S$  term as shown in Equation 1.3.

$$\Delta G = \Delta H - T\Delta S \quad \text{Equation 1.3}$$

G = Gibbs free energy (J), H = enthalpy (J), T = temperature (K), S = entropy (J K<sup>-1</sup>)

The mechanism of ROMP is intrinsically the same as Chauvin's olefin metathesis. The olefin first binds to the metal centre before a 'pseudo 2+2' reaction takes place. This is shown in Scheme 1.7. Since both of the olefins produced in the reaction are still attached to the polymer chain, the metal carbene is still attached to one end of the polymer chain.



**Scheme 1.7:** Mechanism of the ROMP of norbornene using a metal carbene initiator

### 1.2.4 Schrock and Fischer carbenes

As mentioned in 1.2.3, a metal carbene functionality is important to initiate the ROMP of cyclic olefins. Carbenes (CH<sub>2</sub>) are very reactive due to there being only 6 electrons around the carbon.<sup>27</sup> There are two main groups of metal carbene: Fischer and Schrock – named after the scientists who first reported their discovery. Fischer carbenes involve a pair of electrons donated from the carbon to the metal to form the  $\sigma$  bond, then the empty p-orbital can accept electron density from the metal – thus stabilising the carbene (Figure 1.1). Fischer carbenes are electron deficient, so are easily attacked by nucleophiles; and require low oxidation and middle to late transition metals<sup>28</sup> (e.g. W(0), Fe(0), Mo(0)).



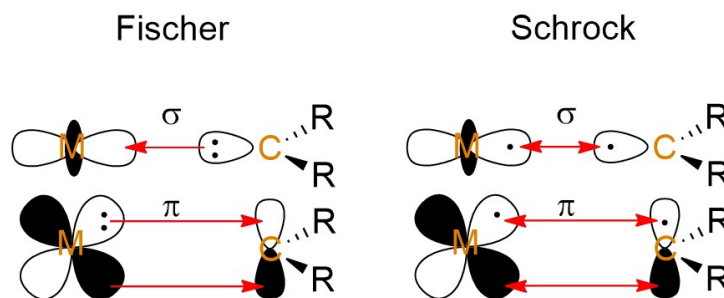


**Figure 1.1:** Orbital diagrams of Fischer and Schrock carbenes, showing the formation of the  $\sigma$  and  $\pi$  bonds

On the other hand, Schrock carbenes are formed from a carbon with two unpaired electrons bonding to two unpaired electrons on a metal (Figure 1.1). Schrock carbenes are electron rich, and so are easily attacked by electrophiles – and are important in metathesis chemistry. Typical metal centres are high oxidation state, early transition metals<sup>28</sup> (e.g. Mo(VI), Ru(IV)).

When an alkyl or aryl group is attached to the carbon instead of two hydrogens, the group technically becomes an alkylidene<sup>27</sup> (Figure 1.2).

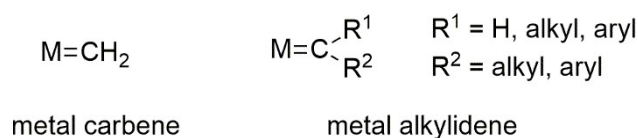
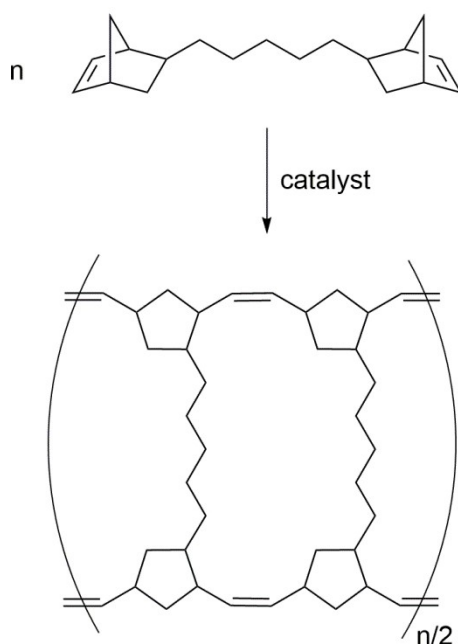


**Figure 1.2:** The difference between a metal carbene (left) and a metal alkylidene (right)

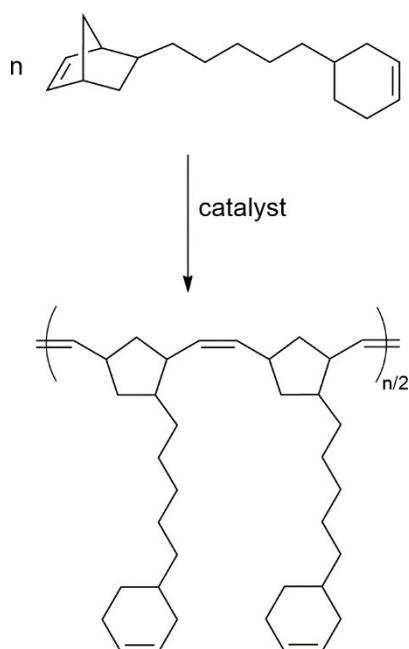
### 1.2.5 ROMP of multifunctional monomers

As shown in Section 1.2.3, the ROMP of monofunctional monomers results in linear polymers. These polymers are usually readily soluble in one or more solvents, and so can easily be studied using varying solution phase techniques. However, if a monomer has two or more strained rings the resulting polymer will be cross-linked, Equation 1.4. This means that the polymer will not be soluble because the polymer chains are joined together by strong, covalent bonds; and means that resolution of the structure is more problematic for these.



**Equation 1.4:** Example of cross-linking due to the ROMP of a difunctional monomer

The polymer becomes less soluble during the reaction and eventually the reaction will become solid – also known as the gel point. The time taken from initiation to this point is known as the gel time. At this point, the reaction can then be analysed by testing how much monomer is left or how much linear polymer has been produced by performing a solvent extraction. Monomer may still be left over if it has become trapped inside the gelled reaction mixture and could therefore no longer continue to react. In the case of a difunctional monomer, the only ways linear polymer could have been produced is if the starting material had contained a monofunctional impurity, or if only one of the rings in the monomer could be ring-opened, Equation 1.5.



**Equation 1.5:** Difunctional monomer which has undergone ROMP and produced a linear polymer, due to the lower strain in the cyclohexene ring<sup>26</sup>

### 1.2.6 ROM copolymerisation

The production of copolymers – polymers produced from the polymerisation of two monomers – can be useful as the product can have properties different from the two homopolymers which could be produced from the two starting monomers. For example, polystyrene can be used as a packaging material; adding in butadiene monomer to the starting materials affords a product with a rubber-like appearance.<sup>29</sup> Using ring-opening metathesis, random and block copolymers, Figure 1.3, are both achievable.<sup>30</sup>

**AAAAAAAAAAAAAAAAAAAAAAAAA** – homopolymer of monomer **A**

**BBBBBBBBBBBBBBBBBBBBBBBBB** – homopolymer of monomer **B**

**ABBBBABABBAAAAABAABABABB** – random copolymer of monomers **A** and **B**

**AAAABBBBAAAABBBBAAAABBBB** – block copolymer of monomers **A** and **B**

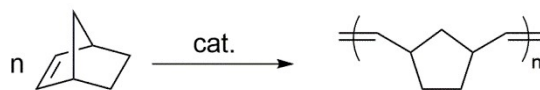
**ABABABABABABABABABABABAB** – alternating copolymer of monomers **A** and **B**

**Figure 1.3:** Example segments of 24 repeating units of two homopolymers, a random copolymer, a block copolymer, and an alternating copolymer

#### 1.2.6.1 Homopolymers

To achieve a homopolymer, Equation 1.6, the monomer (here, norbornene) is added to the initiator, and polymerised. This can be done in either bulk or solvent (depending on the monomer and initiator). To form longer chains more monomer, or less initiator, is added to the reaction mixture. For example, if the ratio in Equation 1.6 of monomer to initiator is 100:1, then the average chain length (DP = 100)

will be 100 monomer units. To double this, the amount of monomer should be doubled; or the amount of initiator utilised could be halved.



**Equation 1.6:** Formation of a homopolymer of norbornene, polynorbornene

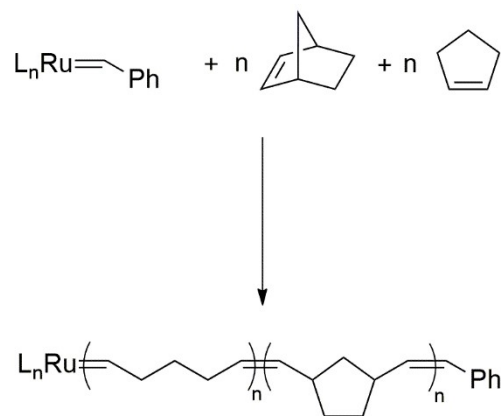
### 1.2.6.2 Random Copolymers

To call them ‘random copolymers’ is perhaps an oversimplification. They are only random when the product of the two reactivity ratios, the likelihood of a monomer to add to a polymer chain, of the copolymers (assuming here there are two) becomes 1. The idea of reactivity ratios was first discussed by Frank Mayo and Frederick Lewis in 1944,<sup>31</sup> and they used it to compare the behaviour in the copolymerisation of styrene and methyl methacrylate. If the product of the two reactivity ratios of the copolymers approaches zero, the polymer becomes increasingly less random, and could be an alternating copolymer or similar to a homopolymer of one monomer if the reactivity ratios.

Assuming that the product of the reactivity ratios of the two comonomers is 1. If the reactivity ratios of each monomer are identical, then the propagation of the polymer will be completely random with each monomer (**A** and **B**) equally likely to add to the polymer chain. If however, the reactivity ratio of **A** is higher than **B**, then more of **A** will initially be incorporated into the polymer chain until the concentration of **A** drops significantly, and **B** will be more likely to add to the polymer chain – and so on. This is called a ‘gradient copolymer’ as gradually, during the course of the polymerisation, the polymer will change from having more **A** than **B** monomers to more **B** than **A**.

If the reactivity ratio of **A** is much greater than **B**, then the start of the polymer will be mainly a homopolymer of **A** until the concentration decreases enough to allow **B** to polymerise. This was investigated using a ROMP system by Nikovia *et al.*<sup>32</sup> when they compared the reactivity ratios of norbornene and cyclopentane. They found this to be 0.87 : 0.02, meaning that the initial polymer formed was very similar to the homopolymer of norbornene since norbornene was 43.5 times more likely to add to the polymer chain.

In order to produce ‘random’ copolymers, Equation 1.7, two (or more) monomers are mixed with the initiating species; again, this can be done in either bulk or solvent. The amount of each monomer can be varied – as mentioned before – to yield different properties, for example to behave more rubber-like or to increase stiffness. The reactivity ratios may have to be taken account of if we need to know that random copolymers are produced.

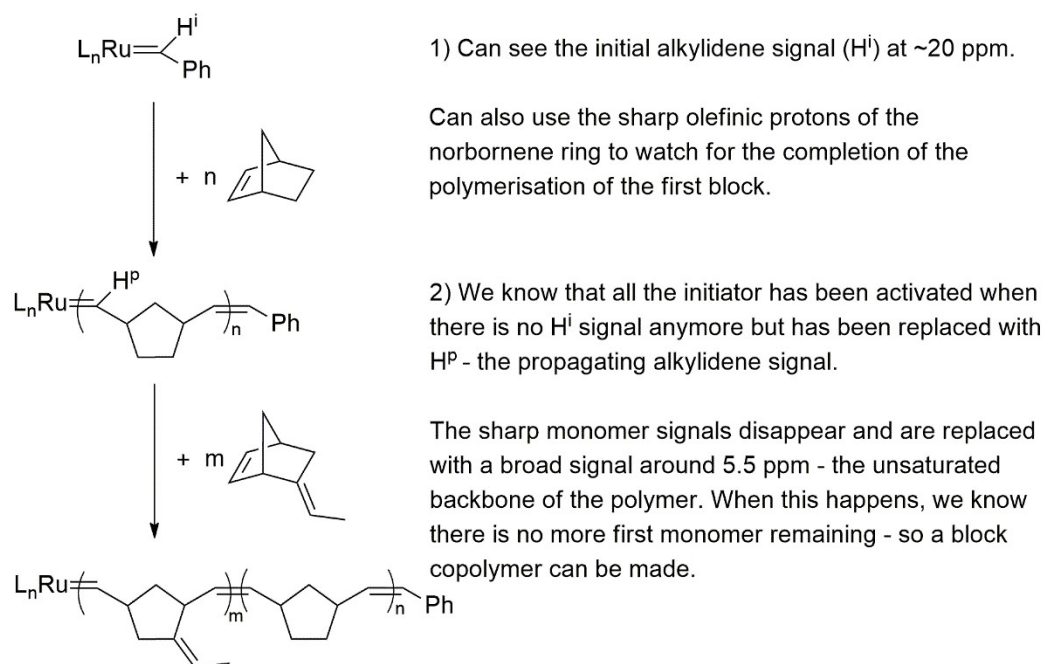


**Equation 1.7:** An example of the statistical copolymerisation of norbornene and cyclopentene performed by Nikovia *et al.* In this example, towards the phenyl end of the polymer, there will be a much higher concentration of the ring-opened norbornene repeat unit due to its much higher reactivity ratio

### 1.2.6.3 Block Copolymers

Finally, block copolymers can be formed using ROMP, Scheme 1.8. This is done by adding one monomer first, and following its polymerisation by  $^1H$  NMR spectroscopy. This study is done by observing the decrease in the strained olefinic protons in the starting monomer, and the increase in the unsaturated backbone protons of the polymer chain. Once there is no monomer remaining, a second – different – monomer is added to the reaction mixture and this is subsequently polymerised. This second block adds onto the end attached to the metal carbene as this is the 'living' part of the polymer (see Section 1.4), and forms what is called a di-block copolymer. Introducing more blocks is possible, which could be the same or different to the original monomer. An alternative way of following the polymerisation of the initial block is by monitoring the initial and propagating alkylidene signals and measuring their ratio. This can be difficult however since the initiator can be very dilute in the reaction mixture.

The only limiting factors that affect how many blocks can be added to a block copolymer are: the lifetime of the initiator, and the solubility (if applicable) of the polymer in solution. Once the living propagating alkylidene has decomposed, the chain end is no longer metathesis active and will not facilitate ROMP any more. And if the polymer is no longer in solution, the mixing of the monomer with the living chain end will be poor to non-existent and so the chain will stop growing.

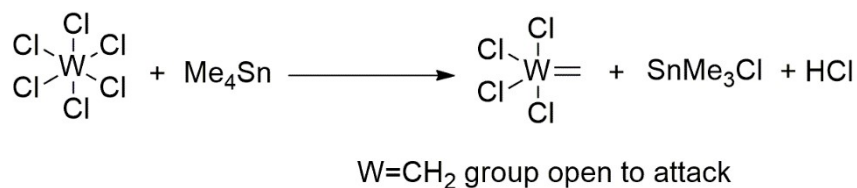


**Scheme 1.8:** An example of the formation of a di-block copolymer using norbornene and ethylidene norbornene; n and m could be the same value, or different. Steps 1 and 2 explain how the reaction can be followed by  $^1\text{H}$  NMR.

### 1.3 ROMP initiators

### 1.3.1 Early ROMP initiators

The earliest ROMP initiators were poorly defined and were made by reacting metal halides (e.g.  $\text{WCl}_6$ ,  $\text{MoCl}_5$ ,  $\text{ReCl}_5$ ,  $\text{IrCl}_3$ ) with activated alkylating species (e.g.  $\text{R}_3\text{Al}$ ,  $\text{R}_2\text{AlCl}$ ,  $\text{R}_4\text{Sn}$ ). These ill-defined initiators do not promote living polymerisation<sup>33</sup> as they are susceptible to termination and chain transfer. The likely activated form if this initiator contains a very reactive metal carbene (Equation 1.8), which is rapidly terminated due to the lack of steric hindrance.<sup>34</sup>

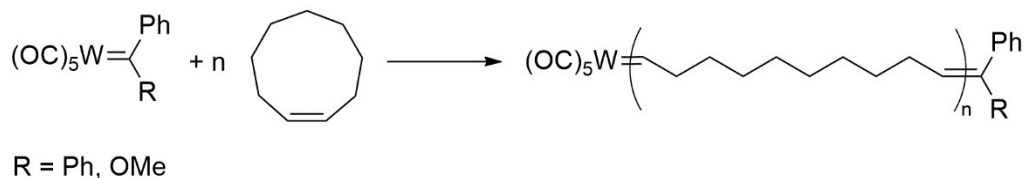


**Equation 1.8:** A possible metathesis-active, ill-defined initiator system

Early initiators have an extremely fast propagation rate, resulting in no molecular weight control. The results are also irreproducible due to this lack of control. Finally, these ill-defined initiators have very limited tolerance for functional groups – only esters can be tolerated. These early initiators were used from the 1960s up until the early 1980s, when more well-defined initiators were starting to be developed.

### 1.3.2 Katz initiator

In 1976, Katz *et al.* developed the first “well-defined” initiator,<sup>35</sup> previously made by Casey *et al.*,<sup>36</sup> which is shown below in Equation 1.9. Katz acknowledged that the metal carbene was an important functionality for a ROMP initiator, so designed his initiator as such.

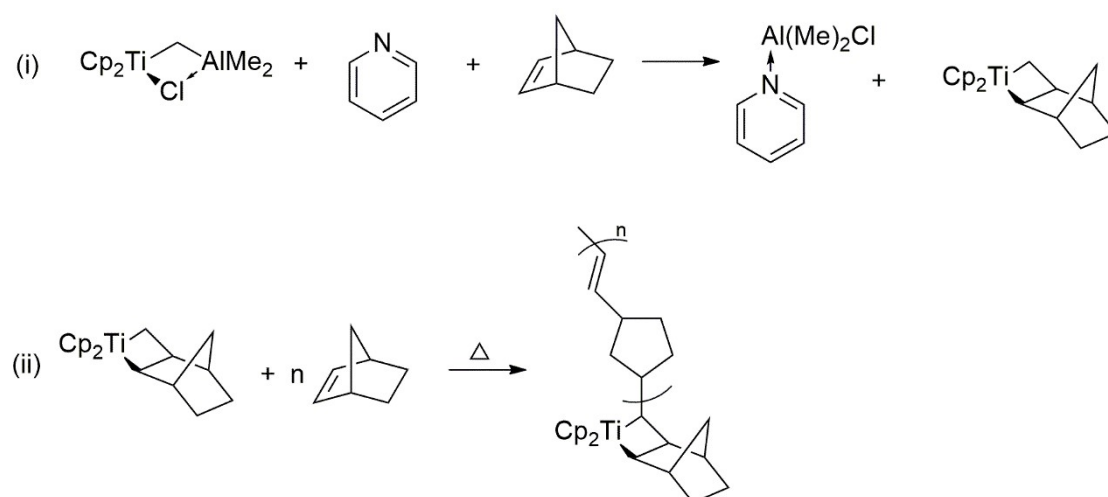


**Equation 1.9:** The ROMP of cyclooctene using Katz’s initiator

This example uses cyclooctene, but would work with most solely olefin-functionalised, strained ring systems. One downside to Katz’s system is the limited tolerance to functionality, and another is the fact that there is little molecular weight control: again the polymerisations are very quick, which results in a broad dispersity ( $\bar{M}_w/\bar{M}_n$ ) of over 1.85. This could suggest that this initiator also suffered from poor initiation characteristics, backbiting, and / or intermolecular metathesis. It was because of these factors that Katz’s tungsten initiator could not be described as promoting living ROMP.

### 1.3.3 Titanium-based ROMP initiators

Titanium-based ROMP initiators were the first single-constituent initiators which were well-defined and, perhaps most importantly, initiated living polymerisation.<sup>37</sup> Titanium complexes are not based on carbenes, but rather titanacyclobutanes. The ‘preinitiator’ is actually a titanium and aluminium containing complex, which is why – in the first stage of the reaction – pyridine is required to sequester the aluminium and activate the initiator – as shown in Scheme 1.9. This activated initiator can then initiate the ROMP of a strained monomer.



**Scheme 1.9:** Titanium-based ROMP of norbornene

The titanocycle produced at the end of reaction (i) in Scheme 1.9 was also proven by Straus and Grubbs to be isolable<sup>38</sup> and they could even perform X-ray crystallography to confirm the structure. In this well-defined initiator, the metallocycle acts like a carbene species when a monomer is added. Unlike ill-defined early initiators and Katz's initiator, titanium-based initiators can catalyse ROMP with much better molecular weight control, resulting in much narrower dispersities, for example the ROMP of norbornene (reaction shown in Scheme 1.7) achieves a dispersity of approximately 1.2. The major downside is that titanium initiators are still reactive with heteroatoms and functional groups because they are Lewis acidic due to their high oxidation state.

### 1.3.4 Tantalum-based ROMP initiators

In 1977, shortly after the discovery of the titanium initiator, Schrock *et al.* started work on a new, well-defined tantalum initiator system.<sup>39</sup> These were the first examples of isolable ROMP initiators that contained a metal alkylidene as can be seen in Figure 1.4.

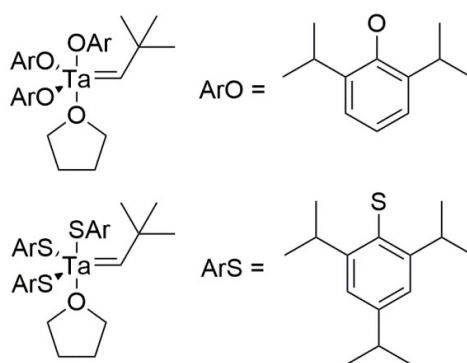


**Figure 1.4:** Examples of an oxygen-based (top) and a sulfur-based (bottom) tantalum initiator<sup>39</sup>

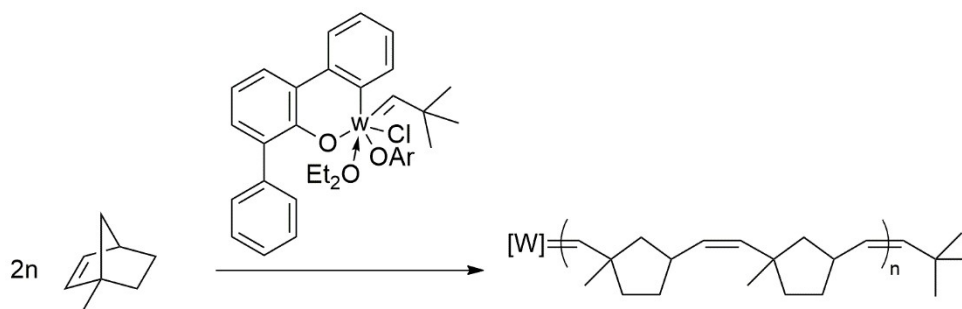
The main advantage of tantalum initiators over their titanium counterparts is their higher activity, although they are still reactive with heteroatoms and functional groups. The tantalum initiator can also be designed for a specific application. If the bulky aryl oxides or aryl mercaptans are not present then the number of side reactions increases. This is perhaps due to the increased number of orientations an olefin could attack from, or the fact that the alkylidene is more exposed, and therefore reactive. The ROMP of norbornene is fairly controllable with respect to molecular weight, *i.e.* if the electron-rich bulky aryloxides are present the dispersity of polynorbornene produced is around 1.1. If however less bulky groups are attached to tantalum, this is increased to 1.6, again showing that adding bulky ligands increases selectivity and narrows dispersity since it decreases the rate of deactivation.

### 1.3.5 Tungsten-based ROMP initiators

In the late 1980s, Basset *et al.* developed tungsten-based metathesis initiators. These were of great interest since, as well as being well-defined, they are also reasonably air-stable<sup>40</sup> and have much greater functional group tolerance. Basset's tungsten initiator – shown in Equation 1.10 – can be used with acetate, cyanide and anhydride groups as well as esters, ethers and glucosides. It also has a



high activity, which means there are increased side reactions. If bulky ligands are attached to the tungsten centre, stereoselective reactions can occur.



**Equation 1.10:** Stereoselective ROMP of methyl norbornene using Basset's tungsten initiator

Schrock *et al.* also developed a tungsten-based initiator that contained an aryl imido group and two alkoxy ligands. These alkoxides could be altered in order to tune the activity of Schrock's tungsten initiator (shown in Figure 1.5). Unlike Basset's initiator, this did not require the addition of a Lewis acid, but was much more intolerant of functionality.

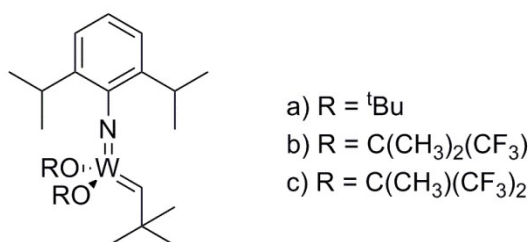


**Figure 1.5:** Schrock's tungsten initiator

If alkoxide **a** is used, Schrock's initiator will not react with cis-2-pentene.<sup>37</sup> However, if **b** or **c** is used, this reaction occurs readily via cross metathesis. As for ROMP of norbornene, this can be performed with a narrow dispersity of 1.03 with **a**, but has multiple side reactions if **b** or **c** as well as much slower initiation.

Ideally, initiators for ROMP – or any other polymerisation for that matter – have a high  $k_i$  (rate of initiation) and low  $k_p$  (rate of propagation). If  $k_p > k_i$ , then not all the initiator will be utilised in the reaction, and some of the chains will grow much longer than ideal (and some will be very short – meaning a broad dispersity). If  $k_p < k_i$ , then all the chains are initiated and then propagate at a slow, steady rate resulting in a far narrower dispersity ( $\bar{D}$ ). This means that for ROMP the bulky, non-fluorinated ligands are preferable (but in this example for the cross metathesis, the fluorinated ligands are a necessity).

### 1.3.6 Molybdenum-based ROMP initiators

As well as his work on tungsten, Richard Schrock is also famous for his work on well-defined, living ROMP initiators based on molybdenum. In 1990, Schrock *et al.* published work<sup>41</sup> announcing the first formation of a molybdenum initiator, shown in Figure 1.6.

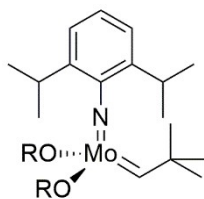
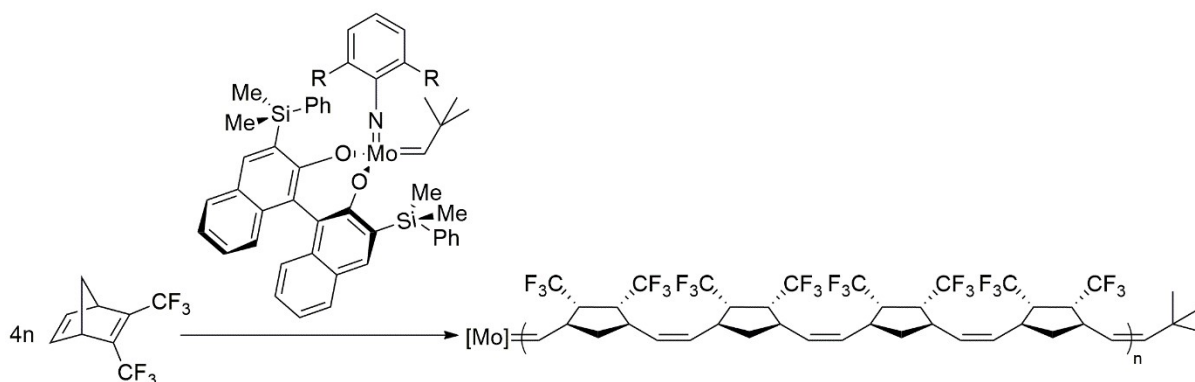


**Figure 1.6:** Schrock's molybdenum initiator

This molybdenum initiator showed very high activity and much higher tolerance for functional groups: esters, amides, imides, ketals, ethers, nitriles, trifluoromethyls and primary halogens all tolerated. Schrock's molybdenum initiator must, however, be used under inert atmosphere conditions – *i.e.* no oxygen or water present. Again the same R groups can be attached to Schrock's tungsten initiator, which again control the reactivity of the initiator – but most reactions with Schrock's molybdenum initiator result in a very narrow dispersity. Utilising chiral ligands, Schrock realised it was also possible to control the stereochemistry of the polymeric product<sup>42</sup> as demonstrated in Equation 1.11 where a regio-controlled polymer is achieved by attaching a bulky binaphthyl group to the molybdenum centre.



**Equation 1.11:** A chiral molybdenum initiator results in a stereochemically-controlled ROMP reaction from an achiral monomer

Another advantage of molybdenum initiators is that the reactions can be carried out at room temperature.<sup>43</sup> Finally, Schrock's molybdenum system suffers from very little, if any, 'backbiting' – which is where the initiator could attack the double bond of the same polymer chain which is being propagated, forming a macrocyclic polymer.

Molybdenum initiators do have disadvantages, however. As mentioned before an inert atmosphere and dry solvent are both necessities. Schrock's initiators are also difficult to synthesise and are expensive (*e.g.* (S)-Schrock-Hoveyda Initiator is £253 for 100 mg).<sup>44</sup>

### 1.3.7 Ruthenium-based ROMP initiators

Many of the ill-defined, early initiators of the 1960s were, at least, partly based on ruthenium – for example  $\text{RuCl}_3$  was a popular metal halide used. This led Robert Grubbs to investigate ruthenium species as ROMP initiators. In 1987, he and Bruce Novak discovered that  $\text{RuCl}_3$  – or similar – in protic media could catalyse the ROMP of unsaturated bicyclic molecules.<sup>45</sup> This was shown, however, to be

a non-living polymerisation. What was encouraging was the use of protic media, and in fact aqueous conditions were shown to be compatible in certain circumstances. This led to the first single component, well-defined, ruthenium-based initiator (Figure 1.7) being developed in 1992.<sup>46</sup> This was shown to be stable towards water, organic acids (e.g. acetic acid) and inorganic acids (e.g. HCl). As well as its stability in different solvents, this ruthenium initiator is also stable in the solid state over long periods of time.

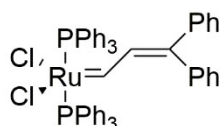
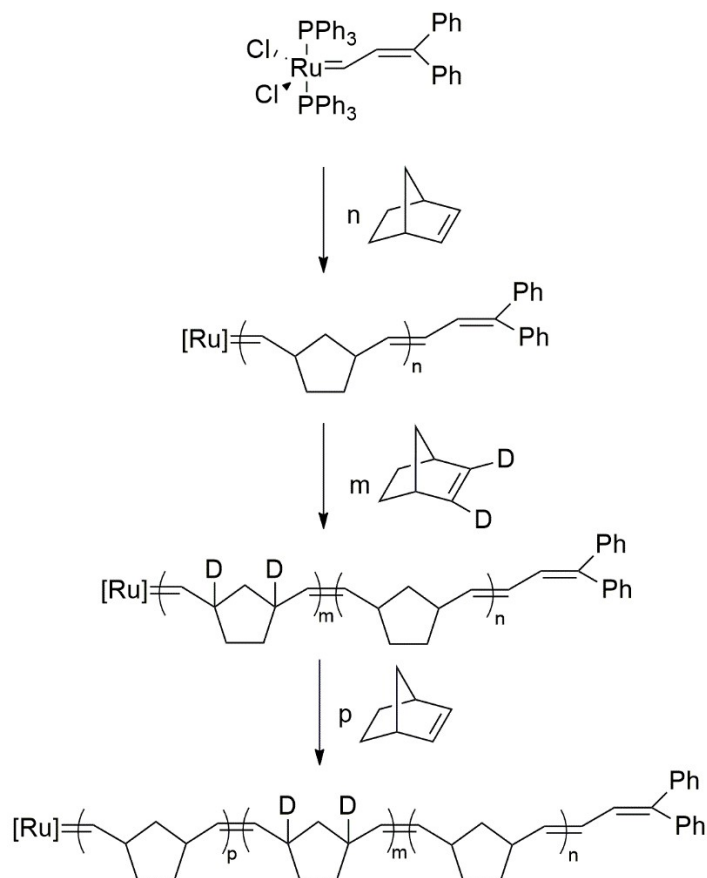


**Figure 1.7:** First single component ruthenium initiator

This ruthenium initiator was also shown by Grubbs *et al.* to catalyse living ring-opening metathesis polymerisation. This was done by the formation of a triblock polymer<sup>37</sup> of norbornene, dideuteronorbornene and then another block of norbornene (Scheme 1.10). This reaction can be followed by <sup>1</sup>H NMR spectroscopy since the proton on the carbene will appear at around 20 ppm and will decrease in intensity as the polymerisation occurs being replaced by another at around 18 ppm for the propagating alkylidene. A doublet at lower chemical shift will also appear at around 5.5 ppm due to the vinylic protons in the polymer backbone, after the norbornene ring has been opened.



**Scheme 1.10:** The formation of a triblock copolymer using the well-defined, ruthenium-based initiator

Grubbs continued his work on ruthenium initiators, and discovered that adding more electron-rich, bulky phosphine ligands (e.g.  $\text{PCy}_3$  – where Cy is cyclohexyl) resulted in a far more active initiator. Fortunately, since the phosphine ligands are so labile, the  $\text{PPh}_3$  and  $\text{PCy}_3$  underwent a facile ligand exchange. Also, since the activity of these initiators was so high (and rate of initiation fairly low) they tended to show very little molecular weight control and thus resulted in broad dispersities, but meant that it was likely that ring systems less strained than norbornene would be reactive with ruthenium-based systems.

In 1995, Grubbs *et al.* published a paper containing the structure of a new ruthenium-based initiator<sup>47</sup> which would later become known as the “Grubbs 1<sup>st</sup> generation initiator”, the structure of which is shown in Figure 1.8. This was shown to be much more reactive than the earlier Ru initiator (Figure 1.7), but maintained the functional group stability and ability to perform reactions in the presence of water as well as being air-stable in the solid state.

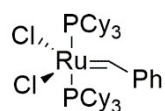


**Figure 1.8:** Grubbs 1<sup>st</sup> generation initiator

Four years later, Grubbs' group synthesised another initiator in which a phosphine ligand is replaced with a non-labile but far more electron donating N-heterocyclic carbene (NHC), which stabilised the reaction intermediates,<sup>48</sup> and makes the initiator far more active. This became known as “Grubbs 2<sup>nd</sup> generation initiator” shown in Figure 1.9. Since the Grubbs 2<sup>nd</sup> generation initiator was slow to initiate, it was modified in 2001, again by a Grubbs-led group,<sup>49</sup> by replacing the phosphine ligand (and a halogen) with more labile pyridine, or bromopyridine, ligands. This third structure is known either as “Grubbs modified 2<sup>nd</sup> generation initiator” and is also shown in Figure 1.9.

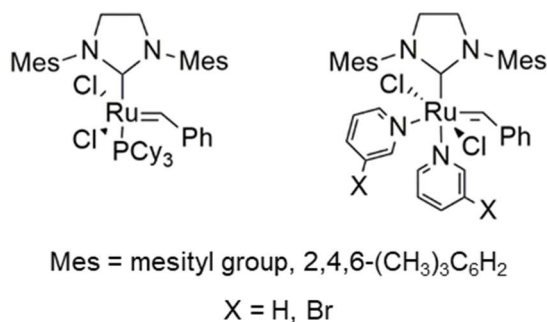
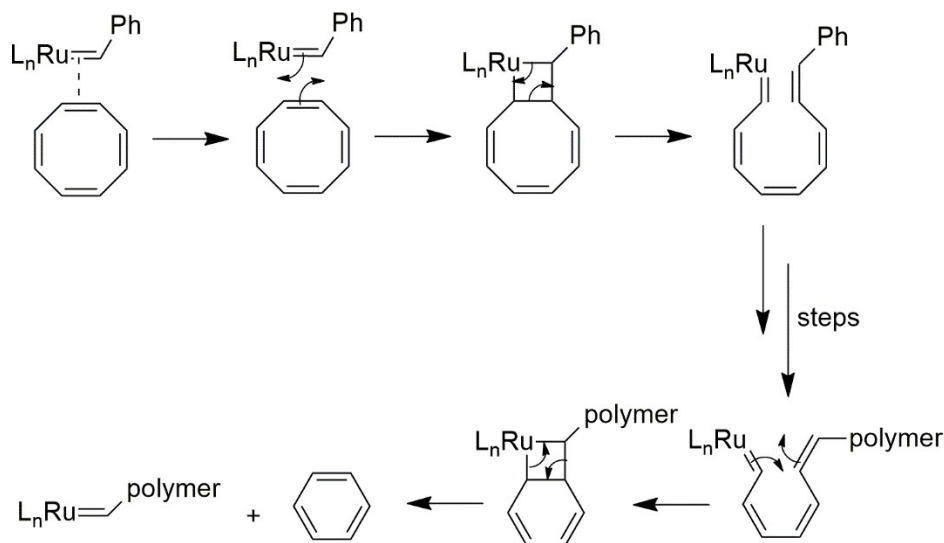


**Figure 1.9:** Grubbs 2<sup>nd</sup> generation initiator (left) and modified 2<sup>nd</sup> generation initiator (right)

Grubbs 1<sup>st</sup> generation initiator – although far less active than 2<sup>nd</sup> generation – can control the molecular weight of polymers far better due to the fact that for the 2<sup>nd</sup> generation, the rate of propagation is much greater than rate of initiation. These two rates are approximately equivalent for 1<sup>st</sup> generation. Modifying the 2<sup>nd</sup> generation with pyridine makes the rate of initiation far greater than

rate of propagation – meaning that this has the greatest control over molecular weight and thus results in the narrowest dispersities.



**Scheme 1.11:** An example of backbiting in the polymerisation of cyclooctatetraene

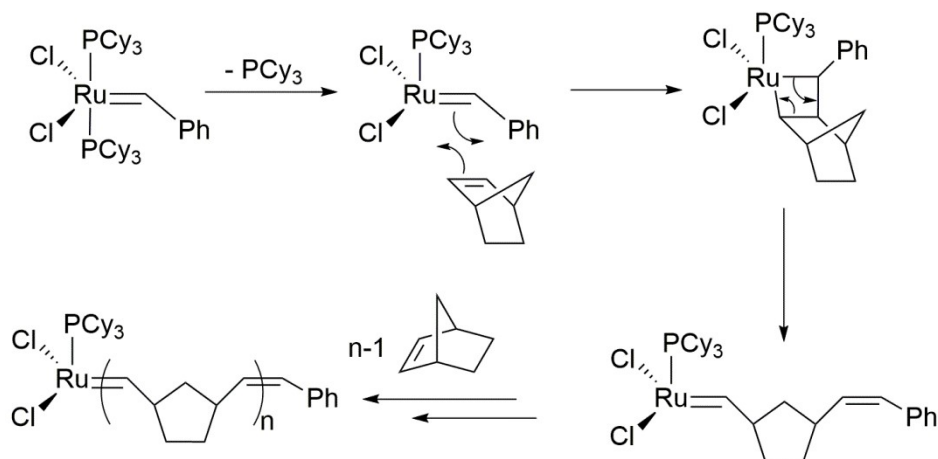
In general, Grubbs ruthenium initiators show a slightly broader dispersity ( $\sim 1.20$ ) than Schrock's molybdenum system ( $\sim 1.05$ ) although this is still an acceptable  $\bar{D}$  for many applications of ROMP. Also, unlike their molybdenum counterparts; ruthenium initiators tend to 'backbite' the living polymer chain (the process of which is shown in Scheme 1.11), which can lead to unexpected products from the polymerisation and also shorter than expected polymer chains.

One major advantage of Grubbs initiators, however, is their ease of synthesis. This makes the ruthenium initiators much cheaper than molybdenum well-defined initiators, despite it being a much more expensive metal.

### 1.3.7.1 Mechanism of ruthenium-catalysed ROMP

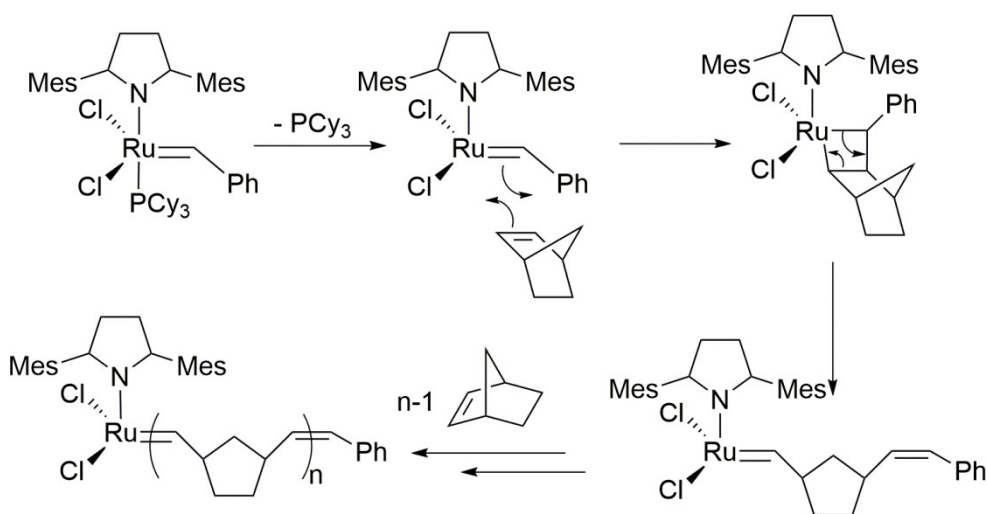
The lability of the phosphine and pyridine ligands is important since these molecules are 'pre-initiators'. They only become active once the phosphine / pyridine has dissociated and thus the metal complex becomes very electron poor (14 electrons), which makes it highly reactive.

When Grubbs 1<sup>st</sup> generation initiator is mixed with a cyclic olefin, the tricyclohexylphosphine ( $\text{PCy}_3$ ) dissociates from the ruthenium centre, producing the active initiator.<sup>47</sup> This active initiator is then electron poor, and is reactive towards the electron-rich double bond of, for example, norbornene (Scheme 1.12).



**Scheme 1.12:** Activation of Grubbs 1<sup>st</sup> generation initiator, and subsequent ROMP of norbornene

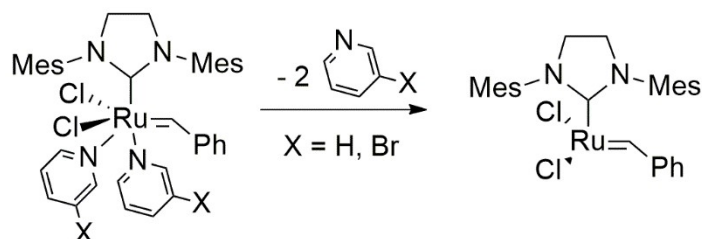
Grubbs 2<sup>nd</sup> generation initiator has a non-labile *N*-heterocyclic carbene ligand added to the ruthenium centre that stabilises the ruthenium carbene. This additional stability is the reason why the rate of propagation is much higher for 2<sup>nd</sup> generation than Grubbs 1<sup>st</sup> generation initiator. However, this means that the PCy<sub>3</sub> is less labile and therefore results in a much lower rate of initiation for the 2<sup>nd</sup> generation initiator.<sup>50</sup> These two factors mean that polymers produced from Grubbs 2<sup>nd</sup> generation initiator, Scheme 1.13, have higher molecular weights than expected, and hence much broader dispersities.



**Scheme 1.13:** Activation of Grubbs 2<sup>nd</sup> generation initiator, and subsequent ROMP of norbornene

In order to improve the initiation characteristics, the PCy<sub>3</sub> ligand on Grubbs 2<sup>nd</sup> generation initiator can be replaced by a pyridine, or bromopyridine, ligand. This increases the rate of initiation by over 1,000,000 times.<sup>51</sup> Once the active form of the initiator is formed, Equation 1.12, the living end of the polymer is identical to that formed from Grubbs 2<sup>nd</sup> generation initiator. This means that the rate of propagation with modified 2<sup>nd</sup> generation initiator is still high, and coupled with its fast initiation

characteristic leads to much more narrowly disperse polymers. Moreover, high molecular weights are still achievable.



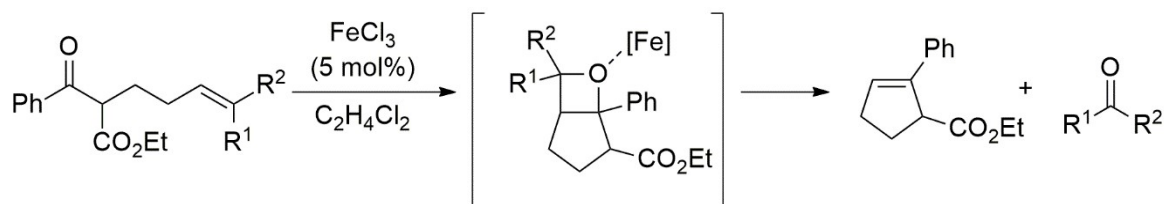
**Equation 1.12:** Formation of the active form of modified Grubbs 2<sup>nd</sup> generation initiator

### 1.3.8 Alternative metal initiators

Osmium-based initiators are extremely rare and tricky to synthesise since they are usually too stable to catalyse olefin metathesis, though some examples do exist.<sup>52</sup> More problems with osmium are its high toxicity (especially its oxide OsO<sub>4</sub>), and its scarcity. In fact osmium is the rarest stable element in the Earth's crust,<sup>53</sup> so using this may not be advisable unless it affords much better properties than any metals seen previously.

Ruthenium is neither a cheap nor a plentiful metal. However, it is in the same Periodic Table triad as iron – which is both inexpensive and abundant. Another advantage of iron is its low toxicity and so its removal post-polymerisation would be less of an issue. For years, there has been research into metathesis-active iron carbene complexes<sup>54</sup>, one example from the Grubbs *et al.*<sup>55</sup> involved the ROMP of a cyclic olefin using an iron carbene. This produced, as expected, a linear unsaturated polymer. Upon attempting to repeat said experiment in a different laboratory – one where no metathesis chemistry had ever taken place – no polymer was formed. It was later discovered that a small amount of residual ruthenium initiator in the first environment had instead initiated the reaction, and the iron carbene system was metathesis inactive.

In 2016, Ludwig *et al.* did however report their findings<sup>56</sup> on the use of iron in a ring closing reaction involving a carbonyl and an olefin (Scheme 1.14). This does not include the use of an explicit iron carbene, but there may be a similar quasicyclobutane intermediate.



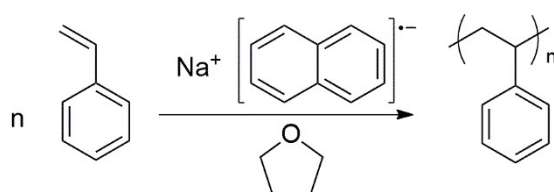
**Scheme 1.14:** An example ring closing reaction performed in the work of Ludwig *et al.*, using the iron catalyst

## 1.4 Living polymerisations

IUPAC defines living polymerisation as, “A chain polymerisation from which chain transfer and chain termination are absent.”<sup>57</sup> This means that the polymerisation should continue indefinitely until the

monomer is completely used up. Living polymerisation should also have three further criteria: the molecular weight should increase linearly; polymerisation can be continued by the addition of more monomer; and the dispersities should be low (ideally  $\bar{D} < 1.1$ ). Taking all of this into account, there are only three methods<sup>58</sup> of truly living polymerisation: living anionic, living cationic, and ROMP.

The first example shown of living anionic polymerisation was by Szwarc *et al.* in 1956<sup>59</sup> and involved the polymerisation of styrene in tetrahydrofuran (THF), using sodium naphthalide as the initiator (Equation 1.13). It was shown to be living since the initiator solution was green and turned red upon the addition of styrene,<sup>60</sup> and this colour persists after exhaustion of the monomer – which suggests that the chain ends are still active and more polymerisation could occur upon further addition of monomer. Anionic polymerisation no longer stays living under basic conditions as these can attack and kill the active chain ends.



**Equation 1.13:** The first example of living anionic polymerisation

One of the first living cationic polymerisations was carried out by Faust and Kennedy in 1986<sup>61</sup> by polymerising isobutylene using boron trichloride and cumyl acetate. They succeeded in achieving rapid initiation, and minimising chain transfer and termination. They were also able to control the rate of propagation to make sure the growth of the chain length was fairly consistent across all chains – leading them to a narrow dispersity.

ROMP using ruthenium-based initiators shares some properties with living polymerisation since, as shown previously, once the monomer has been used up: adding more monomer will continue the polymerisation. Grubbs 2<sup>nd</sup> generation initiator does not facilitate living ROMP since the rate of initiation ( $k_i$ ) is much slower than propagation ( $k_p$ ) which leads to broad dispersities – defying one of the rules of living polymerisation.<sup>57</sup> It could also be argued that since some initiators can suffer from backbiting<sup>62</sup> that this is also not truly living, though the initiator will remain active afterwards and there are no termination reactions until the terminating agent is added. Backbiting is also much less problematic when using Grubbs 1<sup>st</sup> generation.<sup>63</sup> Grubbs modified 2<sup>nd</sup> generation is the most likely to give conditions for living polymerisation (detailed in Table 1.1) as the initiation is rapid, and the rate of termination ( $k_t$ ) is also very small. However, the rate of propagation is high – and chain transfer can be an issue.



**Table 1.1:** A table detailing the properties of living polymerisation, and those polymerisations carried out using Grubbs ruthenium-based initiators

Rate	True living	G1	G2	MG2
$k_i$	fast	slow	very slow	fast
$k_p$	slow	slow*	fast	fast
$k_t$	none	little	little	little
chain transfer	none	little	some	some

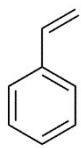
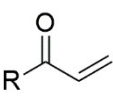
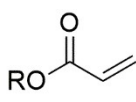
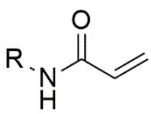
\*Compared to G2 and MG2

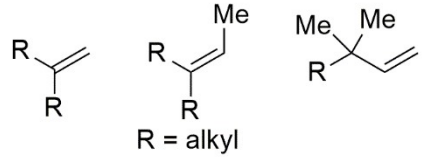
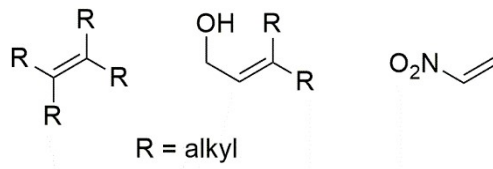
## 1.5 Grubbs' classification of alkenes

**Equation 1.14:** The homodimerisation of propene to form but-2-ene and ethene

In 2013, Chatterjee *et al.* came up with a classification of olefins<sup>64</sup> to describe how easily they underwent homodimerisation (Equation 1.14) during cross metathesis. There were four types of olefins: Type I readily undergo homodimerisation, and the homodimer will still readily undergo homodimerisation itself. Type II undergo slow homodimerisation and the resultant homodimer is very slow to react. Type III show no homodimerisation but will undergo cross metathesis with Types I and II. Finally, Type IV will not undergo cross metathesis but neither do they affect the catalyst – they are said to be “spectators”. From Type I to Type IV: in general, the olefin reactivity decreases; the steric congestion increases; and the electron deficiency increases. Table 1.2 details examples of each type of olefin.

**Table 1.2:** Table showing examples of the four types of olefin in metathesis chemistry

	Dimerisation	Reactivity of homodimer	Examples
<b>Type I</b>	rapid	rapid	$\text{R}-\text{CH}_2\text{CH=CH}_2$ $\text{X}-\text{CH}_2\text{CH=CH}_2$  R = alkyl    X = OH, Hal
<b>Type II</b>	slow	slow	   R = alkyl

<b>Type III</b>	none, but will undergo CM with Type I/II	N/A	
<b>Type IV</b>	unreactive	N/A	

If similar rules of reactivity apply to ROMP of each monomer: an approximation can be made as to which type each could be assigned. Most of the monomers in this work involve sterically unhindered norbornene groups (Figure 1.10), which would lead them to perhaps being Type I or Type II – coupled with the fact that the norbornene ring is highly strained makes these monomers ideal for ROMP reactions. The only monomers which may perhaps have more Type II character are those which include ester or carbamate groups (Figure 1.10) – although these are not positioned next to the olefin (*i.e.* they are not acting as electron withdrawing groups to the olefin).

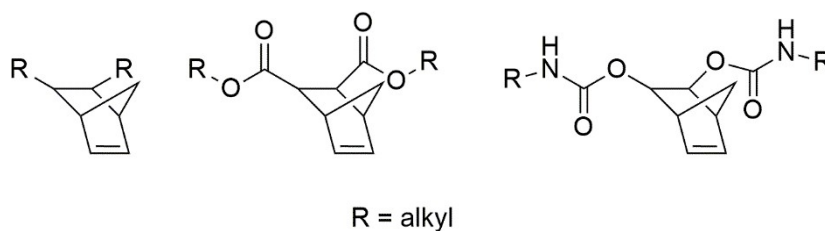


**Figure 1.10:** Example structures of (left to right) sterically unhindered norbornene, ester-functionalised norbornene, and carbamate-functionalised norbornene

## 1.6 Dicyclopentadiene

Dicyclopentadiene (DCPD, structure shown in Figure 1.11) is the product of the Diels-Alder reaction of cyclopentadiene with itself. If DCPD is heated to around 155 °C, it will undergo a de-dimerisation to reform cyclopentadiene, which can be used as a useful ligand precursor in organometallic chemistry. DCPD is formed from the cracking of petroleum fractions<sup>65</sup> including naphtha, *etc.* and was, for many years, a useless by-product meaning that the price of DCPD was extremely low – making it highly attractive commercially as a raw material.



**Figure 1.11:** Dicyclopentadiene

Dicyclopentadiene can undergo ROMP itself – and will form cross-linked material by ring-opening of the cyclopentene ring in higher concentrations as shown in Figure 1.12, and form cross-links within the copolymer. Though in low concentration, the ROMP of DCPD produces a linear polymer.<sup>43</sup>

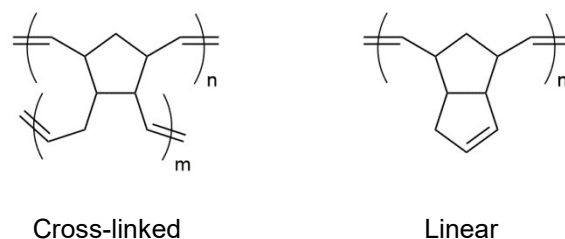
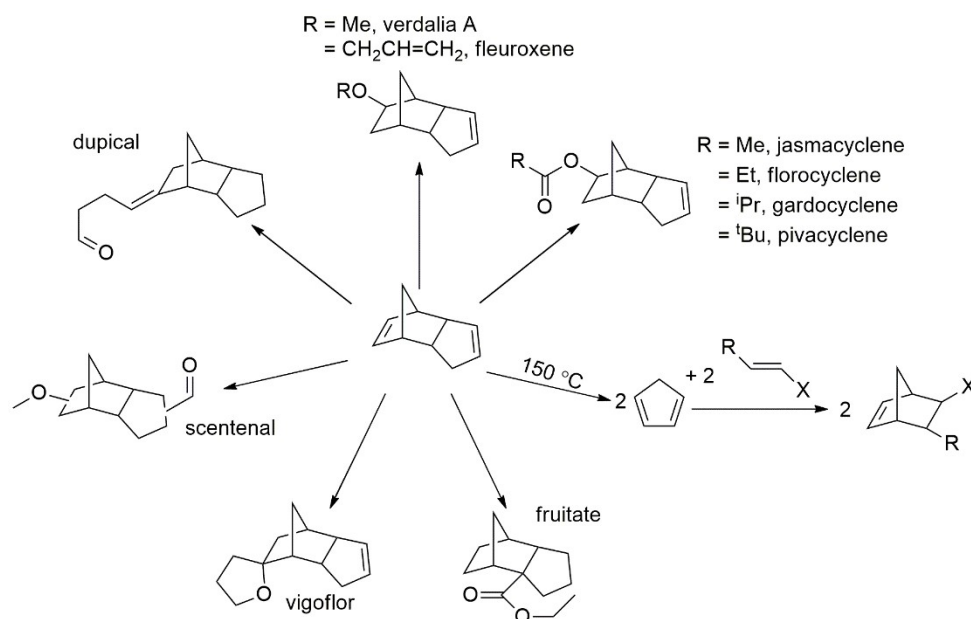


**Figure 1.12:** Poly(DCPD) produced in concentrated (left) and dilute (right) solution

### 1.6.1 Current uses of DCPD

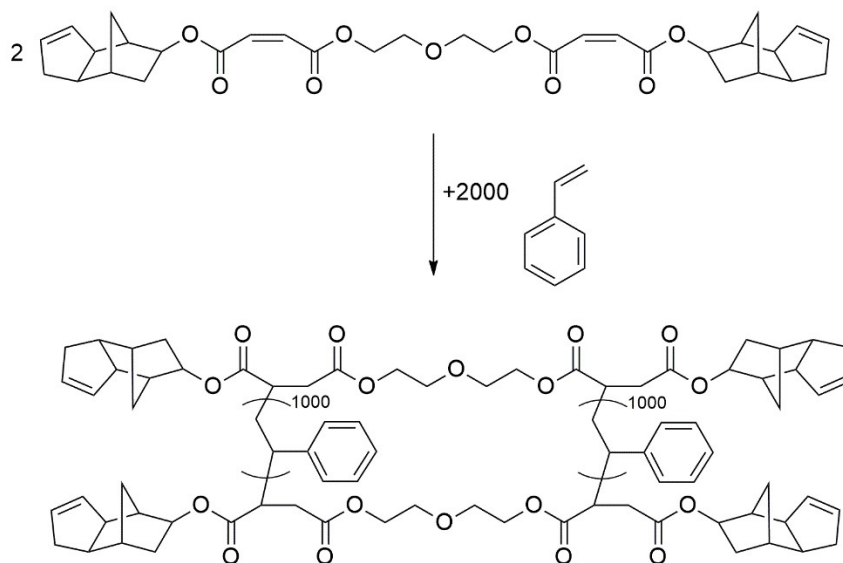
It is known that the double bond of the fused ring of DCPD can be added to by a sufficiently acidic acid, or a glycol with the use of aqueous sulfuric acid. Many adducts have completely different properties from DCPD and the acid or glycol used. For example, DCPD is observed by most to be extremely malodorous. Acetic acid also has a very pungent odour. The DCPD acetate adduct, however, is known as Jasmacyclene and has a pleasant, jasmine-like smell. Many DCPD adducts (like Jasmacyclene) are in fact used in perfumes<sup>66</sup> as shown in Scheme 1.15.



**Scheme 1.15:** Examples of DCPD adducts used in perfumery

DCPD adducts are also used in resins and an example one is based upon DCPD, maleic acid and diethylene glycol (DEG). The unsaturated acid part of this adduct can then be cross-linked (*e.g.* with styrene), as shown in Equation 1.15, to form the required product. The product shown here is much simplified as there will be more than two monomers of the polyester per chain, and the lengths of styrene between each polyester unit will not be the same. The properties of the resin can be tuned by

altering the glycol and/or acid used to perhaps a shorter, less flexible one, or an aromatic one which may stiffen up the polymer backbone resulting in a harder, probably more brittle, resin.

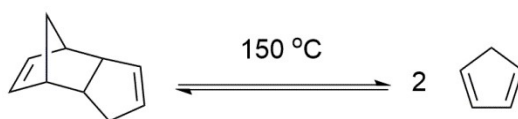


**Equation 1.15:** DCPD maleate diethylene glycol polyester cross-linked with styrene<sup>67</sup>

In order to add across the norbornene double bond of DCPD, the acids used to form adducts need to be sufficiently strong. For maleic acid, the  $pK_a$  is 1.92 which is easily adequate for it to add across the double bond of DCPD. Other acids with higher  $pK_a$  values may require the addition of an aqueous sulfuric acid catalyst. Once the maleic acid adds across the double bond, the  $pK_a$  of the other acid proton increases to 6.07, which is of course less than 1/100,000 as acidic (since  $pK_a$  is logarithmic). This means that the likelihood of maleic acid bridging two DCPD molecules is very low and will instead leave a free acid group. Melting point is also another important factor. Since the cracking temperature of DCPD is around 150 °C<sup>68</sup> and a homogeneous reaction mixture is ideal, then a diacid with a low  $pK_a$  and lower melting point than the cracking temperature is preferable.

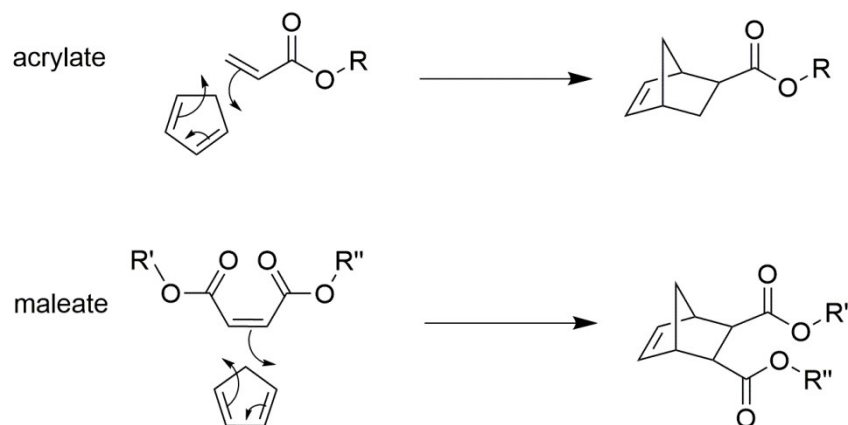
### 1.6.2 Synthesis of norbornene-based monomers

As stated in Section 1.6, dicyclopentadiene can undergo retro-Diels-Alder (or 'cracking') to form cyclopentadiene, Equation 1.16. As this is a diene, it can therefore react with a 'dieneophile' through a Diels-Alder reaction. Of course, the reaction described in Equation 1.16 is reversible and so cyclopentadiene can react with itself to reform dicyclopentadiene. This is why cyclopentadiene must be used immediately after its generation.



**Equation 1.16:** The retro-Diels-Alder of dicyclopentadiene to form cyclopentadiene

The cyclopentadiene produced can also react with an electron deficient double bond in another Diels-Alder reaction to form a molecule with a norbornene ring functionality – which is highly strained, and therefore ideal for ROMP reactions. Examples of good starting materials are acrylates and maleates, Scheme 1.16, due to the electron withdrawing carboxylate groups positioned next to the double bond.



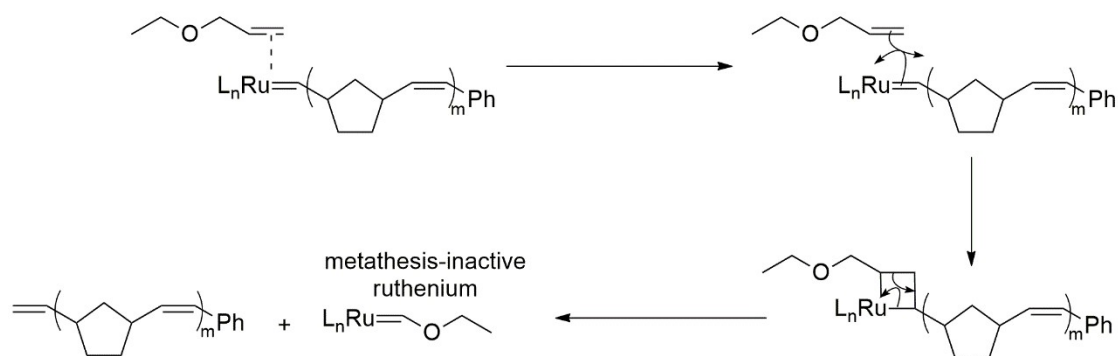
**Scheme 1.16:** Diels-Alder reactions of cyclopentadiene with acrylates and maleates

## 1.7 Green Chemistry

In 1998, Paul Anastas and John Warner made a list of twelve principles by which any process to be described as ‘green’ should abide by<sup>69</sup>. Application of these principles ensure that reactions are as environmentally friendly as possible, for example by reducing energy input by as much as possible as well as trying to limit the usage of non-renewable feedstocks – or to make these as efficient as possible. They also take into account the effect on human health, so toxic and harmful substances should be avoided if alternatives are acceptable. This also means that innocuous solvents (preferably no solvent) should be used. The production of by-products or waste is also severely unfavourable, as this also reduces atom efficiency and also may require treatment before being disposed of in a safe way.

Ruthenium and dicyclopentadiene (DCPD) are both fairly toxic, including to the aquatic environment.<sup>70-72</sup> This would seem to contravene the 3<sup>rd</sup> Principle of Green Chemistry that states that, “synthetic methods and generated substances that minimise toxicity to human health and the environment.” It is used at a level of 1% or less (which is in accordance with the 9<sup>th</sup> Principle – catalytic reagents are better than stoichiometric), which means its effects are reduced – however due to its intrinsic toxicity, it would still be much more preferable to remove it entirely.

The ruthenium can be removed from the reaction mixture by reacting with ethyl vinyl ether (Scheme 1.17), and recycled.<sup>73</sup> If the ruthenium is not removed, it could be seen as a stoichiometric reagent – although it is incorporated into the final product.



**Scheme 1.17:** Mechanism for the termination of ruthenium-based ROMP

Energy expenditure (6<sup>th</sup> Principle) can be quite reasonable when using Grubbs initiators since most ROMP reactions can be performed at room temperature (~25 °C). Unfortunately for less strained (e.g. cyclopentene, cycloheptene) ring systems, the reaction must be cooled – and this can often require more energy than for heating a reaction.

Some of Grubbs' initiators are also soluble in water<sup>74</sup> – meaning an innocuous solvent (5<sup>th</sup> Principle) can be used. Although many of the ROMP targets, like polyester resins, are insoluble in aqueous media meaning this cannot be exploited. Some ROMP reactions can, however, be undertaken in 'bulk' conditions – meaning without, or with very little, solvent. This would, of course, be the ideal solution. Polyester resins are viscous liquids even before setting, so this is not usually possible. A reactive diluent could also be used to lower the viscosity of the reaction however.<sup>75</sup>

Many reactions carried out use dichloromethane or chloroform as a solvent (both good solvents for the resins and initiators) which are both toxic or, at the very least, harmful. This again violates, as mentioned previously, the 3<sup>rd</sup> Principle. The solvents are fairly volatile however, and could be easily removed and recycled if required.

Finally, since there are no by-products, excluding the cleaved ruthenium if terminated in that manner, produced in the ROMP process the 2<sup>nd</sup> Principle is abided by. This states that as many atoms as possible from the starting materials should be incorporated into the final product.

### 1.7.1 E-factor

$$\text{E-factor} = \frac{\text{kg of waste}}{\text{kg of product}} \quad \text{Equation 1.17}$$

One method of measuring how environmentally-friendly a process is, is by calculating its E-factor. This is a simple equation devised by Roger Sheldon in 1992<sup>76</sup> which measures how much waste is created per kg of product produced (Equation 1.17). The more waste produced, the higher a process' E-factor. Thus, as low an E-factor as possible is desired. He calculated the E-factors of a few different industries in his work,<sup>77</sup> shown in Table 1.3. This shows that as the output increases, the E-factor decreases meaning that on the lab scale it would be expected that the E-factor will be significantly higher.

**Table 1.3:** Table showing the E-factors of different industries, according to Sheldon

Industry	Output (tonnes)	E-factor
Oil refining	$10^6 - 10^8$	<0.1
Bulk chemicals	$10^4 - 10^6$	<1 – 5
Fine chemical industry	$10^2 - 10^4$	5 – >50
Pharmaceutical industry	$10 - 10^3$	25 – >100

## 1.8 Mechanical properties of polymers

Since the aim of this work was to prepare styrene-free, cross-linked polyesters, the Young's moduli (a measure of stress *versus* strain, which shows how stiff a material is) of materials produced here *via* ROMP were studied. This can be approximated using the technique of Dynamic Mechanical and Thermal Analysis (DMTA). It could also, more accurately, be calculated by undertaking stress-strain reactions, though these were not performed due to limited supply of both monomers and initiators. The results found using DMTA could then be compared to those of the polyesters currently cross-linked using styrene to see if ROMP offered a viable alternative. Using DMTA,  $E'$  can be observed over a wide range of temperatures: from about  $-190\text{ }^{\circ}\text{C}$  (since the DMTA machine uses liquid nitrogen to cool the sample) to above  $300\text{ }^{\circ}\text{C}$ .

One piece of information that can be found from DMTA is the storage modulus ( $E'$ ). This shows how elastic a material is – and is similar to the Young's modulus although not identical. Another is  $\tan(\delta)$ , which can also be known as damping.<sup>78</sup> A peak in this can show the glass transition temperature ( $T_g$ ), where a sample transitions between behaving like a stiff, glass-like material and becoming a rubber-like material, which is the main focus here. For linear polymers, a peak could also show a melting transition. The final piece of information that DMTA can give is loss modulus ( $E''$ ), which is a measure of how viscous a material is (as opposed to elastic). To put these terms into perspective, steel is an almost perfect elastic material, whereas a liquid would be a viscous material.

$$\tan(\delta) = \frac{E''}{E'} \quad \text{Equation 1.18}$$

Equation 1.18 shows that  $\tan(\delta)$  is the ratio between the loss ( $E''$ ) and storage ( $E'$ ) moduli. As the  $T_g$  is approached, the material becomes more viscous – and less elastic – increasing  $E''$  and decreasing  $E'$ . This leads to a peak in  $\tan(\delta)$ , and thus this can be used to define the  $T_g$  of a material. Above the  $T_g$ , the ability to dissipate energy ( $E'$ ) again decreases, and so  $\tan(\delta)$  decreases again to a relatively constant level. For linear polymers the ratio of  $E'$  to  $E''$ , or  $\tan(\delta)$ , will also display another peak or trough at higher temperature. This peak or trough at higher temperature shows the melting point ( $T_m$ ) of the polymer, where the polymer begins to behave like a viscous liquid as it starts to exhibit flow.

These three pieces of data can then be compared to the currently used polyester resins, and other polymer systems.

## 1.9 Thesis aims and objectives

The main aim in this project is developing a system which:

1. *Incorporates one or more norbornene rings in any monomers synthesised for ROMP*
2. *Can be polymerised using ROMP to yield linear or cross-linked polymers*

The idea for incorporating norbornene rings into the polymer is to make the system ideally suited to ROMP, due to its high ring strain. As mentioned in Section 1.6.2, it is also simple to form norbornene functionalised monomers from simple starting materials. If this is achieved without the production of any side products which may inhibit ROMP, any molecules with norbornene functionality should readily undergo ROMP, affording the desired cross-linked polymer.

3. *Utilises little, or no, styrene*

Reducing styrene would be ideal since its reclassification could be problematic for materials that contain styrene being used. Styrene also regenerates the ruthenium initiator and prevents the propagation of the polymer chain.

4. *Produces products with comparable properties to current unsaturated polyester resins*

Since the polymers produced here are to replace the currently utilised styrene cross-linked polyesters, it is hoped that they will have similar properties to them. However, if they do not then they may have other interesting and novel applications.

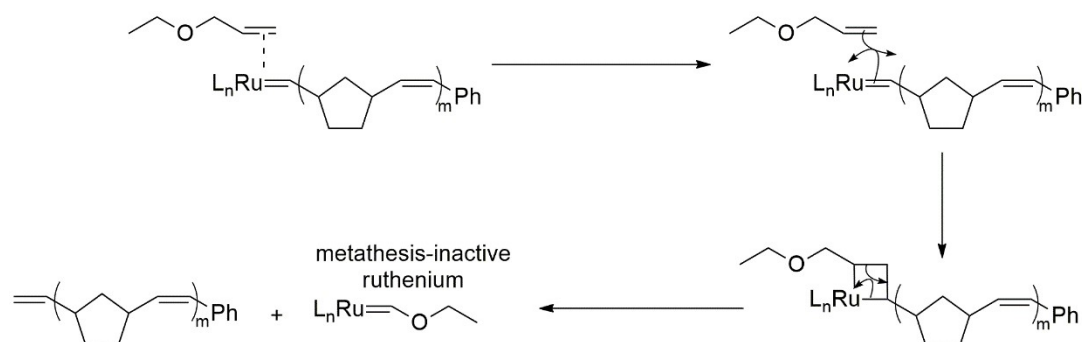
5. *Can be polymerised in solvent, or in the presence of a reactive diluent*

Ideally, polymerisations should be undertaken in bulk as any solvents used affect the properties (e.g. mechanical strength, glass transition temperatures). Good solvents for ruthenium initiators also tend to be chlorinated (for example: chloroform or dichloromethane), which in turn tend to be toxic or carcinogenic. However, sometimes bulk polymerisation is not possible – possibly due to poor solubility of the initiator in the monomer, or the mixing between the two could be unsatisfactory – and so a solvent would have to be used.

6. *Is as environmentally friendly as possible*

If a reaction is environmentally friendly, as few by-products as possible should firstly be produced. In the case of ROMP there are no other products other than the polymer chain as the initiator stays attached to the chain end. If, at the end of the reaction, the ruthenium is cleaved off (e.g. as seen previously by ethyl vinyl ether, Scheme 1.18) then this would need to be removed from the final product due to ruthenium's slight toxicity.<sup>71</sup>





**Scheme 1.18:** Mechanism of the termination of ROMP, and the removal of ruthenium from the chain end

### 7. Is as cost-effective as possible

Finally, ruthenium-based ROMP initiators are expensive and so using these for polymerisations instead of styrene-containing materials may seem counter-intuitive. However, the levels required are very low and so this will keep costs down. All other starting materials (*i.e.* acrylates, maleates, dicyclopentadiene) are fairly cheap so this will help with the aim, and where possible the cheapest monomers will be used. The conditions will also be kept as close to atmospheric conditions as possible for ROMP which will keep the polymerisation cost-effective both on the lab scale, and if it is ever scaled-up.

## 1.10 Summary

Table 1.4 shows that there is a large library of olefin metathesis initiators. However, many monomers have functional groups that are unsuitable for many of the initiator. This limits the number which are suitable. For example, only ruthenium-based initiators, and molybdenum to a lesser extent, have a good tolerance. Another point that this table shows is that certain initiators can control the stereochemistry of the polymer, whereas others will not be able to control this.

Finally, Table 1.4 shows that the number of advantages associated with the initiators increases, in general, from early initiators to ruthenium-based initiators. Similarly, the number of disadvantages decrease as more research was undertaken on olefin metathesis initiators.

**Table 1.4:** A table of the structures and features of important olefin metathesis initiators

Initiator	Example Structure	Advantages	Disadvantages
Early		<ul style="list-style-type: none"> <li>Highly active</li> </ul>	<ul style="list-style-type: none"> <li>High termination rate</li> <li>Uncontrolled polymerisation</li> <li>Requires activating species</li> </ul>

Titanium		<ul style="list-style-type: none"> <li>Promotes living ROMP</li> </ul>	<ul style="list-style-type: none"> <li>Low activity</li> <li>Requires pyridine to be activated</li> <li>Reactive with heteroatoms</li> </ul>
Tantalum		<ul style="list-style-type: none"> <li>High activity</li> </ul>	<ul style="list-style-type: none"> <li>Reactive with heteroatoms</li> </ul>
Tungsten		<ul style="list-style-type: none"> <li>Can be stereoselective</li> <li>Can produce very narrow dispersities</li> </ul>	<ul style="list-style-type: none"> <li>Low functional group tolerance</li> <li>Many side reactions</li> </ul>
Molybdenum		<ul style="list-style-type: none"> <li>Can control tacticity</li> <li>Can achieve narrow dispersities</li> </ul>	<ul style="list-style-type: none"> <li>Air and moisture sensitive</li> <li>Very expensive</li> </ul>
Ruthenium (G1)		<ul style="list-style-type: none"> <li>High tolerance of functional groups</li> </ul>	<ul style="list-style-type: none"> <li>Low activity</li> <li>No stereo control</li> </ul>
Ruthenium (G2)		<ul style="list-style-type: none"> <li>Highly active</li> <li>High tolerance of functional groups</li> </ul>	<ul style="list-style-type: none"> <li>Poor rate of initiation</li> <li>Broad dispersity</li> <li>Expensive</li> <li>No stereo control</li> </ul>
Ruthenium (MG2)		<ul style="list-style-type: none"> <li>High initiation rate</li> <li>High activity</li> <li>Low dispersity</li> <li>High tolerance of functional groups</li> </ul>	<ul style="list-style-type: none"> <li>Expensive</li> <li>No stereo control</li> </ul>

## 1.11 References

1. Kaarnakari, M.; Airola, K.; Tuori, T. Unsaturated polyester gel coats with antifouling properties. WO 2001074953 A1, **2001**.
2. Crystic® Permabright High Performance D-Iso/NPG Polyester Gelcoat. [http://www.scottbader.com/uploads/files/205\\_crystic-permabright-gelcoat-brochure-english.pdf](http://www.scottbader.com/uploads/files/205_crystic-permabright-gelcoat-brochure-english.pdf) (accessed 25th August 2016).
3. Choi, T.-L.; Rutenberg, I. M.; Grubbs, R. H., Synthesis of A,B-Alternating Copolymers by Ring-Opening-Insertion-Metathesis Polymerization. *Angew. Chem., Int. Ed.* **2002**, 41 (20), 3839-3841.
4. Clapham, G.; Shipman, M., Selective Lewis Acid Complexation of 2-Hydroxyethyl Esters using Competitive Diels–Alder Reactions as a Mechanistic Probe. *Tetrahedron* **2000**, 56 (8), 1127-1134.
5. Updegraff, I. H., Unsaturated Polyester Resins. In *Handbook of Composites*, Lubin, G., Ed. Springer US: Boston, MA, **1982**; pp 17-37.
6. Sigma-Aldrich, MSDS - Styrene.
7. Kolstad, H. A.; Juel, K.; Olsen, J.; Lynge, E., Exposure to styrene and chronic health effects: mortality and incidence of solid cancers in the Danish reinforced plastics industry. *Occup. Environ. Med.* **1995**, 52 (5), 320-327.
8. CLH Report for Styrene 100-42-5; Danish EPA: **2011**; pp 17-72.
9. Integrated Risk Information System. <http://www.epa.gov/iris/subst/0104.htm> (accessed 11th August 2016).
10. WHO, Some Traditional Herbal Medicines, Some Mycotoxins, Naphthalene, and Styrene. *IARC Monogr.* **2002**, 82.
11. In *Mosby's Medical Dictionary* 8th ed.; Elsevier: **2008**.
12. Glossary of Terms Used in Physical Chemistry. *Pure Appl. Chem.* **1994**, 66 (5), 1077-1184.
13. Matson, J. B.; Grubbs, R. H., Monotelechelic Poly(oxa)norbornenes by Ring-Opening Metathesis Polymerization using Direct End-Capping and Cross Metathesis. *Macromolecules* **2010**, 43 (1), 213-221.
14. Chiusoli, G. P.; Maitlis, P. M., *Metal-catalysis in Industrial Organic Processes*. RSC: **2008**.
15. Karl Ziegler. In *Encyclopaedia Britannica Online* [Online] **2013**. (accessed 7th May 2013).
16. Bradshaw, C. P. C.; Howman, E. J.; Turner, L., Olefin dismutation: Reactions of olefins on cobalt oxide-molybdenum oxide-alumina. *J. Catal.* **1967**, 7 (3), 269-276.
17. Lewandos, G. S.; Pettit, R., A Proposed Mechanism for the Metal-Catalysed Disproportionation Reaction of Olefins. *Tetrahedron Lett.* **1971**, 11, 789-793.
18. Chauvin, Y., Olefin Metathesis: The Early Days (Nobel Lecture). *Angew. Chem., Int. Ed.* **2006**, 45 (23), 3740-3747.
19. Grubbs, R. H.; Brunck, T. K., Possible intermediate in the tungsten-catalyzed olefin metathesis reaction. *J. Am. Chem. Soc.* **1972**, 94 (7), 2538-2540.
20. Grubbs, R. H.; Burk, P. L.; Carr, D. D., Mechanism of the olefin metathesis reaction. *J. Am. Chem. Soc.* **1975**, 97 (11), 3265-3267.

21. Grubbs, R. H.; Carr, D. D.; Hoppin, C.; Burk, P. L., Consideration of the mechanism of the metal catalyzed olefin metathesis reaction. *J. Am. Chem. Soc.* **1976**, *98* (12), 3478-3483.
22. Howard, T. R.; Lee, J. B.; Grubbs, R. H., Titanium metallocarbene-metallacyclobutane reactions: stepwise metathesis. *J. Am. Chem. Soc.* **1980**, *102* (22), 6876-6878.
23. Anderson, A. W.; Merckling, N. G. Polymeric bicyclo-(2,2,1)-2-heptene. US 2721189 A, **1955**.
24. Lane, P. C.; Tenney, L. P.; Benedikt, G. M.; Strichartz, P. T. Method for preparing cycloolefin copolymers with improved heat stability. US 4899005 A, **1990**.
25. Ludovice, P.; Ahmed, S.; Bidstrup, S. A.; Kohl, P., Stereochemical Structure-Property Relationships in Polynorbornene from Simulation. *Macromol. Symp.* **1998**, *133*, 1-10.
26. Nuyken, O.; Pask, S., Ring-Opening Polymerization—An Introductory Review. *Polymers* **2013**, *5* (2), 361.
27. Atkins, P.; Overton, T.; Rourke, J.; Weller, M.; Armstrong, F., *Inorganic Chemistry*. 4th ed.; Oxford University Press: Oxford, **2006**.
28. <http://chemlabs.princeton.edu/macmillan/wp-content/uploads/sites/6/WSJ-RCM.pdf> (accessed 16th February 2018).
29. Overberger, C. G., Copolymerization: 1. General remarks; 2. selective examples of copolymerizations. *J. Polym. Sci.: Polymer Symposia* **1985**, *72* (1), 67-69.
30. Cannizzo, L. F.; Grubbs, R. H., Block copolymers containing monodisperse segments produced by ring-opening metathesis of cyclic olefins. *Macromolecules* **1988**, *21* (7), 1961-1967.
31. Mayo, F. R.; Lewis, F. M., Copolymerization. I. A Basis for Comparing the Behavior of Monomers in Copolymerization; The Copolymerization of Styrene and Methyl Methacrylate. *J. Am. Chem. Soc.* **1944**, *66* (9), 1594-1601.
32. Nikovia, C.; Maroudas, A.-P.; Goulis, P.; Tzimis, D.; Paraskevopoulou, P.; Pitsikalis, M., Statistical Ring Opening Metathesis Copolymerization of Norbornene and Cyclopentene by Grubbs' 1st-Generation Catalyst *Molecules* **2015**, *20*, 15597-15615.
33. Rankin, D. A. The Design, Synthesis and Controlled Polymerization of Cationic and Zwitterionic Norbornene Derivatives. The University of Southern Mississippi, **2008**.
34. Monsaert, S.; Lozano Vila, A.; Drozdak, R.; Van Der Voort, P.; Verpoort, F., Latent olefin metathesis catalysts. *Chem. Soc. Rev.* **2009**, *38* (12), 3360-3372.
35. <http://willson.cm.utexas.edu/Teaching/Chem367L392N/Files/Metathesis%20Catalysis.pdf> (accessed 14th May 2013).
36. Casey, C. P.; Burkhardt, T. J., (Diphenylcarbene)pentacarbonyltungsten(0). *J. Am. Chem. Soc.* **1973**, *95* (17), 5833-5834.
37. Bielawski, C. W.; Grubbs, R. H., Living Ring-Opening Metathesis Polymerisation. *Prog. Polym. Sci.* **2007**, *32* (1), 1-29.
38. Straus, D. A.; Grubbs, R. H., Titanacyclobutanes: substitution pattern and stability. *Organometallics* **1982**, *1* (12), 1658-1661.
39. Schrock, R. R.; Fellmann, J. D., Multiple metal-carbon bonds. 8. Preparation, characterization, and mechanism of formation of the tantalum and niobium neopentylidene complexes,  $M(\text{CH}_2\text{CMe}_3)_3(\text{CHCMe}_3)$ . *J. Am. Chem. Soc.* **1978**, *100* (11), 3359-3370.

40. Basset, J.-M.; Lefebvre, F.; Leconte, M.; Pagano, S.; Mutch, A., Aryloxy complexes and cyclometallated aryloxy alkylidene complexes of tungsten (VI). Application to the metathesis of functionalized olefins *Polyhedron* **1995**, *14* (22), 3209-3226.
41. Schrock, R. R.; Murdzek, J. S.; Bazan, G. C.; Robbins, J.; DiMare, M.; O'Regan, M., Synthesis of molybdenum imido alkylidene complexes and some reactions involving acyclic olefins. *J. Am. Chem. Soc.* **1990**, *112* (10), 3875-3886.
42. Schrock, R. R.; Bazan, G. C.; Khosravi, E.; Feast, W. J.; Gibson, V. C., Living and highly stereoregular ring-opening polymerization of 5,6-difunctionalized norbornadienes by a well-characterized molybdenum catalyst. *Polym. Commun.* **1989**, *30*, 258-260.
43. Autenrieth, B.; Jeong, H.; Forrest, W. P.; Axtell, J. C.; Ota, A.; Lehr, T.; Buchmeiser, M. R.; Schrock, R. R., Stereospecific Ring-Opening Metathesis Polymerization (ROMP) of endo-Dicyclopentadiene by Molybdenum and Tungsten Catalysts. *Macromolecules* **2015**, *48* (8), 2480-2492.
44. Sanchez, E. M. S.; Zavaglia, C. A. C.; Felisberti, M. I., Unsaturated polyester resins: influence of the styrene concentration on the miscibility and mechanical properties. *Polymer* **2000**, *41*, 765-769.
45. Novak, B. M.; Grubbs, R. H., The ring opening metathesis polymerization of 7-oxabicyclo[2.2.1]hept-5-ene derivatives: a new acyclic polymeric ionophore. *J. Am. Chem. Soc.* **1988**, *110* (3), 960-961.
46. Nguyen, S. T.; Johnson, L. K.; Grubbs, R. H.; Ziller, J. W., Ring-opening metathesis polymerization (ROMP) of norbornene by a Group VIII carbene complex in protic media. *J. Am. Chem. Soc.* **1992**, *114* (10), 3974-3975.
47. Schwab, P.; France, M. B.; Ziller, J. W.; Grubbs, R. H., A Series of Well-Defined Metathesis Catalysts—Synthesis of  $[\text{RuCl}_2(=\text{CHR}')(\text{PR}_3)_2]$  and Its Reactions. *Angew. Chem., Int. Ed.* **1995**, *34* (18), 2039-2041.
48. Scholl, M.; Ding, S.; Lee, C. W.; Grubbs, R. H., Synthesis and Activity of a New Generation of Ruthenium-Based Olefin Metathesis Catalysts Coordinated with 1,3-Dimesityl-4,5-dihydroimidazol-2-ylidene Ligands. *Org. Lett.* **1999**, *1* (6), 953-956.
49. Sanford, M. S.; Love, J. A.; Grubbs, R. H., A Versatile Precursor for the Synthesis of New Ruthenium Olefin Metathesis Catalysts. *Organometallics* **2001**, *20* (25), 5314-5318.
50. Schrodi, J.; Pederson, R. L., Evolution and Applications of Second-Generation Ruthenium Olefin Metathesis Catalysts. *Aldrichimica Acta* **2007**, *40* (2), 45-52.
51. Love, J. A.; Morgan, J. P.; Trnka, T. M.; Grubbs, R. H., A Practical and Highly Active Ruthenium-Based Catalyst that Effects the Cross Metathesis of Acrylonitrile. *Angew. Chem., Int. Ed.* **2002**, *41* (21), 4035-4037.
52. Castarlenas, R.; Esteruelas, M. A.; Oñate, E., N-Heterocyclic Carbene–Osmium Complexes for Olefin Metathesis Reactions. *Organometallics* **2005**, *24* (18), 4343-4346.
53. Hans Wedepohl, K., The composition of the continental crust. *Geochim. Cosmochim. Acta* **1995**, *59* (7), 1217-1232.
54. Poater, A.; Pump, E.; Vummaleti, S. V. C.; Cavallo, L., The activation mechanism of Fe-based olefin metathesis catalysts. *Chem. Phys. Lett.* **2014**, *610–611*, 29-32.

55. Grubbs, R. H. In *Olefin Metathesis Catalysts for the Controlled Synthesis of Large and Small Molecules*, ISOM XXI, Graz, Austria, Graz, Austria, **2015**.
56. Ludwig, J. R.; Zimmerman, P. M.; Gianino, J. B.; Schindler, C. S., Iron(III)-catalysed carbonyl–olefin metathesis. *Nature* **2016**, 533, 374.
57. Jenkins, A. D.; Kratochvíl, P.; Stepto, R. F. T.; Suter, U. W., Glossary of basic terms in polymer science (IUPAC Recommendations 1996). In *Pure Appl. Chem.*, **1996**; Vol. 68, p 2287.
58. Webster, O. W., Living Polymerization Methods. *Science* **1991**, 251 (4996), 887-893.
59. Szwarc, M., 'Living' Polymers. *Nature* **1956**, 178 (4543), 1168-1169.
60. Boskaran, D.; Muller, A. H., Anionic Vinyl Polymerization. *Controlled and living polymerizations: From mechanisms to applications* **2009**.
61. Faust, R.; Kennedy, J. P., Living carbocationic polymerization. *Polym. Bull.* **1986**, 15 (4), 317-323.
62. Blencowe, A.; Qiao, G. G., Ring-Opening Metathesis Polymerization with the Second Generation Hoveyda–Grubbs Catalyst: An Efficient Approach toward High-Purity Functionalized Macrocyclic Oligo(cyclooctene)s. *J. Am. Chem. Soc.* **2013**, 135 (15), 5717-5725.
63. Grela, K., *Olefin Metathesis: Theory and Practice*. John Wiley & Sons: **2014**; p 132-133.
64. Chatterjee, A. K.; Choi, T.-L.; Sanders, D. P.; Grubbs, R. H., A General Model for Selectivity in Olefin Cross Metathesis. *J. Am. Chem. Soc.* **2003**, 125 (37), 11360-11370.
65. DOW, DCPD Specification Sheet.
66. Pybus, D., *The Chemistry of Fragrances*. 2nd ed.; **2006**; p 130.
67. Dholakiya, B., Unsaturated polyester resin for specialty applications. In *Polyester*, InTech: **2012**.
68. DOW, DCPD Product Data Sheet.
69. Anastas, P.; Warner, J., *Green Chemistry: Theory and Practice*. Oxford University Press: New York: **1998**.
70. Dichloro[1,3-bis(2,4,6-trimethylphenyl)-2-imidazolidinylidene][3-(2-pyridinyl)propylidene]ruthenium(II).  
<http://www.sigmaaldrich.com/catalog/product/aldrich/682381?lang=en&region=GB> (accessed 31st August 2016).
71. Ruthenium - biological information. <https://www.webelements.com/ruthenium/biology.html> (accessed 6th July 2017).
72. Dicyclopentadiene.  
<http://www.sigmaaldrich.com/catalog/product/aldrich/454338?lang=en&region=GB> (accessed 10th July 2017).
73. Madkour, A. E.; Koch, A. H. R.; Lienkamp, K.; Tew, G. N., End-functionalized ROMP polymers for Biomedical Applications. *Macromolecules* **2010**, 43 (10), 4557-4561.
74. Tomasek, J.; Schatz, J., Olefin metathesis in aqueous media. *Green Chem.* **2013**, 15 (9), 2317-2338.

75. Reactive Diluents.  
[http://www.adityabirlachemicals.com/products/epoxy\\_resins/reactive\\_diluents.html](http://www.adityabirlachemicals.com/products/epoxy_resins/reactive_diluents.html) (accessed 17th July 2017).
76. Sheldon, R. A., Organic synthesis - past, present and future. (advantages of incorporating catalysis to organic synthesis). *Chem. Ind. (London)* **1992**, 903-906.
77. Sheldon, R. A., The E Factor: fifteen years on. *Green Chem.* **2007**, 9 (12), 1273-1283.
78. Dynamic Mechanical Analysis (DMA): Frequently Asked Questions.  
[http://www.perkinelmer.co.uk/CMSResources/Images/44-74546GDE\\_IntroductionToDMA.pdf](http://www.perkinelmer.co.uk/CMSResources/Images/44-74546GDE_IntroductionToDMA.pdf)  
(accessed 16th August 2016).

## **Chapter 2. Synthesis of Norbornene-Functionalised Monomers and Pre-Polymers**



## 2.1 Introduction

Currently, unsaturated polyesters are cross-linked using divinyl benzene and styrene,<sup>1-3</sup> usually as an active diluent. But as mentioned previously, this is most certainly not ideal due to the health concerns associated with both molecules. In order to form a starting material suitable for ROMP, it must contain a strained olefinic moiety – or more than one if cross-linking is a desired outcome. First tested were dicyclopentadiene (DCPD) adducts with diacids, which could be formed as acids with a low  $pK_a$  and can add across the norbornene double bond in DCPD.<sup>4</sup> These adducts could be made into a polyester by reacting the free acid group with a glycol *via* a condensation reaction. This produced monomers with a terminal cyclopentene group as shown in Figure 2.1.

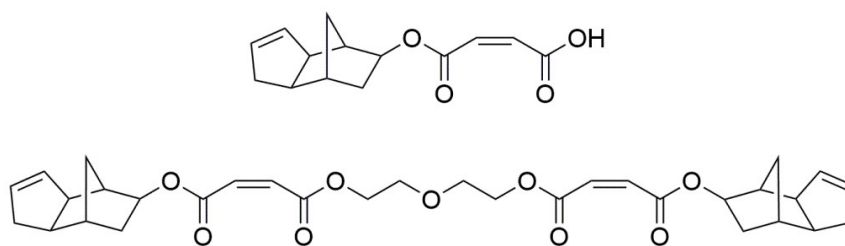
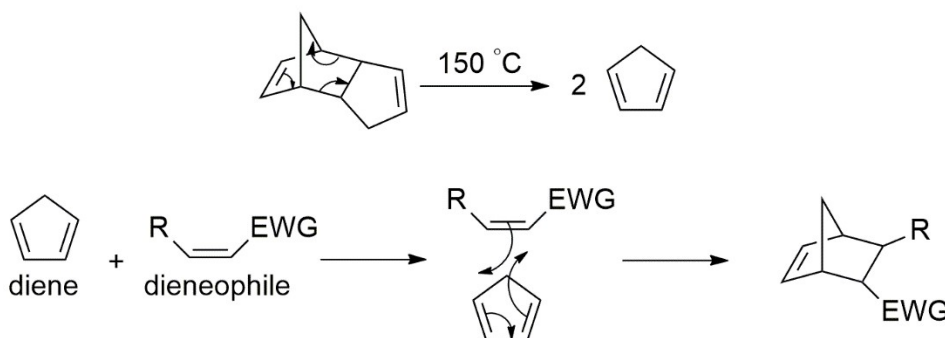


**Figure 2.1:** DCPD maleate (top) and DCPD maleate bis(diethylene glycol diester)

These molecules, due to the maleate unsaturation in the backbone, were still able to be cross-linked using styrene,<sup>5</sup> but it was hoped that the cyclopentene could undergo ROMP and form styrene free polymers. This did not work, however, as there was either: not enough ring strain in the cyclopentene (<6.8 kcal, *cf.* norbornene is 27 kcal),<sup>6</sup> or the maleate double bond was undergoing cross metathesis with the initiator and forming a non-metathesis active product.

It was then realised that norbornene functionality was a necessity. Adding the norbornene moiety can be achieved by cracking DCPD to form two cyclopentadiene molecules (CPD, diene) *via* a retro Diels-Alder reaction. CPD can then add *via* a Diels-Alder addition to electron deficient olefinic species (dienophiles), Scheme 2.1, to form the norbornene group.



**Scheme 2.1:** First step is the retro Diels-Alder to form the CPD.

Second step is the Diels-Alder reaction of CPD with dienophile, R could also be EWG

Ideal dienophiles would be those that can form polyesters, *i.e.* they must take the form of acids or alcohols. Maleic acid was identified as an ideal starting material due to its electron poor double bond,

and its stability at higher temperature that meant the cracking of the DCPD could occur *in situ*. Another species identified as a possibility were functionalised acrylates. These are, however, much more sensitive to temperature and can undergo thermal polymerisation.<sup>7</sup> 2-Hydroxyethyl acrylate was chosen as this was simple to functionalise with norbornene due to the electron poor double bond, but also contained a hydroxyl functionality – which was also easy to react.

This hydroxyl functionalised norbornene species means that norbornene-functionalised carbamates can be formed alongside the aforementioned polyester species, thus broadening the library of the monomers. There are a few commercially available hydroxyl functionalised norbornene-containing monomers,<sup>8-9</sup> but the cost of these tend to be prohibitive. However, the starting materials mentioned here (DCPD, acrylates and maleic anhydride) are all relatively cheap so this becomes a non-issue.

In summary, the main aims of this chapter were to synthesise and characterise several norbornene-functionalised monomers. These could include those with ester and carbamate functionalities to try and increase the range of properties achievable when the monomers are subjected to ROMP. These monomers are an attempt to achieve the overarching aim – discussed in Chapter 1 – of reducing, or even eliminating, styrene wherever possible.

## 2.2 Experimental

### 2.2.1 Materials for all work

Dicyclopentadiene (DCPD, 96 %), pyridine (99.8 %), 2-ethyl-1-hexylamine (98 %), ethyl vinyl ether (99 %), sodium chloride (>99 %), hydroquinone (>99 %), 1,6-hexamethylene diisocyanate (HDI, >99 %), *n*-butyl isocyanate (98 %), glacial acetic acid, styrene (>99 %), Grubbs 1<sup>st</sup> generation ruthenium initiator (G1, 97 %), Grubbs 2<sup>nd</sup> generation ruthenium initiator (G2), Modified Grubbs 2<sup>nd</sup> generation ruthenium initiator (MG2, dichloro(1,3-bis(2,4,6-trimethylphenyl)-2-imidazolidinylidene)(benzylidene)bis(3-bromopyridine)ruthenium(II)) and CDCl<sub>3</sub> were purchased from Sigma Aldrich and used without further purification. 2-Hydroxyethyl acrylate (HEA, 96 %) was purchased from Sigma Aldrich, and purified as detailed in 2.2.1.1 before use. Magnesium sulfate was purchased from VWR International. 5-Norbornene-2,3-dicarboxylic anhydride and 5-norbornene-2-methoxy tetraethylene glycol were previously synthesised in the laboratory. DCM, hexane, toluene and methanol analytical grade solvents were purchased from Fisher Scientific and used as supplied. Polyesters 1 and 2 were synthesised by Scott Bader Co. Ltd. and used without purification. *N*-(2-Ethylhexyl)-5-norbornene-2,3-dicarboximide (EHNBEDC, 99 %) was purchased from Bujno Synthesis (Poland), and used as supplied.

#### 2.2.1.1 Purification of 2-hydroxyethyl acrylate

Following the method of Leng *et al.*,<sup>10</sup> 2-hydroxyethyl acrylate (HEA, 60.0 mL, 60.7 g, 0.522 mol) was dissolved in water (300 mL). This was washed with hexane (10 × 40 mL) and the aqueous layer was treated with sodium chloride (72 g). The monomer was then extracted into diethyl ether (4 × 50 mL), and the organic layers were combined. Hydroquinone (30 mg, 0.05 wt%) was added to the ethereal

fractions, and was then dried over magnesium sulfate. The solution was filtered, and the ether removed under reduced pressure (~10 mbar, 35 °C) – leaving a colourless liquid (57.4 g, 94.6 %).

### 2.2.2 Instrumentation

$^1\text{H}$  and  $^{13}\text{C}$  Nuclear Magnetic Resonance (NMR) spectra were recorded using a Bruker Avance- 400, or Varian VNMRs 700 spectrometer operating at 400 and 700 MHz, respectively;  $J$  values given in Hz.  $\text{CDCl}_3$  was used as deuterated solvent for NMR spectroscopic analysis and the spectra were referenced to the solvent peak at 7.26 ppm for  $^1\text{H}$  NMR spectra, and 77.0 ppm for  $^{13}\text{C}$  NMR spectra. The following abbreviations are used in describing NMR spectra: s = singlet, d = doublet, t = triplet, sp = septet, m = multiplet, b = broad, w = weak, dd = doublet of doublets, dt = doublet of triplets. A  $^{13}\text{C}$  Distortion Enhancement by Polarisation Transfer (DEPT) NMR experiment was used to distinguish between  $-\text{C}-$ ,  $\text{CH}/\text{CH}_3$  and  $-\text{CH}_2$  carbon environments. The quaternary carbon environments do not appear in the DEPT spectrum,  $-\text{CH}_2$  carbon resonances are inverted, whilst  $-\text{CH}$  and  $-\text{CH}_3$  resonances remain the same as in the  $^{13}\text{C}$  NMR spectrum. 2D NMR spectroscopic experiments were also used to fully assign the proton and carbon environments in the products.  $^1\text{H}$ - $^1\text{H}$  Correlation Spectroscopy (COSY) demonstrated proton-proton correlations over two or three bonds.  $^1\text{H}$ - $^{13}\text{C}$  Heteronuclear Shift Correlation Spectroscopy (HSQC) demonstrated correlation between directly bonded proton and carbons atoms.

Molecular weight analysis of polymer molecules was obtained using size exclusion chromatography (SEC). The equipment utilised was a Viscotek TDA 302 using 2 × 300 mL PL gel 5  $\mu\text{m}$  mixed C columns and THF as the eluent (flow rate of 1 mL  $\text{min}^{-1}$ ) at 35 °C. Triple detection (refractive index (RI), viscosity and light scattering (LS) detectors) was used to determine molecular weights. The detectors were calibrated using narrow molecular weight distribution linear polystyrene as a standard. The SEC equipment was calibrated using polystyrene standards. Consequently, the molecular weight information determined directly using this method for polymers whose structure differ significantly from polystyrene (especially in terms of their hydrodynamic radius) will not correspond to the actual molecular weight of the polymers analysed herein. The polymers produced in this thesis have a saturated backbone and are not aromatic, which means that any results acquired in this work using SEC can only be used comparatively against one another and will not give accurate data regarding the actual length of the polymer chain. In order for this to be done, new narrow-dispersity standards, based upon polynorbornene, would have to be synthesised. Dispersity ( $\mathcal{D}$ ) was also calculated automatically using  $M_w/M_n$  or weight-averaged molecular weight divided by the number-averaged molecular weight. The samples were prepared by dissolving in THF for 24 h at a concentration of 1 mg of polymer per 1 mL of solvent. They were then passed through a microfilter to make sure there were no microscopic particles suspended in the solution.

Thermogravimetric analysis (TGA) was carried out using a Perkin Elmer Pyris 1 TGA under air with a sweep rate of 10 °C  $\text{min}^{-1}$ . The retro-Diels–Alder temperature ( $T_{\text{rDA}}$ ) is defined as when the mass of the sample decreases to 95 % of the original mass.

Elemental analysis of small molecules obtained using an Exeter CE-440 elemental analyser.

### 2.2.3 Synthesis of *N*-(2-ethylhexyl)-5-norbornene-2,3-dicarboximide (EHNBEDC)

The synthesis was based on a similar method to Khosravi *et al.*<sup>11</sup> *exo*-5-Norbornene-2,3-dicarboxylic anhydride (18.84 g, 114.5 mmol) was dissolved in glacial acetic acid (25 mL) and 2-ethyl-1-hexylamine (14.88 g, 11.74 mL, 115.1 mmol) was added. The mixture was stirred vigorously and heated, under reflux, to 120 °C for 2 h.

The reaction mixture was then poured into cold distilled water (100 mL) and the cloudy mixture was extracted into toluene (2 × 50 mL). The toluene was then washed with water (2 × 25 mL) and dried over magnesium sulfate. The mixture was filtered and dried under reduced pressure for 6 h, yielding a viscous yellow liquid (21.56 g, 68.4 %), which gave spectra that matched the literature. <sup>1</sup>H NMR (400 MHz; CDCl<sub>3</sub>): δ(ppm) = 0.75 (2 × t, 6 H, *J* = 7.6 Hz, 11, 13); 1.03 – 1.22 (m, 9 H, 4', 8, 9, 10, 12); 1.37 (dt, 1 H, *J*<sub>1</sub> = 10.0 Hz, *J*<sub>2</sub> = 1.6 Hz, 4''); 1.57 (sp, 1 H, *J* = 6.0 Hz, 7); 2.54 (s, 2 H, 3), 3.13 (s, 2 H, 2); 3.23 (d, 2 H, *J* = 7.6 Hz, 6); 6.16 (t, 2 H, *J* = 2.0 Hz, 1); <sup>13</sup>C NMR (101 MHz; CDCl<sub>3</sub>): δ(ppm) = 10.2 (13); 13.9 (11); 22.8 (10); 23.8 (9); 28.3 (8); 30.4 (12); 37.6 (7); 42.3 (6); 42.6 (4); 45.0 (2); 47.6 (3); 137.7 (1); 178.0 (5).

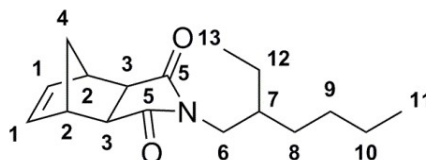


**Figure 2.2:** Numbered structure of *N*-(2-ethylhexyl)-5-norbornene-2,3-dicarboximide (EHNBEDC)

### 2.2.4 Characterisation of norbornene dicarboxylate diethylene glycol phthalic acid polyester (Polyester 1)

Polyester 1 was synthesised and supplied by Scott Bader Company Ltd. Polyester 1 was calculated to have approximately 2.4 mmol of norbornene functionality per gram. The COSY spectrum was complicated, so the NMR spectra of the monomers dimethyl-5-norbornene-2,3-dicarboxylate,<sup>12</sup> diethylene glycol monomethyl ether, and diethylene phthalate were used to identify the most important peaks initially. Then using these, the COSY spectrum could confirm their assignments. <sup>1</sup>H NMR (700 MHz; CDCl<sub>3</sub>): 1.21-1.63 (m, 2 H, 8), 2.71-3.40 (m, 2 H, 3, 6); 3.28-3.40 (m, 2 H, 2, 7); 3.51-4.02 (m, 9 H, 11, 12); 4.22-4.51 (m, 6 H, 10, 13); 5.88-6.29 (m, 2 H, 4, 5); 7.50-7.56 (m, 1 H, 17, 18); 7.70-7.76 (m, 1 H, 16, 19). SEC: *M*<sub>n</sub> = 2.2 × 10<sup>3</sup> g mol<sup>-1</sup>, *M*<sub>w</sub> = 8.8 × 10<sup>3</sup> g mol<sup>-1</sup>, Đ = 3.9. TGA: T<sub>TD</sub> = 250 °C.

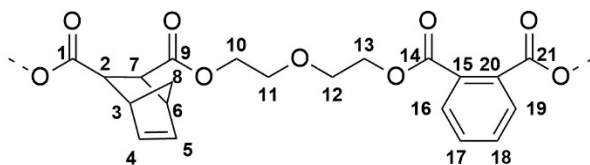


**Figure 2.3:** An example fragment of Polyester 1

### 2.2.5 Characterisation of norbornene dicarboxylate propylene glycol polyester (Polyester 2)

Polyester 2 was synthesised and supplied by Scott Bader Company Ltd. Polyester 2 was calculated to have approximately 4.0 mmol(NBE) g<sup>-1</sup>. Again, since the COSY spectrum was complex, the spectra of the monomers dimethyl-5-norbornene-2,3-dicarboxylate<sup>12</sup> and 1,2-propane diol (propylene glycol) were used to elucidate the main peaks, and the COSY spectrum confirmed the assignments. <sup>1</sup>H NMR (700 MHz; CDCl<sub>3</sub>): 0.78-0.88 (m, 0.3 H,  $\delta_{exo}$ ); 1.09-1.35 (m, 3.6 H,  $\delta_{exo}$ , 12); 1.45 (s, 0.7 H, 8); 1.59 (s, 0.7 H, 8); 1.88-2.03 (m, 0.3 H,  $2_{exo}$ ,  $7_{exo}$ ); 2.07-2.27 (m, 0.3 H,  $3_{exo}$ ,  $6_{exo}$ ); 2.34-2.57 (m, 0.3 H,  $2_{exo}$ ,  $7_{exo}$ ); 2.57-2.77 (m, 0.7 H, 2, 7); 2.77-2.95 (m, 0.3 H,  $3_{exo}$ ,  $6_{exo}$ ); 3.10 (s, 0.7 H, 3, 6); 3.25 (s, 0.7 H, 3, 6); 3.38 (s, br, 0.7 H, 2, 7); 3.83-4.86 (m, 2.2 H, 10); 4.67-5.23 (m, 1.1 H, 11); 5.89-6.32 (m, 2 H, 4, 5); SEC:  $M_n = 2.4 \times 10^3$  g mol<sup>-1</sup>,  $M_w = 41 \times 10^3$  g mol<sup>-1</sup>,  $\bar{D} = 17$ . TGA:  $T_{rDA} = 281$  °C.

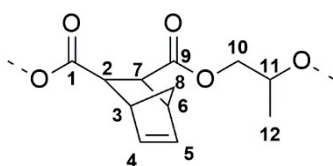


Figure 2.4: An example fragment of Polyester 2

### 2.2.6 Synthesis of hexamethylene-1,6-bis(5-norbornene-2-methoxy tetraethylene glycol carbamate) (DFM1)

Under nitrogen, 5-norbornene-2-methoxy tetraethylene glycol (1.00 g, 3.33 mmol) and HDI (0.21 mL, 280 mg, 1.66 mmol) were stirred at 80 °C for 4 h. The product was analysed by FT-IR, and showed no sign of the isocyanate at 2250 cm<sup>-1</sup>. The temperature was increased to 50 °C for 10 h under reduced pressure (<1 mbar) to remove excess starting materials. When the product cooled it formed a viscous, almost colourless liquid (1.28 g, >99 %). <sup>1</sup>H NMR (700 MHz; CDCl<sub>3</sub>):  $\delta$ (ppm) = 1.03-1.33 (overlapping peaks, 12 H, 3, 5, 10); 1.43-1.49 (m, 4 H, 9); 1.64-1.70 (m, 2 H, 4); 2.72 (s, 2 H, 2''); 2.77 (s, 2 H, 2'); 3.07-3.16 (m, 4 H, 8); 3.25-3.38 & 3.45-3.54 (m, 4 H, 6); 3.54-3.76 (m, 32 H, 7); 4.15-4.31 (m, 4 H, 7 next to urethane); 4.81-5.00 (m, br, NH); 5.89-6.18 (m, 4 H, 1). <sup>13</sup>C NMR (176 MHz; CDCl<sub>3</sub>):  $\delta$ (ppm) = 26.4 (10); 29.8 (5); 29.9 (9); 38.9 (4); 40.9 (8); 41.6 (2'); 43.7 (2''); 45.1 (3); 61.8, 63.9, 69.8, 70.3, 70.4, 70.7, 70.7, 72.6 (all 7); 76.1 (6); 136.6 (1); 156.5 (11). IR (cm<sup>-1</sup>) = 1543 (N-H urethane bend); 1720 (C=O urethane); 2750-3000 (olefinic C-H stretch); 3250-3690 (NH urethane stretch). TGA:  $T_{rDA} = 199$  °C. CHN: Expected: %C = 58.16, %H = 8.31, %N = 4.67; Measured: %C = 62.48, %H = 8.91, %N = 3.64.

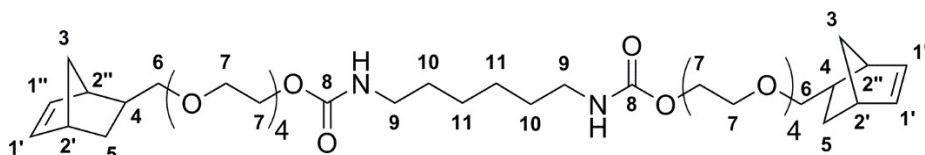


Figure 2.5: Numbered structure of DFM1

### 2.2.7 Synthesis of 2-hydroxyethyl-5-norbornene-2-carboxylate (HE-NBE-CO<sub>2</sub>)

Under nitrogen, DCPD (10.5 g, 0.159 mol) was cracked into CPD at 170 °C and distilled into a second flask containing purified HEA (25 mL, 25.1 g, 0.218 mol) dissolved in DCM (50 mL). The reaction was left for 6 h, after which the DCM containing flask had turned faintly yellow. DCM was subsequently distilled off at room temperature under reduced pressure (<1 mbar), before the temperature was increased to 50 °C for 10 h to remove excess HEA and DCPD, yielding a pale yellow liquid (27.7 g, 70 %). MS: *m/z* ASAP *M*+*H*<sup>+</sup> = 183 Da (HE-NBE-CO<sub>2</sub>). <sup>1</sup>H NMR (700 MHz; CDCl<sub>3</sub>): δ(ppm) = 1.25-1.31 (m, 0.8 H, 3); 1.35-1.46 (m, 2.0 H, 3, 3<sub>exo</sub>, 5, 5<sub>exo</sub>); 1.50-1.55 (m, 0.2 H, 3<sub>exo</sub>); 1.88-1.95 (m, 1 H, 6); 1.95-2.20 (s, br, 1 H, OH); 2.24-2.29 (m, 0.2 H, 4<sub>exo</sub>); 2.88-2.94 (br, overlapping signals, 2', 2'<sub>exo</sub>); 2.96-3.01 (m, 0.8 H, 4); 3.05 (s, 0.2 H, 2''<sub>exo</sub>); 3.22 (s, 0.8 H, 2''); 3.56-3.89 (m, 2 H, 10); 4.04-4.33 (m, 2 H, 9); 5.91-5.95 (m, 0.8 H, 1''); 6.09-6.15 (m, 0.4 H, 1<sub>exo</sub>); 6.17-6.21 (m, 0.8 H, 1'). <sup>13</sup>C NMR (176 MHz; CDCl<sub>3</sub>): δ(ppm) = 29.4 (7), 30.5 (7<sub>exo</sub>), 41.7 (2'<sub>exo</sub>), 42.6 (2'), 43.2 (4<sub>exo</sub>), 43.4 (4), 45.9 (2''), 46.4 (3<sub>exo</sub>), 46.8 (2''<sub>exo</sub>), 49.8 (3), 61.4 (10<sub>exo</sub>), 61.4 (10), 66.0 (9), 66.2 (9<sub>exo</sub>), 132.3 (1''), 135.8 (1'<sub>exo</sub>), 138.0 (1'), 138.2 (1'<sub>exo</sub>), 175.3 (8), 176.8 (8). Smaller peaks can also be seen which are attributed to the carboxylate on C<sub>7</sub>. IR (cm<sup>-1</sup>) = 1718 (ester C=O stretch); 2790-3030 (olefinic C-H stretch); 3160-3620 (O-H stretch). TGA: T<sub>rDA</sub> = 113 °C. CHN: Expected: %C = 65.91, %H = 7.74, %N = 0.00; Measured: %C = 65.05, %H = 7.71, %N = -0.12.

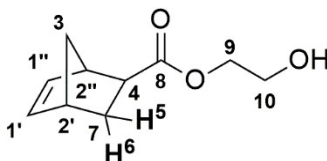


Figure 2.6: Numbered structure of HE-NBE-CO<sub>2</sub>

### 2.2.8 Synthesis of hexamethylene-1,6-bis(5-norbornene-2-carboxylate-2-ethoxy carbamate) (DFM2)

2-hydroxyethyl-5-norbornene-2-carboxylate (3.30 mL, 4.00 g, 0.022 mol) was stirred under nitrogen at 80 °C, HDI (1.76 mL, 1.85 g, 0.011 mol) was added and stirred for 3 h. The mixture increased markedly in viscosity and formed a white solid when cooled to room temperature. The product was then heated to 125 °C under reduced pressure (<1 mbar) for 6 h to remove any starting materials. This yielded an almost colourless, viscous liquid (5.67 g, 98.4 %). MS: *m/z* ASAP *M*+*H*<sup>+</sup> = 533 Da (DFM2). <sup>1</sup>H NMR (700 MHz; CDCl<sub>3</sub>): δ(ppm) = 1.18-1.59 (multiple peaks, 14 H, 3, 3<sub>exo</sub>, 5, 6, 13, 14); 1.82-1.95 (m, 2 H, 6, 6<sub>exo</sub>); 2.22-2.27 (m, 0.4 H, 4<sub>exo</sub>); 2.83-3.54 (multiple peaks, 9.6 H, 2', 2'', 2'<sub>exo</sub>, 2''<sub>exo</sub>, 4, 12); 3.58-4.37 (multiple peaks, 8 H, 9, 10); 4.58 (s, br, 0.4 H, NH<sub>exo</sub>); 4.76 (s, br, 1.6 H, NH); 5.87-5.95 (m, 1.6 H, 1''); 6.06-6.16 (m, 0.8 H, 1<sub>exo</sub>); 6.16-6.24 (m, 1.6 H, 1'). <sup>13</sup>C NMR (176 MHz; CDCl<sub>3</sub>): δ(ppm) = 26.4 (14); 29.4 (7); 30.0 (13); 30.5 (7<sub>exo</sub>); 41.0 (12); 41.8 (2'<sub>exo</sub>); 42.7 (2'); 43.2 (4<sub>exo</sub>); 43.3 (4); 45.9 (2''); 46.5 (3<sub>exo</sub>); 46.8 (2''<sub>exo</sub>); 49.7 (3); 62.5 & 62.8 (9, 10); 132.4 (1''); 135.8 (1'<sub>exo</sub>); 138.0 (1'); 138.3 (1''<sub>exo</sub>); 156.3 (11); 174.6 (8); 176.2 (8<sub>exo</sub>). Smaller peaks can also be seen which are attributed to the carboxylate on C<sub>7</sub>. IR (cm<sup>-1</sup>) = 1524 (N-H urethane bend); 1698 & 1714 (C=O stretch, ester and urethane); 2810-3035 (olefinic C-H stretch); 3235-3450 (N-H urethane stretch). TGA T<sub>rDA</sub> =

249 °C. CHN: Expected: %C = 63.14, %H = 7.57, %N = 5.26; Measured: %C = 62.79, %H = 7.64, %N = 5.72.

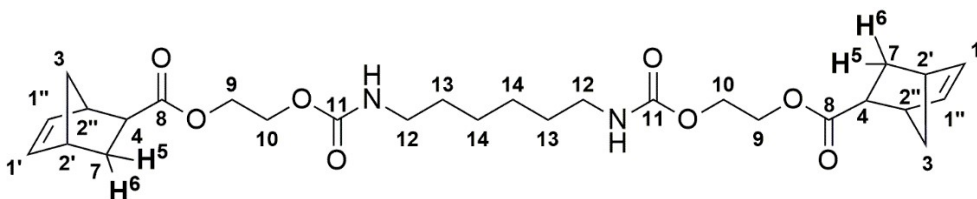


Figure 2.7: Numbered structure of DFM2

## 2.2.9 Synthesis of 2-hydroxyethyl-5-norbornene-2-carboxylate butyl carbamate (MFM)

2-hydroxyethyl-5-norbornene-2-carboxylate (3.30 mL, 4.00 g, 0.022 mmol) was stirred under nitrogen at 60 °C, *n*-butyl isocyanate (2.48 mL, 2.18 g, 0.011 mmol) was added and stirred for 4 h. The mixture increased slightly in viscosity and formed a light orange liquid when cooled to room temperature. The product was then heated to 135 °C under reduced pressure (<1 mbar) for 18 h to remove any starting materials. This yielded a yellowish liquid (5.98 g, 96.8 %). <sup>1</sup>H NMR (700 MHz; CDCl<sub>3</sub>): δ(ppm) = 0.91 (t, *J* = 7.4 Hz, 15); 1.22-1.51 (multiple peaks, 7 H, 3, 5, 13, 14); 1.86-1.93 (m, 1 H, 6); 2.22-2.27 (m, 0.2 H, 4<sub>exo</sub>); 2.87-2.92 (m, 1 H, 2', 2'<sub>exo</sub>); 2.93-3.00 (m, 0.8 H, 4); 3.03 (s, 0.2 H, 2''<sub>exo</sub>); 3.08-3.30 (m, 2.8 H, 2'', 12); 3.40-3.88 & 4.11-4.36 (multiple peaks, 4 H, 9, 10); 4.57 (s, br, 0.2 H, *NH*<sub>exo</sub>); 4.74 (s, br, 0.8 H, *NH*); 5.89-5.94 (m, 0.8 H, 1''); 6.08-6.14 (m, 0.4 H, 1<sub>exo</sub>); 6.15-6.20 (m, 0.8 H, 1'). <sup>13</sup>C NMR (176 MHz; CDCl<sub>3</sub>): δ(ppm) = 13.8 (15); 13.9 (15<sub>exo</sub>); 20.0 (14); 29.4 (7); 30.4 (7<sub>exo</sub>); 32.1 (13); 40.9 (12); 41.8 (2'<sub>exo</sub>); 42.7 (2'); 43.3 (4); 45.8 (2''); 49.7 (3); 61.5, 62.5, 62.7 & 66.0 (9, 10); 132.4 (1''); 135.8 (1<sub>exo</sub>); 137.9 (1'); 138.2 (1<sub>exo</sub>); 156.2 (11); 174.6 (8); 176.1(8<sub>exo</sub>). Smaller peaks can also be seen that are attributed to the carboxylate on C7. IR (cm<sup>-1</sup>) = 1538 (N-H urethane bend); 1625-1795 (C=O stretch, ester and urethane); 2830-3080 (olefinic C-H stretch); 3250-3500 (N-H urethane stretch). TGA: T<sub>IDA</sub> = 167 °C. CHN: Expected: %C = 64.04, %H = 8.24, %N = 4.98; Measured: %C = 63.89, %H = 8.18, %N = 4.00.

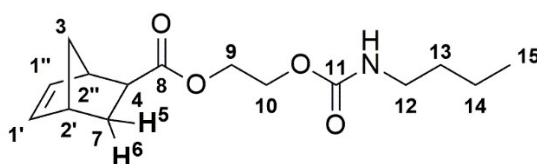
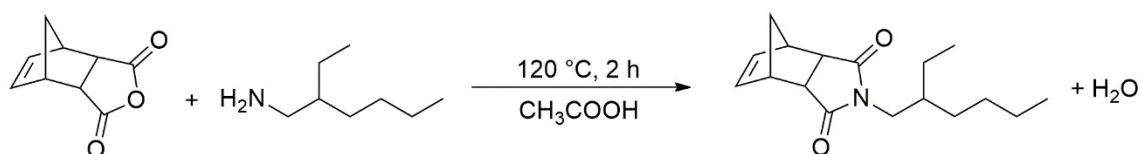


Figure 2.8: Numbered structure of MFM

## 2.3 Results and Discussion

### 2.3.1 Synthesis of *N*-(2-Ethylhexyl)-5-norbornene-2,3-dicarboximide

The monomer, *N*-(2-ethylhexyl)-5-norbornene-2,3-dicarboximide, was prepared by the reaction of *exo*-5-norbornene-2,3-dicarboximide with 2-ethyl-1-hexyl amine (Equation 2.1).



**Equation 2.1:** Synthesis of *N*-(2-ethylhexyl)-5-norbornene-2,3-dicarboximide (EHNBEDC)

Since the 5-norbornene-2,3-dicarboxylic anhydride was 100 % *exo*, and since the reaction to form this molecule does not cause an inversion of symmetry or a racemisation, the product was also found to be *exo*. This can be seen by the fact that there is only one triplet at 6.16 ppm associated with the olefinic, norbornene protons. There are also no broad peaks at around 2 ppm – which are symptomatic of NH protons from the starting material – in the  $^1\text{H}$  NMR spectrum, suggesting the absence of unreacted 2-ethyl-1-hexylamine. The integrations of the  $^1\text{H}$  NMR spectrum confirmed the structure.

The *exo* isomer has been found to be more reactive in the ROMP reactions compared to the *endo* form.<sup>13</sup> This is especially important when used in conjunction with ruthenium G1 which has lower activity than ruthenium G2 and ruthenium MG2. EHNBEDC is also one of a few norbornene-containing species that is liquid at room temperature – which makes it useful as a reactive diluent in bulk copolymerisations.

The E-factor of this reaction was calculated, Table 2.1, as one of the aims of this project was to be as environmentally friendly as possible. The value obtained was around 12.8 which compares to the fine chemicals industry,<sup>14</sup> though this was obviously on a much smaller scale.

**Table 2.1:** A table detailing the calculation of the E-factor for this reaction, (waste = total mass in – product)

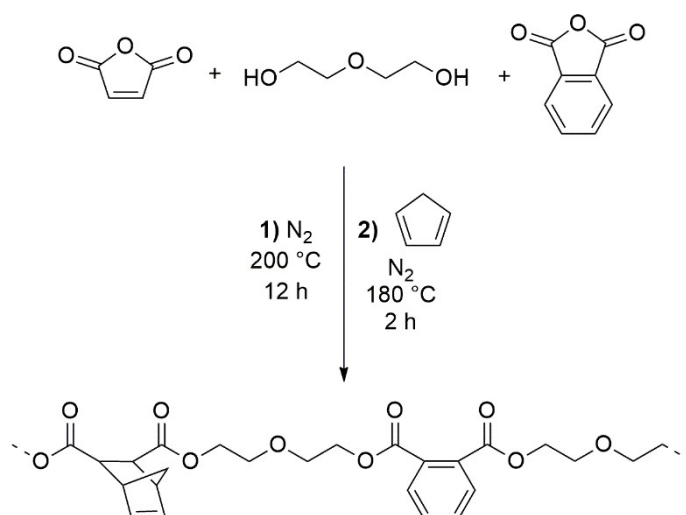
	Volume (mL)	Mass (g)
norbornene dicarboxylic anhydride		18.84
glacial acetic acid	25.00	26.25
ethyl hexylamine	11.74	14.88
water	150.00	150.00
toluene	100.00	87.00
product produced		21.56
waste produced		275.41
<b>E-factor = 12.77</b>		



The actual E-factor for this reaction will actually be slightly higher as the mass of magnesium sulfate added to dry the sample was not recorded – but the magnesium sulfate was simply added to excess.

### 2.3.2 Characterisation of norbornene dicarboxylate diethylene glycol phthalic acid polyester (Polyester 1)

Polyester 1 was synthesised at Scott Bader Company Ltd. by a condensation reaction of 5-norbornene-2,3-dicarboxylic acid, diethylene glycol and phthalic acid (Equation 2.2).



**Equation 2.2:** Synthesis of Polyester 1

Polyester 1's dispersity, calculated using  $M_w/M_n$  from the SEC, is broad ( $\bar{D} = 3.9$ ). This is however not unexpected, since the condensation reaction is uncontrolled and step growth which can have a dispersity well in excess of 2,<sup>15</sup> but here the breadth of said dispersity is unimportant. The NMR spectra produced are broad and also complex. It was therefore decided to characterise Polyester 1 by first using NMR spectra of similar smaller molecules. This worked well, but imperfectly. The molecules chosen were dimethyl-5-norbornene-2,3-dicarboxylate (which gives the norbornene ring in a similar environment to Polyester 1), diethylene glycol monomethyl ether (very similar to DEG), and diethyl phthalate (in order to show approximate environments of the aromatic protons). Arguably the easiest protons to identify are the aromatic protons from phthalic anhydride – these are particularly facile to see due to their characteristic high frequency chemical shift and are the only peaks more highly shifted than the solvent (deuterated chloroform, CDCl<sub>3</sub>), as can be seen in Figure 2.9. This is also characteristic of aromatic protons on a benzene ring system. The only peaks in this area which could not be identified fully are the small, narrow peaks on the shoulders of the main peaks in the aromatic region which could possibly be due to protons at the chain end. This was however not confirmed within this work.

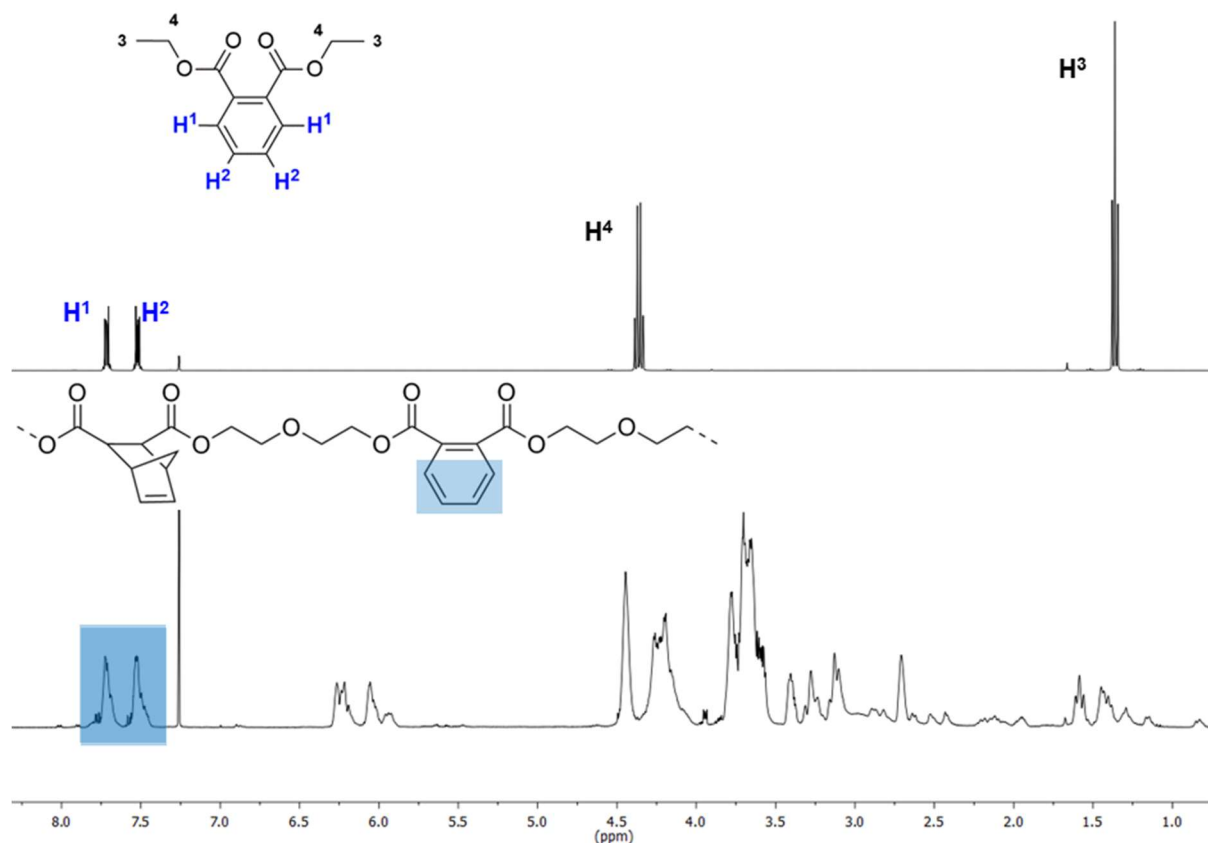


**Figure 2.9:**  $^1\text{H}$  NMR (700 MHz,  $\text{CDCl}_3$ ) spectra showing the identification of the aromatic protons in Polyester 1 (blue) using diethyl phthalate as a reference

The next identifiable peaks are the ones between 5.6 and 6.4 ppm (Figure 2.10). These are indicative of olefinic norbornene protons and are the evidence that a substance contains this functionality – and is therefore extremely important in making ROMP-active polyesters. Due to the broad dispersity of this molecule, and *exo/endo* isomerisation, this leads to many peaks when the idealised molecule has only one or two. There is also a possibility that some chains may contain no norbornene functionality, or many, and the same for the aromatic moiety. Some of the extra peaks could also be chain ends, which could be alcohol or acid groups – another option is that any acid groups could react with the norbornene functionality of DCPD<sup>16</sup> to form an adduct leaving cyclopentene as an end group. The olefinic protons of which would also show up around 5.5 ppm, and there is a little noise here that suggests that this may have occurred to some degree.

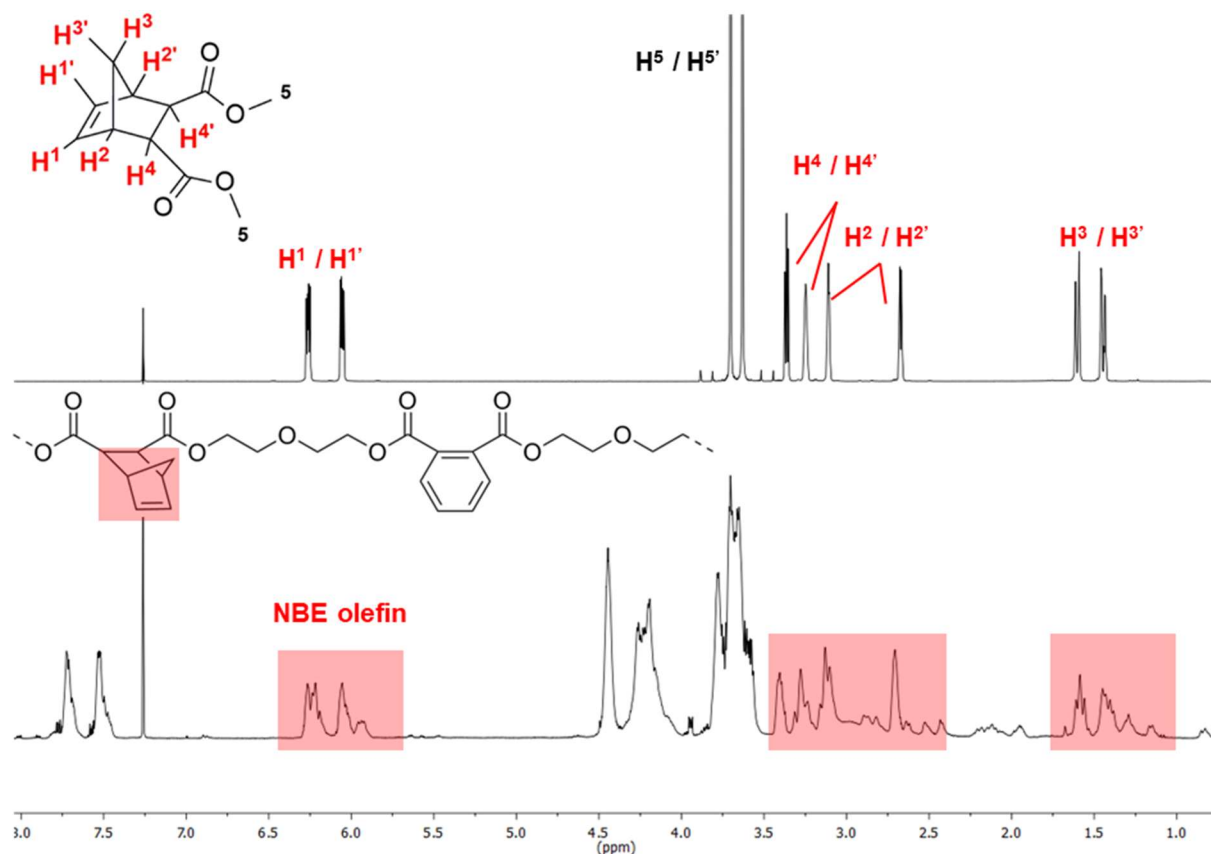


**Figure 2.10:** <sup>1</sup>H NMR (700 MHz, CDCl<sub>3</sub>) spectra highlighting the identification the norbornene ring in Polyester 1 using dimethyl-5-norbornene-2,3-dicarboxylate as the comparable small molecule

The final part to identify is between 3.5 and 4.5 ppm. This is the region of the glycol (Figure 2.11), and the glycol ester protons – these do not appear in the DEG starting material and are as a result of combining with the acid group from phthalic or maleic acid. The formation of these peaks is another piece of evidence to show the successful synthesis of Polyester 1. The region from 3.5 to 4.5 ppm is complex, because the proton environments near the ester groups depend on the acid that reacts with either end of the DEG. The acids could be the same, different, or even non-existent if the glycol is the terminal group. The DEG in the backbone of Polyester 1 makes the polymer quite flexible and results in a very viscous, ‘sticky’ material, which makes handling Polyester 1 somewhat difficult as it tends to adhere to many surfaces.

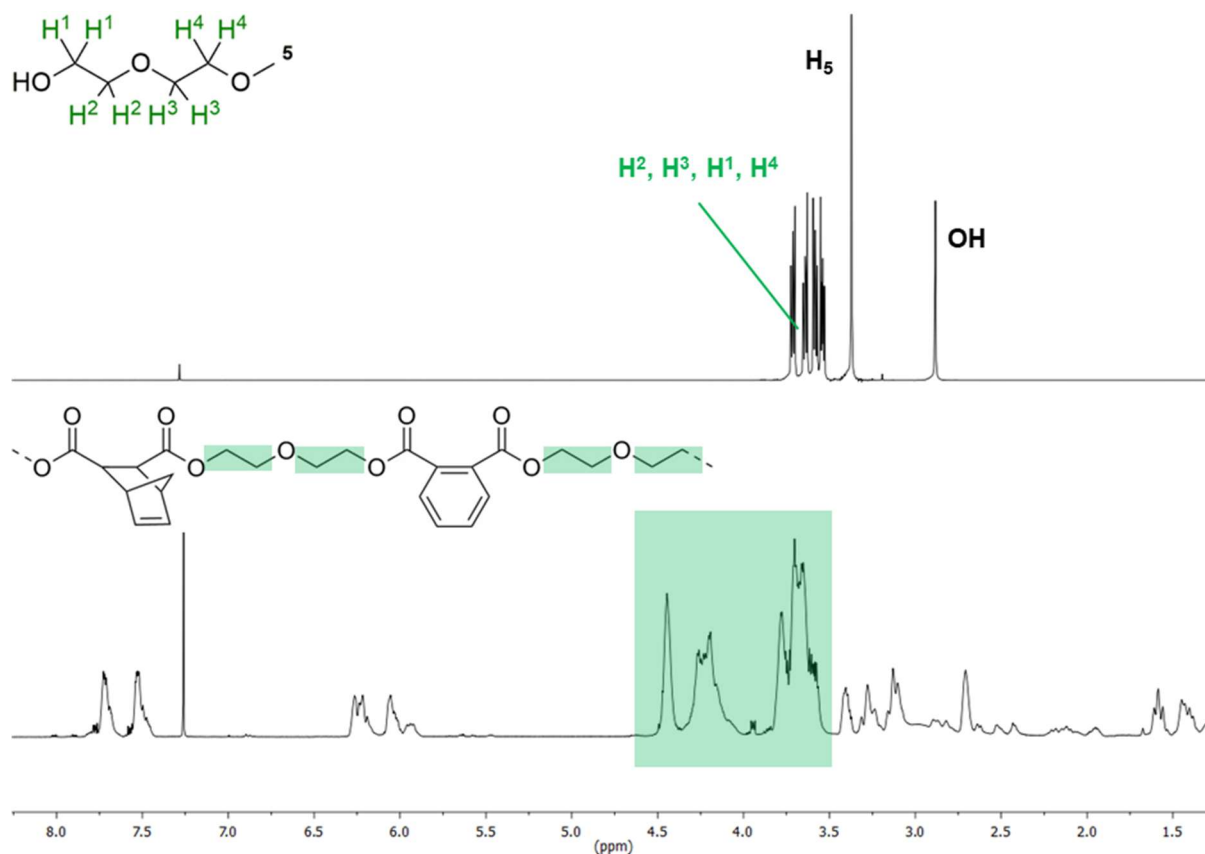
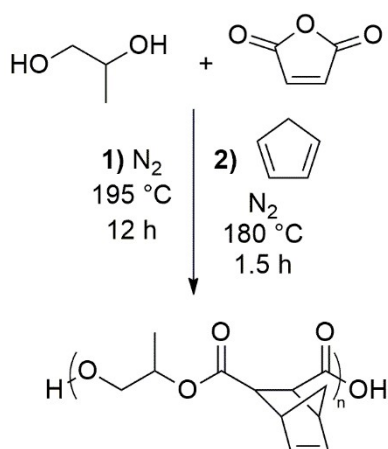


**Figure 2.11:**  $^1\text{H}$  NMR (700 MHz,  $\text{CDCl}_3$ ) spectra highlighting the identification the ether portion of Polyester 1 using diethylene glycol monomethyl ether as the comparable small molecule

### 2.3.3 Characterisation of norbornene dicarboxylate propylene glycol polyester (Polyester 2)

Polyester 2 was synthesised at Scott Bader Company Ltd. by a condensation reaction of propylene glycol and 5-norbornene-2,3-dicarboxylic acid (Equation 2.3).



**Equation 2.3:** Synthesis of Polyester 2

Polyester 2 has a much broader dispersity than Polyester 1 ( $\bar{D}_{PE2} = 17$  compared with  $\bar{D}_{PE1} = 3.9$ ), that could be due to the stiffer glycol in Polyester 2 leading to a more viscous reaction mixture which could lead to more inefficient mixing. Again, due to the step-growth condensation reactions used to produce Polyester 2, such a broad dispersity was not wholly unexpected. Since the dispersity here was so broad, this made the NMR spectroscopic analysis even more problematic – but dimethyl-5-norbornene-2,3-dicarboxylate and propylene glycol (1,2-propane diol) were compared to the spectrum in an attempt to resolve the structure as well as possible.

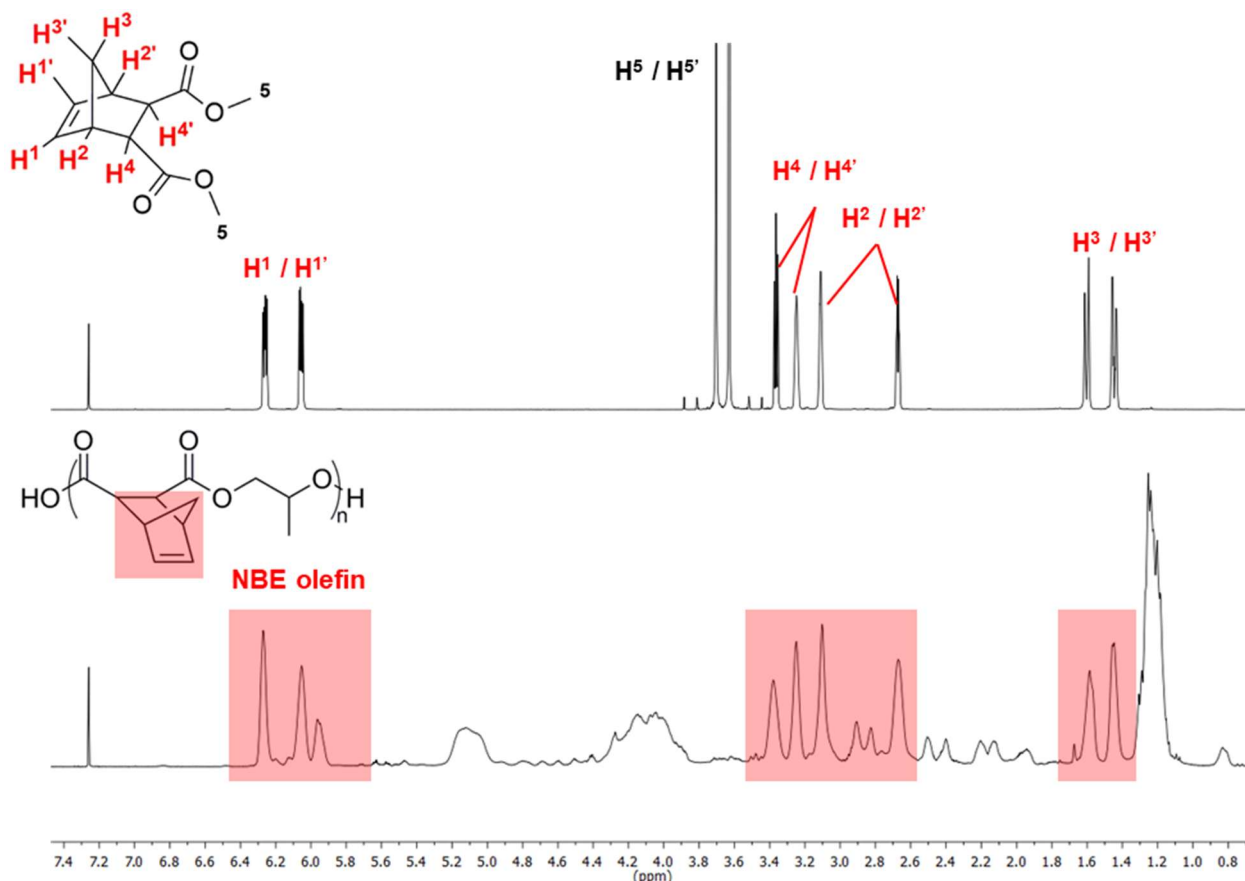


**Figure 2.12:**  $^1\text{H}$  NMR (700 MHz,  $\text{CDCl}_3$ ) spectra highlighting the identification the norbornene ring in Polyester 2 using dimethyl-5-norbornene-2,3-dicarboxylate as the comparable small molecule

The data in Figure 2.12 shows that the incorporation of the norbornene moiety has been successful into Polyester 2. This means that Polyester 2 should be able to undergo ROMP and, if it contains on average 2 or more norbornene groups in the backbone, should form a cross-linked network. Again, as in Polyester 1, a small amount of cyclopentene protons can be seen in the region around 5.5 ppm. It is known for cyclopentene to ring open with ruthenium initiators,<sup>17</sup> but the strain in this cyclic olefin is much lower than norbornene (28.5 *versus* 113.8  $\text{kJ mol}^{-1}$ , respectively).<sup>18</sup>

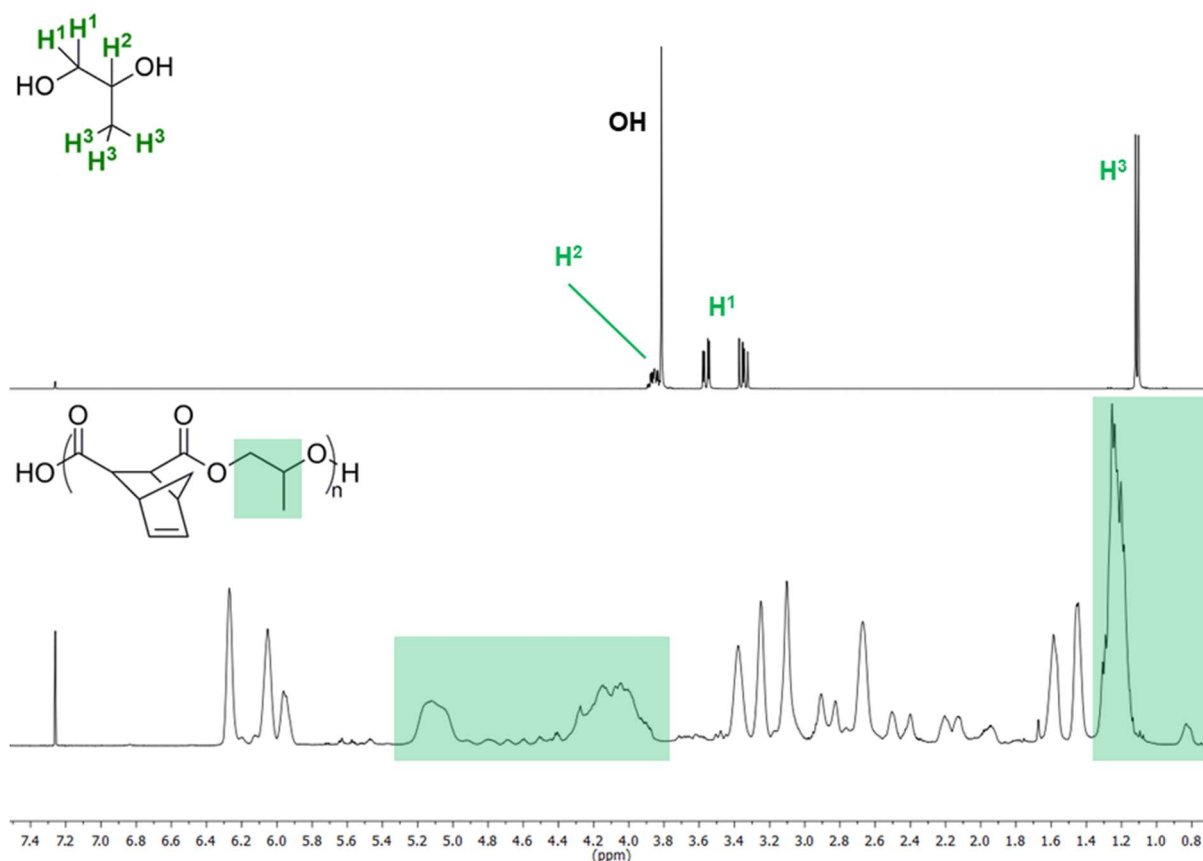


**Figure 2.13:**  $^1\text{H}$  NMR (700 MHz,  $\text{CDCl}_3$ ) spectra highlighting the identification the glycol protons in Polyester 2 using propylene glycol for reference

As seen in Figure 2.13, the protons next to the hydroxyl group in the glycol starting material also appear in Polyester 2. They have a higher shift in the product however (3.8 – 5.2 ppm in Polyester 2 *versus* 3.2 – 3.8 ppm in propylene glycol) due to being adjacent to ester groups. This indicates that the glycol has successfully reacted with the acid groups from maleic acid. There are many proton environments in Polyester 2 despite it looking simple at first glance for two reasons: the norbornene ring system can be *endo* or *exo*; and the glycol is a racemic mixture of R and S since the carbon with the methyl group attached is a chiral centre.

### 2.3.4 Correlation Spectroscopy of Norbornene-Functionalised Polyesters 1 and 2

In order to confirm the structures shown of Polyesters 1 and 2, and their assignment,  $^1\text{H}$ - $^1\text{H}$  Correlation Spectroscopy (COSY) was carried out. This was made difficult due to the broad dispersities of each, but helped confirm what was shown in 2.3.2 and 2.3.3 (*i.e.* the assignments of protons given to each of the polyesters). Figure 2.14 shows the COSY of Polyester 1. Firstly from box A, it can be seen the aromatic protons between 7.3 and 7.9 ppm only couple to each other which is quite obvious and – as mentioned previously – their characteristic high frequency chemical shift makes them extremely clear to see. Region B shows the olefinic protons on the norbornene moiety correlating to the other protons in the bicyclic system. The purple box, C, shows the protons originally associated with DEG – but now  $\text{H}^{10}$  and  $\text{H}^{11}$  are in the ester region, but still correlate to  $\text{H}^{11}$  and  $\text{H}^{12}$  in

the ether region. This is arguably one of the strongest pieces of evidence from this spectrum to prove the polyester has formed.

Polyester 2's COSY spectrum is slightly simpler due to the utilisation of only one acid in its synthesis. It does however have a much broader dispersity which complicates the analysis slightly by also broadening the spectrum and weakening correlations between protons, but assignments were still able to be made. Box E highlights the correlations of the norbornene vinylic protons ( $H^4$  and  $H^5$ ) with  $H^3$  and  $H^6$  also in the ring, and also gives insight into the *exo* : *endo* ratio which is approximately 1 : 3. Figure 2.15 also shows a small amount of cyclopentene functionality in Polyester 2 too, this is again much more difficult to make undergo ROMP than the norbornene moiety – of which, fortunately, there is far more. Region F highlights the  $^1H$ - $^1H$  coupling between the protons in the glycol portion of the polyester. The fact that the methyl group (atom numbered 12 in Figure 2.15) couples with the peaks at 5.2 and 4.0 ppm further proves that the esterification of the glycol has occurred since these shifts are far higher – as previously discussed – than in propylene glycol. The correlations highlighted in region G show the protons on the bridging carbon of norbornene linking to those on the adjacent carbons, further confirming the norbornene bicyclic ring is part of Polyester 2. Finally, area H shows that the extremely low shifted peak at around 1.0 ppm is actually a part of the polyester, although it is due to the minor *exo* isomer, and again is due to the protons on the bridging carbon.

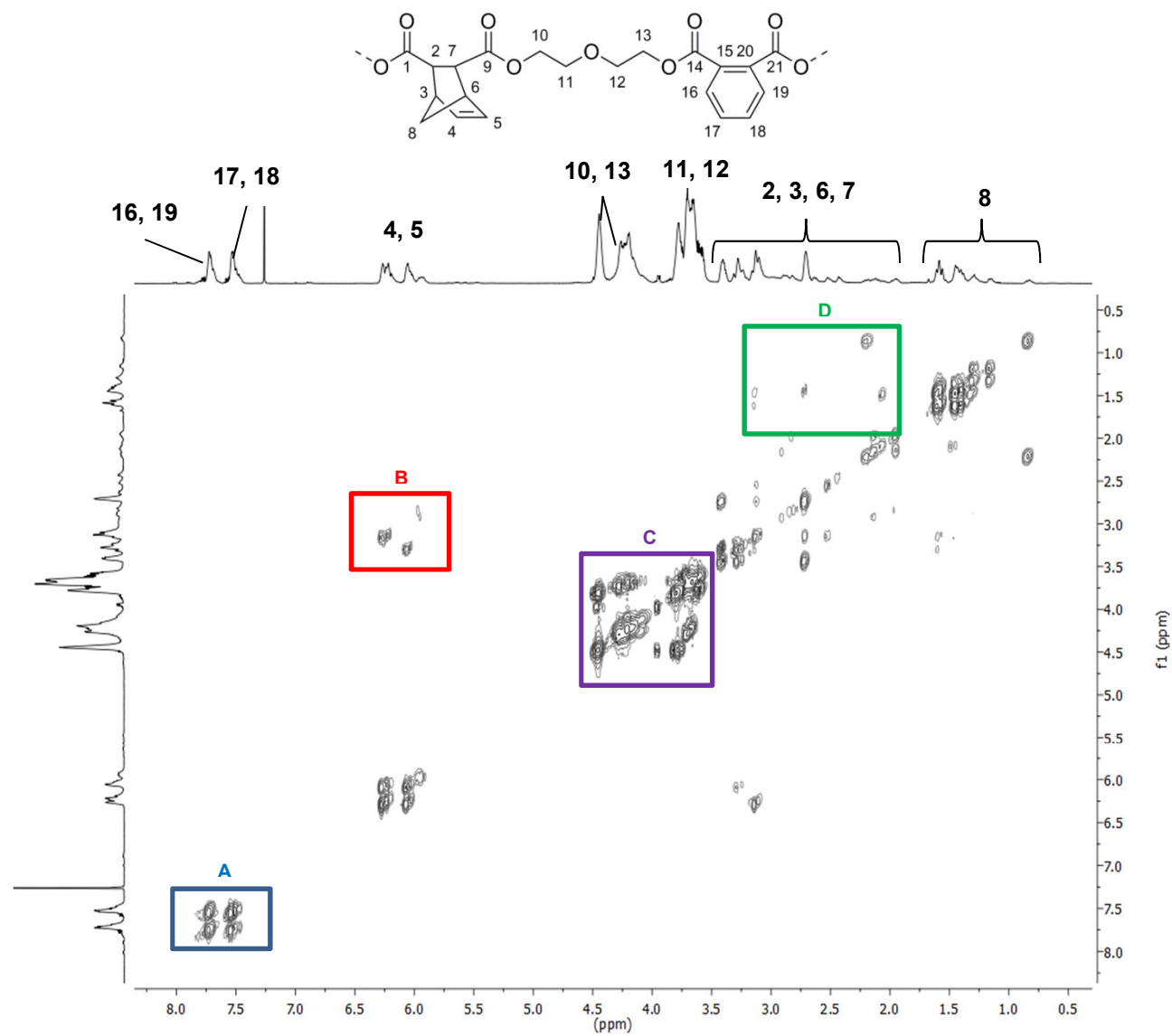


**Figure 2.14:** COSY spectrum (700 MHz, CDCl<sub>3</sub>) of Polyester 1 with important correlations highlighted



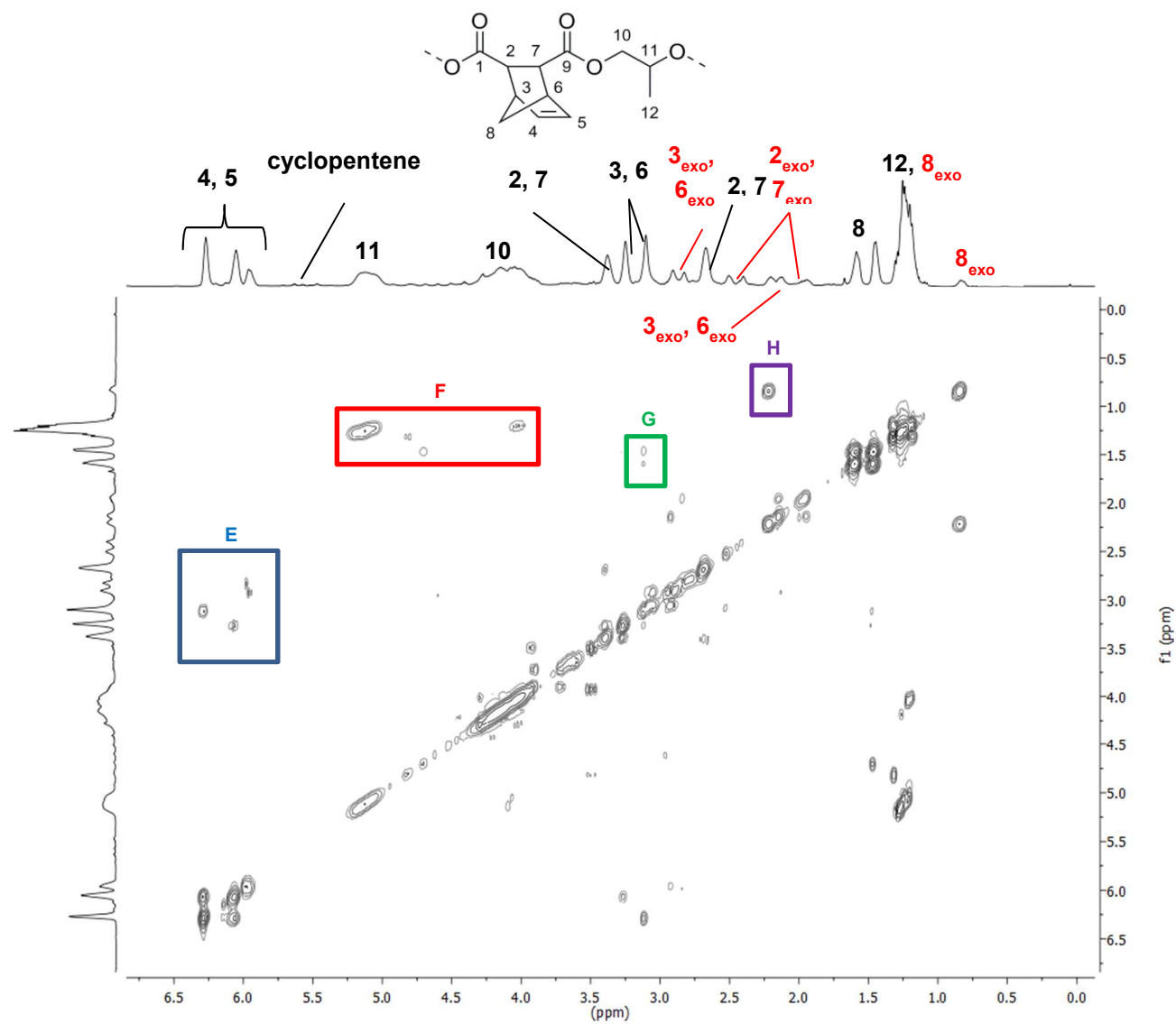


**Figure 2.15:** COSY spectrum (700 MHz, CDCl<sub>3</sub>) of Polyester 2 with important correlations highlighted

### 2.3.5 Structural confirmation of 5-norbornene-2-methoxy tetraethylene glycol

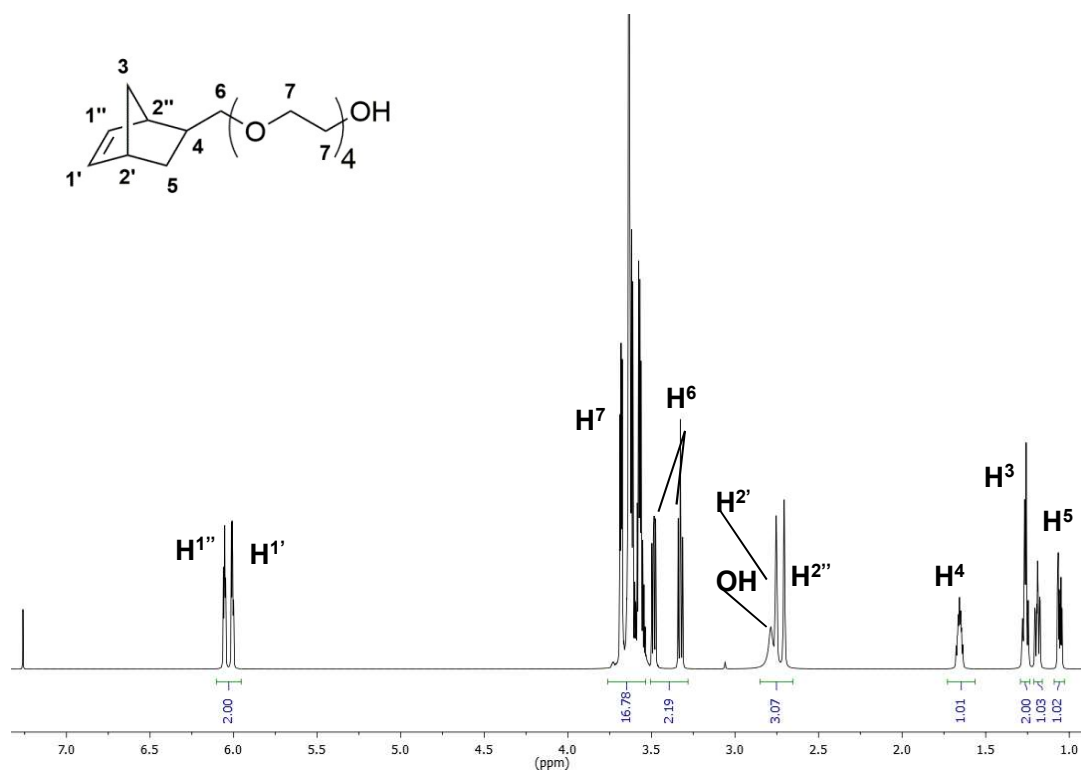


**Figure 2.16:** <sup>1</sup>H NMR (700 MHz, CDCl<sub>3</sub>) spectrum of 5-norbornene-2-methoxy tetraethylene glycol

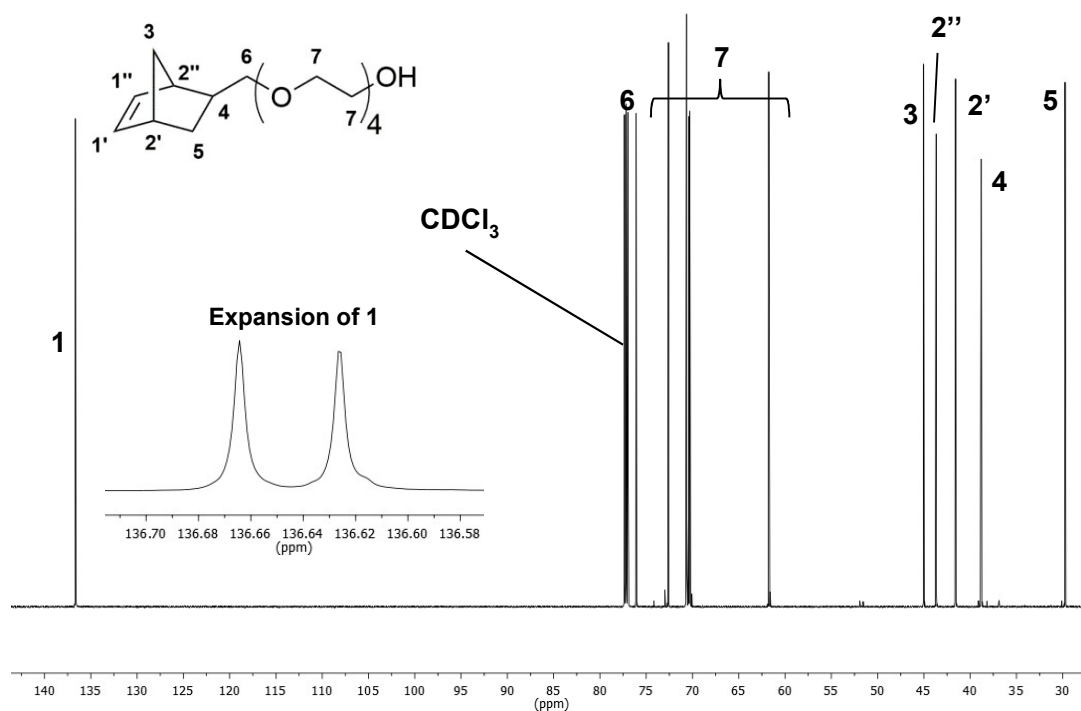


**Figure 2.17:** <sup>13</sup>C NMR (176 MHz, CDCl<sub>3</sub>) spectrum of 5-norbornene-2-methoxy tetraethylene glycol with an inset expansion of the norbornene olefinic region

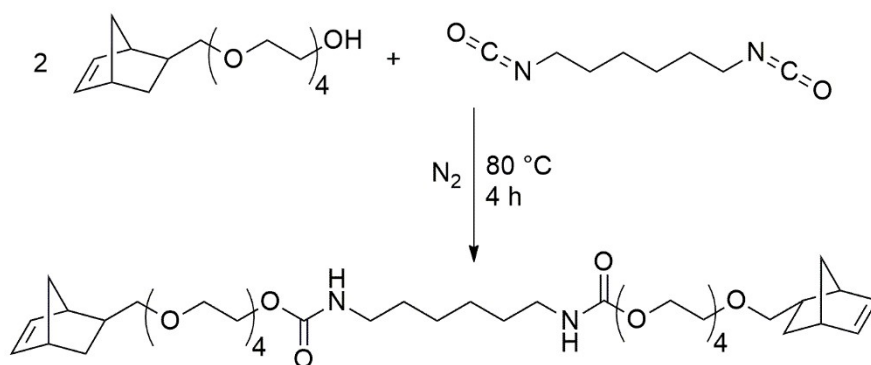
Using the assignment in Figure 2.16 and Figure 2.17 shows that the 5-norbornene-2-methoxy tetraethylene glycol is still unchanged from when it was made. Comparing the integrations of the olefinic protons ( $H^1$ ) at 6.05 ppm with the protons from ethylene glycol ( $H^6$  and  $H^7$ ) between 3.25 and 3.75 ppm shows that there are, on average, 4.2 ethylene glycols attached to the norbornene methanol. All of the other integrations were as expected from the structure, relative to the olefinic norbornene protons.

The  $^1H$  NMR spectrum also shows that the 5-norbornene-2-methoxy tetraethylene glycol is an *exo* isomer. This is confirmed in the  $^{13}C$  NMR spectrum by the fact that there are two peaks due to the two ( $1'$  and  $1''$ ) carbon environments in the olefinic region. In the  $^1H$  NMR spectrum the broad peak due to the hydroxyl group can be clearly seen at around 2.8 ppm, which means that the disappearance of this peak can be used to prove the reaction with isocyanate can be utilised to prove formation of the desired carbamate product.

The  $^{13}C$  NMR spectrum shows various  $C^7$  peaks between 68 and 73 ppm due to the fact that all of these carbons are inequivalent depending where they appear on the oligomeric chain but identifying one from another would be extremely problematic – and unimportant in this case.

### 2.3.6 Synthesis of hexamethylene-1,6-bis(5-norbornene-2-methoxy tetraethylene glycol carbamate) (DFM1)

The compound hexamethylene-1,6-bis(5-norbornene-2-methoxy tetraethylene glycol carbamate), DFM1, was prepared by the reaction of 5-norbornene-2-methoxy tetraethylene glycol with hexamethylene-1,6-diisocyanate (Equation 2.4).



**Equation 2.4:** Synthesis of DFM1

The starting materials are both fairly low viscosity, colourless liquids, but the product is a viscous liquid. This infers that the formation of hexamethylene-1,6-bis(5-norbornene-2-methoxy tetraethylene glycol carbamate) (DFM1) was successful.

The proton NMR spectrum of DFM1 shows the absence of any hydroxyl protons from the starting material and includes a new broad NH peak at 4.81 – 5.00 ppm from the carbamate. It can easily be seen from the COSY spectrum that this is indeed a carbamate NH as this proton correlates to  $H^8$  at 3.07 – 3.16 ppm in Figure 2.18, which would originally have been protons in separate molecules. The

norbornene ring can be resolved clearly in the COSY spectrum since the olefinic protons at 5.89 – 6.18 ppm couple only to H<sup>2'</sup> and H<sup>2''</sup> at 2.77 and 2.72 ppm, respectively, which in turn couple to H<sup>3</sup> (1.03 – 1.33 ppm), H<sup>4</sup> (1.64 – 1.70 ppm) and H<sup>5</sup> (1.03 – 1.33 ppm). Of these, H<sup>3</sup> only couples to H<sup>2</sup> and can therefore be immediately identified as the bridging protons in the bicyclic ring system. What can also be seen is that H<sup>7</sup> splits into glycol (3.54 – 3.76 ppm) and carbamate (4.15 – 4.31 ppm) environments as expected – again further proof of the formation of DFM1. The protons originally from HDI are still found at similar shifts to the starting material and only correlate to one another so are also fairly easy to spot.

The HSQC spectrum (Figure 2.19) of DFM1 shows that the NH peak in the final product does not couple to any carbons, as expected. The <sup>13</sup>C NMR spectrum also contains no peaks in the area attributable to isocyanate carbonyl peaks ( $\delta_c$  = 122.0 ppm in HDI), whereas there is a peak identifiable as a carbamate peak at 156.5 ppm (highlighted in light blue). In the HSQC spectrum, peaks with blue spots on the left and red on the right are CH<sub>2</sub> environments, and the inverse suggests CH or CH<sub>3</sub>. This was one facile way of identifying the olefinic norbornene carbons at 136.6 ppm (correlation highlighted in red) – and also prove that this method works as these, C<sup>2</sup> (at 41.6 and 43.7 ppm) and C<sup>4</sup> (38.9 ppm) are the only CH carbon environments in this molecule. At first glance, C<sup>5</sup> (29.8 ppm) and C<sup>9</sup> (29.9 ppm) appear to only have one peak – but expanding the spectrum shows they are in fact two distinct peaks with C<sup>9</sup> having the slightly higher shift.

The IR spectrum shows no OH or isocyanate peaks in the final product but shows a carbamate C=O peak. This, along with the NMR spectra, suggests that the desired DFM1 has formed.

There are, however, peaks in both the <sup>1</sup>H and <sup>13</sup>C spectra which show small amounts of impurity – presumably from the starting materials as this reaction was carried out in bulk. Another, much less likely, possibility is that the reaction conditions have caused the norbornene ring system to isomerise to the *endo* form – which would be less preferable for ROMP. This is improbable, but the impurities do seem to correlate with some of the peaks in the molecule, for example in the COSY spectrum: the peaks at 2.3 ppm correlate to H<sup>3</sup> and H<sup>5</sup> which could suggest these are H<sup>2-endo</sup>.

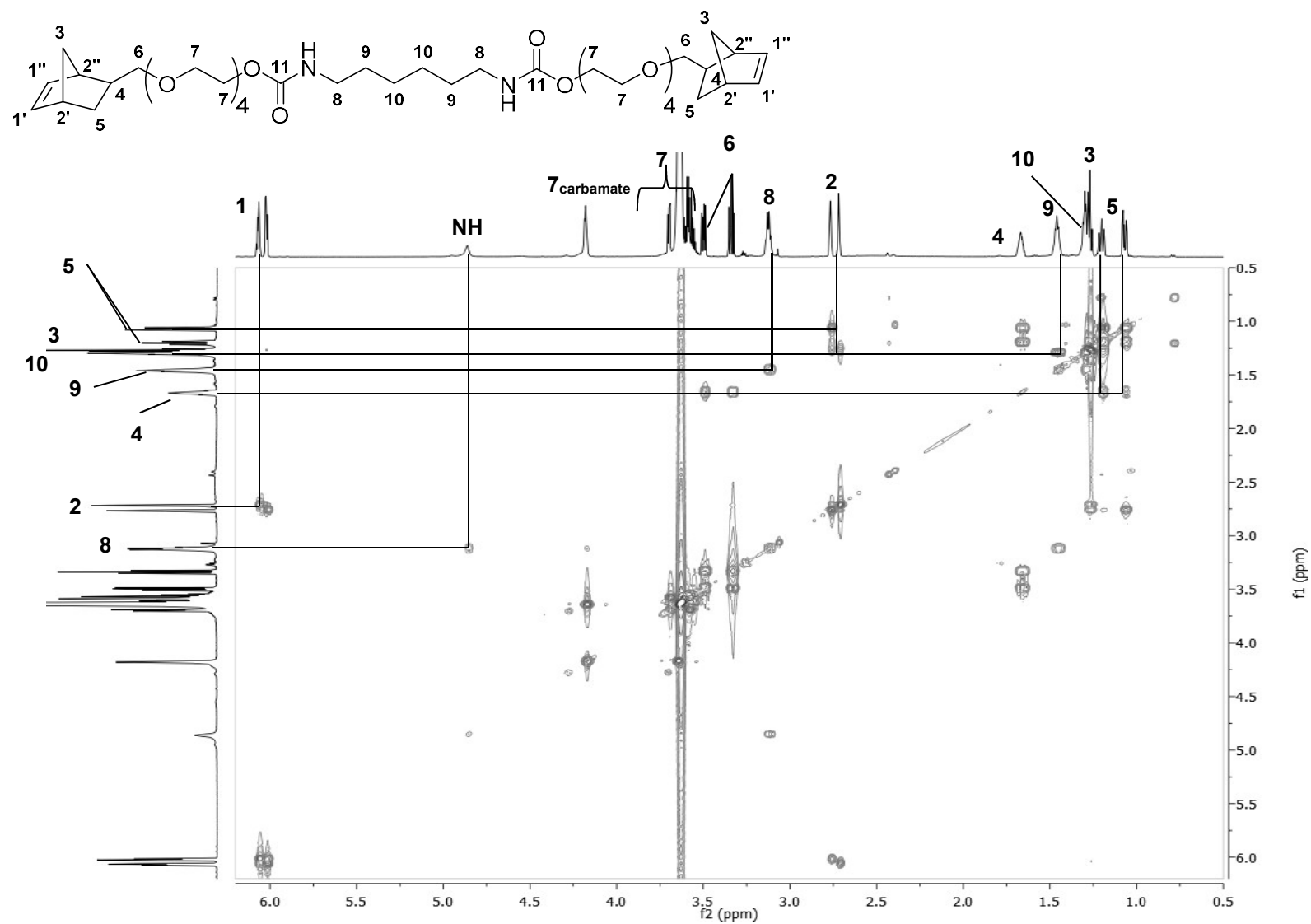


**Figure 2.18:** COSY spectrum (700 MHz, CDCl<sub>3</sub>) of DFM1

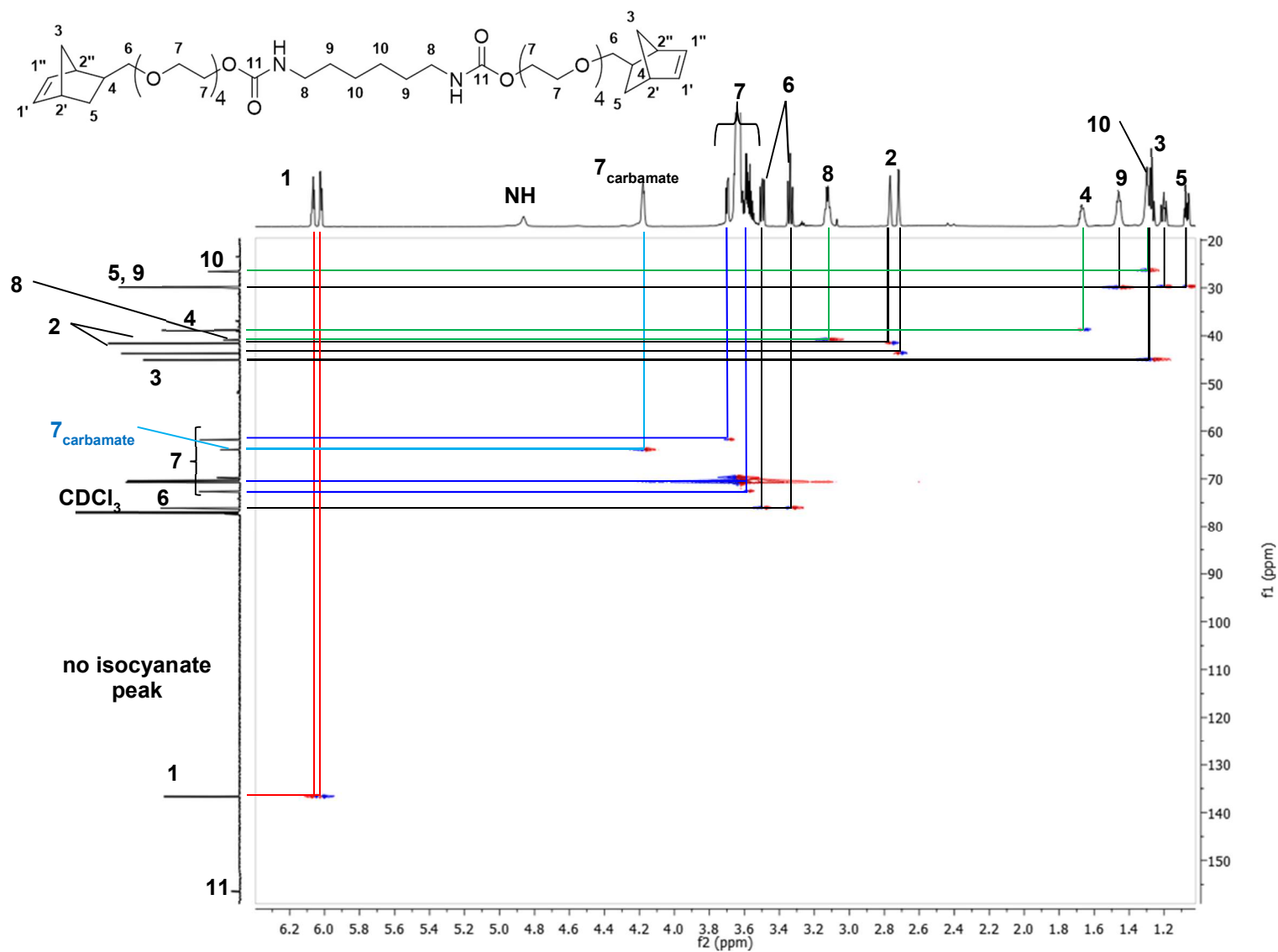


**Figure 2.19:** HSQC spectrum (700 MHz ( $^1\text{H}$ ) and 176 MHz ( $^{13}\text{C}$ ),  $\text{CDCl}_3$ ) of DFM1 with environments originally from HDI highlighted in green for clarity

In the IR spectra of DFM1 (shown in Figure 2.20), the broad OH peak of the norbornene containing starting material has been replaced by a similarly broad NH peak, which is not helpful to show formation of the carbamate species. The isocyanate peak, at  $2256\text{ cm}^{-1}$ , from butyl isocyanate is absent in the product. A new carbamate peak can be seen in the carbonyl region at  $1709\text{ cm}^{-1}$ , although there is a small peak around this area in the starting material as well – although with a much lower intensity. Finally the rest of DFM1's IR spectrum is similar to a combination of both starting materials mixed together, which is to be expected as – with the exception of the newly created carbamate functionality – the structures are by and large the same.

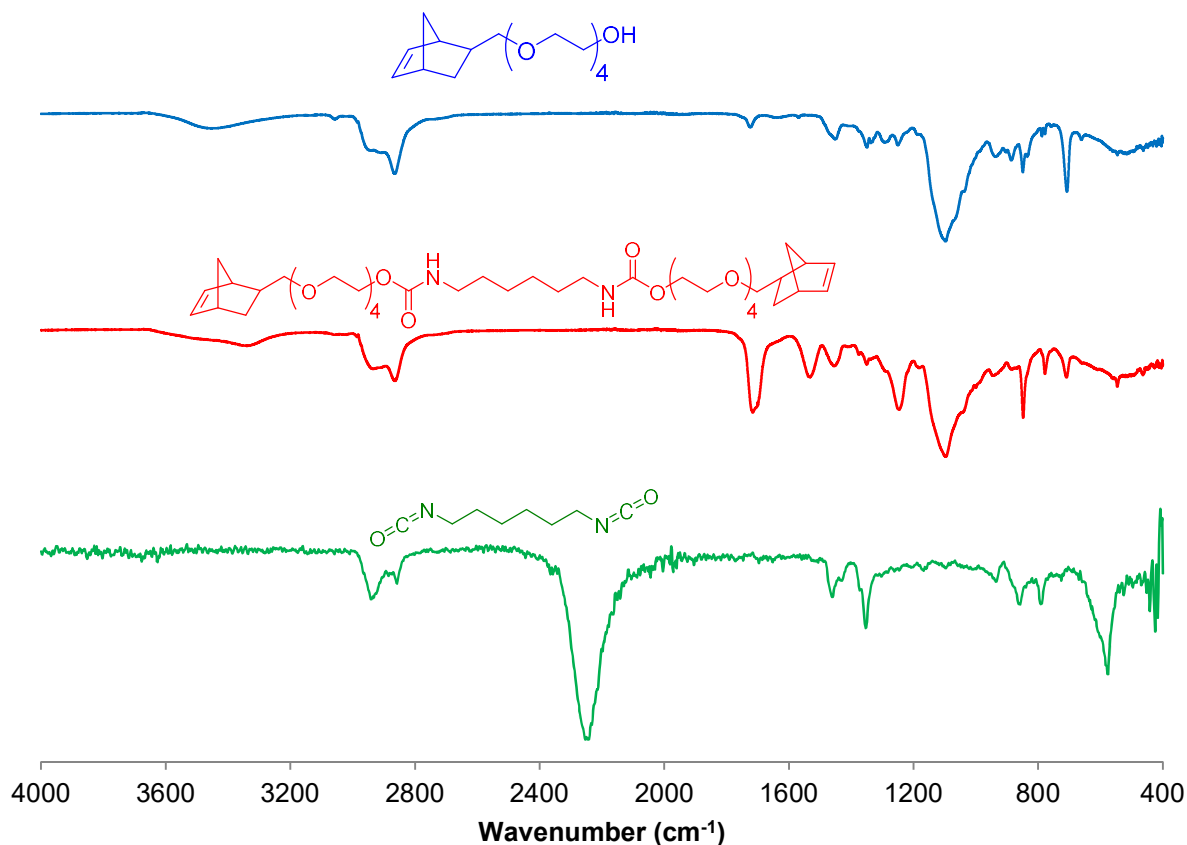
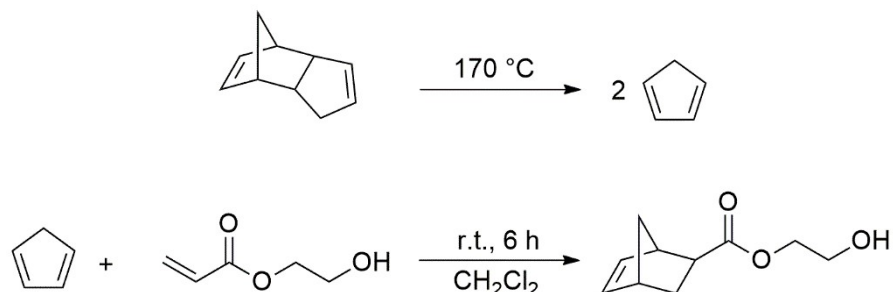


**Figure 2.20:** IR spectra of 5-norbornene-2-methoxy tetraethylene glycol (blue), DFM1 (red) and hexamethylene diisocyanate (green)

The elemental (CHN) analysis of DFM1 does not match up with the percentages of each element, though this could be due to the number of ethylene glycol groups added to the norbornene methanol not being exactly four – as used in the calculations for the analysis. Any slight deviation from tetraethylene glycol side group will change the percentages for C, H and N (as molecular weight of the entire molecule will also change). The NMR spectrum suggested 4.2 ethylene glycols had added, and the CHN seems to suggest more carbon and hydrogen is in the system which would be expected in this case – and also less nitrogen (since molecular weight will have increased slightly). Using this figure of 4.2 gives an expected CHN ratio of: %C = 62.30, %H = 8.92, %N = 3.56, which are much closer to the actual figures (all within 0.18 % of experimental).

### 2.3.7 Synthesis of 2-Hydroxyethyl-5-norbornene-2-carboxylate (HE-NBE-CO<sub>2</sub>)

The compound 2-hydroxyethyl-5-norbornene-2-carboxylate, HE-NBE-CO<sub>2</sub>, was prepared by the reaction of cyclopentadiene (produced from the cracking of dicyclopentadiene) with hydroxyethyl acrylate (Scheme 2.2).



**Scheme 2.2:** Synthesis of HE-NBE-CO<sub>2</sub>

The reaction was successful when the small amount of diacrylate impurity in hydroxyethyl acrylate (HEA) was removed. It was found that the 2-hydroxyethyl-5-norbornene-2-carboxylate (HE-NBE-CO<sub>2</sub>) produced could withstand being heated to the required temperature under reduced pressure without any difficulties.

The NMR spectra of HE-NBE-CO<sub>2</sub> shown here match those published by Clapham *et al.*<sup>19</sup>, which helps identify that the target material has been synthesised. The product also correlates correctly in COSY and HSQC. H<sup>9</sup>, at 4.04 – 4.33 ppm, and H<sup>10</sup> (3.56 – 3.89 ppm) only show a relationship in the COSY (Figure 2.21) to one another. This time, however, the spectrum is slightly complicated by the presence of a major (*endo*) and minor (*exo*) isomer in approximately a 4:1 ratio.



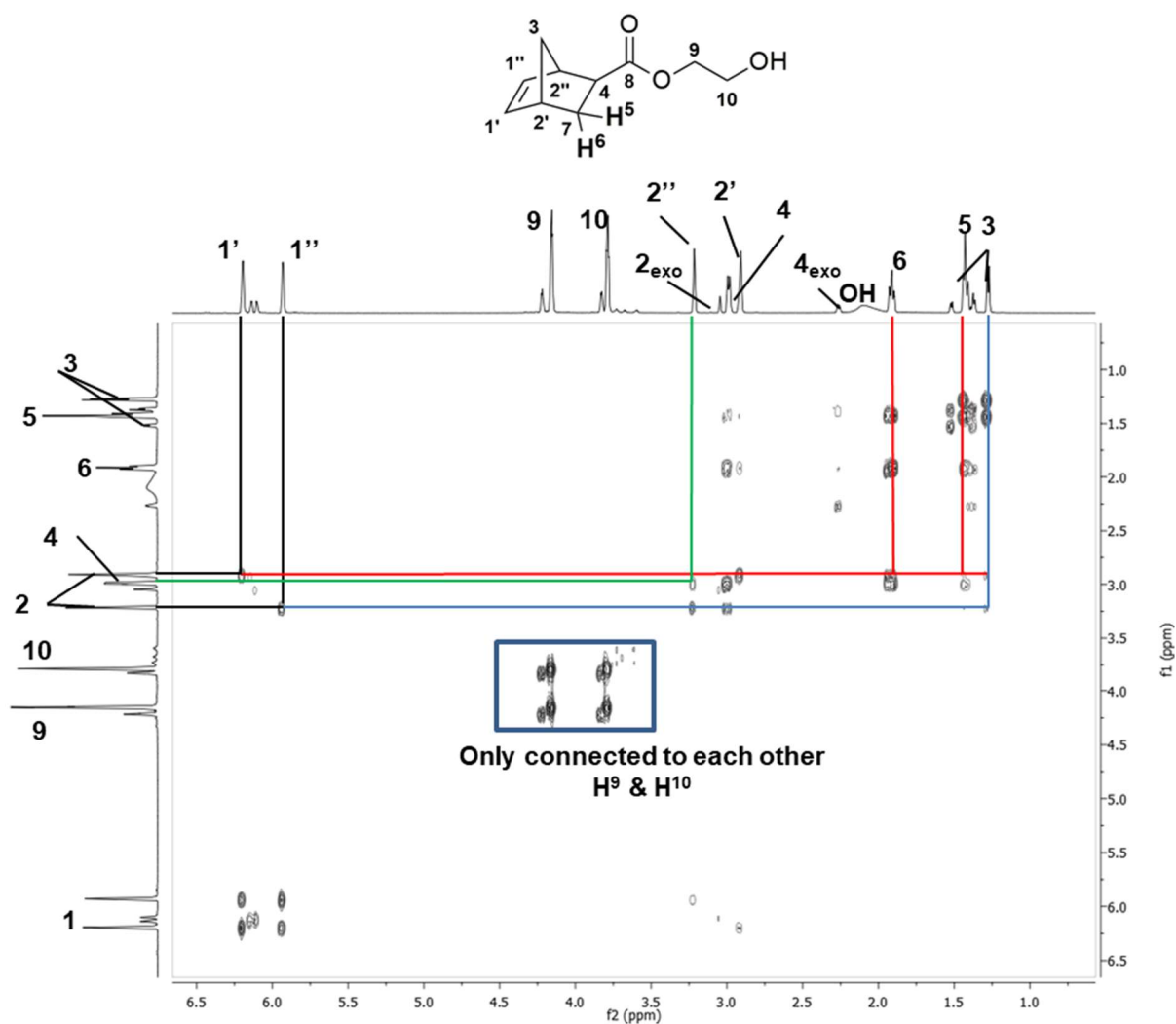


**Figure 2.21:** COSY spectrum (700 MHz, CDCl<sub>3</sub>) of 2-hydroxyethyl-5-norbornene-2-carboxylate

Again the olefinic norbornene protons are shifted higher (5.91 – 6.21 ppm) in the spectrum and to higher frequency – and so the correlations to find H<sup>2'</sup> and H<sup>2''</sup> (and *exo* isomers) at 2.88 – 3.01, 3.05 and 3.22 ppm are simple to observe. One of the H<sup>2</sup> peaks correlates to H<sup>4</sup> (2.24 – 2.29 and 2.96 – 3.01 ppm, green lines); the other to H<sup>5</sup> (1.35 – 1.55 ppm) and H<sup>6</sup> (1.88 – 1.95 ppm, red lines). This allows the resolution of H<sup>2'</sup> and H<sup>2''</sup>, and then from this: H<sup>1'</sup> and H<sup>1''</sup>. H<sup>3</sup>, at 1.25 – 1.55 ppm, correlates to both H<sup>2</sup> signals and nothing else – thus completing the norbornene ring system. The only peak left is at 1.95 – 2.20 ppm, broad, and does not correlate to anything else. The only unassigned proton is the OH group which would be the perfect fit for this. There are also clearly no peaks due to the acrylate or DCPD, which means that the removal of starting materials was successful.

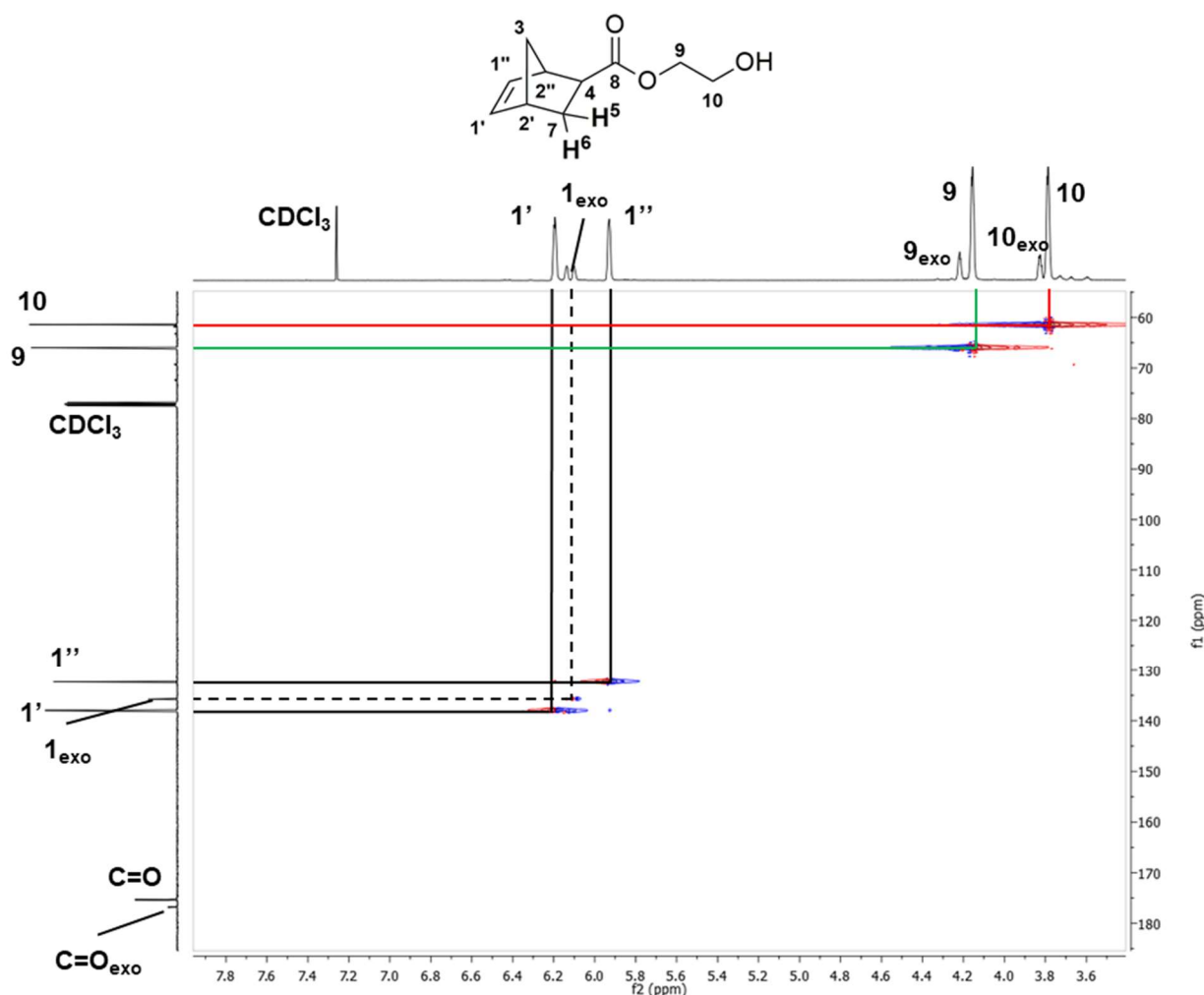


**Figure 2.22:** HSQC spectrum (700 MHz ( $^1\text{H}$ ) and 176 MHz ( $^{13}\text{C}$ ),  $\text{CDCl}_3$ ) of 2-hydroxyethyl-5-norbornene-2-carboxylate for  $\delta_{\text{H}} = 3.5\text{--}7.9$  ppm and  $\delta_{\text{C}} = 50\text{--}190$  ppm

In Figure 2.22, the olefinic norbornene protons can easily be connected to the relevant carbon peaks. Again there are two clear, distinct peaks for  $\text{C}^{1'}$  and  $\text{C}^{1''}$ , at 138.0 and 132.3 ppm, respectively, which are shown to be CH environments. One can also clearly associate the *exo* peak in the proton spectrum with that in the carbon. The carboxylate group is also easy to identify at 175.3 ppm, along with its corresponding *exo* peak at 176.8 ppm, in the carbon spectrum due to its high chemical shift and the fact it does not correlate to the proton spectrum as it is a quaternary carbon environment. Finally  $\text{C}^9$ , 66.0 ppm, and  $\text{C}^{10}$ , 61.4 ppm, show a clear correlation and the DEPT shows up as these (correctly) both being  $\text{CH}_2$ . The *exo* peaks this time are not so easy to spot and probably coincide with the major *endo* peaks as the difference in surroundings for these carbons is vastly reduced for the two isomers opposed to those in the ring.

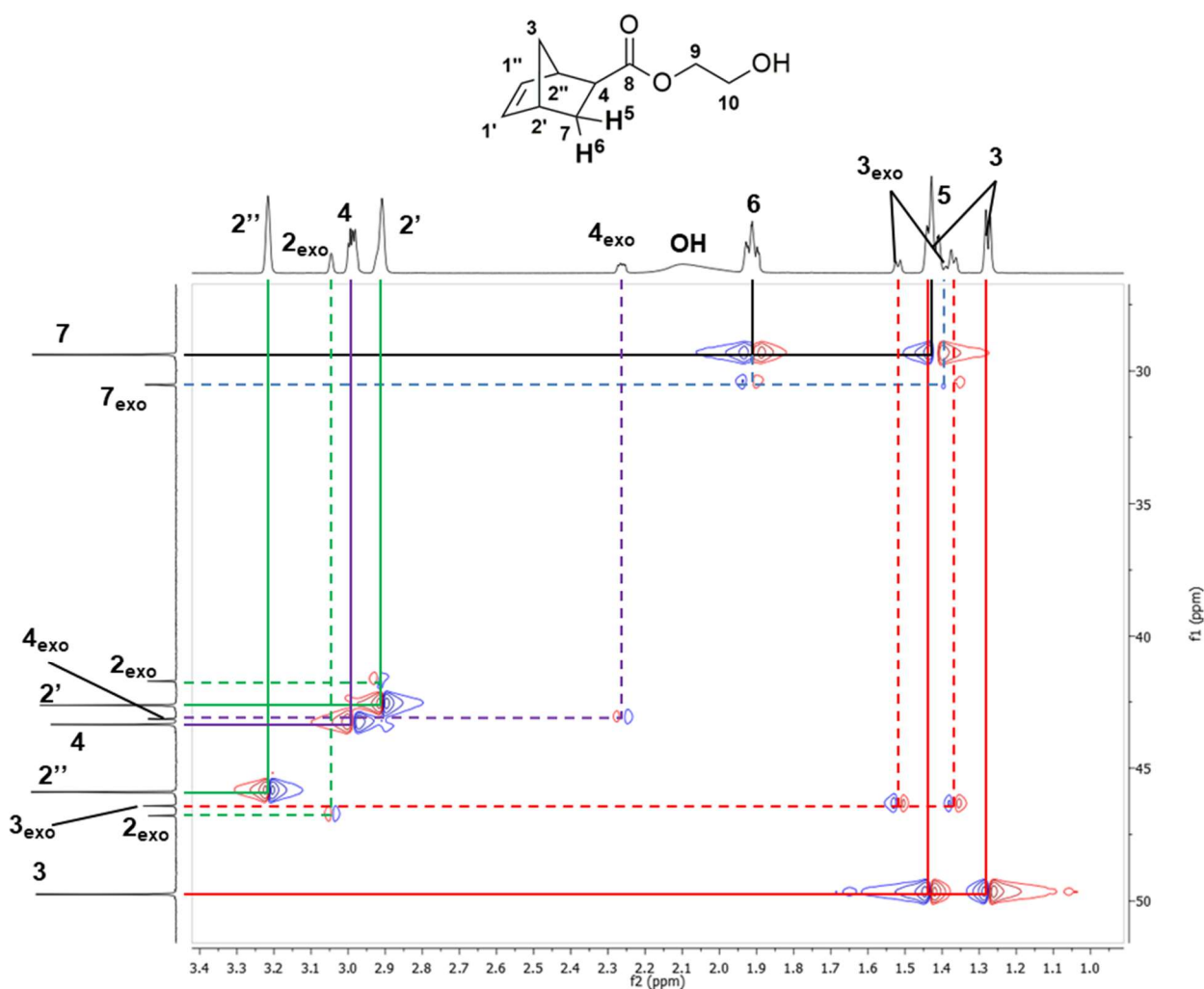


**Figure 2.23:** HSQC spectrum (700 MHz ( $^1\text{H}$ ) and 176 MHz ( $^{13}\text{C}$ ),  $\text{CDCl}_3$ ) of 2-hydroxyethyl-5-norbornene-2-carboxylate for  $\delta_{\text{H}} = 0.9\text{--}3.4$  ppm and  $\delta_{\text{C}} = 27\text{--}50$  ppm

The rest of the molecule is quite complex but, as Figure 2.23 shows, all of the carbons can be successfully assigned. Again (like in the proton spectrum) it is possible to distinguish between  $\text{C}^{2'}$  and  $\text{C}^{2''}$  at 42.6 and 45.9 ppm, respectively, (highlighted in green) and also  $\text{C}^{2\text{-exo}}$  can be seen as two distinct peaks (41.7 and 45.9 ppm) shown with dotted lines. The other *exo* peaks are also shown correlating to the respective protons with dotted lines. The DEPT experiment again shows the differences between the  $\text{CH}_2$  ( $\text{C}^3$  and  $\text{C}^7$ ) and  $\text{CH}$  ( $\text{C}^2$  and  $\text{C}^4$ ) environments; and offers further proof that the assignments are indeed correct. Finally, as one would expect, the hydroxyl group shows no correlation to the carbon spectrum.

HE-NBE- $\text{CO}_2$  had surprisingly good stability – in spite of the low retro Diels-Alder temperature of  $113^\circ\text{C}$  – towards mass spectrometry (specifically electrospray ionisation which normally causes retro Diels-Alder of the norbornene ring), which meant that ASAP could be used and Figure 2.24 shows peaks attributable to both HE-NBE- $\text{CO}_2$  and 5-norbornene-2-carboxylic acid due to the cleaving of the weak ester bond, likely yielding ethylene glycol or ethanol as well although these are below the range of the ASAP spectrometer.

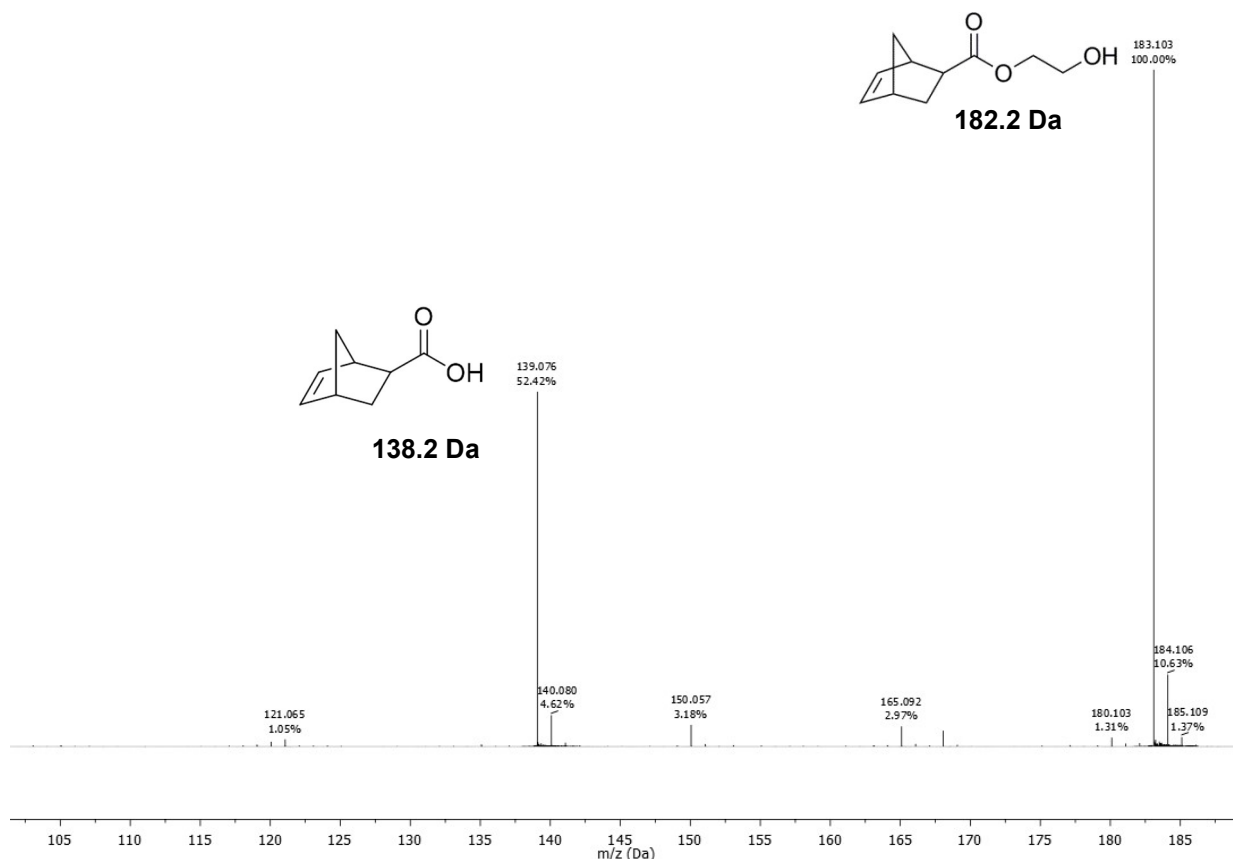


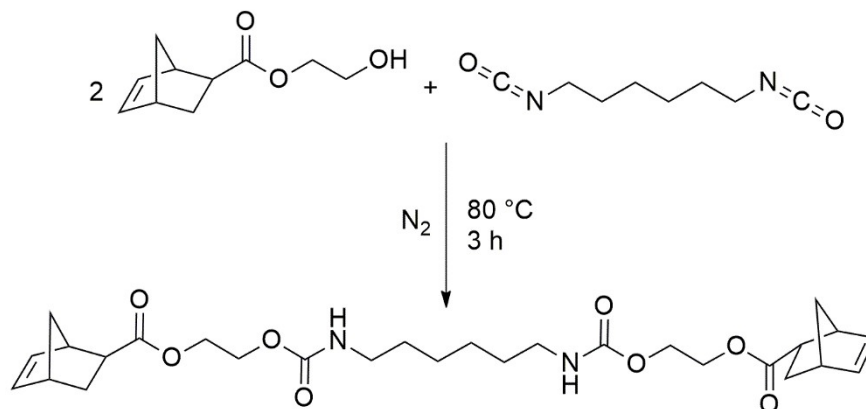
**Figure 2.24:** ASAP-MS of 2-hydroxyethyl-5-norbornene-2-carboxylate

This is a reasonable indication that the desired molecule has been formed as the major peak is the 2-HE-NBE-CO<sub>2</sub> associated with a proton, yielding the m/z of 183. The smaller peak shows 5-norbornene-2-carboxylic acid again showing the M+H<sup>+</sup> peak of 139 this time. Unfortunately, the range of the ASAP does not go below 100 Da (g mol<sup>-1</sup>) which means that if cyclopentadiene (M<sub>w</sub> = 66.1 Da) is produced from the retro Diels-Alder this would also not be seen; although HEA (M<sub>w</sub> = 116.1 Da) would be, but is not observed.

The elemental analysis is extremely close to the expected CHN content of HE-NBE-CO<sub>2</sub> except the carbon is a little high, perhaps due to the presence of inhibitor (hydroquinone) added to the HEA during purification to prevent the free radical or thermal polymerisation of this precursor. The other item of note is that the percentage of nitrogen measured is negative which questions the validity of the results, as it could cast doubt upon the accuracy of the analyser, or perhaps the technique utilised.

### 2.3.8 Synthesis of hexamethylene-1,6-bis(5-norbornene-2-carboxylate-2-ethoxy carbamate) (DFM2)

The compound hexamethylene-1,6-bis(5-norbornene-2-carboxylate-2-ethoxy carbamate), DFM2, was prepared by the reaction of 2-hydroxyethyl-5-norbornene-2-carboxylate with hexamethylene-1,6-diisocyanate (Equation 2.5).



**Equation 2.5:** Synthesis of DFM2

From the COSY spectra in Figure 2.26, one can assign the norbornene ring once again. The red lines show how H<sup>4</sup>, H<sup>5</sup> and H<sup>6</sup> correlate. The olefinic protons, H<sup>1'</sup> and H<sup>1''</sup>, are obvious once again at 5.87 – 6.24 ppm, and show coupling to H<sup>2'</sup> and H<sup>2''</sup> (2.83 – 3.54 ppm) respectively – shown with the black lines. H<sup>9</sup> and H<sup>10</sup>, at 3.58 – 4.37 ppm, can be seen to only correlate to one another once again, as expected. H<sup>13</sup> and H<sup>14</sup>, 1.18 – 1.59 ppm, are in similar regions to the respective proton shifts in HDI,<sup>20</sup> but H<sup>12</sup> shows up slightly differently at 3.15 ppm due to its proximity to a carbamate group rather than an isocyanate. H<sup>12</sup> also shows correlation (as well as to H<sup>13</sup>) to the proton on the carbamate nitrogen at 4.76 ppm, which would be expected as it is on a neighbouring atom. The only peaks that were not possible to identify are those highlighted in the red boxes, though it is possible that these could be due to another isomer of DFM2 (an example is shown in Figure 2.25), which is why the peaks are barely shifted, but appear to have the same relative, to one another, shifts as the main peaks. There are also still the *endo* and *exo* versions of these as well.

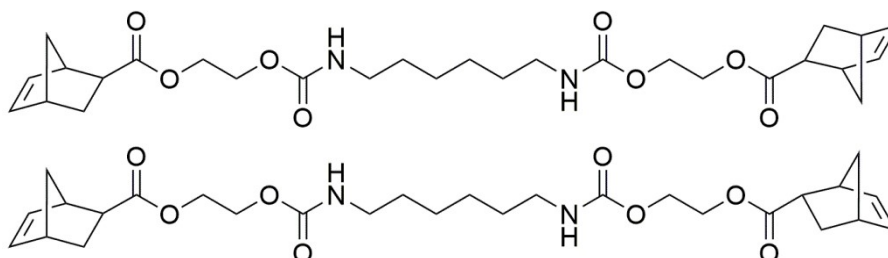


**Figure 2.25:** Two possible isomers of DFM2

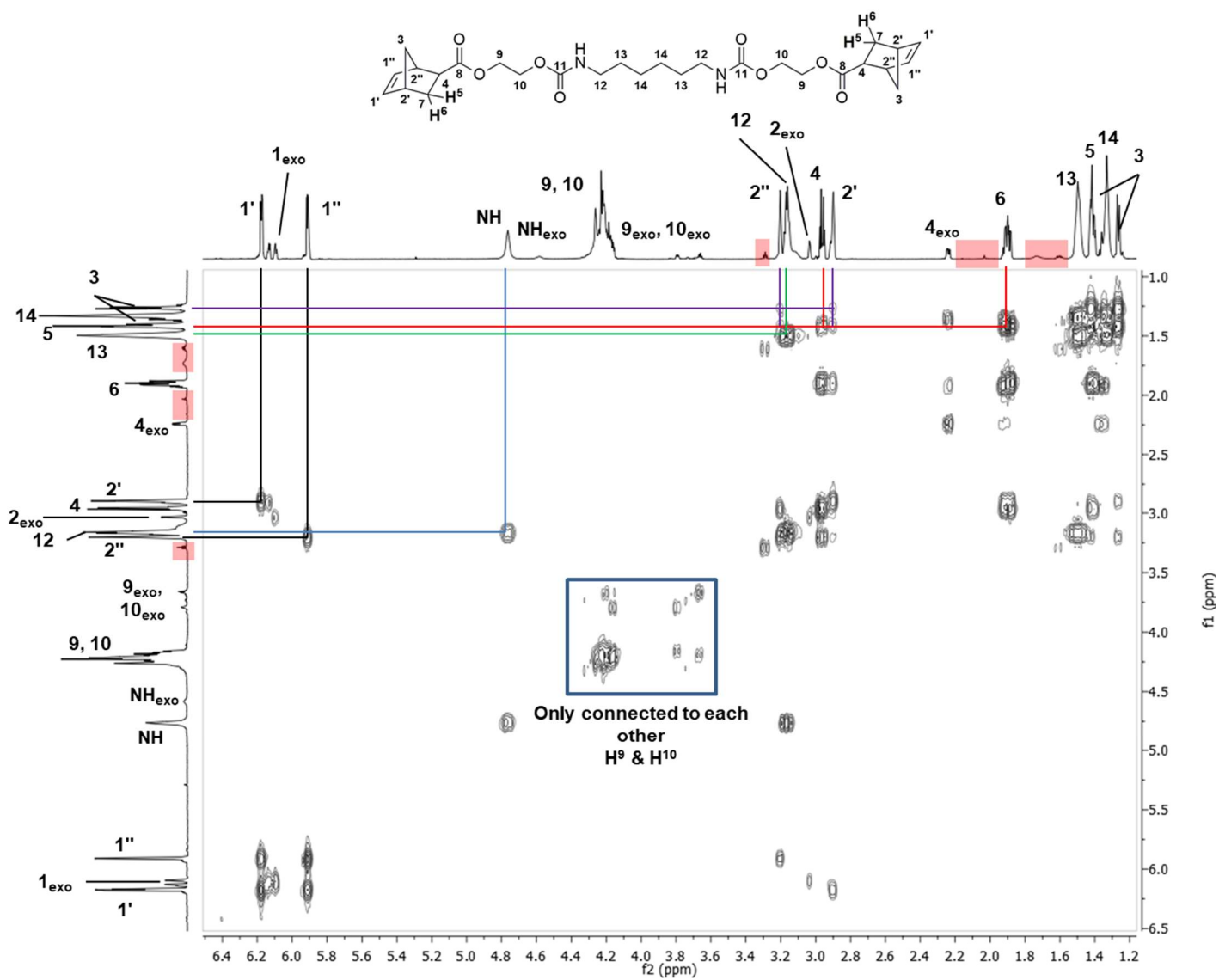
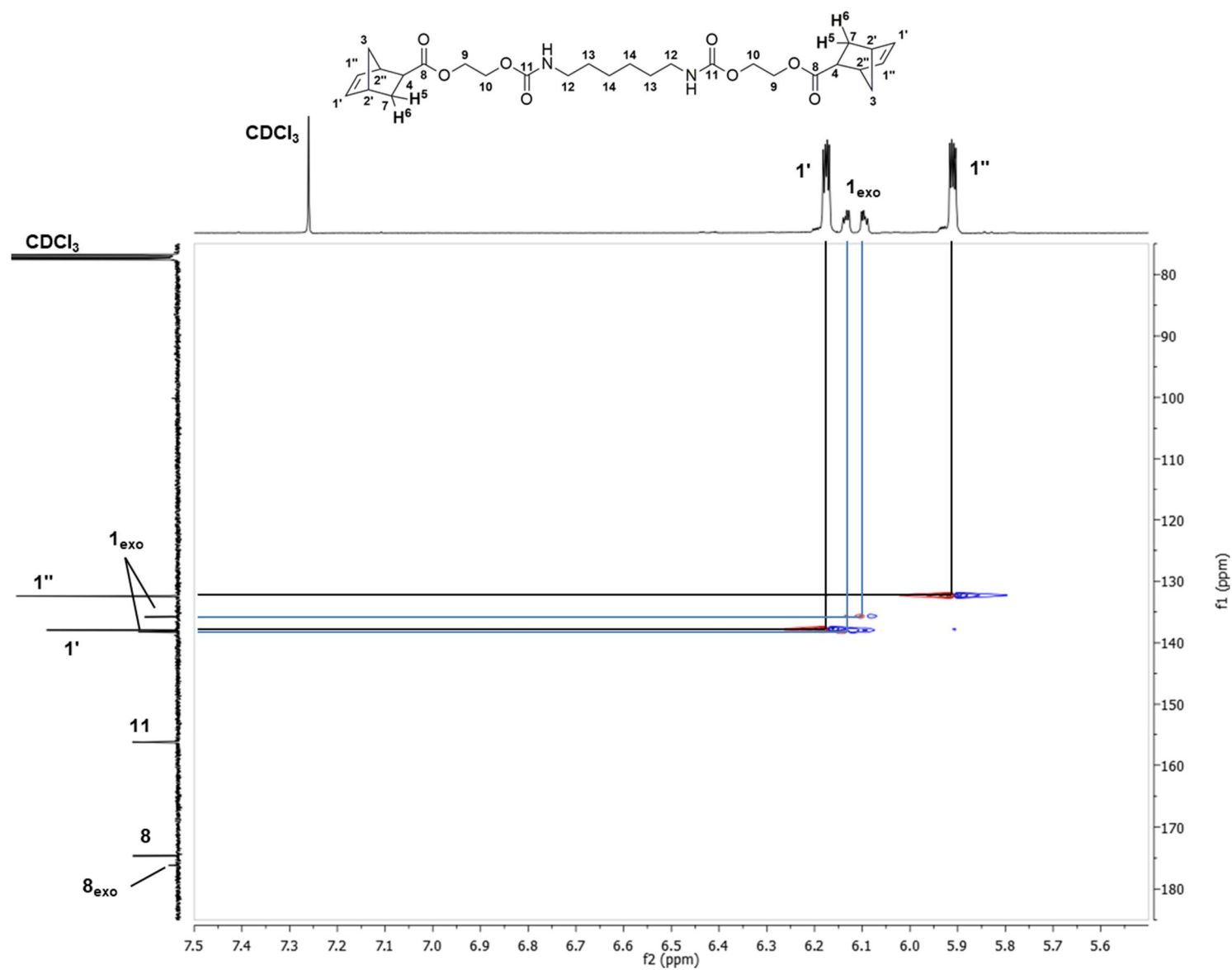


Figure 2.26: COSY spectrum (700 MHz, CDCl<sub>3</sub>) of DFM2

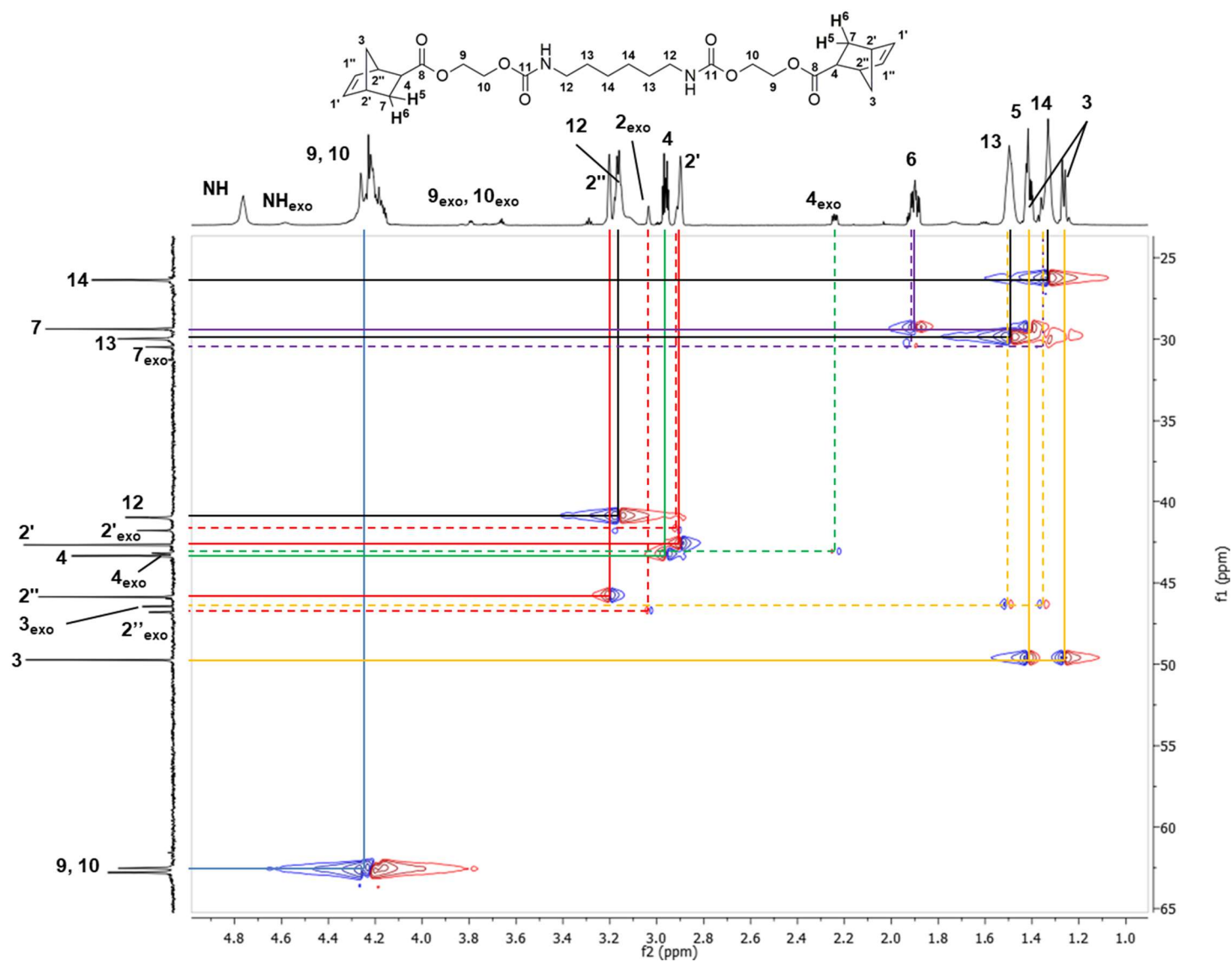
In Figure 2.27, four separate carbon peaks can be seen for the norbornene double bond due to the *exo/endo* isomers at 132.4, 135.8, 138.0 and 138.3 ppm. This was seen before in HE-NBE-CO<sub>2</sub>. What can be seen in the expansion of the <sup>1</sup>H spectrum are the small peaks, slightly shifted to the left of the norbornene olefin peaks – perhaps due to the aforementioned isomers. C<sup>11</sup> appears at 156.3 ppm, which is indicative of a carbamate carbon environment. There is also no correlation here as there are no protons on C<sup>11</sup> as it is a quaternary carbon. The highest shifted peaks, C<sup>8</sup> and C<sup>8-*exo*</sup>, also appear in the correct region of the spectrum at 174.6 and 176.2 ppm, respectively (ester carbons); and again show no correlation. The fact that only two separate carbonyl environments (excluding the *exo* isomer peak) are seen is further proof that the starting materials, HE-NBE-CO<sub>2</sub> and HDI (which would also show an obvious isocyanate peak at 122.0 ppm), have been successfully removed from the product.

Figure 2.28 shows how complicated the spectra of DFM2 are, but all the peaks correlate with one another. One observation that can be easily spotted is that the DEPT signals of C<sup>2'</sup>, at 45.9 ppm, and C<sup>12</sup>, at 41.0 ppm, are the inverse of one another. This is expected as C<sup>2'</sup> is a CH carbon, whereas C<sup>12</sup> is CH<sub>2</sub>. This inversion also helped to assign the overlapping peaks at  $\delta_H = 2.8\text{--}3.2$  ppm, and  $\delta_C = 40\text{--}48$  ppm, mainly because C<sup>2'</sup> (47.2 ppm), C<sup>2''</sup> (45.9 ppm) and C<sup>4</sup> (43.3 ppm) are CH whereas C<sup>3</sup> (49.7 ppm) and C<sup>12</sup> (41.0 ppm) are both CH<sub>2</sub>. The fact that H<sup>5</sup> and H<sup>6</sup> both couple to the same carbon at 29.4 ppm (purple lines, C<sup>7</sup>) helps further resolve the many overlapping peaks with C<sup>3</sup> (orange lines), C<sup>13</sup> and C<sup>14</sup> (at 30.0 and 26.4 ppm correspondingly, black lines), and the *exo* versions of all of these (dotted lines). It is difficult to decide which peak – out of 62.5 and 62.8 ppm – is attributable to C<sup>9</sup> and C<sup>10</sup> as they are very similar environments, though from the NMR of HE-NBE-CO<sub>2</sub> it is likely the slightly higher shifted signal is due to C<sup>9</sup> being more deshielded by the ester group than C<sup>10</sup> by the carbamate – thus increasing the chemical shift of C<sup>9</sup>.



**Figure 2.27:** HSQC spectrum (700 MHz ( $^1\text{H}$ ) and 176 MHz ( $^{13}\text{C}$ ),  $\text{CDCl}_3$ ) of DFM2 for  $\delta_{\text{H}} = 5.5\text{--}7.5$  ppm and  $\delta_{\text{C}} = 75\text{--}185$  ppm

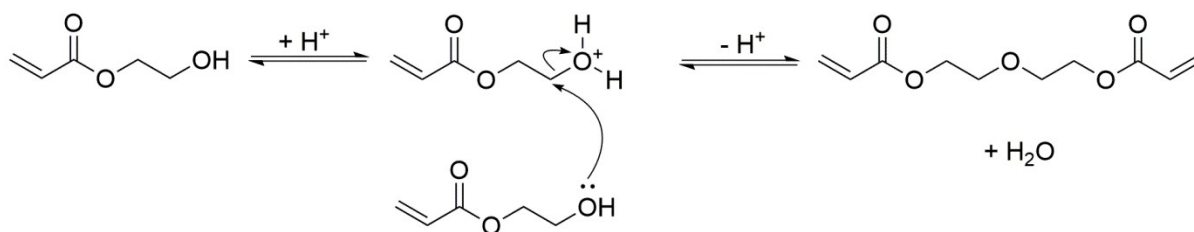




**Figure 2.28:** HSQC spectrum (700 MHz ( $^1\text{H}$ ) and 176 MHz ( $^{13}\text{C}$ ),  $\text{CDCl}_3$ ) of DFM2 for  $\delta_{\text{H}} = 1.0\text{--}5.0$  ppm and  $\delta_{\text{C}} = 25\text{--}65$  ppm

The ASAP mass spectrum of DFM2 (Figure 2.29) shows a peak which could correspond to DFM+H<sup>+</sup> at 533 Da. This is not surprising as DFM2 is shown to be fairly stable to temperature with a much higher T<sub>rDA</sub> than HE-NBE-CO<sub>2</sub>. Some decomposition is seen, however, as highlighted by the two much larger peaks which come as a result of one of the ester groups cleaving (resulting in **A**), and the cleaving of a carbamate group (resulting in **B**). These are two of the weakest bonds in the molecule and so it is unsurprising that these are the species that are seen. It is a little unexpected that the species with acrylates on the end of these molecules, instead of norbornene, are not seen – *i.e.* having undergone a retro Diels-Alder on these species.

The only peak which shows acrylate functionality is at 213 Da, which can be linked to diethylene glycol diacrylate (**C**). This could either be an impurity in the starting material or a product of the mass spectrometry. The starting material was, however, purified to remove this and thus is unlikely to be an impurity. **C** could have formed by the decomposition of DFM2 by retro Diels-Alder and the decomposition of the carbamate groups; thus forming hydroxyethyl acrylate. This newly formed HEA under forcing conditions could undergo self-condensation (Scheme 2.3) when protonated during the ASAP-MS. Of course, unlike the reaction scheme, in order to see product **C** (diethylene glycol diacrylate) in the mass spectrum, the product will stay protonated (*i.e.* no second proton transfer to produce the neutral species).



**Scheme 2.3:** Self-condensation reaction of HEA

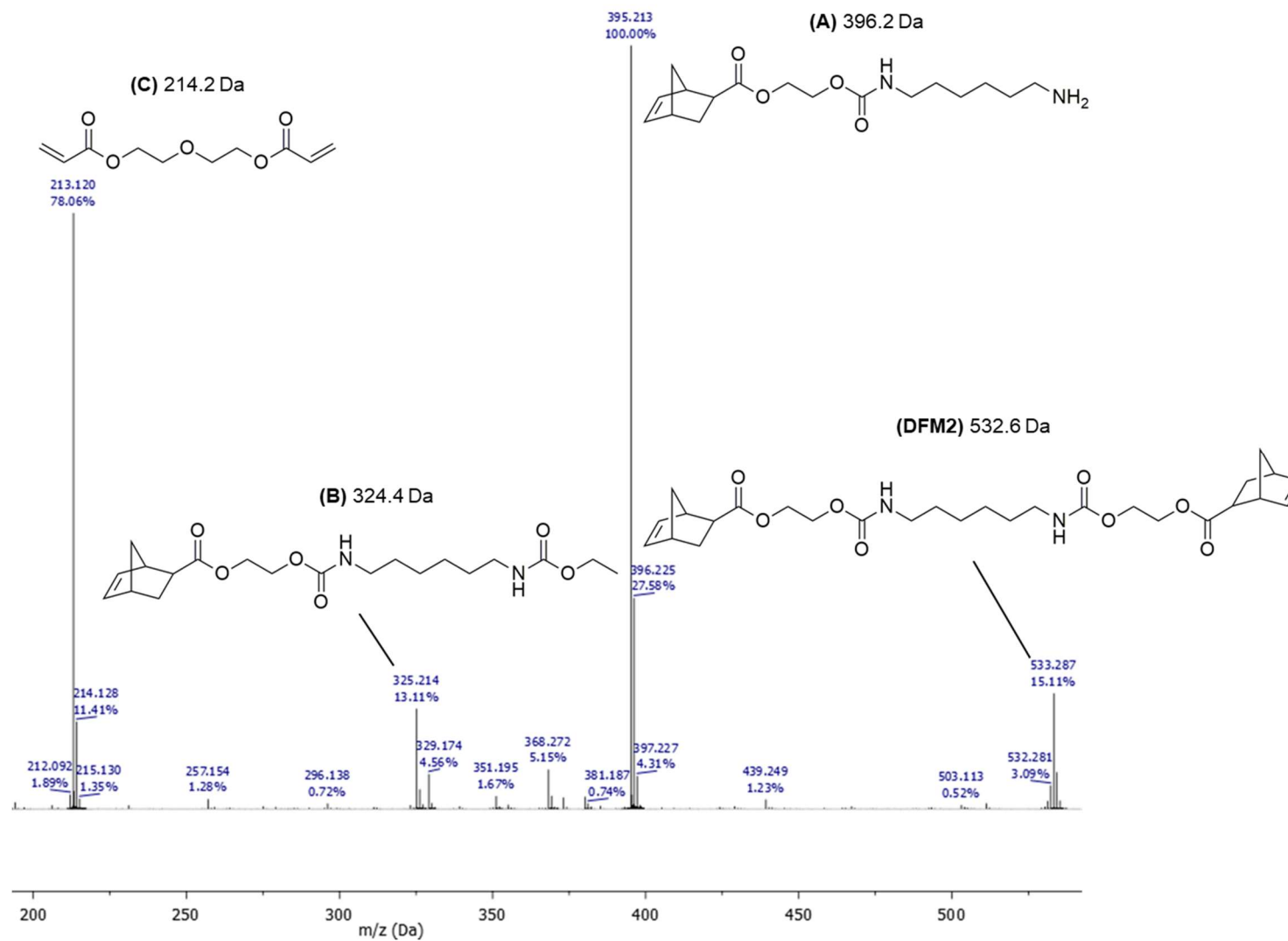
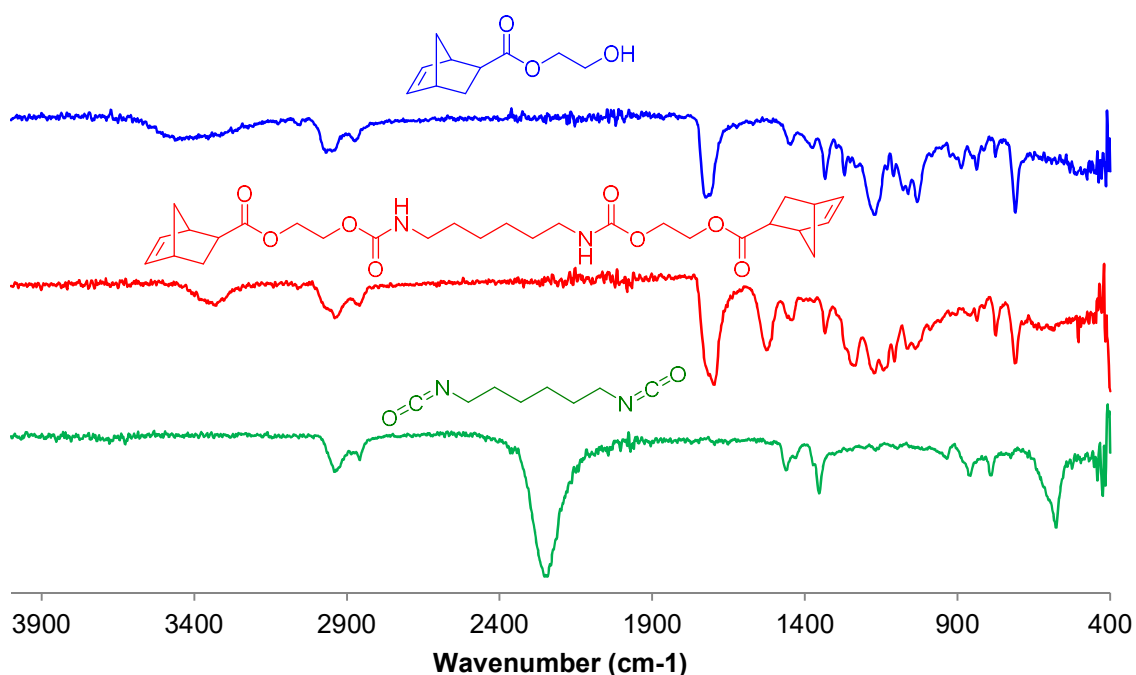


Figure 2.29: ASAP mass spectrum of DFM2 with the major peaks assigned

The IR spectrum, Figure 2.30, of DFM2 shows that the NCO asymmetric stretch around  $2250\text{ cm}^{-1}$  has disappeared which shows that the isocyanate group has fully reacted. At first glance, the broad OH stretch ( $3150\text{--}3600\text{ cm}^{-1}$ ) from the HE-NBE- $\text{CO}_2$  starting material is still in the spectrum of DFM2. This is a much narrower signal, however, ( $3240\text{--}3470\text{ cm}^{-1}$ ) and can actually be assigned to the NH stretch in the carbamate group. In the carbonyl region ( $1500\text{--}1700\text{ cm}^{-1}$ ), it can be seen that HE-NBE- $\text{CO}_2$  only has one (ester) carbonyl group – whereas DFM2 has two separate peaks for its ester and carbamate groups. This again is suggestive of the formation of DFM2 and consumption of both starting materials. Finally, the peak at  $570\text{ cm}^{-1}$  completely disappears from HDI to DFM2 and is not seen in HE-NBE- $\text{CO}_2$ , which perhaps means it is some sort of NCO bend that would obviously not appear in either of the other two molecules.

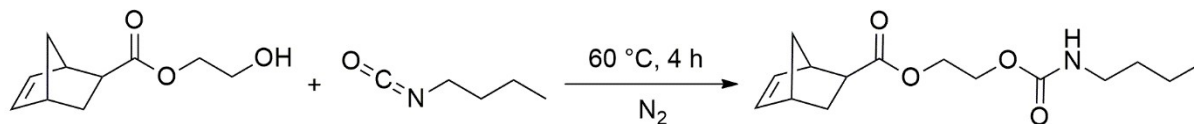


**Figure 2.30:** FT-IR spectra of HE-NBE- $\text{CO}_2$  (blue), DFM2 (red), and HDI (green)

The elemental analysis of hexamethylene-1,6-bis(5-norbornene-2-carboxylate-2-ethoxy carbamate) (DFM2) is close to the expected values, though the %N is a little high (5.72 vs. 5.26). This could be due to the same error shown with the CHN analysis of HE-NBE- $\text{CO}_2$ , which is possibly caused – as discussed previously – by technique used or perhaps by the presence of nitrogen in the oxygen gas in which the sample is combusted.

### 2.3.9 Synthesis of 2-Hydroxyethyl-5-norbornene-2-carboxylate butyl carbamate (MFM)

The compound 2-hydroxyethyl-5-norbornene-2-carboxylate butyl carbamate, MFM, was prepared by the reaction of 2-hydroxyethyl-5-norbornene-2-carboxylate with butyl isocyanate (Equation 2.6).



**Equation 2.6:** Synthesis of MFM

The COSY spectrum of MFM (Figure 2.31) again shows the anticipated correlations between protons in the norbornene ring, confirming its presence in the final material (*i.e.* it has withstood the purification synthesis of the carbamate species from the starting materials). The COSY shows one peak for H<sub>3</sub> that is definite at 1.22 ppm, though the integration did not make sense which made it obvious that H<sub>3</sub> was overlapping with H<sub>5</sub>. Again in the COSY, H<sup>9</sup> and H<sup>10</sup> (at 3.40 – 3.88 and 4.11 – 4.36 ppm) only showed a coupling to one another, since the nearest protons otherwise are 5 bonds away – which would not be seen. The nitrogen proton again at 4.74 ppm (like in the other carbamate species) shows coupling with H<sup>12</sup> (3.08 – 3.30 ppm, orange lines) which in turn couples to H<sup>13</sup> (1.22 – 1.51 ppm) and so on.

The carbamate carbon, C<sup>11</sup>, shows up in the HSQC spectrum (Figure 2.32) in the expected region at 156.2 ppm. Again, there is no isocyanate carbonyl group visible. There are however 3 peaks attributable to the ester carbon (C<sup>8</sup>) in MFM, at 174.6, 175.43 and 176.1 ppm. At first this was assumed to be starting material residue, but none of the other peaks were seen that would suggest this – there was no OH peak in the IR, or the NMR spectrum. This was eventually hypothesised to be a similar phenomenon observed in DFM2 with isomers.

The HSQC spectrum also showed that NH did not correlate to a carbon, which again led to its positive identification (Figure 2.33). The HSQC also proved beyond doubt that the peaks for H<sup>3</sup> and H<sup>5</sup> overlapped since C<sup>7</sup> at 29.4 ppm should correspond to H<sup>5</sup> and H<sup>6</sup> and showed correlation to this mixed peak and H<sup>6</sup> (purple lines). Also, C<sup>3</sup> at 49.7 ppm should only show correlation to H<sup>3</sup> and there was a relation showed between itself and the mixed peak, as well as the lone H<sup>3</sup> peak (orange lines). The carbons C<sup>12</sup> (40.9 ppm), C<sup>13</sup> (32.1 ppm), C<sup>14</sup> (20.0 ppm) and C<sup>15</sup> (13.8 ppm) were also easy to identify, and also further showed the DEPT analysis was valid since C<sup>12</sup>, C<sup>13</sup> and C<sup>14</sup> were shown to be CH<sub>2</sub> environments whereas C<sup>15</sup> is correctly shown to be CH<sub>3</sub>. This technique also shows that C<sup>2</sup> (at 42.7 and 45.8 ppm, red lines) have been correctly identified as CH along with their corresponding exo peaks (all exo correlations shown with dotted lines).

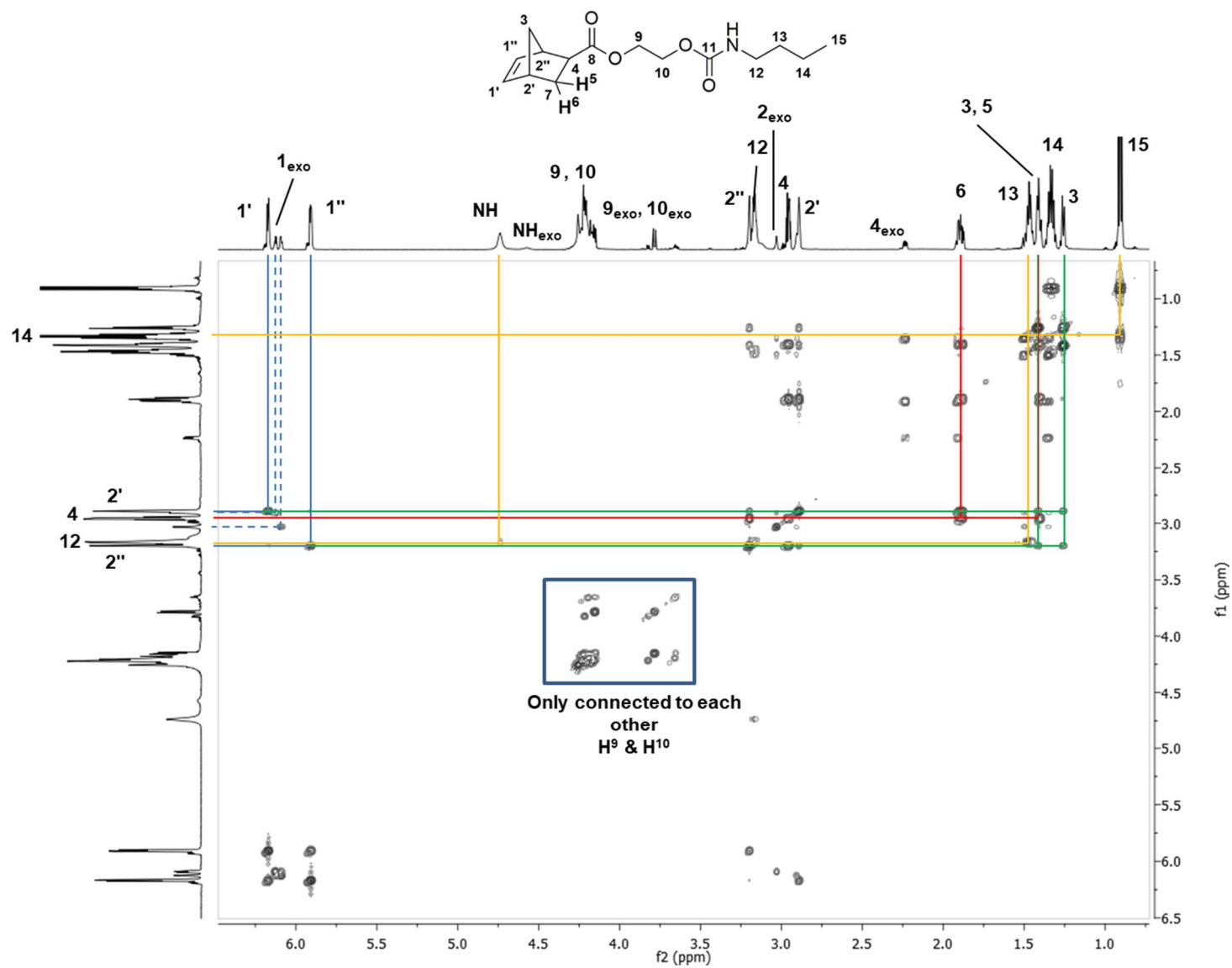


**Figure 2.31:** COSY spectrum (700 MHz,  $\text{CDCl}_3$ ) of MFM

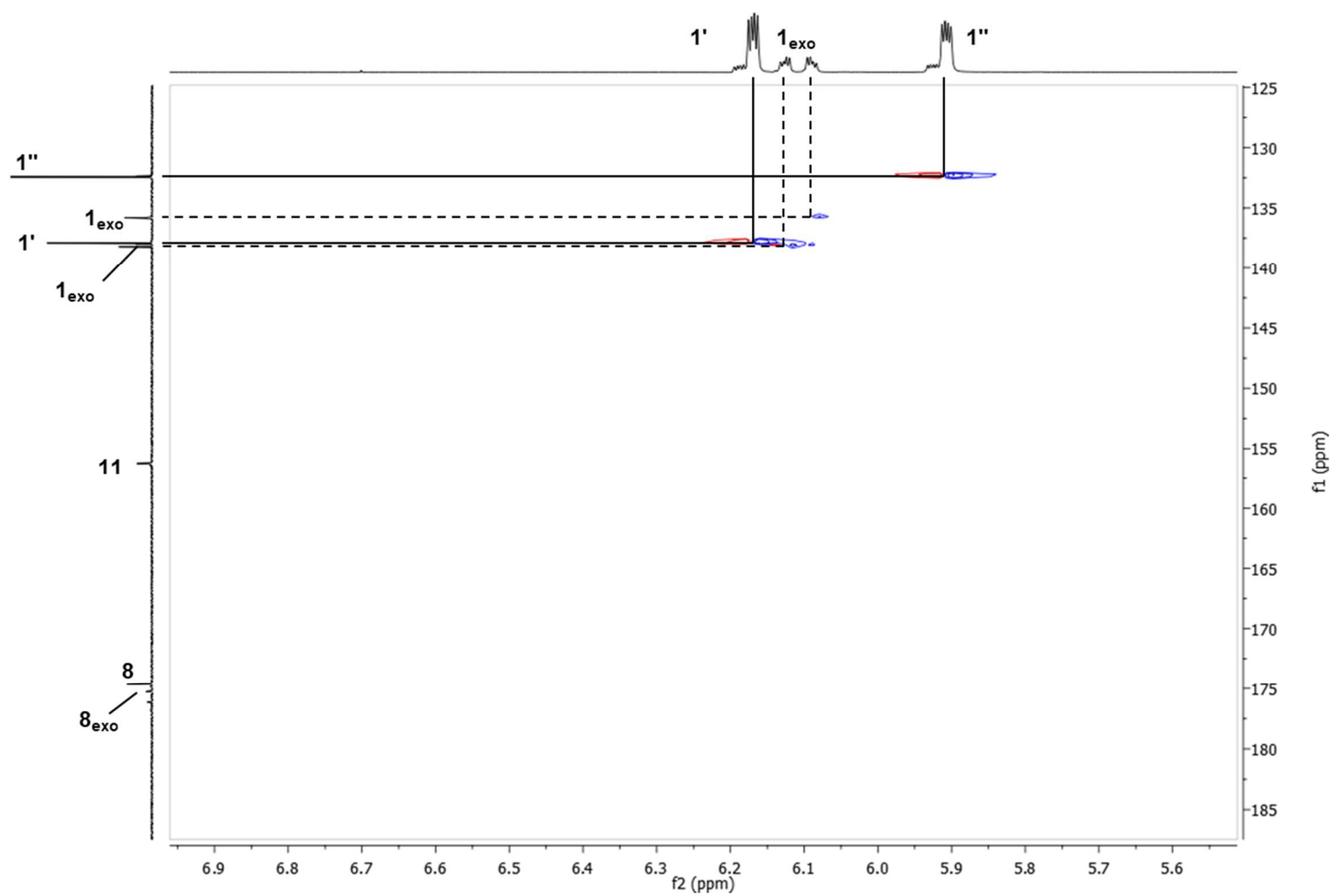
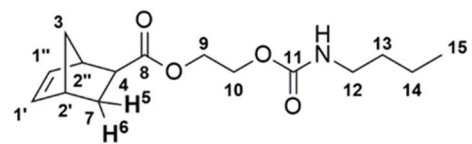


**Figure 2.32:** HSQC spectrum (700 MHz ( $^1\text{H}$ ) and 176 MHz ( $^{13}\text{C}$ ),  $\text{CDCl}_3$ ) of MFM for  $\delta_{\text{H}} = 5.5\text{--}6.9$  ppm and  $\delta_{\text{C}} = 125\text{--}185$  ppm

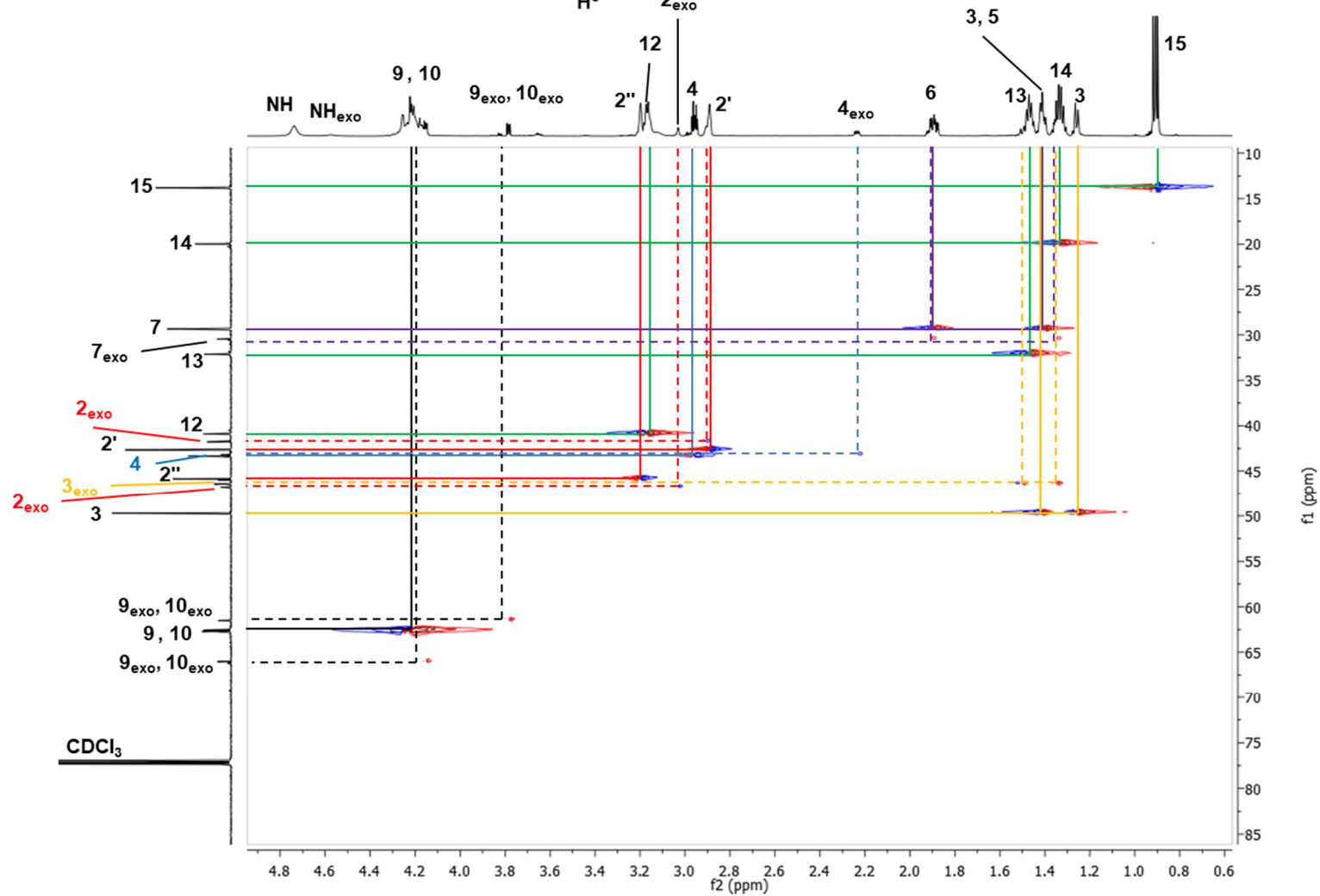


**Figure 2.33:** HSQC spectrum (700 MHz ( $^1\text{H}$ ) and 176 MHz ( $^{13}\text{C}$ ),  $\text{CDCl}_3$ ) of MFM for  $\delta_{\text{H}} = 0.6\text{--}4.9$  ppm and  $\delta_{\text{C}} = 10\text{--}85$  ppm



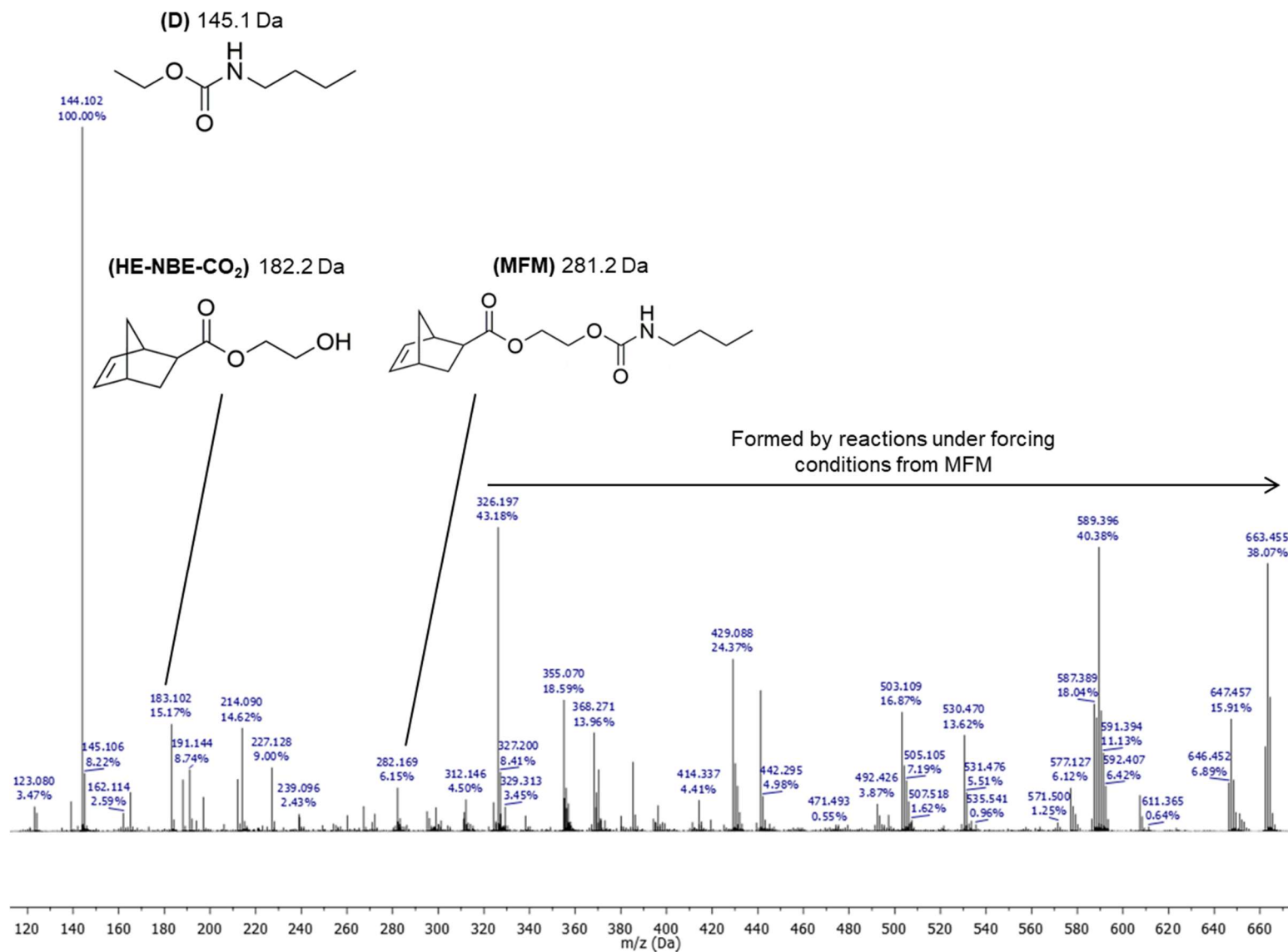
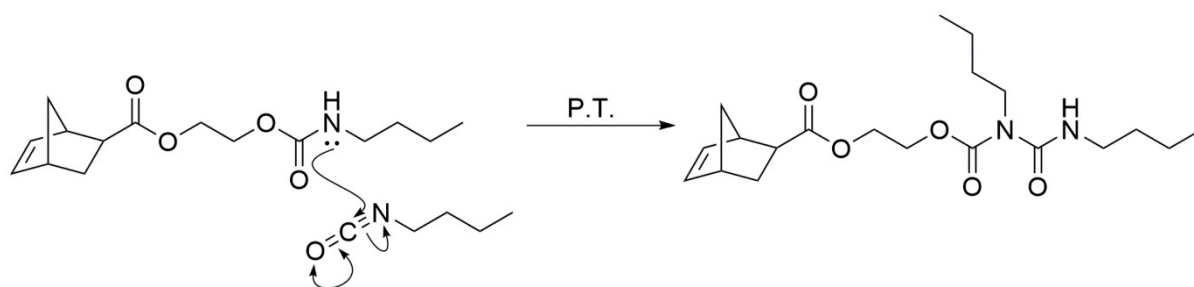


Figure 2.34: ASAP-MS of MFM

Perhaps due to the lower retro Diels-Alder temperature ( $T_{rDA}$ ) of MFM (167 °C), the parent ion in the mass spectrum (Figure 2.34) is much weaker than for DFM2, and even HE-NBE-CO<sub>2</sub>, and the amount of fragmentation seen is much greater. HE-NBE-CO<sub>2</sub>, the starting material of the reaction to form MFM, is seen in this spectrum; as is MFM. This means the peak from HE-NBE-CO<sub>2</sub> could be due to the fragmentation of the weak carbamate group to reform the starting materials. The production of **D** would be due to the fragmentation of the norbornene ester from this species, also forming norbornene carboxylic acid although the peak for this is not observed. It is possible, however, that norbornene carboxylic acid could undergo retro Diels-Alder at an even lower temperature than MFM and form acrylic acid (72.1 Da) and cyclopentadiene (66.1 Da), both of which are lower than the mass threshold of this technique.



**Equation 2.7:** The reaction of *n*-butyl isocyanate with MFM, not the NH in the product which could allow further isocyanate reactions

As is clear, there are many peaks above 282.2 Da which must be combinations of MFM with itself or starting materials (or other fragments). For example, MFM can react through the lone pair on the NH (Equation 2.7) with another butyl isocyanate<sup>21</sup> – the product of which can also react with another isocyanate *etc.* though none of these peaks are seen exactly in the spectrum, but perhaps derivatives of these molecules are (e.g. after retro Diels-Alder, or ester group cleaved).

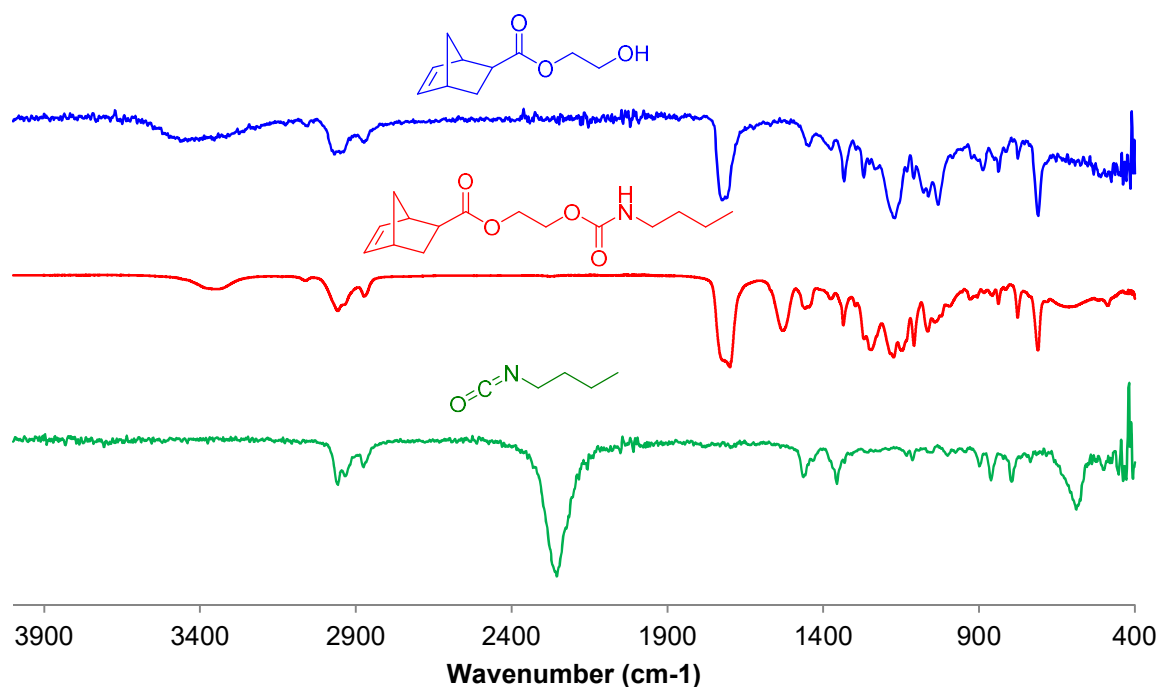


**Figure 2.35:** FT-IR spectra of HE-NBE-CO<sub>2</sub> (blue), MFM (red) and butyl isocyanate (green)

The IR spectrum (Figure 2.35) of MFM shows the absence of both the hydroxyl functionality of HE-NBE-CO<sub>2</sub> around 3150-3600 cm<sup>-1</sup>, and the isocyanate from *n*-butyl isocyanate at 2260 cm<sup>-1</sup>. What can be seen, however, is the important peak at 1540 cm<sup>-1</sup> which is the carbonyl stretch of the carbamate group, and the NH peak at 3400 cm<sup>-1</sup> – also a part of the carbamate group. These all point towards the reaction between the starting materials being successful; and the subsequent removal of them similarly effective. The peak at 590 cm<sup>-1</sup> completely disappears from butyl isocyanate to MFM and is not seen in HE-NBE-CO<sub>2</sub>. There was a corresponding peak at 570 cm<sup>-1</sup> in HDI. This makes it more likely that it was indeed the NCO bend.

The elemental analysis of MFM is again close to the expected percentage make up. The only issue is, once again, with the amount of nitrogen in the system, the possible reasons for which have already been discussed.

### 2.3.10 E-factors

**Table 2.2:** Table of all the E-factors for reactions in Chapter 2

Reaction	Mass of waste (g)	Mass of product (g)	E-factor
Synthesis of EHNBEDC	275.41	21.56	12.77
Synthesis of DFM1	0.00	1.28	0.00
Purification of HEA	781.53	51.40	15.20
Synthesis of HENBECO <sub>2</sub>	74.40	27.70	2.69
Synthesis of DFM2 (from HENBECO <sub>2</sub> )	0.18	5.67	0.03
Synthesis of MFM (from HENBECO <sub>2</sub> )	0.20	5.98	0.03

All the E-factors for reactions in Chapter 2 were calculated, detailed in Table 2.2, which showed that the syntheses of DFM1, DFM2 and MFM were all very 'green' reactions with little or no waste produced. This did not however take into account the production of each of their starting materials. For example, in order to produce the starting material of DFM2 and MFM (HE-NBE-CO<sub>2</sub>), hydroxyethyl acrylate had to be purified. This process of purification had a substantially higher E-factor due to all the solvent being used and repetitive washings. Similarly, the production of HE-NBE-CO<sub>2</sub> itself also involved the use of DCM as a solvent and hence produced 2.7 times as much waste as product was yielded.

The synthesis of DFM1 was seemingly a perfect scenario since all reactants were incorporated into the product, although the synthesis by which 5-norbornene-2-methoxy tetraethylene glycol may have produced waste which was not counted in the E-factor here.

## 2.4 Conclusions

The evidence points towards the fact that all the desired molecules have been successfully synthesised and, where required, purified. In the cases of hexamethylene-1,6-bis(5-norbornene-2-methoxy tetraethylene glycol carbamate) and *N*-(2-ethylhexyl)-5-norbornene-2,3-dicarboximide they are purely the *exo* form, whereas all other molecules are a mixture – and primarily the *endo* isomer. There all have successfully incorporated the norbornene moiety, which was the target to hopefully make them active towards ROMP.

The synthesis of the carbamate containing monomers were shown to be about as green as producing chemicals in the fine chemicals industry,<sup>22</sup> though here the scale is much smaller so hopefully this could be improved upon using a larger scale.

## 2.5 References

1. Stevens, M. P., Preparation and crosslinking of an unsaturated polyester: An organic chemistry experiment. *J. Chem. Educ.* **1967**, *44* (3), 160.
2. Parkyn, B., Chemistry of polyester resins. *Compos.* **1972**, *3* (1), 29-33.
3. Sanchez, E. M. S.; Zavaglia, C. A. C.; Felisberti, M. I., Unsaturated polyester resins: influence of the styrene concentration on the miscibility and mechanical properties. *Polymer* **2000**, *41*, 765-769.
4. DOW, DCPD Product Data Sheet.
5. Updegraff, I. H., Unsaturated Polyester Resins. In *Handbook of Composites*, Lubin, G., Ed. Springer US: Boston, MA, **1982**; pp 17-37.
6. Clark, D. A., *Enyne Metathesis Methods Applied Toward the Total Synthesis of Natural Products*. State University of New York at Buffalo: Buffalo, NY, USA, **2008**.
7. Quan, C.; Soroush, M.; Grady, M. C.; Hansen, J. E.; Simonsick, W. J., High-Temperature Homopolymerization of Ethyl Acrylate and n-Butyl Acrylate: Polymer Characterization. *Macromolecules* **2005**, *38* (18), 7619-7628.
8. Schrock, R. R.; Bazan, G. C.; Khosravi, E.; Feast, W. J.; Gibson, V. C., Living and highly stereoregular ring-opening polymerization of 5,6-difunctionalized norbornadienes by a well-characterized molybdenum catalyst. *Polym. Commun.* **1989**, *30*, 258-260.
9. Schrock, R. R.; Murdzek, J. S.; Bazan, G. C.; Robbins, J.; DiMare, M.; O'Regan, M., Synthesis of molybdenum imido alkylidene complexes and some reactions involving acyclic olefins. *J. Am. Chem. Soc.* **1990**, *112* (10), 3875-3886.
10. Leng, X.; Nguyen, N. H.; van Beusekom, B.; Wilson, D. A.; Percec, V., SET-LRP of 2-hydroxyethyl acrylate in protic and dipolar aprotic solvents. *Polym. Chem.* **2013**, *4* (10), 2995-3004.
11. Khosravi, E.; Al-Hajaji, A. A., Ring Opening Metathesis Polymerisation of N-Alkyl Norbornene Dicarboximides Using Classical Initiators. *Eur. Polym. J.* **1998**, *34* (2), 153-158.
12. Rajsfus, D. E.; Alter-Zilberfarb, S.; Frimer, A. A., The synthesis of fluorinated endcaps: Part 1. The effect of C-7 fluorination on the base-catalyzed monohydrolysis of 5-norbornenyl-2,3-diester. *J. Fluorine Chem.* **2013**, *148*, 49-58.
13. Lapinte, V.; Brosse, J.-C.; Fontaine, L., Synthesis and Ring-Opening Metathesis Polymerization (ROMP) Reactivity of endo-and exo-Norbornenylazlactone Using Ruthenium Catalysts. *Macromol. Chem. Phys.* **2004**, *205* (6), 824-833.
14. Sheldon, R. A., The E Factor: fifteen years on. *Green Chem.* **2007**, *9* (12), 1273-1283.
15. Dotson, N. A., *Polymerization process modeling*. VCH: New York ; Cambridge, **1995**; p 260-279.
16. Adrian, J. H. M. Dicyclopentadiene-dicarboxylic acid reaction products and polyesters thereof. US3306868 A, **1967**.
17. Tuba, R.; Grubbs, R. H., Ruthenium catalyzed equilibrium ring-opening metathesis polymerization of cyclopentene. *Polym. Chem.* **2013**, *4* (14), 3959-3962.
18. Schleyer, P. v. R.; Williams, J. E.; Blanchard, K. R., Evaluation of strain in hydrocarbons. The strain in adamantane and its origin. *J. Am. Chem. Soc.* **1970**, *92* (8), 2377-2386.

19. Clapham, G.; Shipman, M., Selective Lewis Acid Complexation of 2-Hydroxyethyl Esters using Competitive Diels–Alder Reactions as a Mechanistic Probe. *Tetrahedron* **2000**, 56 (8), 1127-1134.
20. Polenz, I.; Schmidt, F. G.; Spange, S., Kinetic studies on the imine base/isocyanate-induced radical polymerization of vinyl monomers. *J. Polym. Sci., Part A: Polym. Chem.* **2012**, 50 (16), 3324-3331.
21. Ulrich, H.; Tucker, B.; Sayigh, A. A. R., Base-catalyzed reactions of isocyanates. Synthesis of 2,4-dialkylallophanates. *J. Org. Chem.* **1967**, 32 (12), 3938-3941.
22. Sheldon, R. A., Organic synthesis - past, present and future. (advantages of incorporating catalysis to organic synthesis). *Chem. Ind. (London)* **1992**, 903-906.

## **Chapter 3. ROMP of Norbornene-Functionalised Polyesters**

### 3.1 Introduction

In 2013, Chih-Pin Hsu *et al.*<sup>1</sup> reported the synthesis of ‘styrene-free unsaturated polyesters’ by ROMP of norbornene-functionalised polyesters using a variety of initiators. Most of the polyester pre-polymers reported by Hsu were multifunctional (Figure 3.1) and when they had undergone ROMP, cross-linked networks were formed. In Chapter 2 it was shown that it was possible to synthesise norbornene-functionalised polyesters. It was therefore decided to investigate whether these pre-polymers could be polymerised using Grubbs ruthenium initiators to produce styrene-free polyesters. The pre-polymers synthesised here contain multiple norbornene groups, and so the gel contents of each could also be investigated as well as the choice of initiator. They also reported that each polyester had a broad dispersity and high  $M_w$ , whereas there are also a few well-defined carbamate monomers in this work (for example, MFM and DFM2).

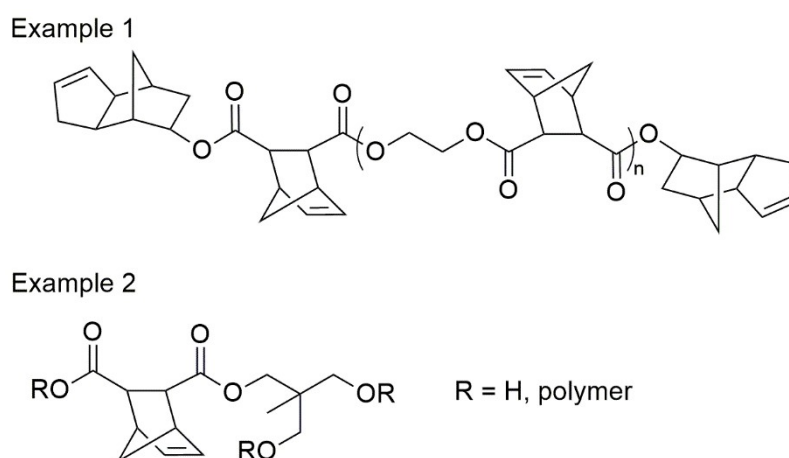


**Figure 3.1:** Two example pre-polymers for ROMP from the patent by Hsu *et al.*

The three initiators used here are Grubbs 1<sup>st</sup> generation, Grubbs 2<sup>nd</sup> generation and modified Grubbs 2<sup>nd</sup> generation (Figure 3.2). They were selected for their high tolerance of functional groups,<sup>2,3</sup> including oxygen and water, which means there is no need for an inert atmosphere. All three initiators also have a high activity for ROMP of norbornene derivatives.

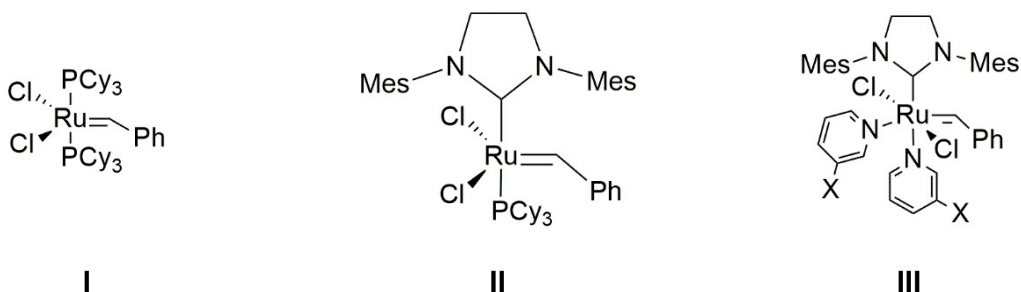


**Figure 3.2:** I) Grubbs 1<sup>st</sup> generation, II) 2<sup>nd</sup> generation, III) modified 2<sup>nd</sup> generation

One of the issues of these initiators, however, is colouring of the resultant polymer, especially at the levels utilised here. At 1 % all polymers produced are dark brown or orange. The exceptions are linear



polymers where the ruthenium can easily be removed from the chain by adding ethyl vinyl ether. This also lowers the ruthenium content of the polymer, which may be advantageous due to its slight toxicity and its high retention in bones.

The extent of cross-linking is established using the sol-gel extraction process. This involves boiling the ground down, cross-linked polymer in DCM under reflux. The idea behind this is that any linear polymer will dissolve in the DCM leaving behind only the insoluble, cross-linked material.

## 3.2 Experimental

### 3.2.1 Instrumentation

Samples were prepared for Dynamic Mechanical and Thermal Analysis (DMTA) by utilising a Specac Thermal Press, Figure 3.3.



**Figure 3.3:** Specac Thermal Press used to form all samples

Following their formation in the thermal press, samples were then analysed using a dual cantilever, Figure 3.4, in a TA Instruments DMA Q800 with liquid nitrogen cooling.

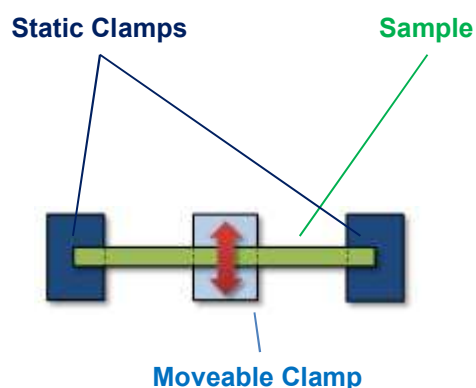


**Figure 3.4:** A photo of a dual cantilever,<sup>4</sup> and a diagram of a cross-section through one<sup>5</sup>

### 3.2.2 Synthesis of pyridine-modified Grubbs 2<sup>nd</sup> generation ruthenium initiator (MG2)

Following the literature method of Grubbs *et al.*,<sup>6</sup> Grubbs 2<sup>nd</sup> generation ruthenium initiator (G2, 100 mg, 0.118 mmol) was dissolved in pyridine (43 mg, 0.05 mL, 0.54 mmol) and the mixture was stirred for 30 min. The solution turned from orange to a bright green colour. The reaction mixture was then precipitated into ice-cold hexane (10 mL). The precipitate was then dried (<1 mbar, 50 °C, 24 h), yielding a green powder (56 mg, 65.3 %). The NMR spectroscopic characterisation was in agreement with the literature.<sup>6</sup>

### 3.2.3 ROMP of *N*-(2-ethylhexyl)-5-norbornene-2,3-dicarboximide (EHNBEDC)

#### 3.2.3.1 ROMP of EHNBEDC with G1

G1 (10 mg, 0.0122 mmol) was dissolved in DCM (2 mL). In a second vial, *N*-(2-ethylhexyl)-5-norbornene-2,3-dicarboximide (EHNBEDC, 336 mg, 1.22 mmol) was dissolved in DCM (2 mL). The monomer containing solution was then added to the initiator, and stirred. The reaction mixture turned from purple to an orange colour. After 24 h, ethyl vinyl ether (EVE, 5 mg) was added to terminate the polymerisation, and the reaction was stirred for a further 10 min – whereupon the mixture was added dropwise to vigorously stirring, ice-cold methanol. The off-white precipitate was dried under reduced pressure (<1 mbar, 50 °C, 24 h). The polymer produced was weighed (214 mg, 63.7 %) and analysed by SEC and NMR spectroscopy. <sup>1</sup>H NMR (700 MHz; CDCl<sub>3</sub>): δ(ppm) = 0.76-0.96 (m, 6 H, 11, 13); 1.11-1.35 (m, 8 H, 8, 9, 10, 12); 1.52-1.84 (m, 2 H, 3); 2.01-2.25 (m, 1 H, 7); 2.57-2.79 (2 × s, br, 2 H, 2) 2.93-3.13 (m, 2 H, 4); 3.16-3.39 (m, 2 H, 6); 5.45-5.54 (m, 0.35 H, 1<sub>trans</sub>); 5.68-5.79 (m, 1.65 H, 1<sub>cis</sub>); <sup>13</sup>C NMR (176 MHz; CDCl<sub>3</sub>): δ(ppm) = 10.5 (13); 14.2 (11); 23.1 (10); 24.0 (9); 28.6 (8); 30.6 (12); 37.4 (7); 41.1 (w, 3) 42.4 (br, 3, 6); 46.0 (2); 46.2 (2); 50.9 (4); 51.1 (4); 52.6 (w, 4); 131.9 (1<sub>trans</sub>); 132.1 (1<sub>cis</sub>); 178.7 (5). SEC:  $M_n = 4.1 \times 10^4$  g mol<sup>-1</sup>,  $M_w = 4.7 \times 10^4$  g mol<sup>-1</sup>, Đ = 1.2.

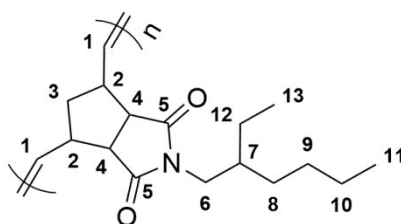


Figure 3.5: Numbered structure of poly(EHNBEDC)

#### 3.2.3.2 ROMP of EHNBEDC with G2

G2 (10 mg, 0.0118 mmol) was dissolved in DCM (2 mL). In a second vial, EHNBEDC (325 mg, 1.18 mmol) was dissolved in DCM (2 mL). The monomer containing solution was then added to the initiator, and stirred. The reaction mixture stayed orange, but the viscosity increased markedly. After 24 h, ethyl vinyl ether (EVE, 5 mg) was added to terminate the polymerisation, and the reaction was stirred for a further 10 min – at which point the mixture was added dropwise to vigorously stirring, ice-cold methanol. The off-white precipitate was dried under reduced pressure (<1 mbar, 50 °C, 24 h). The polymer produced was weighed (285 mg, 87.7 %) and analysed by SEC and NMR spectroscopy.

The NMR spectrum matched the polymer produced using G1. SEC:  $M_n = 5.5 \times 10^5 \text{ g mol}^{-1}$ ,  $M_w = 11 \times 10^5 \text{ g mol}^{-1}$ ,  $\bar{D} = 1.9$ .

### 3.2.3.3 ROMP of EHNBEDC with MG2

MG2 (10 mg, 0.0137 mmol) was dissolved in DCM (2 mL). In a second vial, EHNBEDC (377 mg, 1.37 mmol) was dissolved in DCM (2 mL). The monomer containing solution was then added to the initiator, and stirred. The reaction mixture turned immediately from green to a brown colour. After 24 h, ethyl vinyl ether (EVE, 5 mg) was added to terminate the polymerisation, and the reaction was stirred for a further 10 min – immediately after which the mixture was added dropwise to vigorously stirring, ice-cold methanol. The off-white precipitate was dried under reduced pressure (<1 mbar, 50 °C, 24 h). The polymer produced was weighed (284 mg, 75.3 %) and analysed by SEC and NMR spectroscopy. The NMR spectrum matched the polymer produced using G1. SEC:  $M_n = 4.4 \times 10^4 \text{ g mol}^{-1}$ ,  $M_w = 4.7 \times 10^4 \text{ g mol}^{-1}$ ,  $\bar{D} = 1.1$ .

## 3.2.4 ROMP of norbornene dicarboxylate diethylene glycol phthalic acid polyester (Polyester 1)

### 3.2.4.1 ROMP of Polyester 1 with G1

Polyester 1 (1030 mg, 2.43 mmol(norbornene)) was dissolved in DCM (4 mL) for 16 h. This solution was then added to G1 (20 mg, 0.0243 mmol) and the mixture was agitated. The mixture went solid after 21 min, and could withstand inversion without deforming. The gelled reaction was left for a further 24 h before being broken up into smaller pieces, and stirred under reflux at 40 °C in DCM (40 mL) for 3 h. The brown solid pieces were then isolated by filtration and dried under reduced pressure (<1 mbar, 50 °C, 72 h). The pieces were weighed and the average gel content was calculated. This reaction was repeated three times (567 mg,  $54 \pm 4 \%$ ).

### 3.2.4.2 ROMP of Polyester 1 with G2

Polyester 1 (996 mg, 2.36 mmol(norbornene)) was dissolved in DCM (4 mL) for 16 h. This was then added to G2 (20 mg, 0.0236 mmol) and the mixture was agitated. The mixture went solid after 9 min, and could withstand inversion without deforming. The gelled reaction was left for a further 24 h before being broken up into smaller pieces, and stirred under reflux at 40 °C in DCM (40 mL) for 3 h. The brown solid pieces were then isolated by filtration and dried under reduced pressure (<1 mbar, 50 °C, 72 h). The pieces were weighed and the average gel content was calculated. This reaction was repeated three times (891 mg,  $87 \pm 1 \%$ ).

### 3.2.4.3 ROMP of Polyester 1 with MG2

Polyester 1 (954 mg, 2.26 mmol(norbornene)) was dissolved in DCM (4 mL) for 16 h. This was then added to MG2 (20 mg, 0.0226 mmol) and the mixture was agitated. The mixture went solid after 15 s, and could withstand inversion without deforming. The gelled reaction was left for a further 24 h before being broken up into smaller pieces, and stirred under reflux at 40 °C in DCM (40 mL) for 3 h. The solid pieces were isolated by filtration and dried under reduced pressure (<1 mbar, 50 °C, 72 h). The

pieces were weighed and the average gel content was calculated. This reaction was repeated three times (838 mg,  $87 \pm 1$  %).

### 3.2.5 ROMP of norbornene dicarboxylate propylene glycol polyester (Polyester 2)

#### 3.2.5.1 ROMP of Polyester 2 with G1

Polyester 2 (608 mg, 2.43 mmol(norbornene)) was dissolved in DCM (4 mL) for 16 h. This was then added to G1 (20 mg, 0.0243 mmol) and the mixture was agitated. The mixture went solid after 31 min, and could withstand inversion without deforming. The gelled reaction was left for a further 24 h before being broken up into smaller pieces, and stirred under reflux at 40 °C in DCM (40 mL) for 3 h. The brown solid pieces were then isolated by filtration and dried under reduced pressure (<1 mbar, 50 °C, 72 h). The pieces were weighed and the average gel content was calculated. This reaction was repeated three times (304 mg,  $50 \pm 3$  %).

#### 3.2.5.2 ROMP of Polyester 2 with G2

Polyester 2 (590 mg, ~2.36 mmol(norbornene)) was dissolved in DCM (4 mL) for 16 h. This was then added to G2 (20 mg, 0.0236 mmol) and the mixture was agitated. The mixture went solid after 12 min, and could withstand inversion without deforming. The gelled reaction was left for a further 24 h before being broken up into smaller pieces, and stirred under reflux at 40 °C in DCM (40 mL) for 3 h. The brown solid pieces were then isolated by filtration and dried under reduced pressure (<1 mbar, 50 °C, 72 h). The pieces were weighed and the average gel content was calculated. This reaction was repeated three times (555 mg,  $91 \pm 2$  %).

#### 3.2.5.3 ROMP of Polyester 2 with MG2

Polyester 2 (566 mg, ~2.26 mmol(norbornene)) was dissolved in DCM (4 mL) for 16 h. This was then added to MG2 (20 mg, 0.0226 mmol) and the mixture was agitated. The mixture went solid after 17 s, and could withstand inversion without deforming. The gelled reaction was left for a further 24 h before being broken up into smaller pieces, and stirred under reflux at 40 °C in DCM (40 mL) for 3 h. The solid pieces were then isolated by filtration and dried under reduced pressure (<1 mbar, 50 °C, 72 h). The pieces were weighed and the average gel content was calculated. This reaction was repeated three times (517 mg,  $88 \pm 1$  %).

### 3.2.6 ROM copolymerisation of norbornene dicarboxylate diethylene glycol phthalic acid polyester (Polyester 1) with *N*-(2-ethylhexyl)-5-norbornene-2,3-dicarboximide (EHNBEDC)

Polyester 1 (5/10/15 %) was dissolved in EHNBEDC (95/90/85 %) for 24 h. To this was then added the initiator (G1/G2, 1/100<sup>th</sup> equivalent with respect to norbornene (NBE)). The reaction mixture was left for 24 h, and then stirred under reflux at 40 °C in DCM (30 mL) for 3 h. The insoluble gel product was isolated by filtration, and dried under reduced pressure (<1 mbar, 50 °C, 72 h). The gel contents were calculated (11 – 64 %).

### 3.2.7 ROM copolymerisation of norbornene dicarboxylate propylene glycol polyester (Polyester 2) with *N*-(2-ethylhexyl)-5-norbornene-2,3-dicarboximide (EHNBDIC)

Polyester 2 (5/10/15 %) was dissolved in EHNBDIC (95/90/85 %) for 24 h. To this was then added the initiator (G1/G2, 1/100<sup>th</sup> equivalent with respect to NBE). The reaction mixture was left for 24 h, and then stirred under reflux at 40 °C in DCM (30 mL) for 3 h. The insoluble gel product was isolated by filtration, and dried under reduced pressure (<1 mbar, 50 °C, 72 h). The gel contents were calculated (30 – 74 %).

### 3.2.8 In-mould bulk ROM copolymerisation of *N*-(2-ethylhexyl)-5-norbornene-2,3-dicarboximide (EHNBDIC) and norbornene dicarboxylate diethylene glycol phthalic acid polyester (Polyester 1) for DMTA testing

Norbornene dicarboxylate diethylene glycol phthalic acid polyester (Polyester 1) (0 – 143 mg, 0.00 – 0.34 mmol(NBE)) was dissolved in *N*-(2-ethylhexyl)-5-norbornene-2,3-dicarboximide (EHNBDIC) (529 – 622 mg, 1.92 – 2.26 mmol) in a vial at 100 °C, overnight. To this, MG2 (10 mg, 0.113 mmol) was added, vigorously stirred for 5 s, and transferred to a rectangular mould (20 × 10 × 0.5 mm). The sample was transferred to the thermal press and pressed for 40 min (85 °C, 6 – 8 tonnes). The sample was placed in the DMTA clamp and subjected to an amplitude of 1 µm at 1 Hz. The temperature was then raised from -120 °C to 200 °C at a rate of 2 ° per min. The storage and loss moduli, and tan(δ), were monitored, and the T<sub>g</sub> was calculated (27.6 – 70.8 °C).

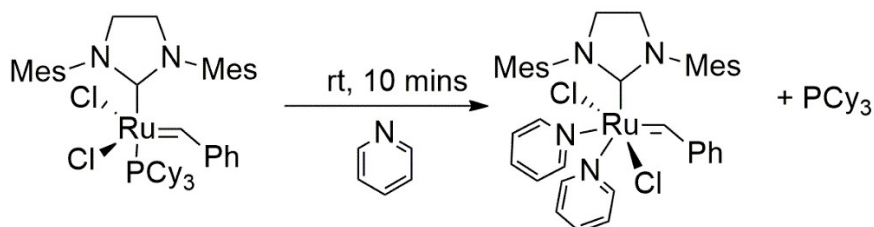
### 3.2.9 In-mould bulk ROM copolymerisation of *N*-(2-ethylhexyl)-5-norbornene-2,3-dicarboximide (EHNBDIC) and norbornene dicarboxylate propylene glycol polyester (Polyester 2) for DMTA testing

Norbornene dicarboxylate propylene glycol polyester (Polyester 2) (0 – 85 mg, 0.00 – 0.34 mmol(NBE)) was dissolved in EHNBDIC (529 – 622 mg, 1.92 – 2.26 mmol) in a vial at 100 °C, overnight. To this, MG2 (10 mg, 0.113 mmol) was added, vigorously stirred for 5 s, and transferred to a rectangular mould (20 × 10 × 0.5 mm). The sample was transferred to the thermal press and pressed for 40 min (85 °C, 6 – 8 tonnes). After this, the sample was placed in the DMTA clamp and subjected to an amplitude of 1 µm at 1 Hz. The temperature was then raised from -120 °C to 200 °C at a rate of 2 ° per min. The storage and loss moduli, and tan(δ), were monitored, and the T<sub>g</sub> was calculated (29.8 – 70.8 °C).

### 3.3 Results and Discussion

#### 3.3.1 Synthesis of pyridine-modified Grubbs 2<sup>nd</sup> generation ruthenium initiator (MG2)

Modified Grubbs 2<sup>nd</sup> generation ruthenium initiator (Dichloro[1,3-bis(2,4,6-trimethylphenyl)-2-imidazolidinylidene](benzylidene)bis(pyridine)ruthenium(II), MG2), was prepared by the reaction of Grubbs 2<sup>nd</sup> generation ruthenium initiator (G2) with pyridine (Equation 3.1).<sup>6</sup>



**Equation 3.1:** The synthesis of MG2 from G2

This reaction is fast, and can be undertaken at ambient conditions – achieving as much as 89 % yield with 10 equivalents of pyridine.<sup>7</sup> This produces MG2: a quicker activating version of G2 – due to the increased lability, under olefin metathesis conditions, of the pyridine ligand. The <sup>1</sup>H NMR spectrum matched the literature,<sup>6</sup> including the alkylidene proton signal at 19.17 ppm. A colour change of orange-brown to bright green also confirms the synthesis of MG2 from G2. A comparison of the three alkylidene peaks in the <sup>1</sup>H NMR spectra of G1, G2 and MG2 can be seen in Figure 3.6.

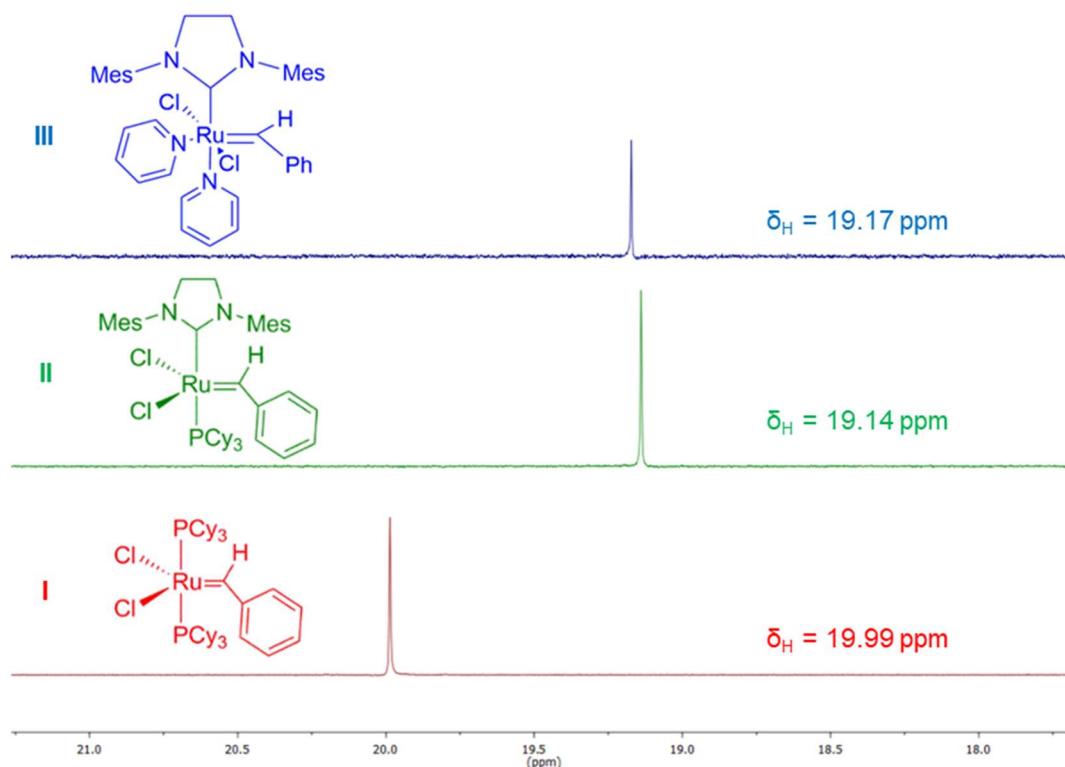
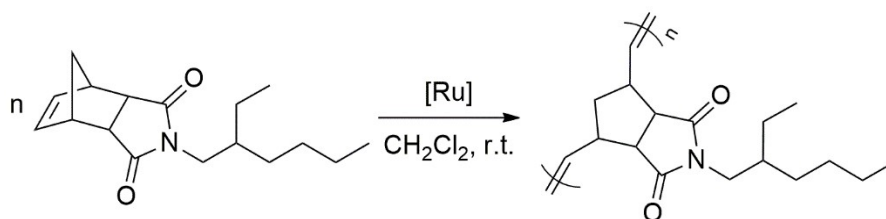


**Figure 3.6:** <sup>1</sup>H NMR (700 MHz, CDCl<sub>3</sub>) spectra showing the alkylidene protons of I) MG2, II) G2, and III) G1

### 3.3.2 ROMP of *N*-(2-ethylhexyl)-5-norbornene-2,3-dicarboximide (EHNBEDC)

EHNBEDC was subjected to ROMP using Grubbs ruthenium initiators to prepare poly(EHNBEDC) (Equation 3.2).



**Equation 3.2:** ROMP of EHNBEDC with ruthenium initiators G1, G2 or MG2

The polymerisation of EHNBEDC, and other alkyl norbornene dicarboximides, is well studied.<sup>8-9</sup> Using G1, G2 and MG2 to polymerise EHNBEDC produced identical NMR spectra, except for the *cis/trans* ratios. The NMR of poly(EHNBEDC) produced utilising G1 was used to determine all of the peaks. In Figure 3.7, the backbone unsaturation ( $H^1$ ) can easily be seen between 5.42 and 5.79 ppm – with *trans* occurring at a higher shift than *cis*.<sup>10-11</sup> This can immediately help us find  $H^2$  at 2.57 – 2.79 ppm as these are the only other protons to correlate to  $H^1$  in the COSY, shown by the black lines.  $H^2$  shows correlation too to  $H^3$  (at 2.01 – 2.22 ppm) and  $H^4$  (between 2.93 and 3.13 ppm). The only ways to tell the difference with these is the fact that  $H^4$  will be more deshielded, and thus appear at a higher chemical shift; or that  $H^3$  is in a  $CH_2$  environment and  $H^4$  is CH. This shows up in the DEPT spectrum when correlated to their relevant carbons (Figure 3.9), with  $C^3$  appearing at 42.4 ppm and  $C^4$  at 50.9 and 51.1 ppm, confirming their original assignment.  $H^{6-12}$  appear in roughly the same regions as the EHNBEDC monomer, and also correlate correctly as shown that  $H^6$  (3.16 – 3.39 ppm) relates to  $H^7$  (red line, 1.52 – 1.84 ppm). This in turn correlates to  $H^8$  and  $H^{12}$  (green) but these overlap, along with  $H^9$  and  $H^{10}$  with all of them appearing between 1.11 and 1.35 ppm. The correlation to  $H^{11}$  and  $H^{13}$  can still be seen however, as shown with the orange lines. These appear in the  $^1H$  NMR overlapping between 0.76 and 0.96 ppm.

$C^5$  can easily be identified in Figure 3.8 as it has the highest chemical shift in the polymer, at 178.7 ppm, and is a quaternary carbon environment – *i.e.* does not show up in the DEPT.  $C^1$  is facile to locate too, at 132.1 (*cis*) and 131.9 ppm (*trans*), as these are found in the double bond region of the carbon NMR spectrum, clearly correlate to  $H^1$ , and are CH environments. Figure 3.9 shows three carbon peaks for  $C^4$  at 50.9, 51.1 and 52.6 ppm (black lines), which suggest that there could be some isomerisation of the two rings (*i.e.* *endo/exo*) even though the starting material for producing EHNBEDC was enantiomerically pure. This could have been during the initial production of EHNBEDC or its polymerisation and would also explain why so many of the environments have more than expected peaks attributable. This also shows us that  $C^2$  (46.0 and 46.2 ppm) and  $C^7$  (37.4 ppm) are also CH groups as expected – clearly differentiating the peaks relating to 7 (green) and 3 (yellow). DEPT also shows that the peaks attributed to 4 are correctly assigned and do not belong to 6 – which is a  $CH_2$  environment.

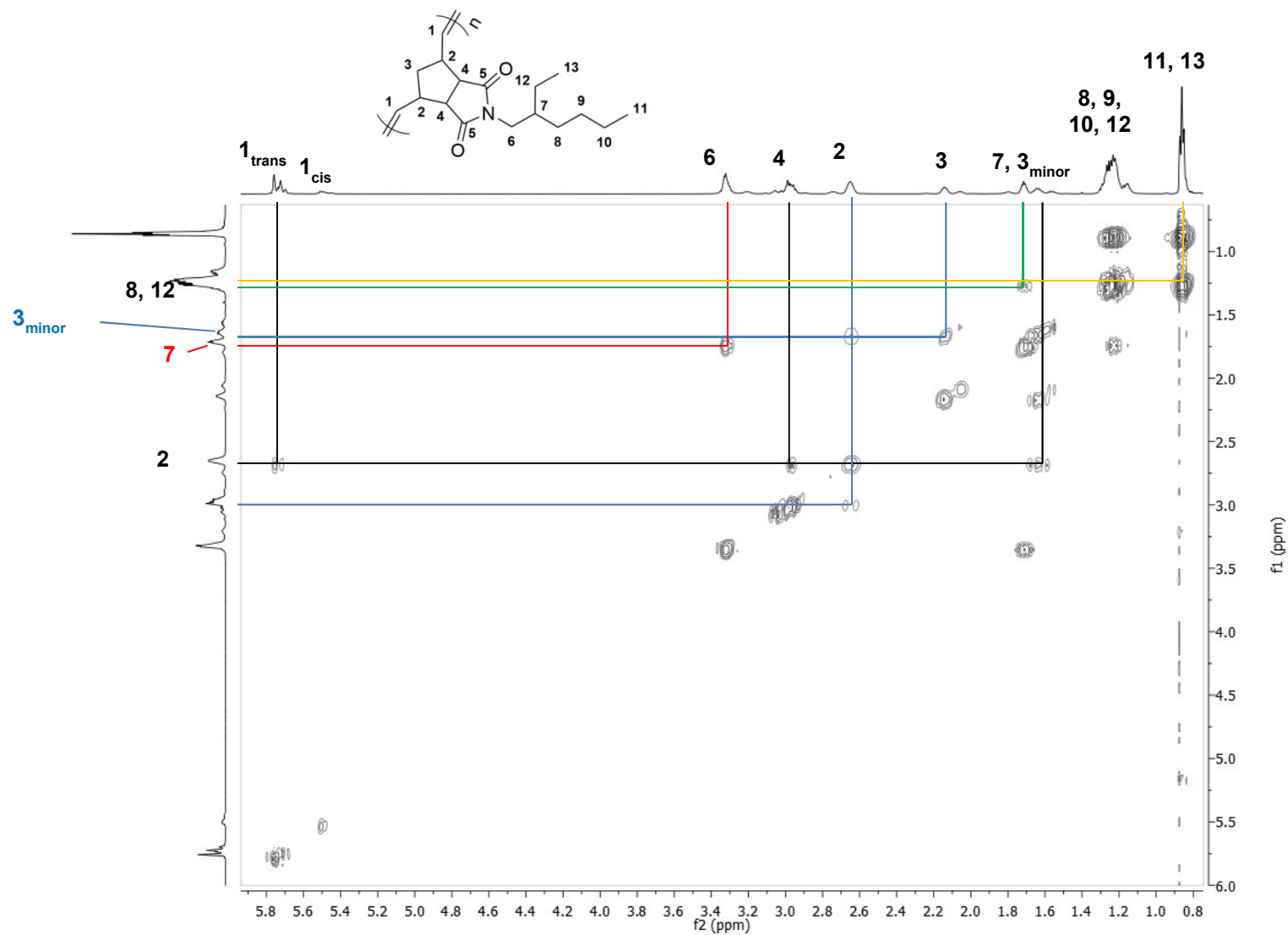


**Figure 3.7:** COSY spectrum (700 MHz,  $\text{CDCl}_3$ ) of poly(EHNBEDC)



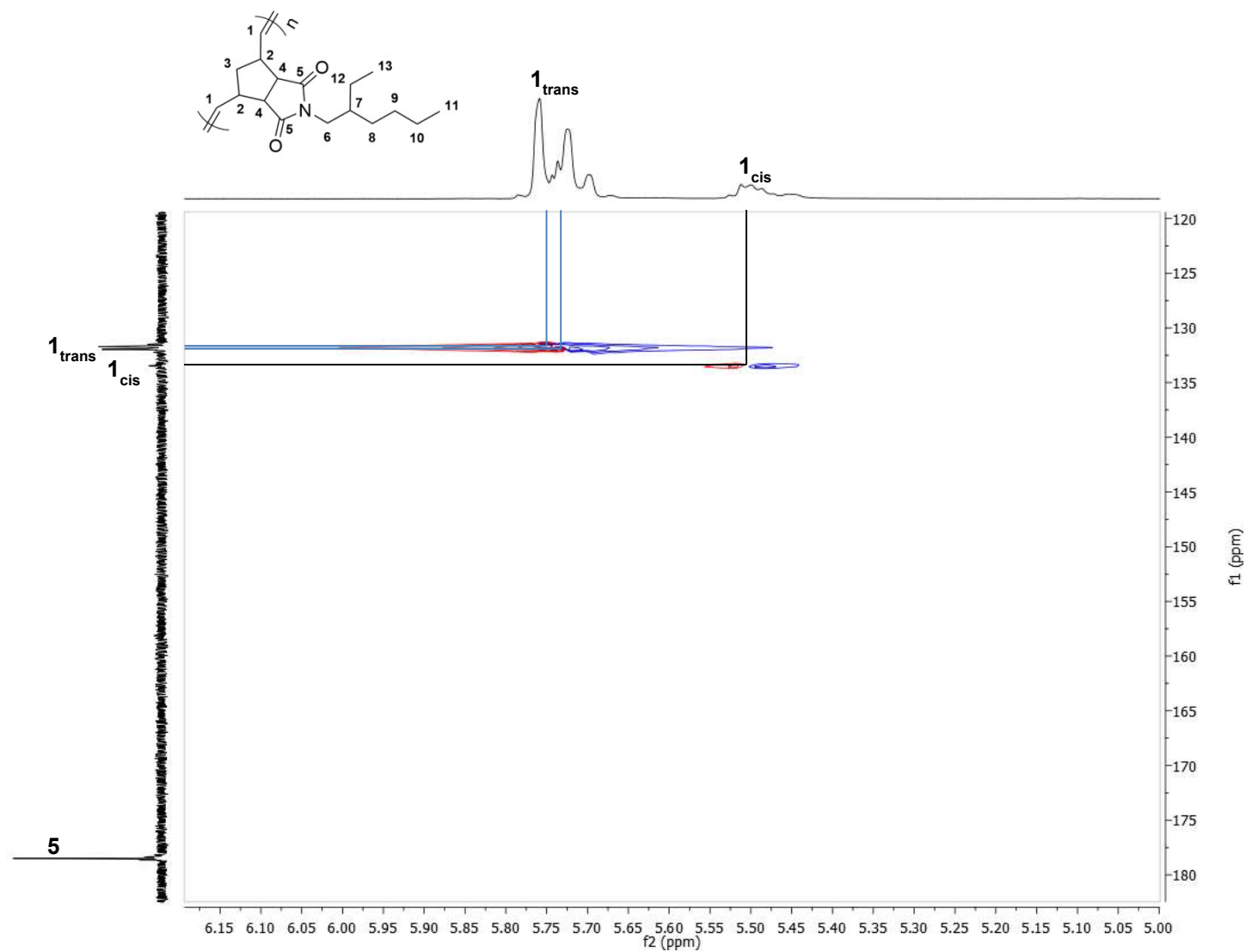


**Figure 3.8:** HSQC spectrum (700 MHz ( $^1\text{H}$ ) and 176 MHz ( $^{13}\text{C}$ ),  $\text{CDCl}_3$ ) of poly(EHNBEDC) for  $\delta_{\text{H}} = 5.0\text{-}6.2$  ppm and  $\delta_{\text{C}} = 120\text{-}185$  ppm

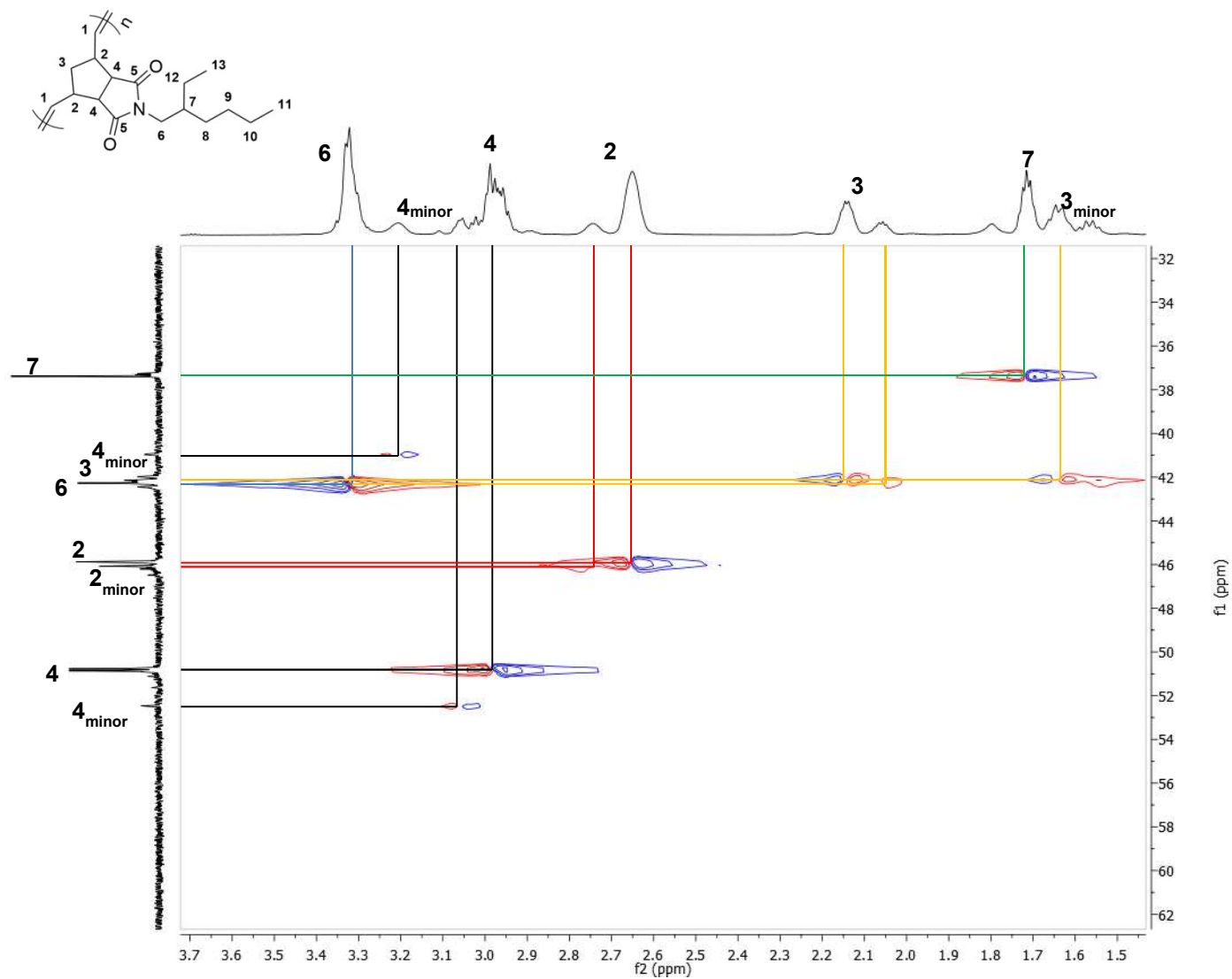


**Figure 3.9:** HSQC spectrum (700 MHz ( $^1\text{H}$ ) and 176 MHz ( $^{13}\text{C}$ ),  $\text{CDCl}_3$ ) of poly(EHNBEDC) for  $\delta_{\text{H}} = 1.4\text{--}3.7$  ppm and  $\delta_{\text{C}} = 32\text{--}62$  ppm

The final part of the spectrum contain multiple protons (Figure 3.10) overlapped but the  $^{13}\text{C}$ , Heteronuclear Single Quantum Correlation experiment (HSQC) and DEPT correctly show that there should be four  $\text{CH}_2$  ( $\text{C}^8$ ,  $\text{C}^9$ ,  $\text{C}^{10}$ ,  $\text{C}^{12}$ ) and two  $\text{CH}_3$  ( $\text{C}^{11}$  and  $\text{C}^{13}$ ) peaks in this region. These  $^{13}\text{C}$  shifts roughly correspond to the monomer's peaks, and so EHNBEDC was used to assign all the peaks – which match the polarity shown; which is expected since the environments of these carbons, from monomer to polymer, is unlikely to have altered considerably. Those assignments are summarised in Table 3.1.

**Table 3.1:** Summary of some  $^{13}\text{C}$  NMR (176 MHz,  $\text{CDCl}_3$ ) shifts in poly(EHNBEDC)

Carbon	$\delta_{\text{c}}(\text{ppm})$
$\text{C}^8$	28.6
$\text{C}^9$	24.0
$\text{C}^{10}$	23.1
$\text{C}^{11}$	14.2
$\text{C}^{13}$	10.5

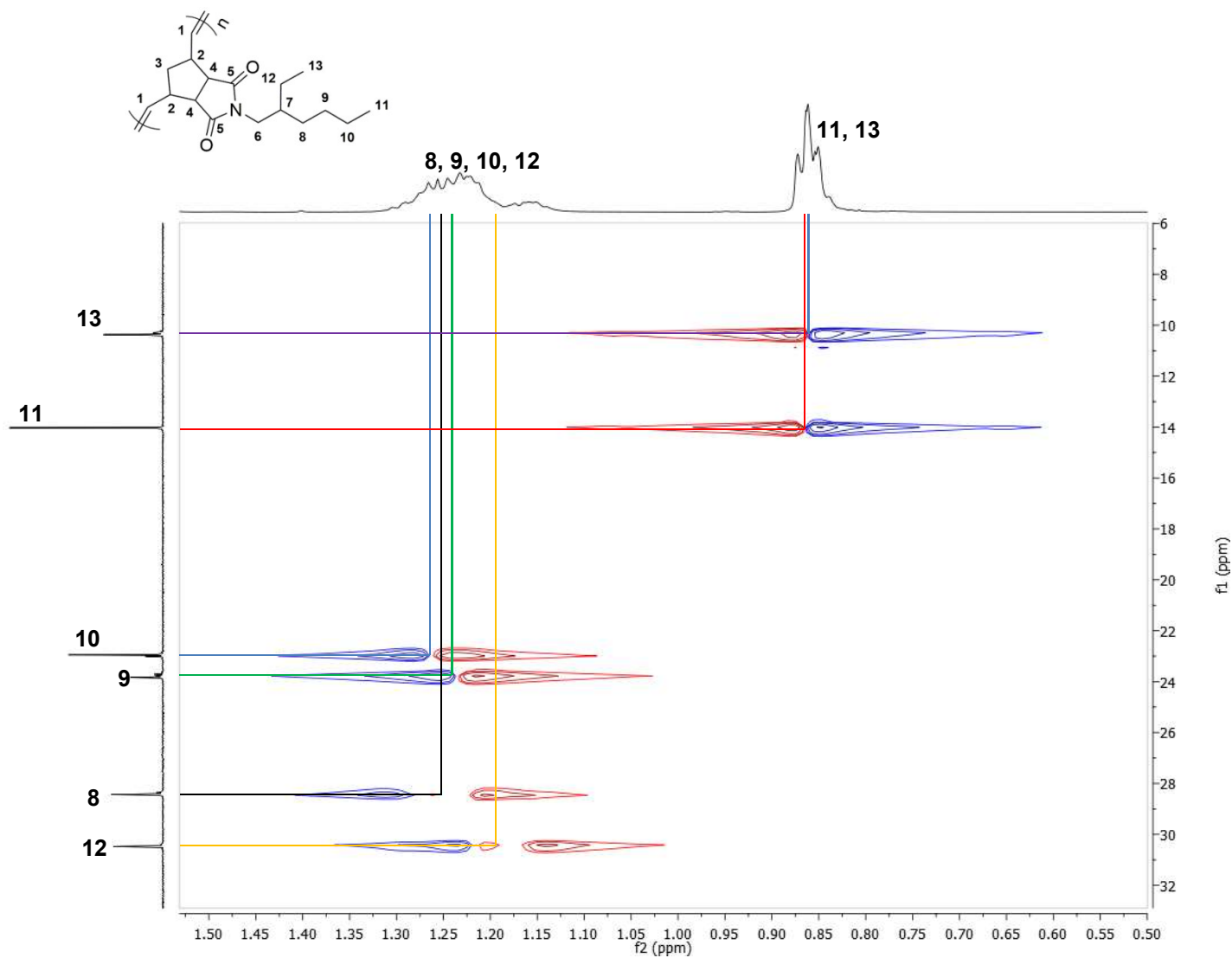


**Figure 3.10:** HSQC spectrum (700 MHz ( $^1\text{H}$ ) and 176 MHz ( $^{13}\text{C}$ ),  $\text{CDCl}_3$ ) of poly(EHNBEDC) for  $\delta_{\text{H}} = 0.5\text{--}1.5$  ppm and  $\delta_{\text{C}} = 6\text{--}32$  ppm

The yields of polymer achieved varied according to the initiator used and the SEC shows the three initiators produce polymers with varied molecular weights ( $M_n$  and  $M_w$ ) and dispersities ( $\bar{D}$ ), Table 3.2.

**Table 3.2:** SEC and theoretical data for ROMP of EHNBEDC with different initiators

Polymer	Initiator	M : I	Yield (%)	<i>cis</i> : <i>trans</i>	$M_n^{th}$	$M_n^{SEC}$ ( $\times 10^3 \text{ g mol}^{-1}$ )	$M_w^{SEC}$	$\bar{D}$
<b>E</b>	G1	100 : 1	63.7	1 : 2.8	28	41	47	1.2
<b>F</b>	G2	100 : 1	87.7	1 : 2.1	28	550	1100	1.9
<b>G</b>	MG2	100 : 1	75.3	1 : 0.9	28	44	47	1.1

Since G1 is the least active of the three initiators it is no surprise that the yield is lower. G2 is very slow to initiate, almost 1/100<sup>th</sup> as quick to initiate as G1,<sup>12</sup> but the propagation rate is reported to be high.<sup>13</sup> This means that the dispersity is vastly broadened due to perhaps only a small percentage of the initiator being active at any one time, as can be seen in Table 3.2. This also results in a much larger monomer to initiator ratio than the theoretical, and therefore we see much higher  $M_n$  and  $M_w$  than when using the other initiators.

These polymers were only made once and analysed by SEC once, meaning there is an increased chance of error both due to synthetic and measurement. Coupled to this is the fact that the SEC was calibrated with polystyrene standards that are not representative of the polymer systems used in this work. This means that the dispersity and molecular weights are perhaps slightly unreliable and only really comparable to one another.

Finally, what can be noted is that SEC measured  $M_n$  for **E** and **G** are roughly 1.5 times that of the theoretical values – giving approximate chain lengths of 146 and 157, respectively, rather than 100 monomer units. Although G1 and MG2 have much better initiating characteristics (than G2), one possible explanation could be that the ROMP of EHNBEDC is still rapid in comparison due to high ring strain of the norbornene moiety.

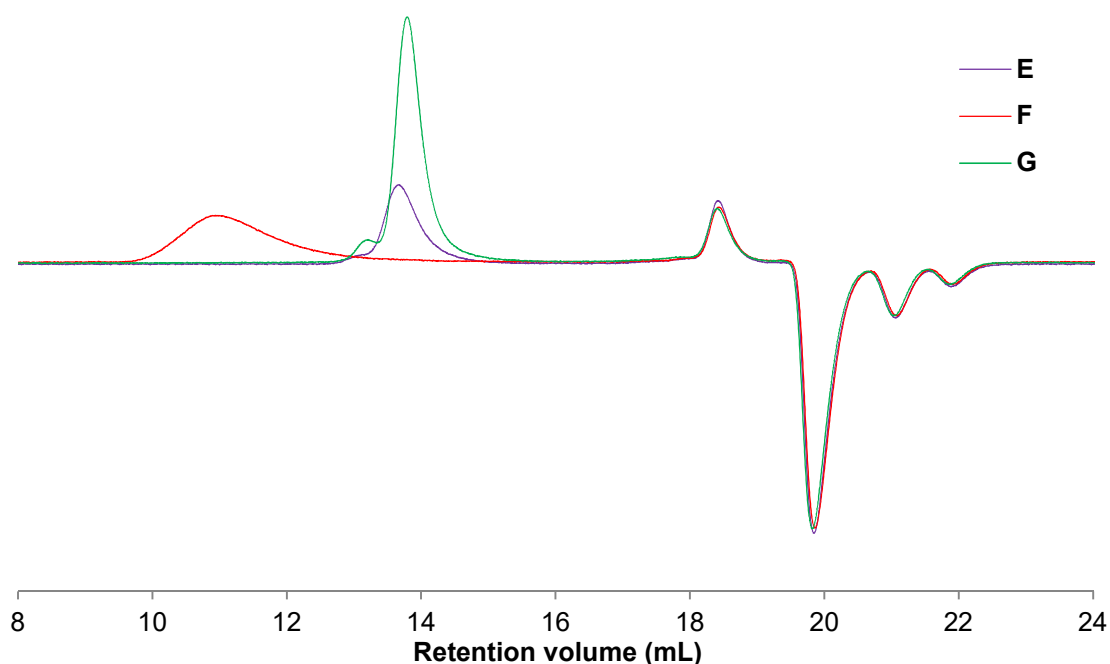


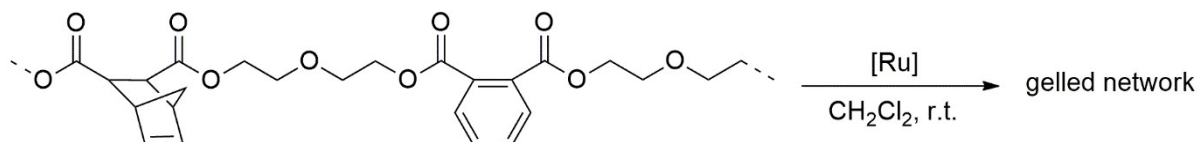
**Figure 3.11:** SEC-RI trace of poly(EHNBEDC) produced using G1 (**E**, purple), G2 (**F**, red), and MG2 (**G**, green)

In SEC, Figure 3.11, **F** elutes earlier than **E** or **G** which proves it is higher molecular weight, confirming the values from the table. The peak due to **F** is also much broader than the other peaks. This shows that the dispersity is much broader – caused by the slow initiation ( $k_i$ ) and rapid propagation ( $k_p$ ) of the 2<sup>nd</sup> generation initiator.<sup>14</sup>

The only slight surprise is that the trace of **G** shows a slight bimodal distribution with a small higher molecular weight peak (at about 13.5 mL). Possible reasons for this could be poor mixing or perhaps back-biting as described in Chapter 1. Usually polymerisation with MG2 is the most controlled since rate of initiation ( $k_i$ ) and propagation are both rapid.<sup>14</sup>

### 3.3.3 ROMP of norbornene dicarboxylate diethylene glycol phthalic acid polyester (Polyester 1)

Polyester 1 was subjected to ROMP using Grubbs ruthenium initiators: G1, G2 and MG2 (Equation 3.3).



**Equation 3.3:** ROMP of Polyester 1 with G1, G2 or MG2 ([Ru])

Firstly, the fact this formed a gel proves the polymerisation was successful. It also indicates that there must be more than one norbornene group – on average – per chain in norbornene dicarboxylate diethylene glycol phthalic acid polyester (Polyester 1), or else the cross-linked network would be unachievable.

The gel content was calculated using a DCM extraction. Drying the gel was achieved over several days since the DCM could become trapped inside the gel and would inflate the mass disproportionately; which is also why the gel was weighed periodically.

**Table 3.3:** Gel contents and times of poly(Polyester 1)

Polymer	Initiator	Gel content (%)	Gel time (s)
<b>H</b>	G1	54 ± 4	1260
<b>I</b>	G2	87 ± 1	540
<b>J</b>	MG2	87 ± 1	15

The data in Table 3.3 shows that – as expected – the choice of Grubbs initiator has a massive effect on gel time of Polyester 1. Grubbs 1<sup>st</sup> generation is the least active and therefore it is no surprise that it takes the longest to gel, as the polymerisation will be much slower than the other two initiators. Grubbs 2<sup>nd</sup> generation is slow to initiate but quick to propagate. The modified Grubbs 2<sup>nd</sup> generation initiator retains G2's quick propagation rate, but also is activated much faster – it is therefore no surprise that **J** has such a short gel time as the ROMP will be rapid.

The data in Table 3.3 also shows that the choice of initiator may have an effect on the gel content. Each polymer was prepared a total of three times in order to quantify the error and show that the fact the gel content of **H** was definitely lower than **I** or **J** rather than just within experimental error. The fact that **H** has such a low gel content is most likely due to the lower activity of G1 in comparison to G2 and MG2. G2 and MG2 result in two almost identical gel contents which suggests that this is probably the maximum gel content achievable with Polyester 1 due to MG2's characteristic high activity and swift activation.

The soluble part of the DCM extraction was also investigated by NMR spectroscopy (Figure 3.12). The NMR spectrum quite clearly shows that the extract contains Polyester 1, suggesting that the gelation prevents the completion of the reaction despite the presence of free norbornene groups in the mixture. The integration of the norbornene double bonds, between 5.83 and 6.27 (highlighted in red), has actually decreased in the final product, with respect to the rest of the peaks, by about a third. This means that as well as norbornene functionalised chains in this extract, we are also left with chains containing no norbornene-functionality attached. This reduces the relative integration of the norbornene double bond with respect to the peaks from the phthalic acid (7.38 – 7.80 ppm, highlighted in blue) and diethylene glycol (3.45 – 4.47 ppm, highlighted in green) moieties.

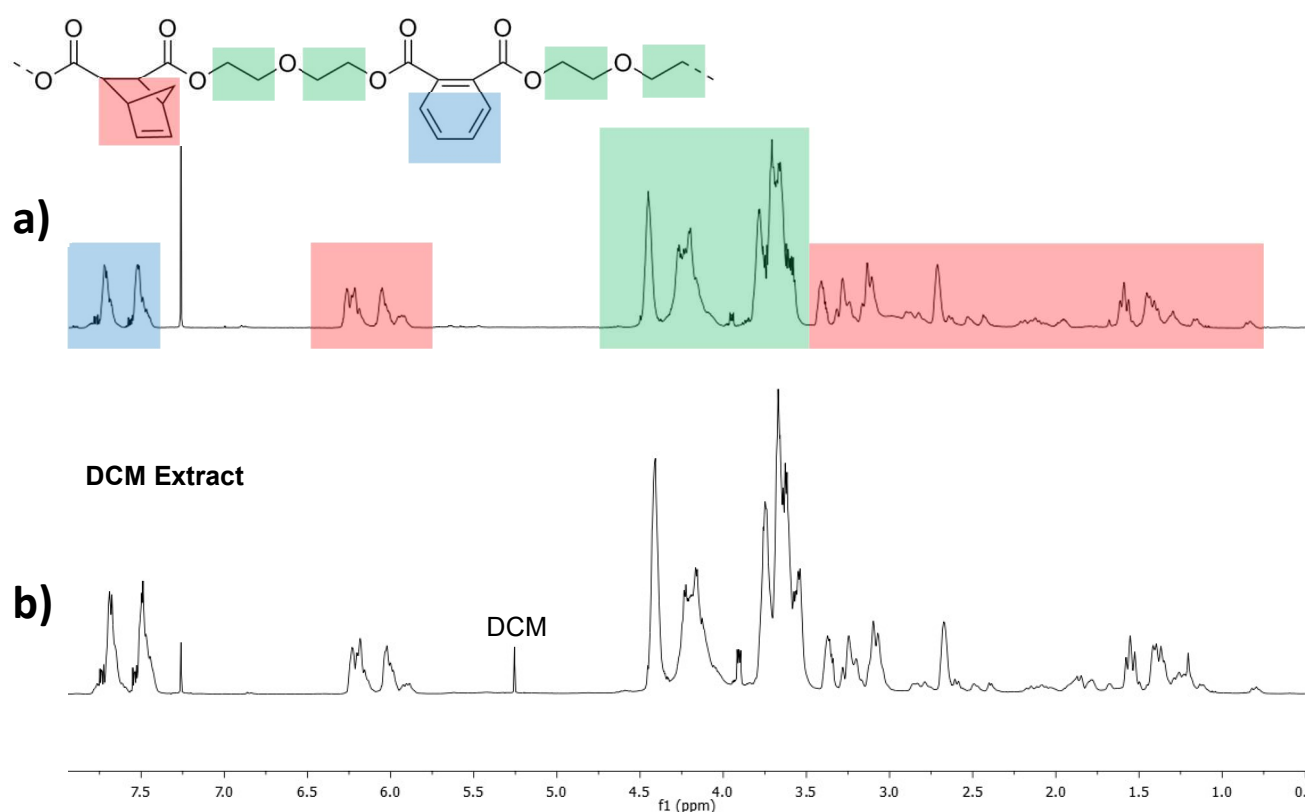
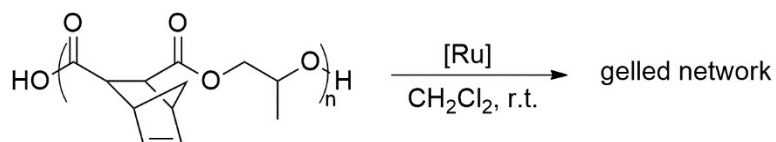


**Figure 3.12:**  $^1\text{H}$  NMR spectra (700 MHz,  $\text{CDCl}_3$ ) of a) Polyester 1 with regions highlighted for clarity, and b) DCM extract of ROMP product

### 3.3.4 ROMP of norbornene dicarboxylate propylene glycol polyester (Polyester 2)

Polyester 2 was subject to ROMP using Grubbs ruthenium initiators: G1, G2 and MG2 (Equation 3.4).



**Equation 3.4:** ROMP of Polyester 2 with G1, G2 or MG2 ( $[\text{Ru}]$ )

The ROMP reaction successfully forms a cross-linked network using each of the three initiators. This also indicates that Polyester 2 – on average – contains two or more norbornene functional groups per chain. The extraction of poly(Polyester 2) was treated exactly the same as that for Polyester 1.



**Table 3.4:** Gel contents and times of poly(Polyester 2)

Polymer	Initiator	Gel content (%)	Gel time (s)
<b>K</b>	G1	50 ± 3	1860
<b>L</b>	G2	91 ± 2	720
<b>M</b>	MG2	88 ± 1	17

As shown in Table 3.4, **K** has the lowest gel content due to the lower reactivity of G1. This again means that Polyester 2 is not polymerised to a great degree as with G2 or MG2. **L** has the highest gel content, and therefore – in all likelihood – the highest degree of cross-linking. This is due to the high reactivity of G2, though it may be surprising therefore that MG2 produces **M** with the same gel content, within experimental error.

The DCM fraction of the ROMP product shows some peaks attributable to the starting material (Polyester 2) in Figure 3.13. The relative ratio between the proton integration of the norbornene olefin (peaks appearing between 5.90 and 6.33 ppm) and glycol (3.83 – 5.24 ppm) barely changes between the starting material and the DCM fraction. This suggests that most chains must have at least one norbornene group attached. If not, after ROMP of the polyester, the DCM fraction would see a relative decrease in olefinic protons.

Unlike Polyester 1, where phthalic and maleic acid are in competition to react with the glycol, Polyester 2 only contains one acid and one glycol. This means that all the acid incorporated into the pre-polymer backbone must be norbornene functionalised. If the acid is not incorporated, the result would simply be monomeric propylene glycol – and this would have been removed when placed under high vacuum, which was used to remove the dicyclopentadiene when Polyester 2 was initially synthesised.

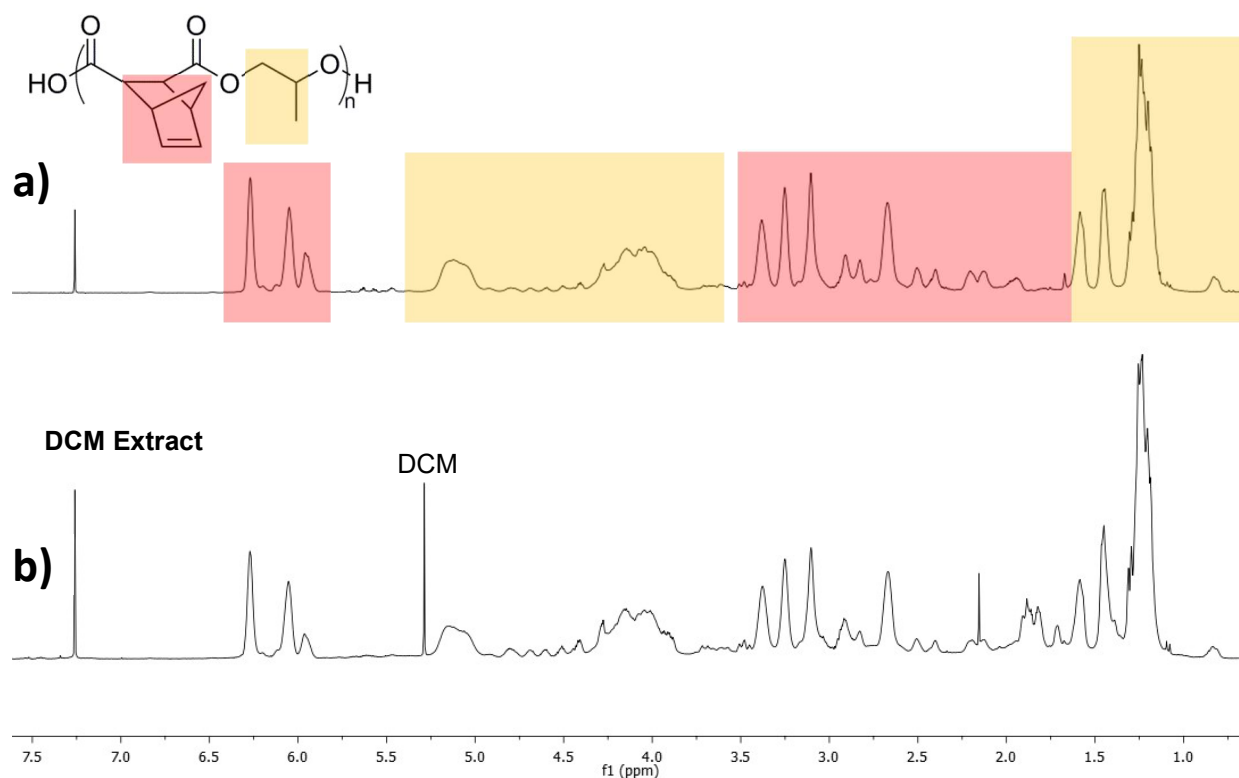


**Figure 3.13:**  $^1\text{H}$  NMR spectrum (400 MHz,  $\text{CDCl}_3$ ) of a) regions of Polyester 2 highlighted for clarity, and b) DCM extract of ROMP product

### 3.3.5 ROM copolymerisation of norbornene dicarboxylate diethylene glycol phthalic acid polyester (Polyester 1) and *N*-(2-ethylhexyl)-5-norbornene-2,3-dicarboximide (EHNBEDC)

Ring Opening Metathesis Copolymerisation of Polyester 1 and EHNBEDC, a reactive diluent, was performed in the bulk using Grubbs ruthenium initiators G1 and G2.

Figure 3.14 shows that increasing the level of Polyester 1 in the reaction mixture does indeed increase the gel content. The gel content at 5 % polyester is higher for G1 than G2. One reason may be if G2 has a higher affinity for polymerising EHNBEDC than Polyester 1. This would indicate that G2 polymerises EHNBEDC faster than Polyester 1, resulting in more poly(EHNBEDC) in the reaction product. This would not increase the gel content. Beyond 15 % it is quite difficult to dissolve any more Polyester 1 in EHNBEDC. One limitation of this experiment is that it was not repeated, and so it was not possible to incorporate error bars into the figure – which could show if any results were within error of one another.

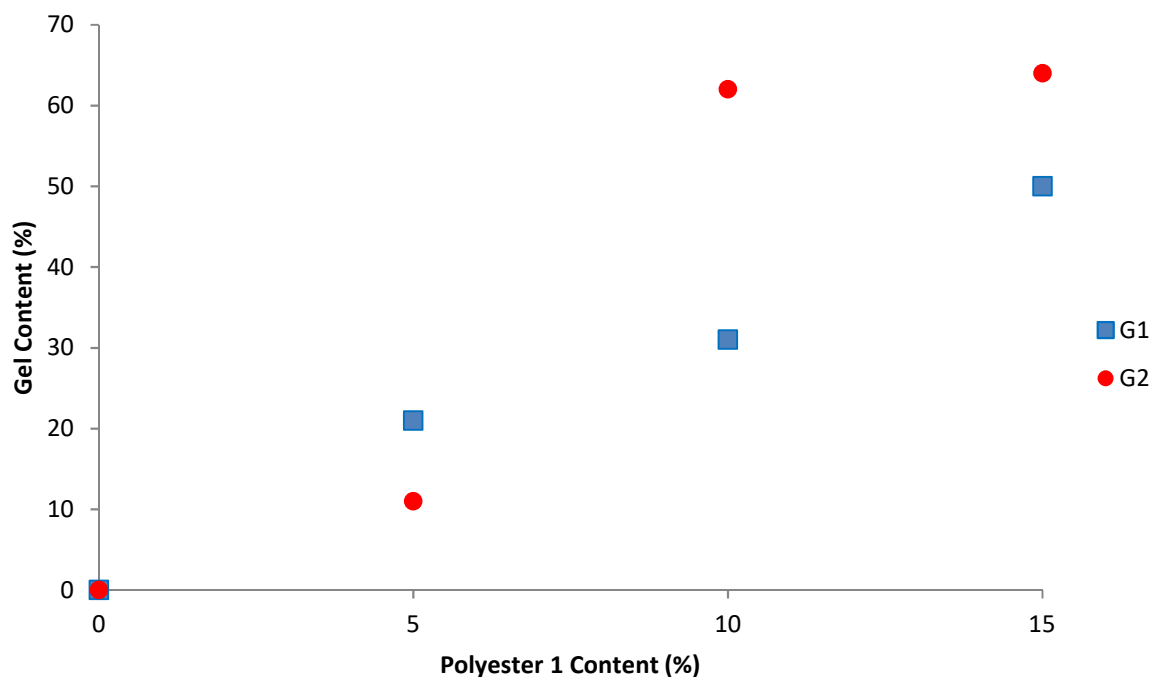


**Figure 3.14:** A chart showing the gel contents of copolymers of Polyester 1 and EHNBEDC produced from ROMP with G1 and G2, depending on the content of Polyester 1

The DCM soluble fractions were analysed by  $^1\text{H}$  NMR spectroscopy (10 % Polyester 1 is shown in Figure 3.15). The DCM fraction with 0 % Polyester 1, as expected, contains the homopolymer of EHNBEDC, and no sign of the monomer. This indicates that the polymerisation can occur to a high degree in this situation before the reaction mixture becomes too viscous.

When studying the extraction contents of the copolymers, 10 % Polyester 1 gave the best spectrum to analyse since the gel content for 15 % polyester level was high – meaning that there was very little in the DCM soluble fraction. The multiplets between 5.35 and 5.79 ppm are indicative of the ring-opened olefinic backbone protons. In the aromatic region, between 7.34 and 7.82 ppm (highlighted in blue on the chart), peaks can be seen in the DCM soluble fraction of the attempted copolymer. This shows that some of the polyester is either not getting polymerised, due to being in bulk or because there are no norbornene groups on the chain, or that there is linear polymer present. As well as the phthalic acid peaks above 7.34 ppm, one can also clearly see small peaks appearing in the glycol region between 3.35 and 4.56 ppm, highlighted in green with a particularly strong peak showing at 4.47 ppm. These all offer evidence for some presence of Polyester 1, as well as poly(EHNBEDC) in the DCM soluble fraction.

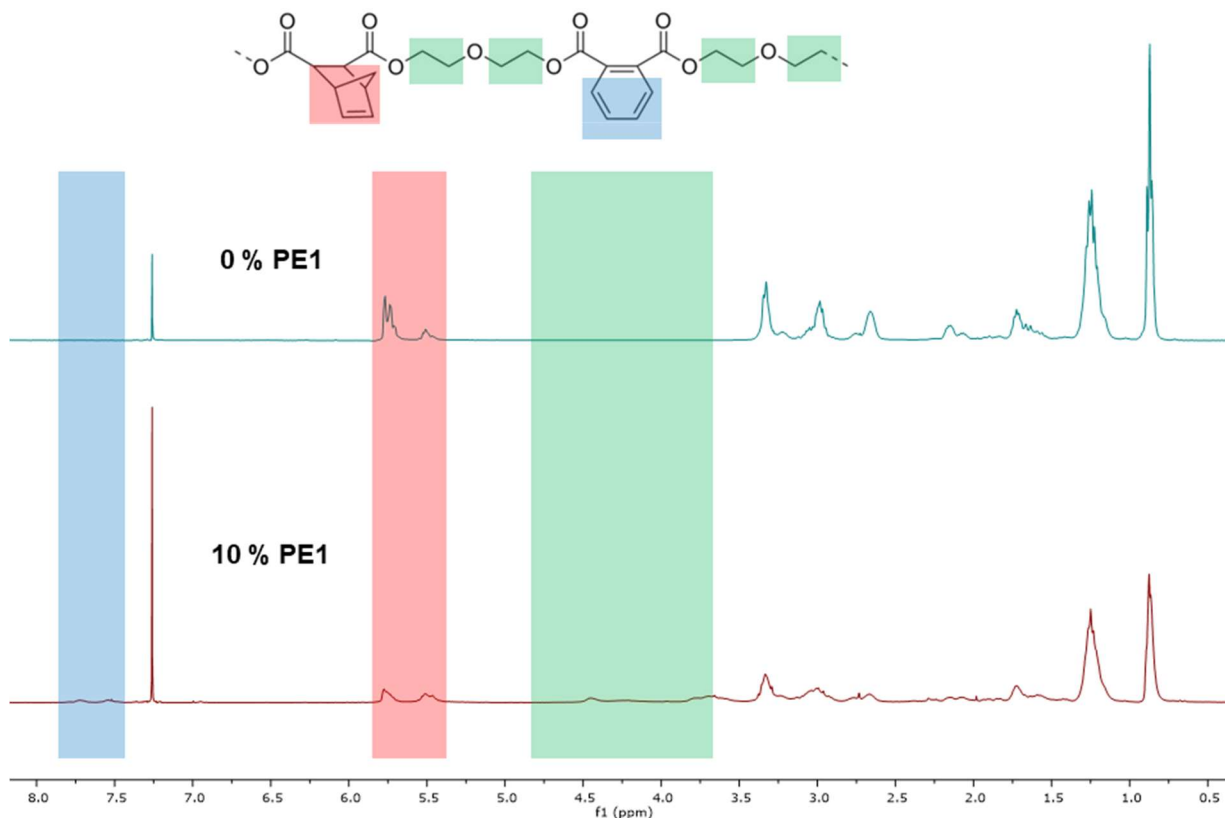


**Figure 3.15:**  $^1\text{H}$  NMR (400 MHz,  $\text{CDCl}_3$ ) spectra of in-bulk ROMP of EHNBEDC and in-bulk copolymerisation of Polyester 1 (PE1) in EHNBEDC using G1

### 3.3.6 ROM copolymerisation of norbornene dicarboxylate propylene glycol polyester (Polyester 2) and *N*-(2-ethylhexyl)-5-norbornene-2,3-dicarboximide (EHNBEDC)

Ring Opening Metathesis Copolymerisation of Polyester 2 and EHNBEDC, a reactive diluent, was performed in bulk using Grubbs ruthenium initiators G1 and G2.

The results of the investigation involving the gel content for the ROMP of Polyester 2 are shown in Figure 3.16. 10 % Polyester 2 with Grubbs 1<sup>st</sup> generation is slightly lower than expected. Furthermore, the gel contents of 5 % and 10 % Polyester 2 are within error of each other, 30 %. One possible reason could be due to poorer solubility of Polyester 2 in EHNBEDC and poorer mixing during this reaction. Above 15 %, it becomes incredibly difficult to dissolve Polyester 2 in EHNBEDC. Again error bars are not shown as this reaction was only performed once.

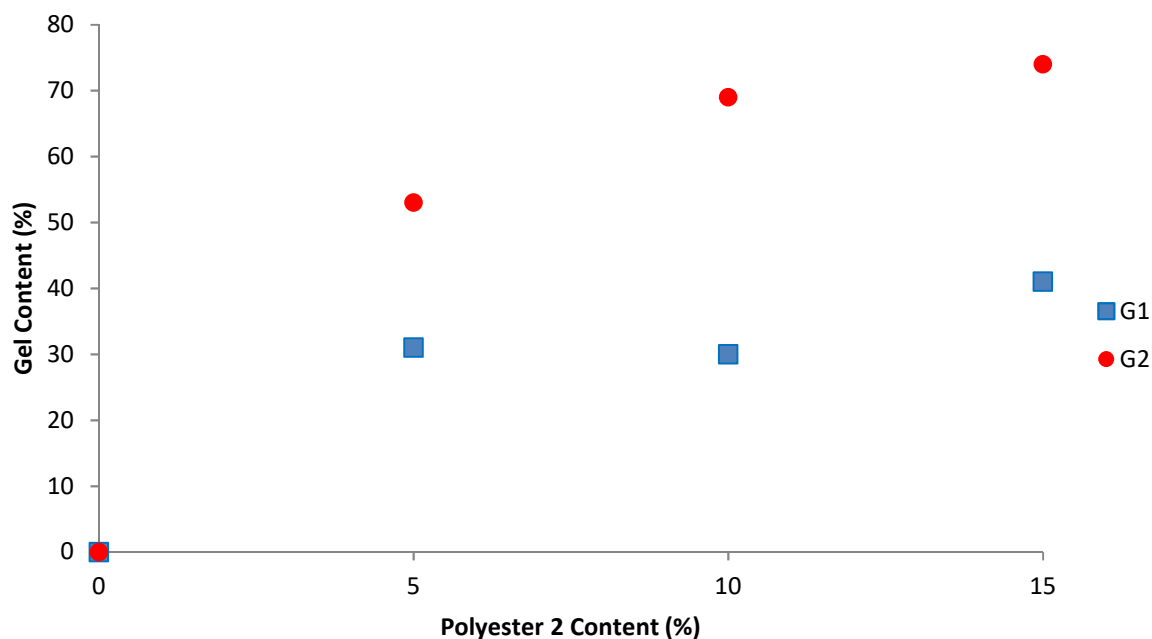


**Figure 3.16:** A chart showing the gel contents of copolymers of Polyester 2 and EHNBEDC produced from ROMP with G1 and G2, depending on the content of Polyester 2

The DCM soluble fractions of these bulk polymerisations were investigated by  $^1\text{H}$  NMR, Figure 3.17. These all showed the presence of poly(EHNBEDC), confirmed by the presence of the multiplets between 5.35 and 5.81 ppm, which are indicative of the ring-opened olefinic backbone protons. At 10 % level of the polyester, the spectra appears to have no peaks appearing due to Polyester 2. To highlight this, the region of the spectrum where the glycol part of the polyester would show up is highlighted in orange. Here there are no overlapping with peaks corresponding to EHNBEDC. There is only one very small, broad peak in this area between 3.5 and 5.5 ppm, from the 0 % Polyester 2 spectrum. This suggests that there is very little Polyester 2 which is not incorporated into the gelled fraction, and that in the DCM fraction the vast majority is poly(EHNBEDC).

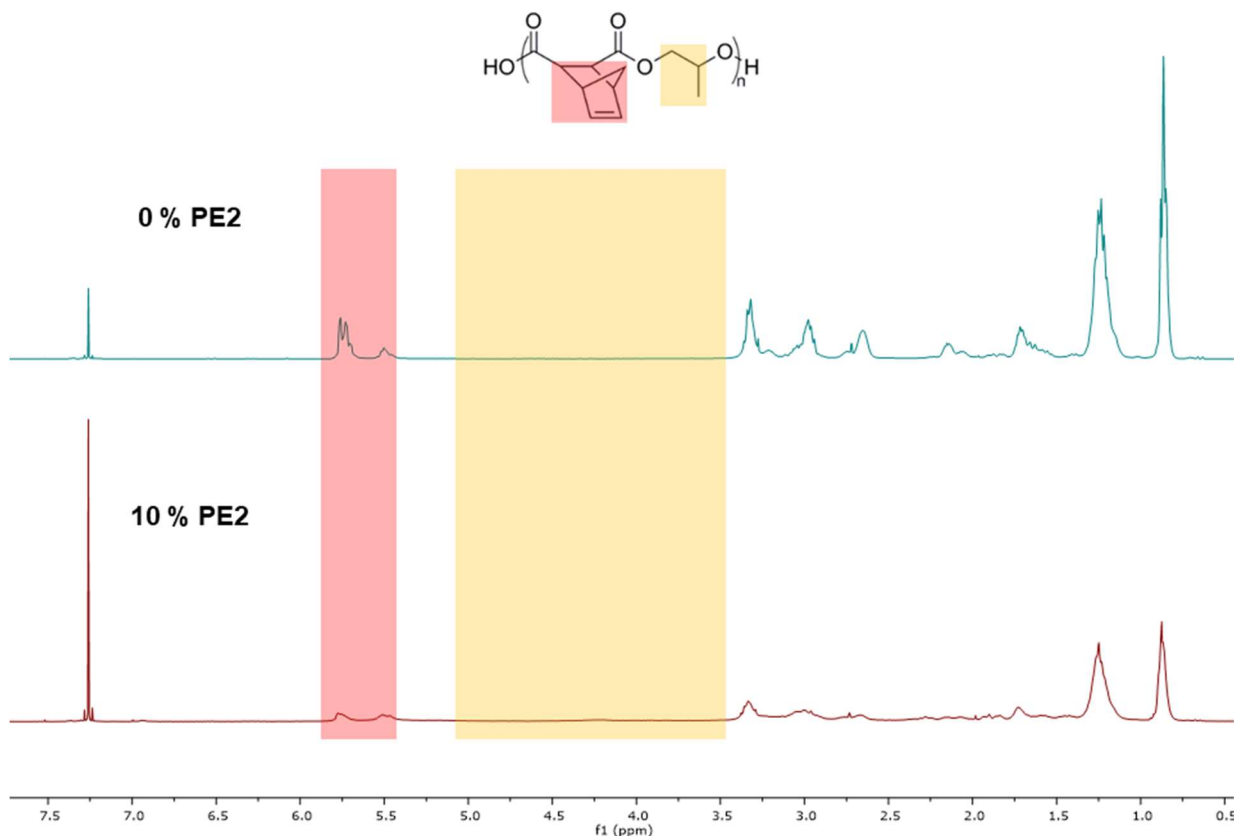


**Figure 3.17:** <sup>1</sup>H NMR (400 MHz, CDCl<sub>3</sub>) spectra of in-bulk ROMP of EHNBEDC and in-bulk copolymerisation of Polyester 2 (PE2) in EHNBEDC using G1

### 3.3.7 Comparing poly(norbornene dicarboxylate diethylene glycol phthalic acid polyester) and poly(norbornene dicarboxylate propylene glycol polyester)

#### 3.3.7.1 Homopolymerisations

The data in Figure 3.18 shows, that for all three initiators, the gel contents for the ROMP products of Polyester 1 and Polyester 2 are the same within experimental error. This would suggest that the lower concentration of norbornene groups in Polyester 1 (2.4 mmol g<sup>-1</sup>) compared to Polyester 2 (4.0 mmol g<sup>-1</sup>) does not play a significant role in the gel contents.

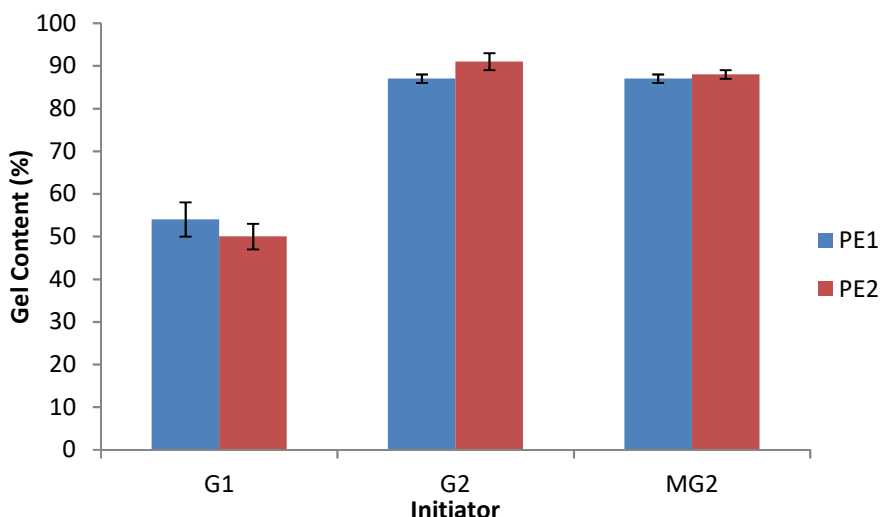


**Figure 3.18:** Comparison of the gel contents of the ROMP products of Polyesters 1 and 2 using the three initiators

On the other hand when the gel time is examined, Figure 3.19, a clear difference can be observed. The gel time of Polyester 2 is much greater (by about 40 %) than Polyester 1, and this is seen across all three initiators. One source of error could include observing when gelation has occurred, which is done manually by inverting the reaction mixture every few seconds (dependent on the length of experiment). This is a source of error since it is both a subjective observance and because gelation will probably occur at some point between two inversions. Another source of error could be due to any mixing, especially with reactions involving MG2 where the gel time is quite short. If the reaction mixture is not well mixed before being left to polymerise, this could greatly change the time it takes to form a solid. As Figure 3.19 shows, this error is actually very small in these experiments and so the differences in gel time are not purely error. What this chart also emphasises is how much quicker the gel is achieved using MG2 over G1, or even G2.

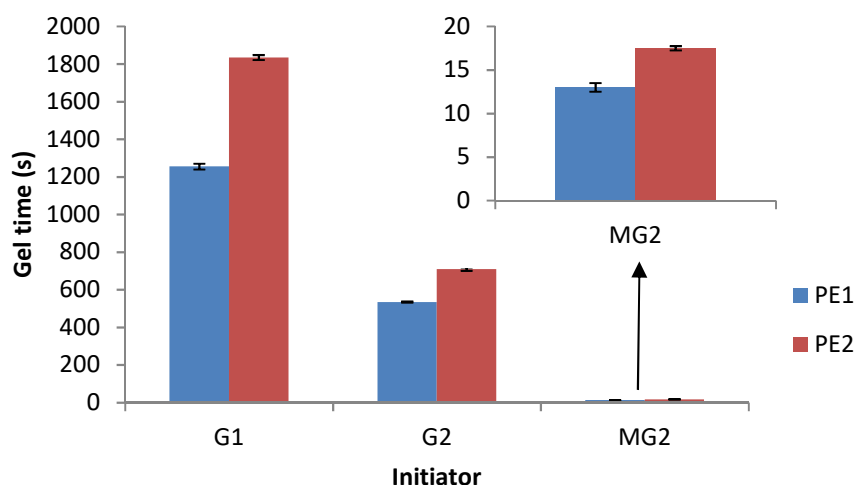


**Figure 3.19:** Comparison of the gel times of the ROMP products of Polyesters 1 and 2 using the three initiators

One possible reason for the difference in gel times between the two polyesters is solubility. Polyester 2 is slightly less soluble in DCM, and therefore less available to undergo ROMP. This slows down the reaction enough to give this difference which is observable with all three initiators.

### 3.3.7.2 Copolymerisations

The gel contents for bulk copolymerisations using both Grubbs 1<sup>st</sup> generation and Grubbs 2<sup>nd</sup> generation initiators were compared. For G1, there is a very small difference in gel contents between Polyester 1 and Polyester 2, Figure 3.20. These could in fact be within error, but the reaction was only performed once and so error bars could not be calculated.

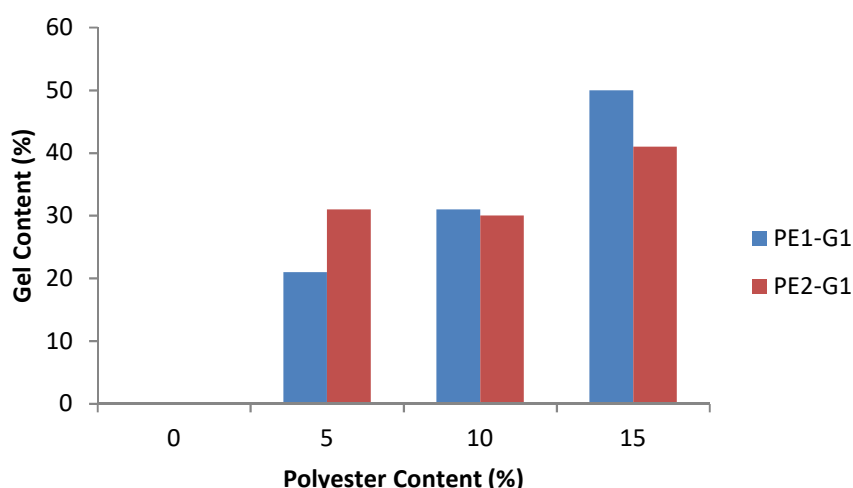


**Figure 3.20:** Chart showing the gel contents for the copolymers produced by bulk ROM copolymerisation of Polyesters 1 and 2 dissolved in varying levels of EHNBEDC using G1

Polyester 2 has a stiffer glycol in its backbone than Polyester 1 (propylene glycol *versus* diethylene glycol), leading to a higher viscosity. Polyester 1 is very viscous, whereas Polyester 2 is a brittle solid. Due to this, at higher polyester content, the copolymerisation of Polyester 2 and EHNBEDC will gel quicker than the corresponding copolymer with Polyester 1 – possibly rationalising the lower gel content achieved by Polyester 2 at higher concentrations shown in Figure 3.20.

Using Grubbs 2<sup>nd</sup> generation initiator yields rather surprising results (Figure 3.21). The ROM copolymerisation of Polyester 2 and EHNBEDC results in higher gel contents than the analogous reaction using Polyester 1. For every concentration of polyester, up to 15 %, that Polyester 2 results in higher gel contents than Polyester 1. One reason behind this perhaps is that G2 polymerises EHNBEDC faster than Polyester 2, but slower than Polyester 1. This would mean that the increase in viscosity is slower than expected for the copolymerisation with Polyester 2 meaning that the polymerisation can propagate for longer, resulting in the higher level of cross-linking. The viscosity increase will also be retarded by the slow initiation rate of G2.



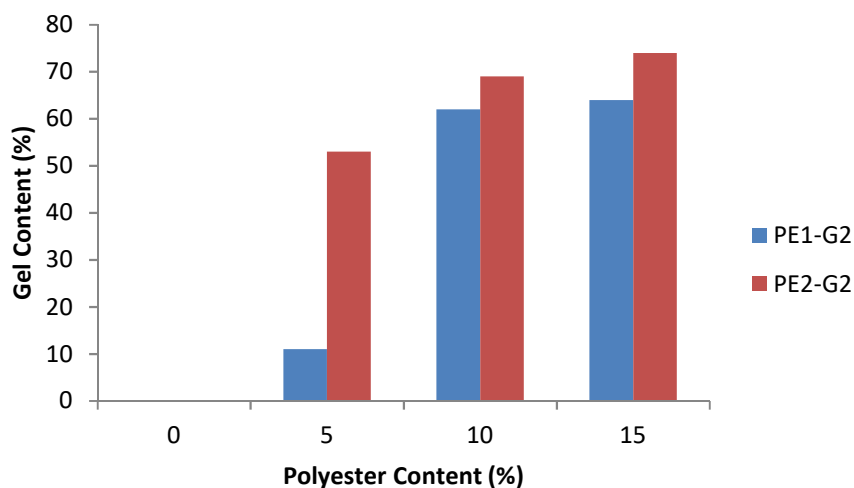


**Figure 3.21:** Chart showing the gel contents for the copolymers produced by bulk ROM copolymerisation of Polyesters1 and 2 dissolved in varying levels of EHNBEDC using G2

### 3.3.8 Mechanical Testing

#### 3.3.8.1 Equivalents of monomers for DMTA

A total of 200 equivalents of monomer were used for each DMTA run. Due to the size of the moulds utilised, this allowed two good quality samples to be formed (see Figure 3.22), rather than run the risk of one poor quality sample if 100 equivalents were used without doubling up the amount of Grubbs initiator added to the mixture, which would have used up the ruthenium initiators far too quickly.

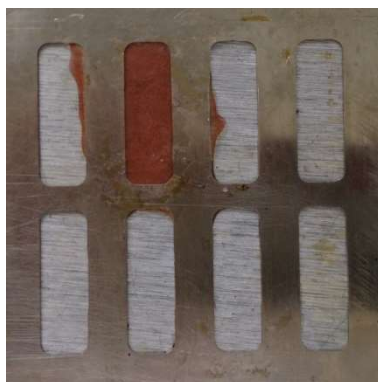


**Figure 3.22:** An example of a good quality pressed sample in the second well which has shown some overflow to other wells

Since the production of samples required for DMTA were carried out in bulk, good mixing between the initiator and the monomers was also necessary. This was attainable when using 200 monomer equivalents, whereas 100 monomer equivalents suffered from poor mixing due to the solid initiators. However, using a larger quantity of monomers resulted in more homogeneous, better quality samples.

### 3.3.8.2 Choice of Initiator

Grubbs 2<sup>nd</sup> generation initiator was the first to be ruled out as the choice of initiator for DMTA due to its slow rate of initiation and rapid rate of propagation. Since the mixing in bulk is much less effective than in solution, as close as possible to 100 % of the initiator needed to be active so the final product is as regular as possible. What is also known, however, is that initiators G2 and MG2 have much better thermal stability than G1,<sup>15</sup> and in fact 1<sup>st</sup> generation initiators may start to decompose noticeably at temperatures as low as 55 °C. As shown in the methods, temperatures of 60-85 °C were required as the heat press temperature to achieve a satisfactory product.

Grubbs 1<sup>st</sup> generation initiator also has another drawback in that its activity is much lower than the second-generation initiators. As the DMTA trace in Figure 3.23 shows, there was still a considerable amount of monomer present after being heat pressed for 40 min when using G1. This resulted in the clear downward shift in  $T_g$ , called plasticisation. This did not occur with MG2 and as can be seen, the peak in the trace of  $\tan(\delta)$  is also much sharper which infers a more homogeneous sample.

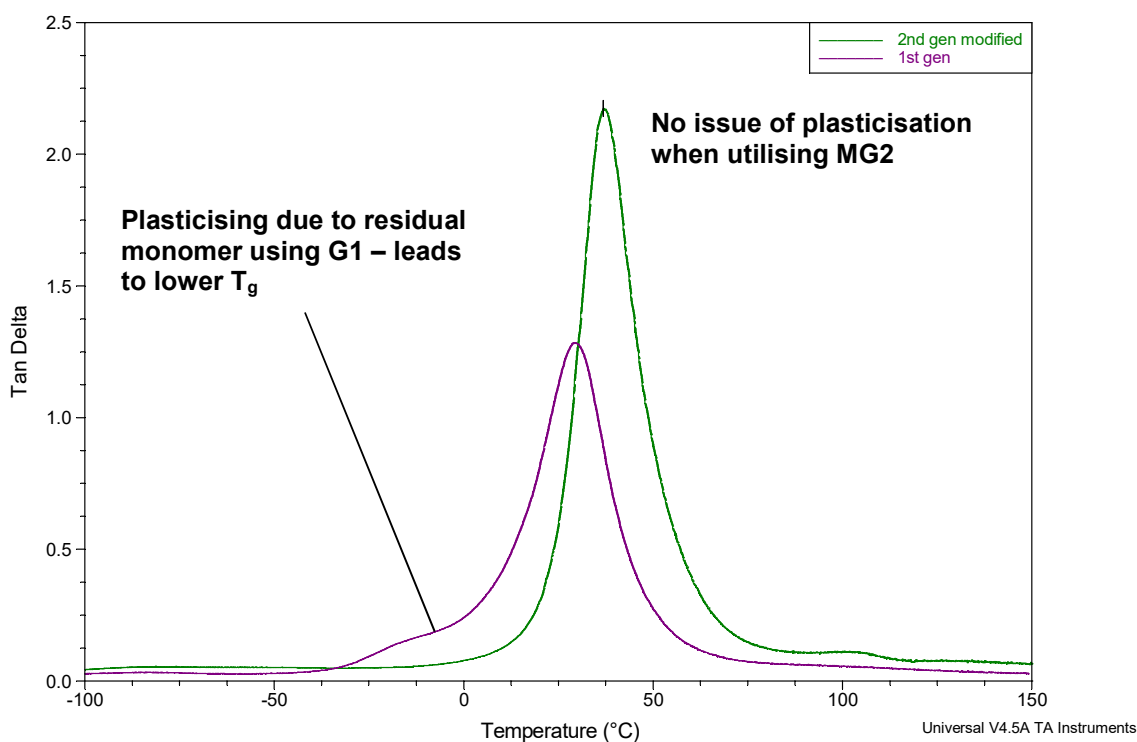


**Figure 3.23:** Example DMTA (-100 to 100 °C) traces of a polymer formed using G1 (purple) and MG2 (green), the peak in each shows the  $T_g$

Its rapid rates of initiation and propagation indicated MG2 as the best choice of initiator for DMTA, although the reaction times being very short became problematic as it was difficult on occasion to transfer the reaction mixture to the mould before it gelled, or became too viscous. If this happened, the mixture was not able to be heat pressed in to a good quality sample. This also meant that repeats for many of the experiments were not possible due to limited supply of the initiator.

### 3.3.8.3 In-mould bulk ROM copolymerisation of *N*-(2-ethylhexyl)-5-norbornene-2,3-dicarboximide (EHNBEDC) and norbornene dicarboxylate diethylene glycol phthalic acid polyester (Polyester 1)

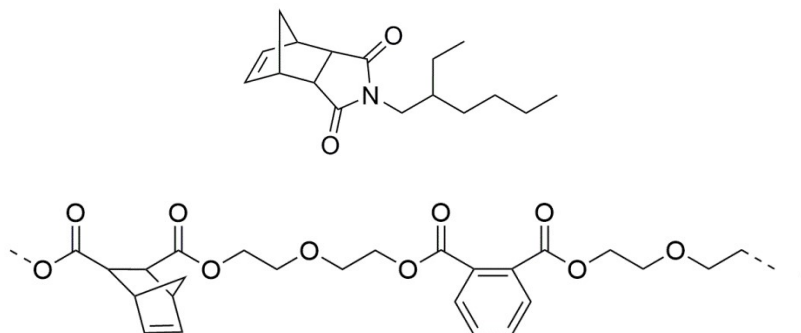


**Figure 3.24:** Structure of EHNBEDC (top) and Polyester 1 (bottom)

Norbornene dicarboxylate diethylene glycol phthalic acid polyester (Polyester 1, Figure 3.24) was shown to be soluble in *N*-(2-ethylhexyl)-5-norbornene-2,3-dicarboximide (EHNBEDC, Figure 3.24) up to around 15 %. It was thought having multiple norbornene groups in some of the chains could lead to higher achievable  $T_g$ 's, perhaps further than already high  $T_g$ 's of polynorbornene dicarboximides.<sup>16-18</sup>

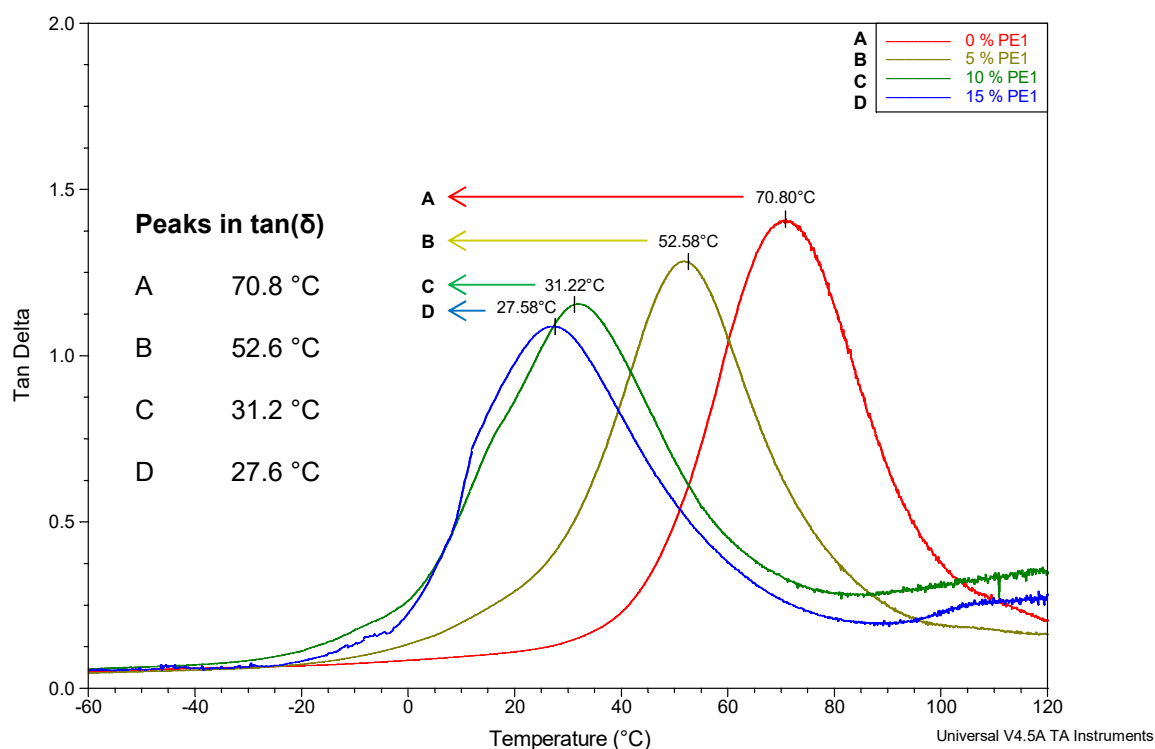


**Figure 3.25:** DMTA trace (-60 to 120 °C) of EHNBEDC/Polyester 1 copolymers initiated with MG2, showing  $\tan(\delta)$  – a peak in which shows the  $T_g$  of the material

As the content of Polyester 1 increases from 0 – 15 % in these polymers, the  $T_g$  steadily decreases from 70.8 °C to 27.6 °C, Figure 3.25. At first this seems counterintuitive, though as mentioned

previously, polynorbornene dicarboximides have a high  $T_g$  (here, poly(EHNBEDC) has a  $T_g$  of 70.8 °C). As more Polyester 1 is added into the reaction mixture, the content of EHNBEDC is therefore declining (from 100 % to 85 %) and that accounts for the steady decrease in  $T_g$  to 52.6 °C at 95 % EHNBEDC content; and to 31.2 °C at 90 % EHNBEDC content.

As can be seen in the blue trace (D in Figure 3.25), with 15 % Polyester 1, there is a significant deviation in the peak from -10 to 10 °C which is likely due to a defect in the sample which could not be controlled beyond the visual inspection to check for consistency. For example, this could have been caused by slightly less effective mixing of the reaction or perhaps an air bubble disrupting the mixture.

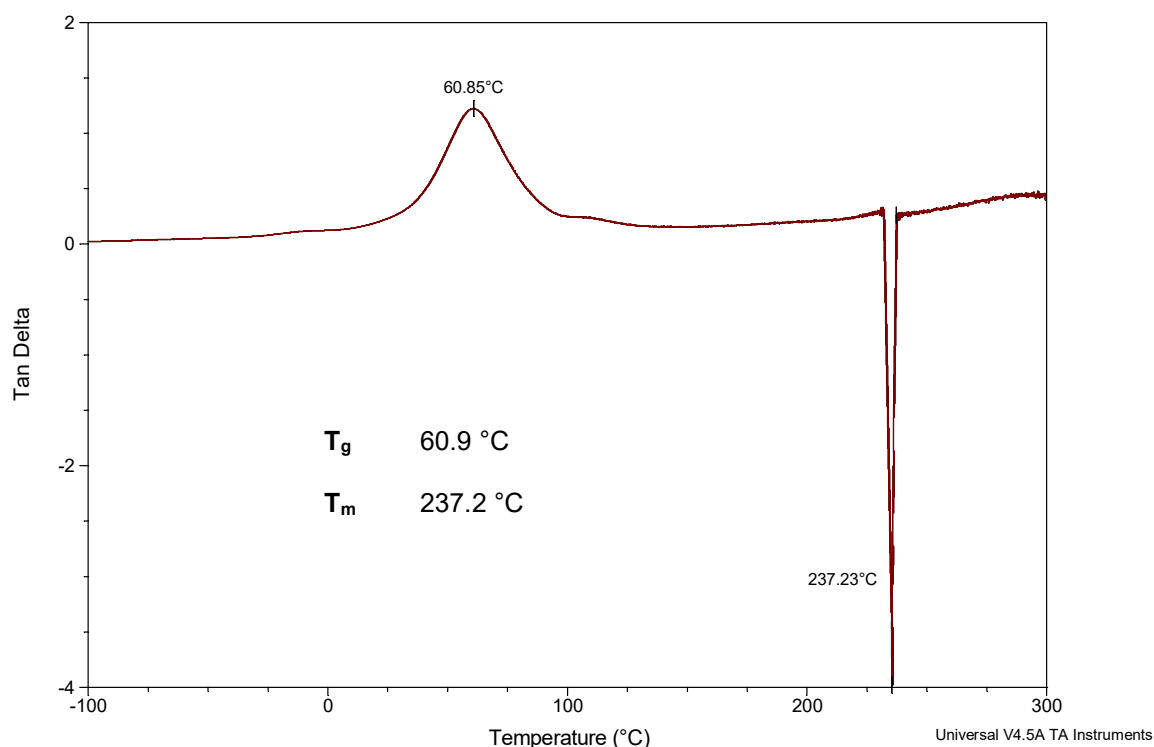


**Figure 3.26:** DMTA trace (-100 to 300 °C) of poly(EHNBEDC) produced using MG2 initiator with  $T_g$  and  $T_m$  highlighted

Poly(EHNBEDC) showed a melting transition ( $T_m$ ) at 237.2 °C, shown in Figure 3.26, in addition to its  $T_g$  of 60.9 °C before it thermally decomposed. This was assigned as  $T_m$ , since the sample exhibited flow and hence properties of a liquid.

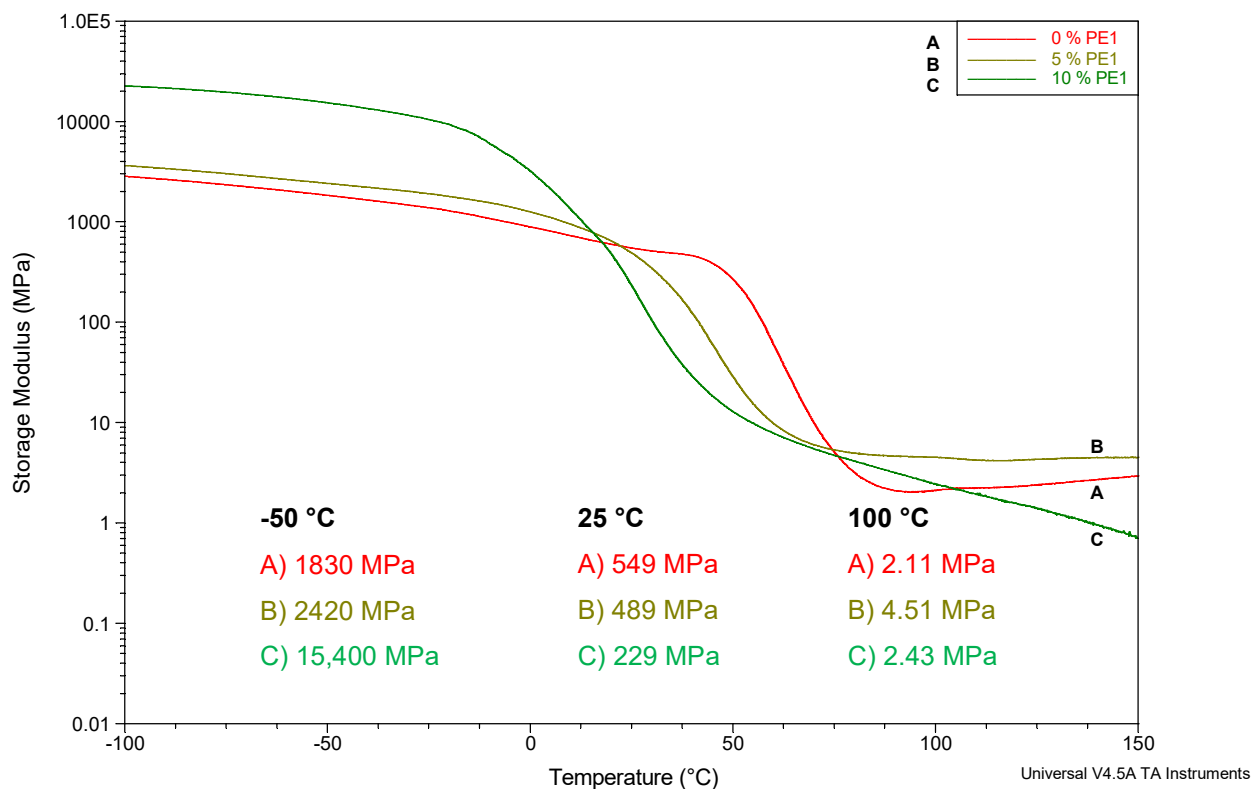


**Figure 3.27:** Storage moduli traces of EHNBEDC/Polyester 1 copolymers

$E'$  was measured at -50 °C (below all polymers'  $T_g$ 's), 25 °C (room temperature) and 100 °C (above all polymers'  $T_g$ 's). As Figure 3.27 shows the incorporation of Polyester 1 below the  $T_g$  has a large effect on  $E'$ , for example changing the Polyester 1 content between 0 %, 5 % and 10 % leads to  $E'$  values of 1830 MPa, 2420 MPa and 15,400 MPa, respectively. This means that the more Polyester 1 is incorporated into the polymer, the stiffer the material produced. Temperature also has a large effect on  $E'$ : at -50 °C the value of 15,400 MPa is akin to the stiffness of bone,<sup>19</sup> although by room temperature the material is again similar to rubber (229 MPa).

This figure again shows up the differences in  $T_g$  of the three materials, shown in Figure 3.27 where each trace has the first turning point. This shows that 10 % Polyester 1 content has the lowest  $T_g$  of the three (transition starts at around 0 °C); followed by 5 % Polyester 1 content (starts around 25 °C); and then pure poly(EHNBEDC) has the highest (around 60 °C).

### 3.3.8.4 In-mould bulk ROM copolymerisation of *N*-(2-ethylhexyl)-5-norbornene-2,3-dicarboximide (EHNBEDC) and norbornene dicarboxylate propylene glycol polyester (Polyester 2)

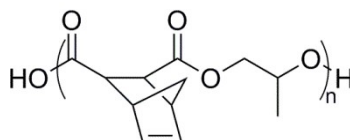


**Figure 3.28:** Structure of Polyester 2

Norbornene dicarboxylate propylene glycol polyester (Polyester 2, Figure 3.28) was shown to be soluble in EHNBEDC up to concentrations of around 15 %, allowing the mechanical testing to be performed on the mixture.

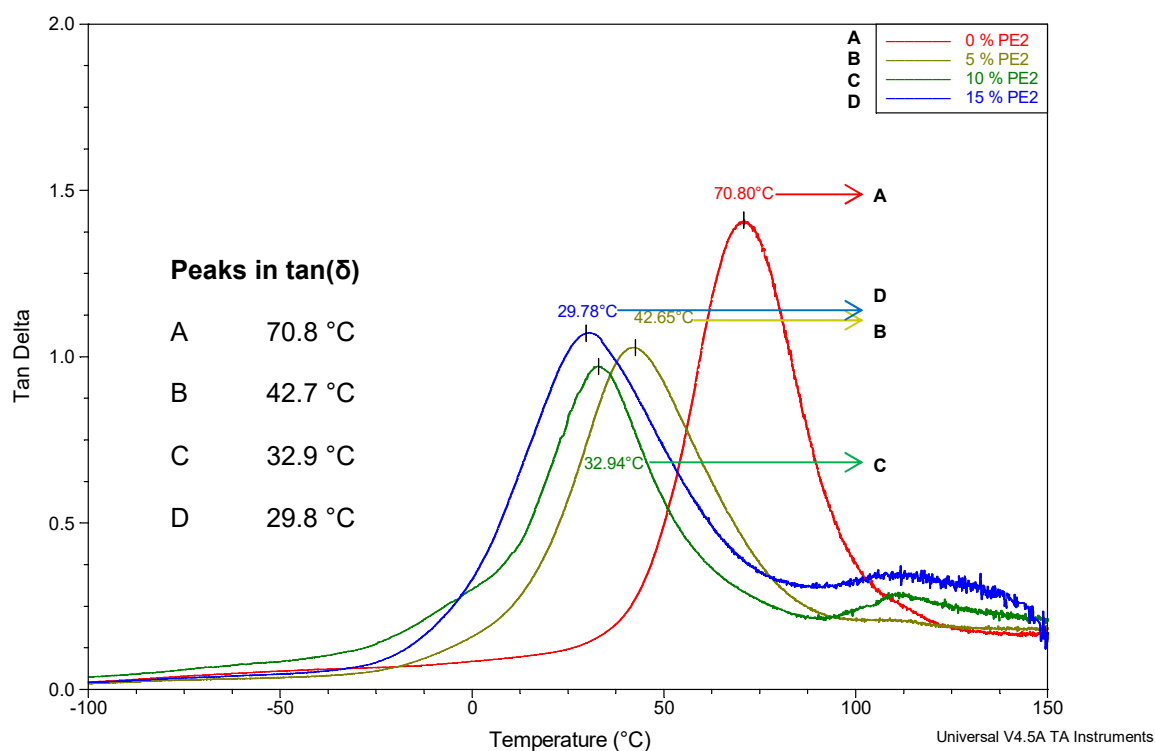


**Figure 3.29:** DMTA trace (-100 to 150 °C) of EHNBEDC/Polyester 2 copolymers initiated with MG2, showing  $\tan(\delta)$  – a peak in which shows the  $T_g$  of the material

Similarly to Polyester 1, incorporating Polyester 2 in to the copolymer structure decreases the  $T_g$ , this time from 70.8 °C to 29.8 °C, as shown in Figure 3.29. This is probably due to the high  $T_g$  of poly(EHNBEDC) and the fact that the ROMP of Polyester 2 produces a polymer with a gel content of, maximum, 74 %. This means that almost a quarter of the non-gelled product will be monomer or linear polymeric material from the ROMP of Polyester 2, which may help plasticise the material, which may be shown by the large shoulders on the left side of the peaks in  $\tan(\delta)$  in the three traces: **B**, **C**

and **D**. Increasing plasticisation could be the reason for the decreasing  $T_g$ 's of: 42.7 °C, 32.9 °C and 29.8 °C, respectively.

Some of the copolymers (for example, **B** with 5 % Polyester 2 content) have another slight peak at around 100 °C which may be attributable to the homopolymer, poly(EHNBEDC) as different chain lengths may have a higher  $T_g$ .

Polyester 2 is a much stiffer pre-polymer due to the shorter glycol in its structure, it was hoped that this would produce materials with a much higher storage modulus than Polyester 1 when copolymerised with EHNBEDC.

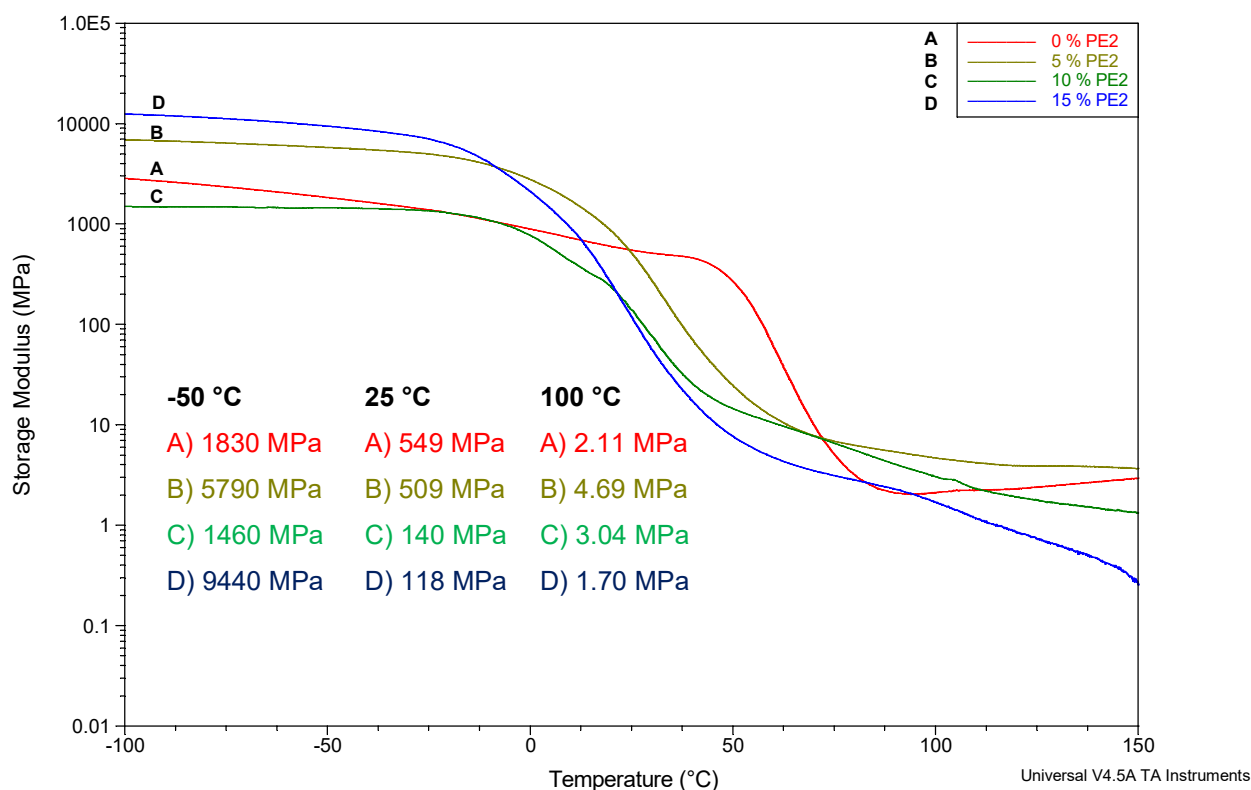


**Figure 3.30:** Storage moduli traces of EHNBEDC/Polyester 2 copolymers

Here,  $E'$  was measured at -50 °C (below the  $T_g$  of all the copolymers), 25 °C (room temperature) and 100 °C (above the  $T_g$  of all copolymers). The first observation from Figure 3.30 is that 10 % Polyester 2 is less stiff than it ought to be: 1460 MPa at -50 °C, whereas it should be between 5790 and 9440 MPa using the figures from 5 % and 15 % Polyester 2 content. This perhaps suggests that this sample was inferior to the others. This could be due to poor mixing or pressing – although all samples in this experiment were pressed at the same temperature for similar periods of time. The mixing was difficult to keep constant, since it could only be done for a very short time. The mixture had to be transferred to the heat press before it gelled – and with modified 2<sup>nd</sup> generation this occurred within one min, so stirring could only be applied for a very short time.

Surprisingly, these polymers have a lower stiffness (1460-9440 MPa) below their  $T_g$ 's compared to the copolymers containing Polyester 1 (1830-15,400 MPa). This could possibly be due to the low

concentrations (maximum 15 %), and so the characteristics of poly(EHNBEDC) take priority. The stiffness of Polyester 2 pre-polymer appears to have very little, if any, effect therefore on  $E'$  of the final material.

Again, the trend seen in  $T_g$  can also be observed in Figure 3.30. This can be seen by the fact that with increasing Polyester 2 contents, the turning point (indicating the  $T_g$  onset) in the trace decreases in temperature. The rough  $T_g$  starting points are: the sample containing 0 % Polyester 2 content is around 60 °C; 5 % undergoes this transition from around 10 °C; 10 and 15 % Polyester 2 content both start the transition just below 0 °C. This confirms that as the Polyester 2 content was increased the  $T_g$  reduced, since the increase in Polyester 2 content results in lowering of the onset of  $T_g$ . This means that the stiffness could indirectly be altered – for example at 25 °C due to the transitions occurring the stiffness could be reduced by a factor of around five by introducing 15 % of Polyester 2, reducing  $E'$  from 549 MPa to 118 MPa. This effect is possibly caused by the increasing plasticisation with increasing Polyester 2 due to leftover monomer in the sample – which was shown previously in Figure 3.29.

Above the transition, all four polymers (with Polyester 2 contents of 0 – 15 %) again have an appearance, or stiffness, analogous to rubber. There is, at these temperatures, very little difference in  $E'$  between the four materials (lowest is 1.70 MPa with 15 % Polyester 2 content, and the highest is 4.69 MPa).

### 3.3.9 Evaluation of Green Chemistry aspects

#### 3.3.9.1 E-factor

**Table 3.5:** Table of all the E-factors linear polymerisations in Chapter 3

Reaction	Mass of waste (mg)	Mass of product (mg)	E-factor
ROMP of EHNBEDC (G1)	84 457	214	395
ROMP of EHNBEDC (G2)	84 375	285	296
ROMP of EHNBEDC (MG2)	84 428	284	297

The E-factors for the ROMP of EHNBEDC are high (Table 3.5), and these do not include the synthesis of the monomer. Similar to previous reactions, one of the major reasons for these having a high E-factor is because the scale which they are produced on is very small. Secondly, due to the usage of a non-solvent (100 mL of methanol), this has inflated the mass of waste produced. If this stage was not performed it would reduce the E-factor by a factor of around 10. However, without this stage, the quality of the polymers produced would not be as good and may include some residual



monomer. An interesting point from these data is that the E-factor for the G1 produced polymer is significantly higher than the other two, mainly due to its lower yield.

The E-factors for the cross-linked polymers are not detailed here since they are zero as all material is incorporated into the final product. This changes however if a gel extraction takes place and will significantly increase the E-factor as the yield decreases and the amount of waste produced increases.

### 3.3.9.2 Compostable polymers

A polymer can be described as biodegradable if “capable of undergoing decomposition into carbon dioxide, methane, water, inorganic compounds, or biomass in which the predominant mechanism is the enzymatic action of microorganisms, that can be measured by standardized (*sic*) tests, in a specified period of time, reflecting available disposal condition.”<sup>20</sup> However, since most of the polymers developed in this work do not contain biological molecules – and were not tailored to biodegrade, it is unlikely that they will do so. What is possible however, is that they may be compostable, “capable of undergoing biological decomposition in a compost site as part of an available program, such that the plastic is not visually distinguishable and breaks down to carbon dioxide, water, inorganic compounds and biomass, at a rate consistent with known compostable materials (e.g. cellulose)”.<sup>20</sup> It is more probable that the polymers produced in this work are compostable due to their abundance of ester linkages which are easily hydrolysed during composting in aromatic-aliphatic systems,<sup>21</sup> similar to Polyester 1, and aliphatic only systems<sup>22</sup> similar to Polyester 2.

## 3.4 Conclusions

EHNBEDC was successfully polymerised with all three ruthenium-based initiators: G1, G2 and MG2. This resulted in high yields with all initiators, with G1 and MG2 also producing fairly narrowly disperse polymers ( $\bar{M}_w = 1.2$  and  $1.1$ , respectively). All three polymers produced were also successfully characterised by  $^1\text{H}$  and  $^{13}\text{C}$  NMR spectroscopy.

Polyester 1 was polymerised in DCM with G1, G2 and MG2; and produced cross-linked products with gel contents of 54, 87 and 87 %, respectively. The gel time also varied between 15 s, for MG2, and 21 min for G1. Polyester 2 was also polymerised in DCM using the same three initiators; producing materials with gel contents of 50, 91 and 88 %, respectively. The gel time again varied over a wide range, from 17 s to 31 min. The DCM soluble fractions for all six polymerisations were characterised using  $^1\text{H}$  NMR spectroscopy.

Polyester 1 was also copolymerised in bulk, using EHNBEDC as a reactive diluent. The gel content could be increased from zero to 50 % using G1, and from zero to 64 % using G2, by changing the amount of polyester added to the reaction mixture. This indicates that the copolymers' levels of cross-linking can be tailored by varying the ratios of the starting materials. Repeating these reactions with Polyester 2 instead, the gel content increased from zero to 41 % using G1, and from zero to 74 % using G2. This also suggests that changing the ratios of EHNBEDC and Polyester 2 can change the

level of cross-linking markedly.  $^1\text{H}$  NMR spectra of the DCM soluble fractions from these experiments was also successfully resolved.

When investigating copolymerisations of Polyester 1 with EHNBEDC, the  $T_g$  decreased with increasing the amount of Polyester 1 as shown in **Error! Reference source not found.**. In fact, with only 15 % Polyester 1 composition, the  $T_g$  was decreased to 27.6 °C from 70.8 °C. No more equivalents were attempted, however, as the solubility of Polyester 1 in EHNBEDC was poor above this level. As this table also shows, storage moduli were not calculated for this level of Polyester 1, due to the brittleness of these polymers. The three other polymers showed an increasing trend in storage modulus with increasing Polyester 1 contents when below the  $T_g$ , from 1830 to 2420 MPa, and up to a maximum of 15,400 MPa with 10 % Polyester 1 contents. The three moduli calculated above the  $T_g$  may be within error of one another (2.11, 4.51 and 2.43 MPa), though this will only be able to be confirmed if the DMTA experiments are repeated.

It was shown that adding Polyester 2 to EHNBEDC decreases the  $T_g$  from 70.8 °C to 29.8 °C at 15 % Polyester 2 contents. The reduction in  $T_g$  of 41.0 °C is almost as high as the reduction of  $T_g$  seen in the copolymers of EHNBEDC with Polyester 1 (43.2 °C). The storage moduli at -50 °C show a slight trend upwards with more Polyester 2 (1830 MPa with 0 %, up to 9440 MPa with 15 % Polyester 2 contents), however there is a possible anomaly at 10 % polyester which has  $E'$  of only 1460 MPa (that would need to be repeated). One trend in storage moduli that can be seen is at 25 °C, due to the differences in  $T_g$  some of the copolymers are glassy and others are rubbery.

It was found that increasing Polyester 2 concentration at 25 °C results in a lower value of  $E'$ , for example: increasing Polyester 2 contents from zero to 15 % in 5 % increments decreases the storage moduli to: 549, 509, 140, and 118 MPa, respectively. Above the  $T_g$ , once more the moduli become much smaller than they were at -50 °C – in fact by about a factor of 100 again, for example at 15 % Polyester 2 contents  $E'$  reduces from 9440 MPa to 1.7 MPa.

### 3.5 References

1. Hsu, C. P.; Zhao, M. Y.; Voeks, S. L. Styrene-free unsaturated polyester. EP 2621999 A1, **2013**.
2. Schwab, P.; France, M. B.; Ziller, J. W.; Grubbs, R. H., A Series of Well-Defined Metathesis Catalysts—Synthesis of  $[\text{RuCl}_2(=\text{CHR}')(\text{PR}_3)_2]$  and Its Reactions. *Angew. Chem., Int. Ed.* **1995**, 34 (18), 2039-2041.
3. Scholl, M.; Trnka, T. M.; Morgan, J. P.; Grubbs, R. H., Increased ring closing metathesis activity of ruthenium-based olefin metathesis catalysts coordinated with imidazolin-2-ylidene ligands. *Tetrahedron Lett.* **1999**, 40 (12), 2247-2250.
4. Autenrieth, B.; Jeong, H.; Forrest, W. P.; Axtell, J. C.; Ota, A.; Lehr, T.; Buchmeiser, M. R.; Schrock, R. R., Stereospecific Ring-Opening Metathesis Polymerization (ROMP) of endo-Dicyclopentadiene by Molybdenum and Tungsten Catalysts. *Macromolecules* **2015**, 48 (8), 2480-2492.

5. Sanchez, E. M. S.; Zavaglia, C. A. C.; Felisberti, M. I., Unsaturated polyester resins: influence of the styrene concentration on the miscibility and mechanical properties. *Polymer* **2000**, *41*, 765-769.
6. Grubbs, R.; Love, J.; Sanford, M.; Trnka, T.; Moore, J. Hexacoordinated ruthenium or osmium metal carbene metathesis catalysts. US2002177710 (A1), **2002**.
7. Love, J. A.; Morgan, J. P.; Trnka, T. M.; Grubbs, R. H., A Practical and Highly Active Ruthenium-Based Catalyst that Effects the Cross Metathesis of Acrylonitrile. *Angew. Chem., Int. Ed.* **2002**, *41* (21), 4035-4037.
8. Khosravi, E.; Al-Hajaji, A. A., Ring opening metathesis polymerisation of n-alkyl norbornene dicarboxyimides using well-defined initiators. *Polymer* **1998**, *39* (23), 5619-5625.
9. Majchrzak, M.; Hine, P. J.; Khosravi, E., An autonomous self-healing system based on ROMP of norbornene dicarboximide monomers. *Polymer* **2012**, *53* (23), 5251-5257.
10. Floros, G.; Saragas, N.; Paraskevopolou, P.; Psaroudakis, N.; Koinis, S.; Pitsikatis, M.; Hadjichristidis, N.; Mertis, K., Ring Opening Metathesis Polymerization of Norbornene and Derivatives by the Triply Bonded Ditungsten Complex  $\text{Na}[\text{W}_2(\mu\text{-Cl})_3\text{Cl}_4(\text{THF})_2]\cdot(\text{THF})_3$ . *Polymers* **2012**, *4* (4), 1657-1673.
11. Vergas, J.; Santiago, A. A.; Gavino, R.; Cerda, A. M.; Tlenkopatchev, M. A., Synthesis and ring-opening metathesis polymerization (ROMP) of new N-fluoro-phenylnorbornene dicarboximides by 2nd generation ruthenium alkylidene catalysts. *Express Polym. Lett.* **2007**, *1* (5), 274-282.
12. Nelson, D. J.; Manzini, S.; Urbina-Blanco, C. A.; Nolan, S. P., Key processes in ruthenium-catalysed olefin metathesis. *Chem. Commun.* **2014**, *50* (72), 10355-10375.
13. Sanford, M. S.; Love, J. A.; Grubbs, R. H., Mechanism and Activity of Ruthenium Olefin Metathesis Catalysts. *J. Am. Chem. Soc.* **2001**, *123* (27), 6543-6554.
14. Love, J. A.; Morgan, J. P.; Trnka, T. M.; Grubbs, R. H., A Practical and Highly Active Ruthenium-Based Catalyst that Effects the Cross Metathesis of Acrylonitrile. *Angew. Chem., Int. Ed.* **2002**, *41* (21), 4035-4037.
15. Schrodi, J.; Pederson, R. L., Evolution and Applications of Second-Generation Ruthenium Olefin Metathesis Catalysts. *Aldrichimica Acta* **2007**, *40* (2), 45-52.
16. Asrar, J.; Hurlbut, J. B., Synthesis, rheology, and physical properties of a metathesis polymer. *J. Appl. Polym. Sci.* **1993**, *50* (10), 1727-1732.
17. Madan, R.; Anand, R. C.; Varma, I. K., Metathesis polymerization of N-aryl norbornene dicarboximides. I. *J. Polym. Sci., Part A: Polym. Chem.* **1997**, *35* (14), 2917-2924.
18. Khosravi, E.; Feast, W. J.; Al-Hajaji, A. A.; Leejarkpai, T., ROMP of n-alkyl norbornene dicarboxyimides: from classical to well-defined initiators, an overview. *J. Mol. Catal. A: Chem.* **2000**, *160* (1), 1-11.
19. Rho, J. Y.; Ashman, R. B.; Turner, C. H., Young's modulus of trabecular and cortical bone material: Ultrasonic and microtensile measurements. *J. Biomech.* **1993**, *26* (2), 111-119.
20. Song, J. H.; Murphy, R. J.; Narayan, R.; Davies, G. B. H., Biodegradable and compostable alternatives to conventional plastics. *Philos. Trans. R. Soc. London, Ser. B* **2009**, *364* (1526), 2127-2139.

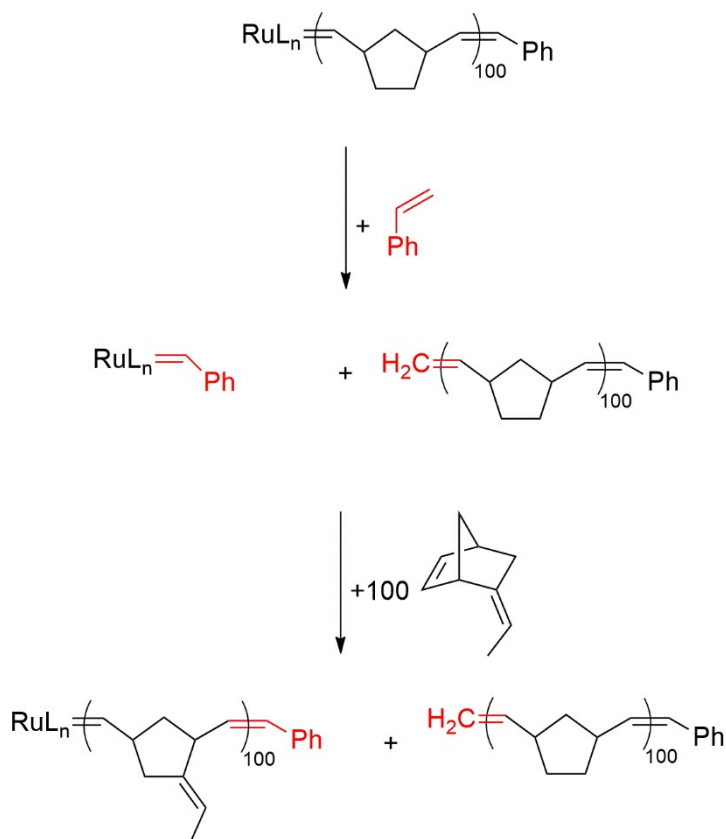
21. Kijchavengkul, T.; Auras, R.; Rubino, M.; Selke, S.; Ngouajio, M.; Fernandez, R. T., Biodegradation and hydrolysis rate of aliphatic aromatic polyester. *Polym. Degrad. Stab.* **2010**, 95 (12), 2641-2647.
22. Rydz, J.; Sikorska, W.; Kyulavska, M.; Christova, D., Polyester-Based (Bio)degradable Polymers as Environmentally Friendly Materials for Sustainable Development. *Int. J. Mol. Sci.* **2015**, 16 (1), 564-596.

## **Chapter 4. Gelation Control by the Addition of Styrene in ROMP of Norbornene-Functionalised Polyesters**

## 4.1 Introduction

Since Hsu *et al.*<sup>1</sup> had only investigated the production of ‘styrene-free’ polyesters that were able to undergo ROMP, it was decided to see if incorporating styrene into the system had any effect on gel content, gel time or any other physical properties. This seemingly goes against Aim 4 of the project, that the polymer system, “utilises little, or no, styrene”. However, the levels used here are still much lower than those currently used to cross-link UPRs as styrene can be used as the solvent or reactive diluent.<sup>2</sup>

Previously, in 2010, Khosravi *et al.*<sup>3</sup> studied the effect of adding styrene to systems involving Grubbs ruthenium initiators and observed that adding styrene to a living polymer chain regenerates the initiator, a so-called chain transfer agent (CTA). This led to their discovery that this would be ideal for creating blends of polymers and copolymers of varying molecular weights, shown in Scheme 4.1. The reason styrene makes such a good CTA is because it is a Type I olefin<sup>4</sup> and reacts rapidly with the initiator, separating the polymer chain from the ruthenium.



**Scheme 4.1:** Utilising styrene to create a blend of poly(norbornene) and poly(ethylidene norbornene),  $L_nRu$  can represent any of Grubbs ruthenium initiators

The initiator is able to be regenerated by the styrene present in solution. It was hoped that keeping the initiator living for a longer timeframe may drive the polymerisations to higher gel contents. Or, the styrene may undergo cross metathesis with the ruthenium carbene on the chain ends – leading to

shorter chains, which would lead to longer polymerisation processes perhaps hence higher levels of cross-linking.

The idea of this project was to produce styrene-free polyester resins, and so introducing styrene into this system seems counterintuitive. In the ROMP-based systems described in this thesis a maximum of five equivalents of styrene with respect to the initiator is added – which equates to around a 5 % styrene content excluding the solvent. This can be reduced by increasing the monomer to initiator ratio.

## **4.2 Experimental**

### **4.2.1 Gel Content Investigations in the presence of styrene**

#### **4.2.1.1 ROMP of norbornene dicarboxylate diethylene glycol phthalic acid polyester (Polyester 1) with G1**

Polyester 1 (1030 mg, ~2.43 mmol(NBE)) was dissolved in DCM (4 mL) that contained styrene (0-2 eq. with respect to G1) for 16 h. This was then added to G1 (20 mg, 0.0243 mmol) and the mixture was agitated. The reaction mixture had turned solid after 24 h, and so was broken into smaller pieces and stirred under reflux at 40 °C in DCM (40 mL) for 3 h. The brown solid pieces were separated by filtration and dried under reduced pressure (<1 mbar, 50 °C, 72 h). These reactions were repeated three times. The pieces were weighed – and the average gel content was calculated (59 – 64 %).

#### **4.2.1.2 ROMP of norbornene dicarboxylate propylene glycol polyester (Polyester 2) with G1**

Polyester 2 (608 mg, ~2.43 mmol(NBE)) was dissolved in DCM (4 mL) that contained styrene (0-2 eq. with respect to G1) for 16 h. This was then added to G1 (20 mg, 0.0243 mmol) and the mixture was agitated. The reaction mixture had turned solid after 24 h, and so was broken into smaller pieces and stirred under reflux at 40 °C in DCM (40 mL) for 3 h. The brown solid pieces were separated by filtration and dried under reduced pressure (<1 mbar, 50 °C, 72 h). These reactions were repeated three times. The pieces were weighed – and the average gel content was calculated (47 – 57 %).

#### **4.2.1.3 ROMP of Polyester 1 with G2**

Polyester 1 (996 mg, ~2.36 mmol(NBE)) was dissolved in DCM (4 mL) that contained styrene (0-2 eq. with respect to G2) for 16 h. This was then added to G2 (20 mg, 0.0236 mmol) and the mixture was agitated. The reaction mixture had turned solid after 24 h, and so was broken into smaller pieces and stirred under reflux at 40 °C in DCM (40 mL) for 3 h. The brown solid pieces were separated by filtration and dried under reduced pressure (<1 mbar, 50 °C, 72 h). These reactions were repeated three times. The pieces were weighed – and the average gel content was calculated (87 – 90 %).

#### **4.2.1.4 ROMP of Polyester 2 with G2**

Polyester 2 (996 mg, ~2.36 mmol(NBE)) was dissolved in DCM (4 mL) that contained styrene (0-2 eq. with respect to G2) for 16 h. This was then added to G2 (20 mg, 0.0236 mmol) and the mixture was agitated. The reaction mixture had turned solid after 24 h, and so was broken into smaller pieces and stirred under reflux at 40 °C in DCM (40 mL) for 3 h. The brown solid pieces were separated by

filtration and dried under reduced pressure (<1 mbar, 50 °C, 72 h). These reactions were repeated three times. The pieces were weighed – and the average gel content was calculated (84 – 97 %).

#### 4.2.1.5 ROMP of Polyester 1 with MG2

Polyester 1 (954 mg, ~2.26 mmol(NBE)) was dissolved in DCM (4 mL) that contained styrene (0-2 eq. with respect to MG2) for 16 h. This was then added to MG2 (20 mg, 0.0226 mmol) and the mixture was agitated. The reaction mixture had turned solid after 24 h, and so was broken into smaller pieces and stirred under reflux at 40 °C in DCM (40 mL) for 3 h. The solid pieces were separated by filtration and dried under reduced pressure (<1 mbar, 50 °C, 72 h). These reactions were repeated twice. The pieces were weighed – and the average gel content was calculated (80 – 86 %).

#### 4.2.1.6 ROMP of Polyester 2 with MG2

Polyester 2 (566 mg, ~2.26 mmol(NBE)) was dissolved in DCM (4 mL) that contained styrene (0-2 eq. with respect to MG2) for 16 h. This was then added to MG2 (20 mg, 0.0226 mmol) and the mixture was agitated. The reaction mixture had turned solid after 24 h, and so was broken into smaller pieces and stirred under reflux at 40 °C in DCM (40 mL) for 3 h. The solid pieces were separated by filtration and dried under reduced pressure (<1 mbar, 50 °C, 72 h). These reactions were repeated twice. The pieces were weighed – and the average gel content was calculated (82 – 90 %).

### 4.2.2 Gel Time Investigations in the presence of styrene

Gel times were measured using a simple inversion test. The end point is where the reaction was cross-linked enough to be able to hold its shape (*i.e.* not deform) when turned upside-down.

#### 4.2.2.1 ROMP of Polyester 1 with G1

Polyester 1 (1030 mg, ~2.43 mmol(NBE)) was dissolved in DCM (4 mL) that contained styrene (0-5 eq. with respect to G1) for 16 h. This was then added to G1 (20 mg, 0.0243 mmol) and the mixture was agitated. The vial was gently shaken every 15 s until the mixture held its shape – and continued to do so when inverted. This was defined as the gel time for these and all future reactions. These reactions were repeated three times, and the average was calculated over the three experiments (1255 – 1880 s).

#### 4.2.2.2 ROMP of Polyester 2 with G1

Polyester 2 (608 mg, ~2.43 mmol(NBE)) was dissolved in DCM (4 mL) that contained styrene (0-5 eq. with respect to G1) for 16 h. This was then added to G1 (20 mg, 0.0243 mmol) and the mixture was agitated. The vial was gently shaken every 15 s until the mixture held its shape – and continued to do so when inverted. These reactions were repeated three times, and the average was calculated over the three experiments (1835 – 2630 s).

#### 4.2.2.3 ROMP of Polyester 1 with G2

Polyester 1 (996 mg, ~2.36 mmol(NBE)) was dissolved in DCM (4 mL) that contained styrene (0-5 eq. with respect to G2) for 16 h. This was then added to G2 (20 mg, 0.0236 mmol) and the mixture was agitated. The vial was gently shaken every 15 s until the mixture held its shape – and continued to do



so when inverted. These reactions were repeated three times, and the average was calculated over the three experiments (535 – 580 s).

#### 4.2.2.4 ROMP of Polyester 2 with G2

Polyester 2 (590 mg, ~2.36 mmol(NBE)) was dissolved in DCM (4 mL) that contained styrene (0-5 eq. with respect to G2) for 16 h. This was then added to G2 (20 mg, 0.0236 mmol) and the mixture was agitated. The vial was gently shaken every 15 s until the mixture held its shape – and continued to do so when inverted. These reactions were repeated three times, and the average was calculated over the three experiments (710 – 735 s).

#### 4.2.2.5 ROMP of Polyester 1 with MG2

Polyester 1 (954 mg, ~2.26 mmol(NBE)) was dissolved in DCM (4 mL) that contained styrene (0-5 eq. with respect to MG2) for 16 h. This was then added to MG2 (20 mg, 0.0226 mmol) and the mixture was agitated. The vial was gently shaken constantly until the mixture held its shape – and continued to do so when inverted. These reactions were repeated twice, and the average gel time was calculated over both experiments (13 – 15 s).

#### 4.2.2.6 ROMP of Polyester 2 with MG2

Polyester 2 (566 mg, ~2.26 mmol(NBE)) was dissolved in DCM (4 mL) that contained styrene (0-5 eq. with respect to MG2) for 16 h. This was then added to MG2 (20 mg, 0.0226 mmol) and the mixture was agitated. The vial was gently shaken constantly until the mixture held its shape – and continued to do so when inverted. These reactions were repeated twice, and the average gel time was calculated over both experiments (16 – 19 s).

### 4.3 Results and Discussion

#### 4.3.1 Calculation of Error

Experiments measuring gel time and gel contents; using Polyesters 1 and 2; and using all G1 and G2 initiators, were repeated three times in order to give a reasonable idea of the error involved. Those experiments using MG2 were repeated twice due to availability and cost of the initiator. The error is both positive and negative from the mean value and is calculated as half the standard deviation (Equation 4.1) of the three values. It is used for seeing if the results achieved show any trend or are more or less identical.

$$\sigma = \sqrt{\frac{\sum(x - \bar{x})^2}{N}}$$

Equation 4.1

Where  $\sigma$  = standard deviation,  $x - \bar{x}$  = difference of value from mean, N = number of measurements in data set.

### 4.3.2 Gel Content Investigations in the presence of styrene

The polyesters were dissolved in DCM and varying levels of styrene from zero to two equivalents with respect to the initiator. This was to see if the addition of styrene had any effect on the gel content of the ROMP products of either polyester using G1, G2 or MG2.

#### 4.3.2.1 ROMP of Polyester 1

The gel contents were calculated to the nearest whole percent and seemed to generate reasonably large errors with G1 – though this is not unsurprising using DCM extraction especially with these broadly disperse polyester starting materials. From studying the data in Table 4.1 and Table 4.2, it would appear there is no overall trend with styrene content and gel content with Polyester 1 and any initiator– though a graphical form gives a better idea.

**Table 4.1:** Table detailing the gel contents the ROMP products from Polyester 1 in the presence of styrene with G1 and G2 ruthenium initiators

Grubbs Initiator	Equivalents of styrene	Gel Content (%)			Mean Gel Content (%)	Error ( $\sigma/2$ )
		1	2	3		
<b>G1</b>	<b>0.0</b>	65	51	62	59.3	3.7
	<b>0.5</b>	47	67	72	62.0	6.6
	<b>1.0</b>	64	70	53	62.3	4.3
	<b>1.5</b>	69	61	62	64.0	2.2
	<b>2.0</b>	63	63	56	60.7	2.0
<b>G2</b>	<b>0.0</b>	87	85	90	87.3	1.3
	<b>0.5</b>	88	86	91	88.3	1.3
	<b>1.0</b>	87	88	88	87.7	0.3
	<b>1.5</b>	90	88	91	89.7	0.8
	<b>2.0</b>	87	84	90	87.0	1.5

**Table 4.2:** Table detailing the gel contents the ROMP products from Polyester 1 in the presence of styrene with MG2 ruthenium initiator

Grubbs Initiator	Equivalents of styrene	Gel Content (%)		Mean Gel Content (%)	Error ( $\sigma/2$ )
		1	2		
MG2	0.0	87	86	86.5	0.4
	0.5	79	85	82.0	2.1
	1.0	85	84	84.5	0.4
	1.5	85	79	82.0	2.1
	2.0	88	84	86.0	1.4

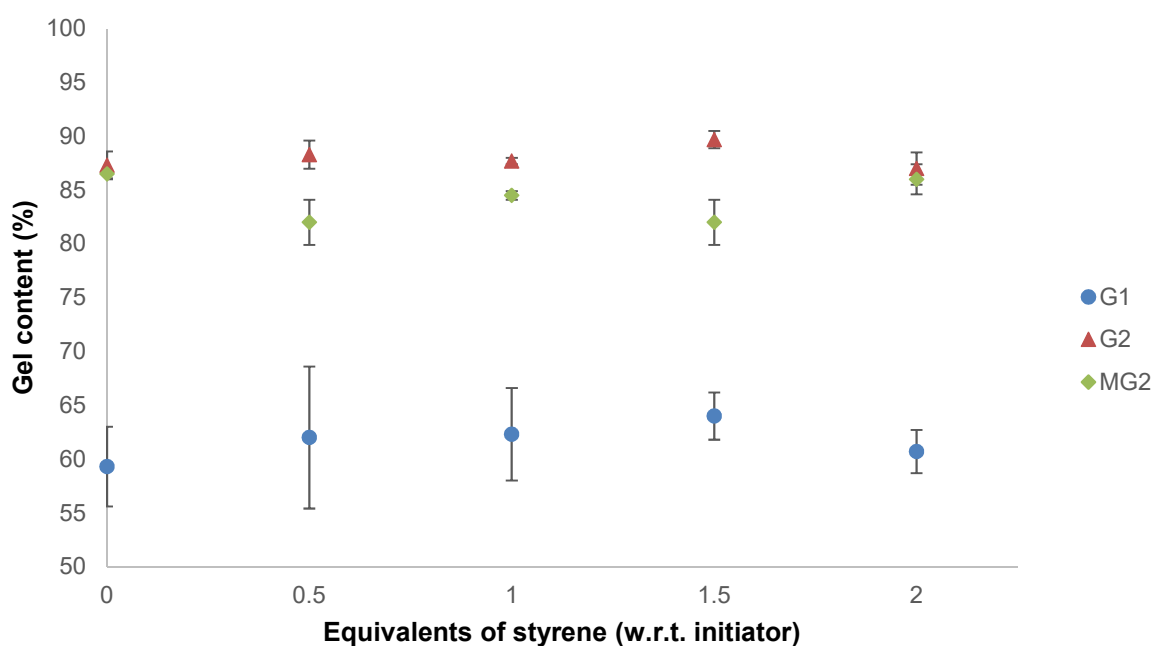


**Figure 4.1:** Gel contents of cross-linked networks formed from ROMP of Polyester 1 in the presence of styrene

As Figure 4.1 clearly shows, from 0-2 equivalents of styrene, the gel contents of the ROMP product of Polyester 1 are within error of one another for G1, G2 and MG2 as the initiator. The errors for G2 and MG2 are surprisingly very small compared to G1, in spite of the fact that these reactions achieve gelation much quicker. What can also be seen is that the gel content when using MG2 is slightly lower than any of the experiments using G2, and the gel content using G1 is significantly lower. This is what was also found without any addition of styrene in Chapter 3.

The  $^1\text{H}$  NMR spectra (Figure 4.2) show that styrene has no effect on what is contained in the DCM soluble fraction and – by inference – likely has no effect on the cross-linked network part either. The level of styrene used is too low to see by NMR spectroscopy. As seen previously in the ROMP of Polyester 1 (Chapter 3), all the DCM soluble fractions contain the norbornene moiety, as shown by the olefinic proton peaks between 5.75 and 6.31 ppm. This suggests that the cross-linking becomes too dense – *i.e.* the mixture gels before all the strained olefin groups are ring opened.

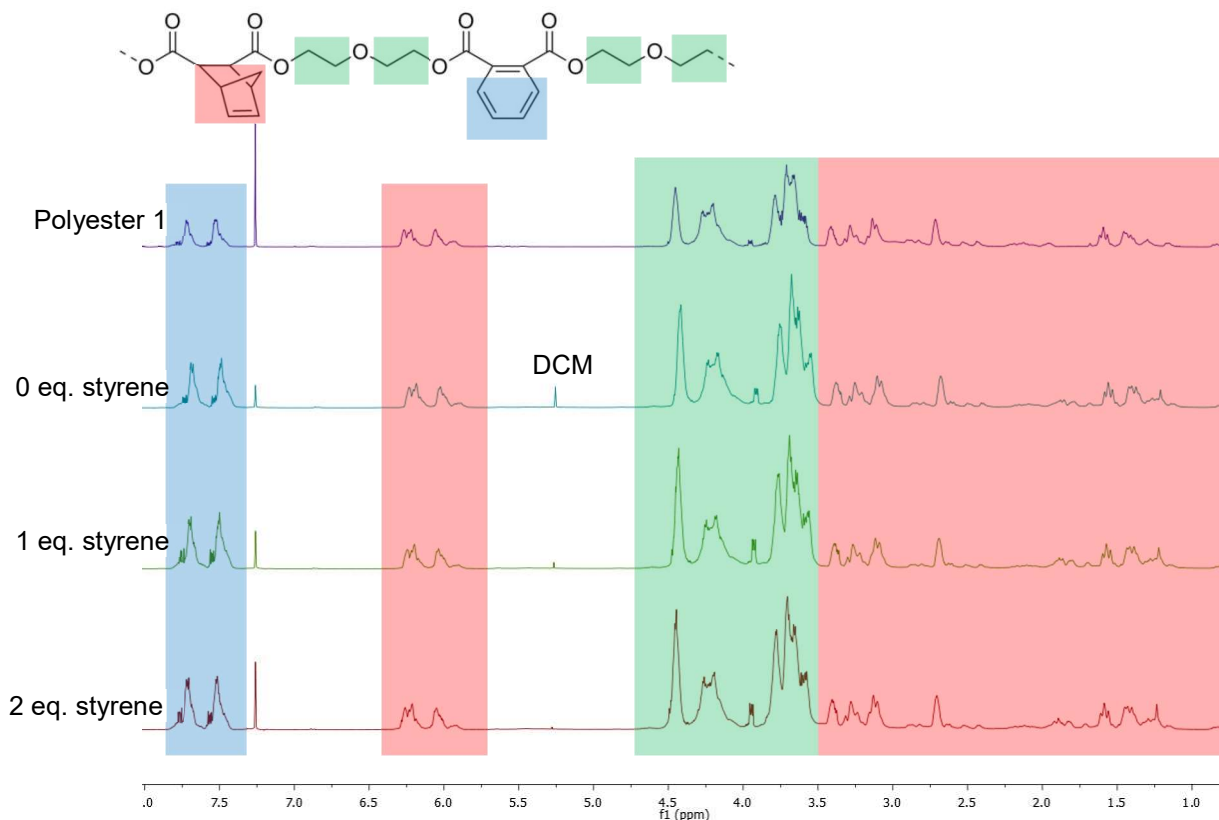


**Figure 4.2:**  $^1\text{H}$  NMR ( $\text{CDCl}_3$ , 400 MHz) spectra of ROMP of Polyester 1 and DCM fractions of gels formed using varying levels of styrene

#### 4.3.2.2 ROMP of Polyester 2

Unexpectedly, generally the errors using Polyester 2 are much smaller than the polymers produced using Polyester 1 as shown in Table 4.3. This could possibly be due to the fact that Polyester 2 is a brittle solid, meaning it can be ground down to a fine powder and is therefore easier to measure accurately. The other possibility is that Polyester 2 is an alternating copolymer (Polyester 1 is a random copolymer) meaning that the spacing of the norbornene groups is much more regular, *i.e.* it is less likely there will be any copolymer chains without norbornene functionality. This would mean that the gel content is likely to be more consistent.

There are anomalous results (highlighted in the table in red), with one equivalent of styrene with respect to G2 giving a gel content of 73 %, when the expected value is around 90-95 %. This results in the gel content average reducing significantly to 86 % although, due to the increase in the standard deviation because of this anomaly, the point is still within error of the rest of the experimental values.

Similarly, with 0.5 equivalents with respect to MG2: the gel content is lower than expected. This time however, the fact that this is purely an error cannot be confirmed definitively as these experiments were only performed twice.

**Table 4.3:** Table detailing the gel contents the ROMP products from Polyester 2 in the presence of styrene

Initiator	Equivalents of styrene	Gel Content (%)			Mean Gel Content (%)	Error ( $\sigma/2$ )
		1	2	3		
<b>G1</b>	<b>0.0</b>	51	56	56	54.3	1.4
	<b>0.5</b>	49	62	56	55.7	3.3
	<b>1.0</b>	58	56	53	55.7	1.3
	<b>1.5</b>	49	44	64	52.3	5.2
	<b>2.0</b>	52	54	51	52.3	0.8
<b>G2</b>	<b>0.0</b>	94	87	93	91.3	1.9
	<b>0.5</b>	97	94	95	94.3	1.5
	<b>1.0</b>	73	94	91	86.0	5.7
	<b>1.5</b>	91	90	91	90.7	0.3
	<b>2.0</b>	90	95	87	90.7	2.0
<b>MG2</b>	<b>0.0</b>	87	88		87.5	0.4
	<b>0.5</b>	75	88		81.5	4.6
	<b>1.0</b>	88	88		88.0	0.0
	<b>1.5</b>	88	88		88.0	0.0
	<b>2.0</b>	90	88		89.0	1.4

What can readily be seen from Figure 4.3 is that the gel content is not affected by the presence (either positively or negatively) of styrene. A straight line could almost be drawn through these points,

and certainly within the error bars. As before, there is very little difference in gel content from the ROMP of Polyester 2 using Grubbs 1<sup>st</sup> generation initiator.

Using G2 as the initiator, the gel content with half an equivalent of styrene shows a much larger than expected error due to the extremely low recorded gel content of 75 % (around 88 % would be expected), whereas the rest of the points have very small errors and are more or less in a straight line. Again, the ROMP product of Polyester 2 formed using MG2 exhibits a gel content very similar to Polyester 2 that was polymerised using G2; and again, much greater than that utilising G1.

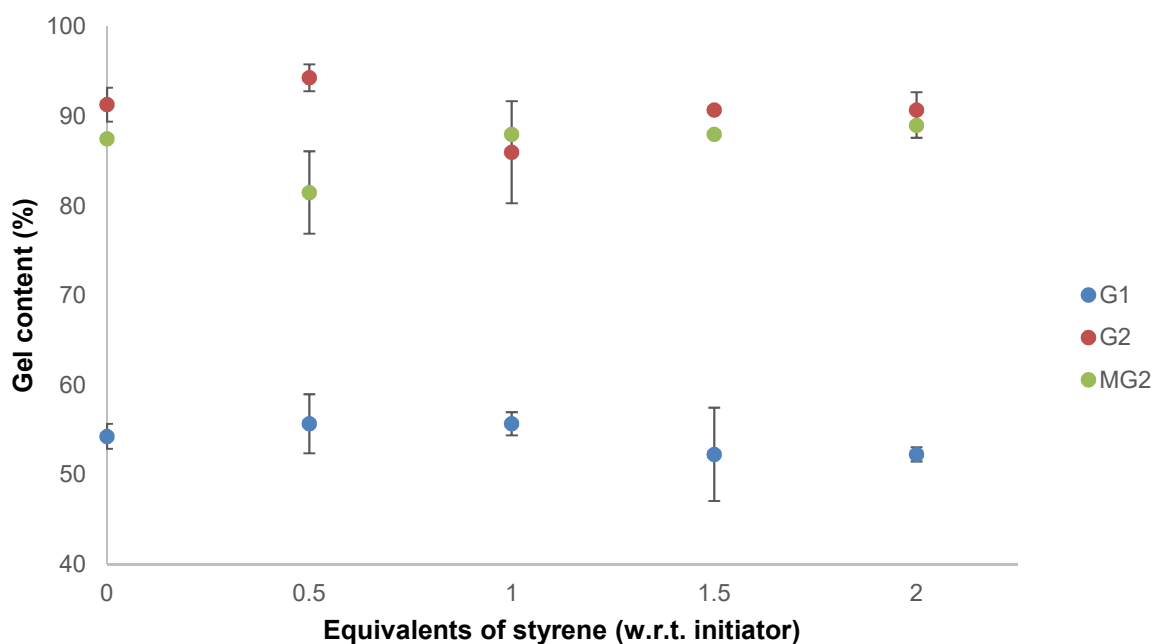


**Figure 4.3:** Gel contents of cross-linked networks formed from ROMP of Polyester 2 in the presence of styrene

From <sup>1</sup>H NMR (Figure 4.4) spectra, it can be seen that adding styrene has no effect on the DCM soluble fraction (and therefore no change in the insoluble fraction). In each spectrum we do see a large DCM peak which is still present after several days of drying. What can also be seen, especially when 2 equivalents of styrene are used, are some peaks around the chloroform peak at 7.26 ppm. These could possibly be due to the presence of styrene in the DCM soluble fraction and it is not removed under reduced pressure. The other possibility is that this is due to the presence of small quantities of residual Grubbs 1<sup>st</sup> generation initiator.

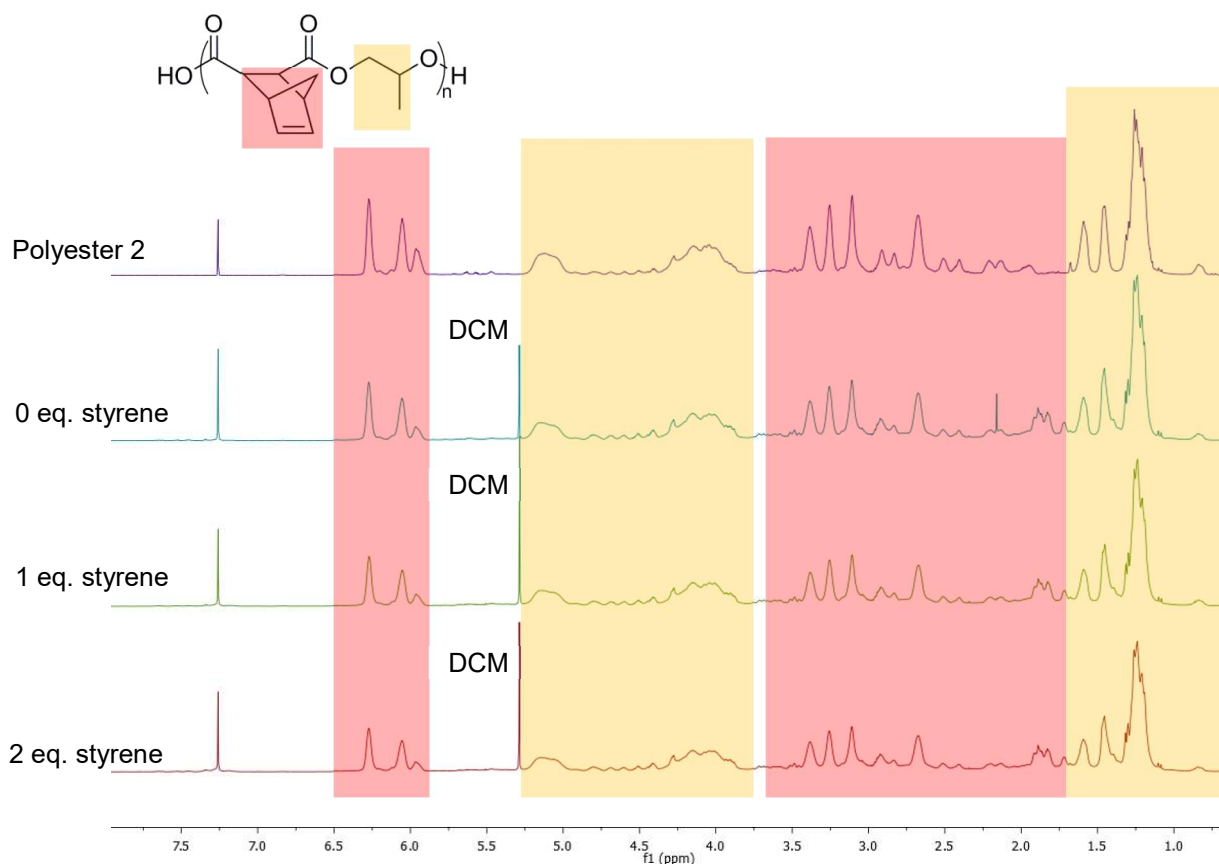


**Figure 4.4:** <sup>1</sup>H NMR (CDCl<sub>3</sub>, 400 MHz) spectra of ROMP of Polyester 2 with G1 and DCM fractions of gels formed using varying levels of styrene

All other peaks in Figure 4.4 remain largely unchanged including the norbornene olefinic protons between 5.85 and 6.30 ppm, and some of the glycol protons, which are visibly separate from the norbornene ring peaks, between 3.85 and 5.25 ppm.

### 4.3.3 Gel Time Investigations in the Presence of Styrene

It was noticed that the experiments with higher styrene contents appeared to be taking longer to gel, and so this phenomenon was investigated. In order to highlight any changes seen, the range in styrene equivalents was changed from 0 – 2 equivalents to 0 – 5 equivalents with respect to the initiator. This would also mean that the experiments would more likely still show a trend if the errors were large.

#### 4.3.3.1 ROMP of Polyester 1 with G1

As can be seen from the data in Table 4.4, as the level of styrene is increased the gel time in this system is steadily increased. With no styrene the gel time is just less than 21 min, rising to 31 min if 5 equivalents of styrene are added. Considering the fact styrene previously appeared to have no effect on the gel contents, it is a surprise how much of an effect it has on the gel time – slowing the reaction by almost 50 % with the maximum concentration utilised in this investigation. Also, this cannot be a concentration (of the polyester or initiator) effect slowing the reaction rate since the styrene is added

in dilute solution, and it is made sure that the volume of the reaction stays constant over all the polymerisations.

**Table 4.4:** Table detailing the gel time of the ROMP product of Polyester 1 using G1 with varying levels of styrene

Equivalents of styrene	Gel Time (s)			Mean Gel Time (s)	Error ( $\sigma/2$ )
	1	2	3		
0	1290	1230	1245	1255	13
1	1455	1470	1350	1425	27
2	1560	1485	1530	1525	15
3	1695	1635	1695	1675	14
4	1770	1755	1800	1775	9
5	1890	1875	1875	1880	4

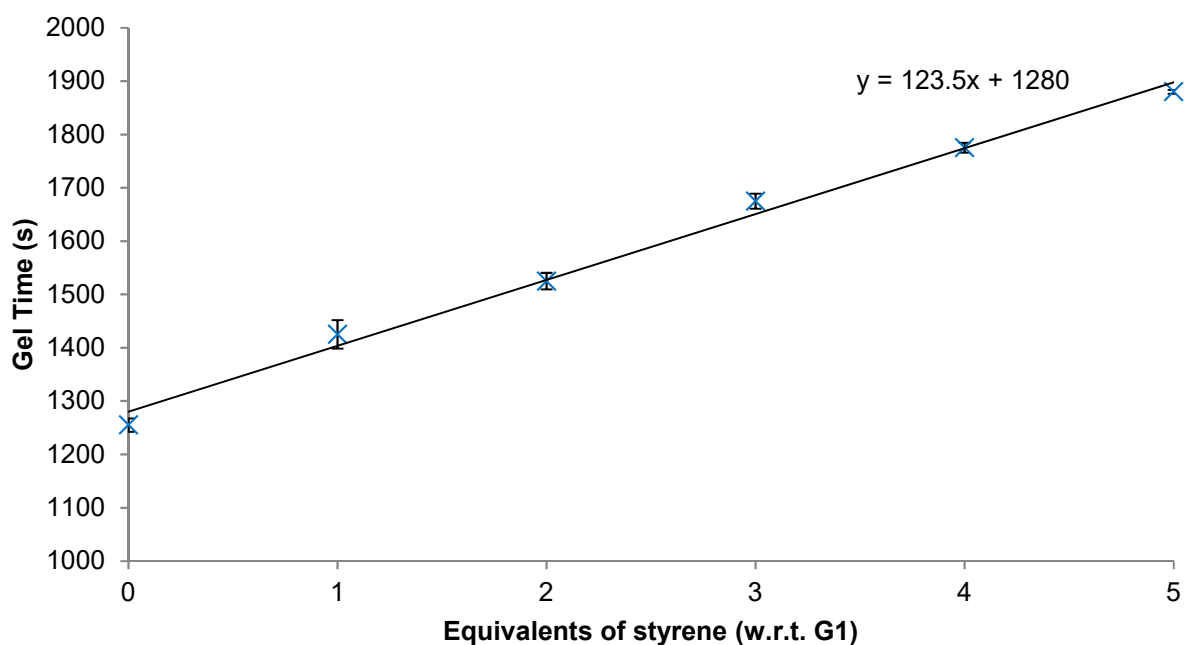


**Figure 4.5:** Gel times for the ROMP of Polyester 1 with G1 in the presence of styrene, (the y-axis starts at 1000 s for clarity)



The first thing that can be seen by looking at the data in Figure 4.5 is the fact that there appears to be a linear relationship between gel time and styrene concentration of up to 5 equivalents. In order to double the gel time, using the equation shown on the graph and below in Equation 4.2, it would appear that you would require just over 10 equivalents of styrene with respect to Grubbs 1<sup>st</sup> generation initiator. Although there is no change in gel content, styrene could be used to slow down the gel time and allow the addition of copolymers to the reaction more easily.

$$\text{Gel time} = 123.5 (\text{equivalents of styrene}) + 1280$$

**Equation 4.2:** Equation for the line of best fit for the gel time for the ROMP of Polyester 1 with G1 in the presence of styrene

The error bars on this graph are small, suggesting that although the inversion test (agitating the mixture every 15 s) is a fairly basic test, it proffers extremely reliable results – especially over these large timescales.

#### 4.3.3.2 ROMP of Polyester 2 with G1

The data in Table 4.5 reveals that all the gel times for the ROMP of Polyester 2 are much slower than when using Polyester 1. This could be due to the higher intrinsic viscosity of the system due to the much less flexible glycol moiety, although the reaction is undertaken in DCM so this effect is likely to be only slight. The other immediately noticeable comparison is that the error is much larger for the ROMP of Polyester 2. This is the reverse of what occurred with the gel content investigations. This could possibly be due to the much broader dispersity of Polyester 2 than Polyester 1 (16.9 *versus* 3.9), meaning that Polyester 2 may have a much less well-defined structure than Polyester 1 and so the range in times at which the cross-links start to occur will vary greatly.

**Table 4.5:** Table detailing the gel time of the ROMP product of Polyester 2 using G1 with varying levels of styrene

Equivalents of styrene	Gel Time (s)			Mean Gel Time (s)	Error ( $\sigma/2$ )
	1	2	3		
0	1830	1800	1875	1835	15
1	1935	1980	2085	2000	31
2	2130	2250	2310	2230	37
3	2205	2355	2550	2370	71
4	2655	2430	2625	2570	50
5	2700	2565	2625	2630	28

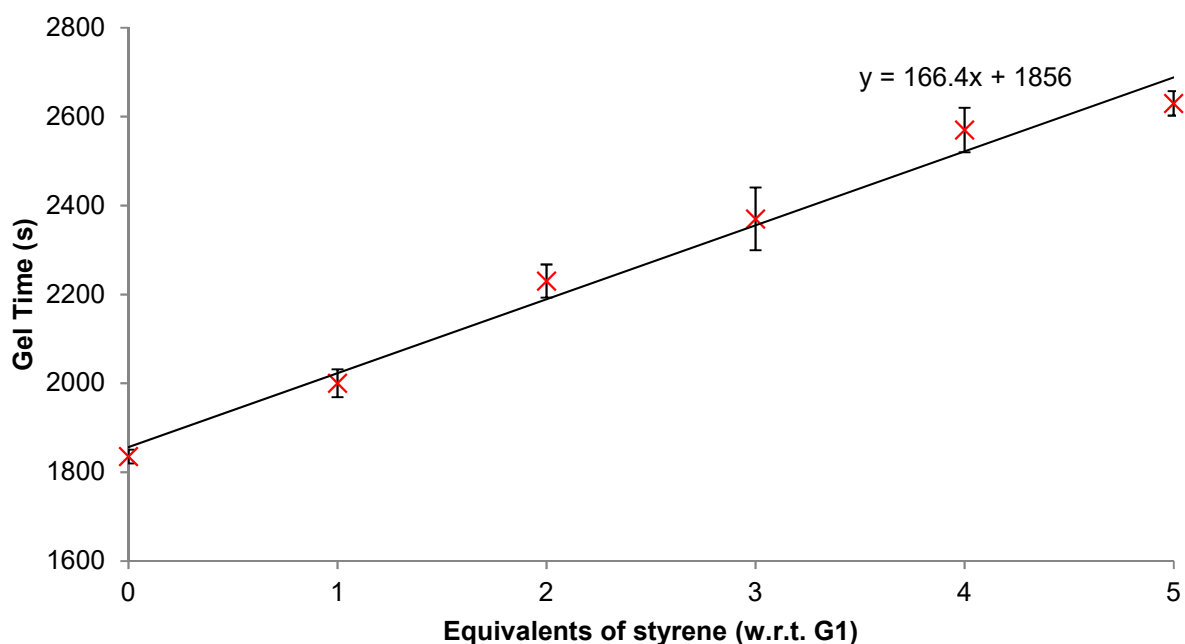


**Figure 4.6:** Gel times for the reaction between Polyester 2 and G1, the y-axis starts at 1600 s for clarity

The data in Figure 4.6 shows that the gel time is steadily increased from 30.5 to 44 min from zero to five equivalents of styrene. This suggests that using Grubbs 1<sup>st</sup> generation to polymerise Polyester 2 can be slowed markedly using up to five equivalents of styrene. The errors seen in this graph are

small and do not overlap one another – meaning that the gel time differences between the reactions are significant, and not within errors.

#### 4.3.3.3 ROMP of Polyester 1 with G2

The data in Table 4.6 immediately shows how much quicker gelation is attained using G2 than G1 in this system – taking approximately half the time (just under 9 min for zero styrene). What can also be seen is that there is far less of an effect of styrene on the gel time, possibly due to the much quicker propagation characteristics of G2, which may also affect how reliable the gel times are due to the rudimentary technique of measuring them.

**Table 4.6:** Table detailing the gel time of the ROMP product of Polyester 1 using G2 with varying levels of styrene

Equivalents of styrene	Gel Time (s)			Mean Gel Time (s)	Error ( $\sigma/2$ )
	1	2	3		
0	540	540	525	535	4
1	570	585	570	575	4
2	555	555	570	560	4
3	555	570	600	575	9
4	555	570	570	565	4
5	570	570	600	580	7

There appears to be no general trend in styrene affecting the gel time up to five equivalents of styrene. There is however a significant difference (greater than error) between zero styrene and added styrene with gelation slowed by at least 25 s, or 5 %. This is not the sort of level of retardation seen with G1 but could still be significant.

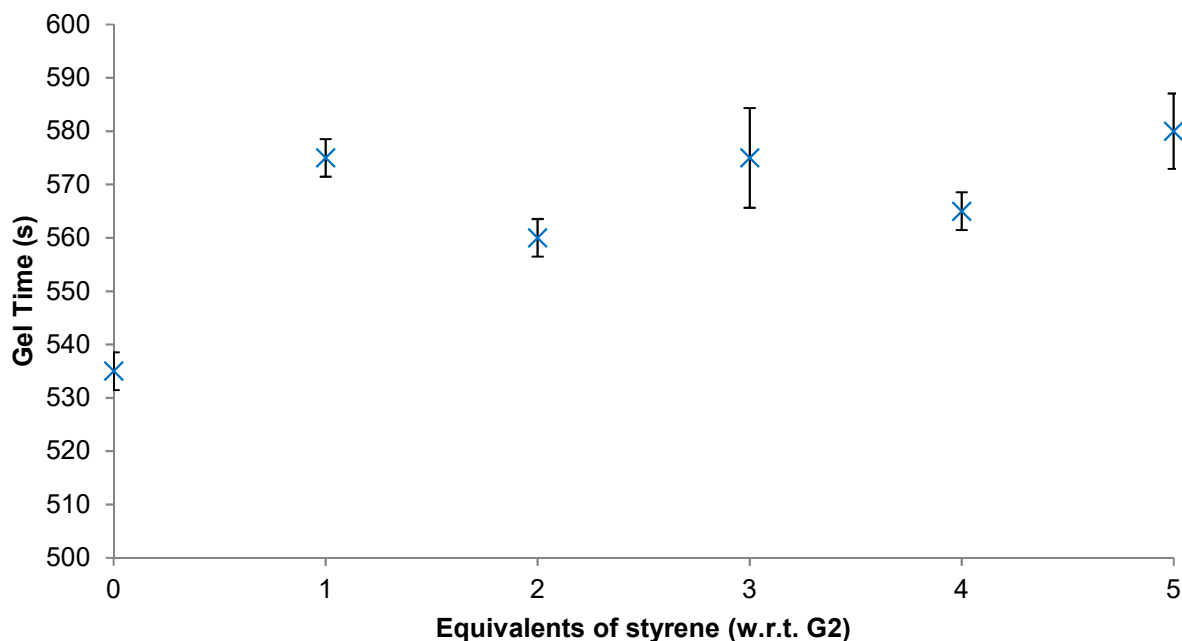


**Figure 4.7:** Gel times for the ROMP of Polyester 1 with G2 in the presence of styrene, (the y-axis starts at 500 s for clarity)

The data in Figure 4.7 shows clearly that increasing the styrene level has no effect on the gel time. In fact, the points from 1 to 5 equivalents of styrene are pretty much within error of one another. Taking into account the data point with zero styrene, it can be said that styrene has an effect of slowing the gel time but adding additional styrene seemingly has no effect.

#### 4.3.3.4 ROMP of Polyester 2 with G2

The first thing that can be seen from the data in Table 4.7 is that the gel times are slower again when compared with Polyester 2. This is in agreement with all previous results. The observed error is similar too though the effect is slightly less significant due to the slightly longer gel times here.

**Table 4.7:** Table detailing the gel time of the ROMP product of Polyester 2 using G2 with varying levels of styrene

Equivalents of styrene	Gel Time (s)			Mean Gel Time (s)	Error ( $\sigma/2$ )
	1	2	3		
0	690	705	735	710	9
1	705	750	750	735	11
2	705	750	750	735	11
3	705	750	735	730	9
4	705	750	735	730	9
5	705	750	735	730	9

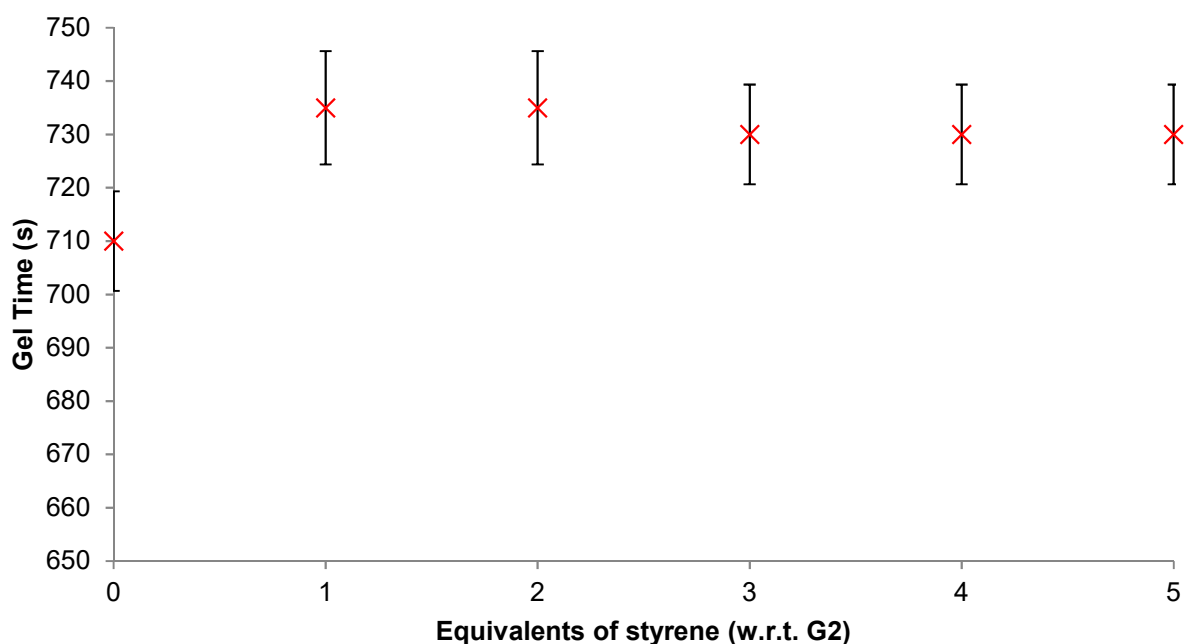


**Figure 4.8:** Gel times for the ROMP of Polyester 2 with G2 in the presence of styrene, (the y-axis starts at 650 s for clarity)

Furthermore, the data in Figure 4.8 clearly shows that the utilisation of styrene slows down the gel time in this system by up to 30 s (4 %). However, adding more than 1 equivalent appears to have no

effect. It could be said that the presence of styrene has an effect of slowing the ROMP of Polyester 2 by G2 but adding in more than 1 equivalent of styrene will not lengthen the gel time any further.

#### 4.3.3.5 ROMP Polyesters 1 and 2 using MG2

As was the case with gel content reactions, only two repeats were possible when using Grubbs modified 2<sup>nd</sup> generation initiator due to its limited supply. The data shown in Table 4.8 show the gel times seen for the ROMP of Polyester 1 with MG2 are much quicker than seen with Grubbs 1<sup>st</sup> or 2<sup>nd</sup> generation initiators. This is due to its much faster rate of initiation and high rate of propagation.

**Table 4.8:** Table detailing the gel time of the ROMP product of Polyesters 1 and 2 using MG2 with varying levels of styrene

Polyester	Equivalents of styrene	Gel Time (s)		Mean Gel Time (s)	Error ( $\sigma/2$ )
		1	2		
Polyester 1	0	12	14	13.0	0.5
	1	14	16	15.0	0.5
	2	14	14	14.0	0.0
	3	13	15	14.0	0.5
	4	14	15	14.5	0.3
	5	13	14	13.5	0.3
Polyester 2	0	17	18	17.5	0.3
	1	18	18	18.0	0.0
	2	18	19	18.5	0.3
	3	16	18	17.0	0.5
	4	17	19	18.0	0.5
	5	17	19	18.0	0.5

The ROMP of each polyester is shown to be much more rapid with MG2 than G2 and G1. This is expected due to the rapid rates of initiation and propagation of the modified 2<sup>nd</sup> generation initiator.<sup>5</sup> In fact, the time taken to achieve gelation has decreased from the order of minutes to seconds. However, despite the much shorter timescale, the size of error is very small. The only issue is that the

experiments using MG2 in this work were only carried out twice, so the small errors may have increased with an extra set of results. Also due to the rapid gelation time, MG2 polymerised systems will be affected far more by quality of the mixing beforehand since if any polyester or initiator is not well dissolved in the solvent, then it will not take part in the reaction.

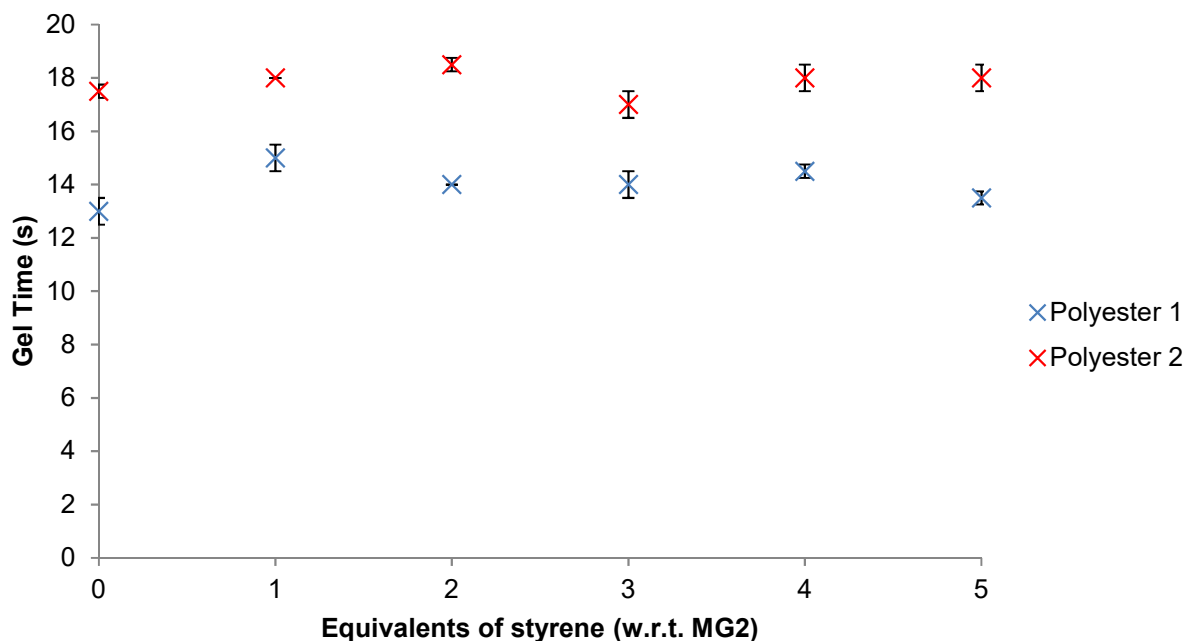


**Figure 4.9:** Gel times for the ROMP of Polyester 1 and Polyester 2 with MG2 in the presence of styrene

The data in Figure 4.9 show, for both Polyester 1 and Polyester 2, styrene content appears to have no effect on gelation time when modified 2<sup>nd</sup> generation initiator is used. There is not even a difference between styrene and no styrene.

## 4.4 Conclusions

The presence of styrene has no effect on the gel content of the products of the ROMP of Polyester 1 or 2 using any of the three initiators. Grubbs 1<sup>st</sup> generation initiator also constantly produces cross-linked networks with lower gel contents than either of the 2<sup>nd</sup> generation and modified 2<sup>nd</sup> generation initiators – which produce similar gel contents. Polyester 1 and 2 starting materials are the main constituents of the soluble fraction of these reactions suggesting that these reactions gel before going to completion.

For Grubbs 1<sup>st</sup> generation initiator, the presence of styrene has a strong effect on the gel time of the polyesters, slowing both of them down significantly even at one equivalent of styrene. The relationship also appears to be linear and is therefore still increasing the gel time significantly from 4 to 5 equivalents. Grubbs 2<sup>nd</sup> generation also has an effect on the gel time – slowing it by up to 5 % upon addition of five equivalents of styrene. This is, however, a much smaller effect than with G1. This is likely due to its much quicker propagation rate, not allowing the styrene to affect the rate of ROMP. G2 may also perhaps preferentially polymerise norbornene moieties *via* ROMP over the cross-

metathesis reaction with styrene. Using higher numbers of equivalents of styrene with Grubbs 2<sup>nd</sup> generation initiator may show more of a trend. The use of modified 2<sup>nd</sup> generation initiator appears to have no influence on the gel time. This again is probably due to either its high rate of propagation (remembering the gel takes only 15 s to form in these experiments compared to 30 min with G1), or perhaps it preferentially polymerises norbornene moieties *via* ROMP over the cross-metathesis reaction with styrene. The error was very small even on these experiments, which are on timescales of a dozen seconds or so. Even at these much shorter timescales, Polyester 2 takes longer to gel than Polyester 1, a common trend seen throughout all of these experiments.

The fact we can slow down the rate of gelation so significantly with G1, and to a certain extent with G2, may allow us to add in extra reactants to the polymer. These may help us alter the polymer characteristics that would require further investigation. Another option that this slowing of gelation could be is that it would help control the curing of any resin using this system, meaning that – for example – if used as a coating, there would be more time available for its application before the polymer gels and becomes unworkable.

## 4.5 References

1. Hsu, C. P.; Zhao, M. Y.; Voeks, S. L. Styrene-free unsaturated polyester. EP 2621999 A1, **2013**.
2. Sanchez, E. M. S.; Zavaglia, C. A. C.; Felisberti, M. I., Unsaturated polyester resins: influence of the styrene concentration on the miscibility and mechanical properties. *Polymer* **2000**, 41 (2), 765-769.
3. Khosravi, E.; Kenwright, A. M.; Yu, Z.; Haigh, D. M.; Hobson, L. Olefin metathesis polymerisation. WO 2010083881 A1, **2010**.
4. Chatterjee, A. K.; Choi, T.-L.; Sanders, D. P.; Grubbs, R. H., A General Model for Selectivity in Olefin Cross Metathesis. *J. Am. Chem. Soc.* **2003**, 125 (37), 11360-11370.
5. Love, J. A.; Sanford, M. S.; Day, M. W.; Grubbs, R. H., Synthesis, Structure, and Activity of Enhanced Initiators for Olefin Metathesis. *J. Am. Chem. Soc.* **2003**, 125 (33), 10103-10109.



## **Chapter 5. ROMP of Norbornene-Functionalised Urethanes**

## 5.1 Introduction

For the formation of styrene-free unsaturated polymers, one of the easiest monomers to target was thought to be norbornene-functionalised polyurethanes. The details of the syntheses of these materials is described in Chapter 2. Preliminary investigations involving mixing ruthenium initiators with linear carbamates, without a norbornene moiety, showed that the free proton on the carbamate NH would not interact with or deactivate the ruthenium-based initiators. This was shown by the fact that the alkylidene proton (seen in G1, G2 and MG2) did not shift according to  $^1\text{H}$  NMR spectroscopy, and that monomers featuring norbornene moieties (e.g. ethylidene norbornene) could still undergo ROMP. Previously, Angeletakis *et al.*<sup>1</sup> also showed the polymerisation of norbornene-functionalised polyethers and polyurethanes – reinforcing the results of the preliminary work here.

Hexamethylene-1,6-bis(5-norbornene-2-methoxy tetraethylene glycol carbamate) (DFM1, Figure 5.1) was the first monomer to be investigated to test the ability to ROMP molecules with carbamate moieties.

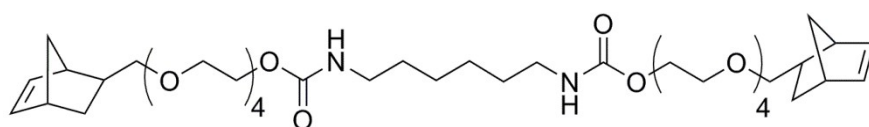


**Figure 5.1:** Structure of hexamethylene-1,6-bis(5-norbornene-2-methoxy tetraethylene glycol carbamate) (Difunctional Monomer 1, DFM1)

Another difunctional monomer which was synthesised was hexamethylene-1,6-bis(5-norbornene-2-carboxylate-2-ethoxy carbamate) (DFM2, Figure 5.2). If this can form a gelled network, then this will also confirm that there are two norbornene rings found in the structure – offering further confirmation of DFM2's synthesis.

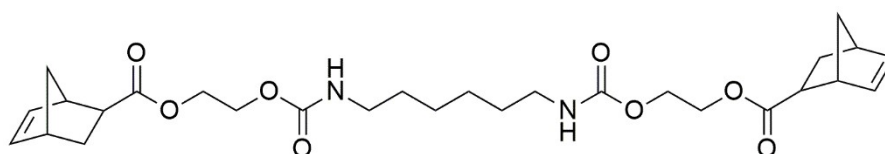


**Figure 5.2:** Structure of hexamethylene-1,6-bis(5-norbornene-2-carboxylate-2-ethoxy carbamate) (Difunctional Monomer 2, DFM2)

The ROMP of 2-hydroxyethyl-5-norbornene-2-carboxylate butyl carbamate (MFM, Figure 5.3) will confirm if the removal of dicyclopentadiene (DCPD) from the starting material of 2-hydroxyethyl-5-norbornene-2-carboxylate was successful. If there is no residual DCPD, no gel will form due to the formation of poly(DCPD).

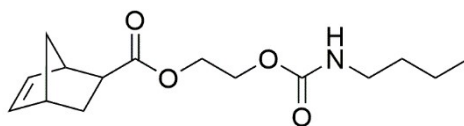
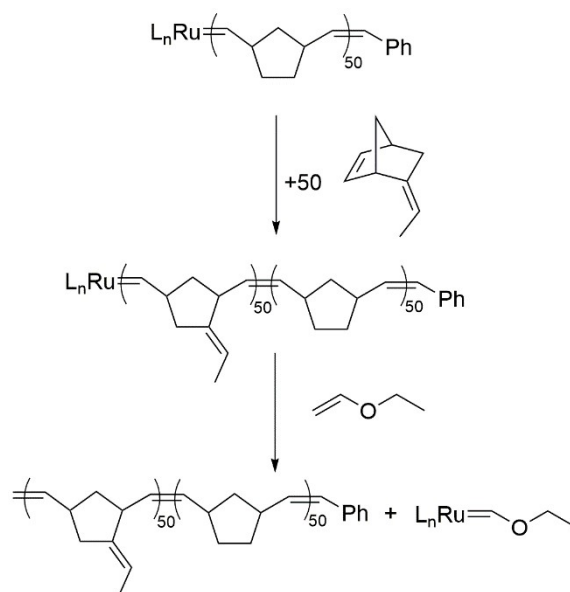


**Figure 5.3:** Structure of 2-hydroxyethyl-5-norbornene-2-carboxylate butyl carbamate (Monofunctional Monomer, MFM)

ROMP can be an example of a living polymerisation<sup>2</sup> as discussed previously, and is a useful technique for producing block copolymers,<sup>3</sup> for example with norbornene and ethylidene norbornene as shown in Scheme 5.1. In this example 50 equivalents of norbornene, with respect to the ruthenium initiator, is polymerised. At this stage the reaction mixture can be analysed by IR spectroscopy for any peaks related to the C=C bond in norbornene, if none are seen the reaction has gone to completion. The other technique which can be used is <sup>1</sup>H NMR spectroscopy as the monomer will have protons from the norbornene olefin at around 6 ppm (in CDCl<sub>3</sub>), whereas the olefinic backbone protons of the polymer chain appear closer to 5.5 ppm.

When the first block has been completely polymerised, 50 equivalents of ethylidene norbornene are added in and the reaction is allowed to go to completion. To terminate the reaction, ethyl vinyl ether is added which cleaves the propagating alkylidene from the polymer chain.



**Scheme 5.1:** Formation of a block copolymer of norbornene, then ethylidene norbornene including the termination step of adding ethyl vinyl ether

Block copolymers using MFM and *N*-(2-ethylhexyl)-5-norbornene-2,3-dicarboximide (EHNBEDC) (Figure 5.4), and 2-hydroxyethyl-5-norbornene-2-carboxylate (HE-NBE-CO<sub>2</sub>, Figure 5.5) were investigated. Since these all contain only one norbornene functionality, they should produce linear polymers.

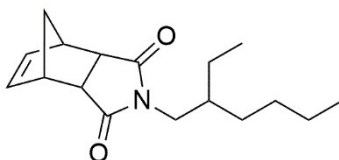


**Figure 5.4:** Structure of *N*-(2-ethylhexyl)-5-norbornene-2,3-dicarboximide

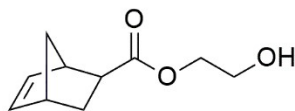


**Figure 5.5:** Structure of 2-hydroxyethyl-5-norbornene-2-carboxylate (HE-NBE-CO<sub>2</sub>)

## 5.2 Experimental

### 5.2.1 ROMP of hexamethylene-1,6-bis(5-norbornene-2-methoxy tetraethylene glycol carbamate) (DFM1)

#### 5.2.1.1 ROMP of DFM1 with G1

DFM1 (568 mg, 1.22 mmol) was dissolved in DCM (1 mL). In a separate vial, G1 (10 mg, 0.0122 mmol) was dissolved in DCM (1 mL) and the two vials were mixed. The reaction mixture turned from purple to orange, and solidified – and could withstand being inverted – after 25 min. After 24 h, the reaction mixture was broken into small pieces, and these were then stirred under reflux at 40 °C in DCM (20 mL) for 3 h. After this, the solid pieces were isolated by filtration, and dried under reduced pressure (<1 mbar, 50 °C, 72 h). The pieces were weighed – and the gel content was calculated (133 mg, 23 %).

#### 5.2.1.2 ROMP of DFM1 with G2

DFM1 (552 mg, 1.18 mmol) was dissolved in DCM (1 mL). In a separate vial, G2 (10 mg, 0.0118 mmol) was dissolved in DCM (1 mL) and the two vials were mixed. The reaction mixture turned from orange to brown, and solidified – and could withstand being inverted – after 4 min. After 24 h, the reaction mixture was broken into small pieces, and these were then stirred under reflux at 40 °C in DCM (20 mL) for 3 h. After this, the solid pieces were isolated by filtration, and dried under reduced pressure (<1 mbar, 50 °C, 72 h). The pieces were weighed – and the gel content was calculated (264 mg, 47 %).

#### 5.2.1.3 ROMP of DFM1 with MG2

DFM1 (530 mg, 1.13 mmol) was dissolved in DCM (1 mL). In a separate vial, MG2 (10 mg, 0.0113 mmol) was dissolved in DCM (1 mL) and the two vials were mixed. The reaction mixture turned from purple to orange, and solidified – and could withstand being inverted – after roughly 8 s. After 24 h, the reaction mixture was broken into small pieces, and these were then stirred under reflux at 40 °C in DCM (20 mL) for 3 h. After this, the solid pieces were isolated by filtration, and dried under

reduced pressure (<1 mbar, 50 °C, 72 h). The pieces were weighed – and the gel content was calculated (70 mg, 13 %).

## **5.2.2 ROMP of hexamethylene-1,6-bis(5-norbornene-2-carboxylate-2-ethoxy carbamate) (DFM2)**

### **5.2.2.1 ROMP of DFM2 with G1**

DFM2 (650 mg, 1.22 mmol) was dissolved in DCM (1 mL). In a separate vial, G1 (10 mg, 0.0122 mmol) was dissolved in DCM (1 mL) and the two vials were mixed. The reaction mixture turned from purple to orange, and solidified – and could withstand being inverted – after 8 min. After 24 h, the reaction mixture was broken into small pieces, and these were then stirred under reflux at 40 °C in DCM (20 mL) for 3 h. After this, the solid pieces were isolated by filtration, and dried under reduced pressure (<1 mbar, 50 °C, 72 h). The pieces were weighed – and the gel content was calculated (656 mg, 99 %).

### **5.2.2.2 ROMP of DFM2 with G2**

DFM2 (627 mg, 1.18 mmol) was dissolved in DCM (1 mL). In a separate vial, G2 (10 mg, 0.0118 mmol) was dissolved in DCM (1 mL) and the two vials were mixed. The reaction mixture turned from orange to brown, and solidified – and could withstand being inverted – after about 1 min. After 24 h, the reaction mixture was broken into small pieces, and these were then stirred under reflux at 40 °C in DCM (20 mL) for 3 h. After this, the solid pieces were isolated by filtration, and dried under reduced pressure (<1 mbar, 50 °C, 72 h). The pieces were weighed – and the gel content was calculated (620 mg, 97 %).

### **5.2.2.3 ROMP of DFM2 with MG2**

DFM2 (602 mg, 1.13 mmol) was dissolved in DCM (1 mL). In a separate vial, MG2 (10 mg, 0.0113 mmol) was dissolved in DCM (1 mL) and the two vials were mixed. The reaction mixture turned from purple to orange, and solidified – and could withstand being inverted – instantaneously. After 24 h, the reaction mixture was broken into small pieces, and these were then stirred under reflux at 40 °C in DCM (20 mL) for 3 h. After this, the solid pieces were isolated by filtration, and dried under reduced pressure (<1 mbar, 50 °C, 72 h). The pieces were weighed – and the gel content was calculated (612 mg, 100 %).

## **5.2.3 ROMP of 2-hydroxyethyl-5-norbornene-2-carboxylate butyl carbamate (MFM)**

### **5.2.3.1 ROMP of MFM with G1**

MFM (341 mg, 1.22 mmol) was dissolved in DCM (2 mL). In a separate vial, G1 (10 mg, 0.0122 mmol) was dissolved in DCM (2 mL). The two vials were mixed and stirred for 24 h, turning from purple to orange. After this, ethyl vinyl ether (5 mg) was added and stirred for a further 10 min before being added dropwise to vigorously stirring dry ice cooled hexane (40 mL). The resulting black solid was then dried under reduced pressure (<1 mbar, 50 °C, 48 h) and weighed (309 mg, 90.6 %), and then analysed by NMR spectroscopy and SEC. <sup>1</sup>H NMR (700 MHz; CDCl<sub>3</sub>): δ(ppm) = 0.89 (t, *J* = 7.3 Hz, 3 H, 13); 1.27-1.40 (m, 2 H, 12); 1.40-1.50 (m, 2 H, 11); 1.58-1.81 (m, 2 H, 4);

1.81-2.12 (m, 2 H, 3); 2.37-2.82 (m, 2 H, 2); 2.92 (s, br, 1 H, 5); 3.04-3.21 (m, 2 H, 10); 3.55-4.46 (multiple peaks, 2 H, 7, 8); 4.88-5.52 (multiple peaks, 3 H, 1, *NH*);  $^{13}\text{C}$  NMR (151 MHz;  $\text{CDCl}_3$ ):  $\delta(\text{ppm}) = 13.8$  (13); 20.0 (12); 20.1 (12<sub>cis</sub>); 32.1 (11); 32.4 (11<sub>cis</sub>); 35.4-40.3 (multiple peaks, 3, 4); 40.6 (10<sub>cis</sub>); 40.8 (10); 42.7 (br, 2); 45.6 (br, 2); 48.2 (br, 5); 61.0 (7<sub>cis</sub>, 8<sub>cis</sub>); 62.6 (7, 8); 129.5-134.7 (1); 156.3 (9); 174.6 (br, 6). SEC:  $M_n = 1.1 \times 10^4 \text{ g mol}^{-1}$ ,  $M_w = 1.5 \times 10^4 \text{ g mol}^{-1}$ ,  $\bar{D} = 1.4$ .

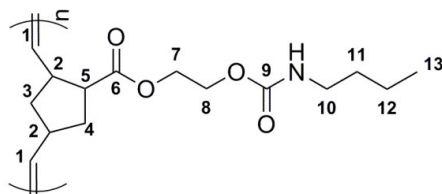


Figure 5.6: Numbered structure of poly(MFM)

### 5.2.3.2 ROMP of MFM with G2

MFM (332 mg, 1.18 mmol) was dissolved in DCM (2 mL). In a separate vial, G2 (10 mg, 0.0118 mmol) was dissolved in DCM (2 mL). The two vials were mixed and stirred for 24 h, turning from orange to brown. After this, ethyl vinyl ether (5 mg) was added and stirred for a further 10 min before being added dropwise to vigorously stirring dry ice cooled hexane (40 mL). The resulting black solid was then dried under reduced pressure (<1 mbar, 50 °C, 48 h) and weighed (304 mg, 91.6 %). NMR spectroscopic analysis matched that of the polymer produced with G1. SEC:  $M_n = 6.1 \times 10^4 \text{ g mol}^{-1}$ ,  $M_w = 1.1 \times 10^5 \text{ g mol}^{-1}$ ,  $\bar{D} = 1.8$ .

### 5.2.3.3 ROMP of MFM with MG2

MFM (385 mg, 1.37 mmol) was dissolved in DCM (2 mL). In a separate vial, MG2 (10 mg, 0.0137 mmol) was dissolved in DCM (2 mL). The two vials were mixed and stirred for 24 h, turning from green to orange. After this, ethyl vinyl ether (5 mg) was added and stirred for a further 10 min before being added dropwise to vigorously stirring dry ice cooled hexane (40 mL). The resulting brown solid was then dried under reduced pressure (<1 mbar, 50 °C, 48 h) and weighed (343 mg, 89.1 %). NMR spectroscopic analysis matched that of the polymer produced with G1. SEC:  $M_n = 5.0 \times 10^4 \text{ g mol}^{-1}$ ,  $M_w = 7.9 \times 10^4 \text{ g mol}^{-1}$ ,  $\bar{D} = 1.5$ .

## 5.2.4 ROM copolymerisations of 2-hydroxyethyl-5-norbornene-2-carboxylate butyl carbamate (MFM) and N-2-ethylhexyl norbornene dicarboximide (EHNBEDC)

### 5.2.4.1 Random ROM copolymerisation of MFM and EHNBEDC with G1

EHNBEDC (168 mg, 0.608 mmol) and MFM (172 mg, 0.608 mmol) were dissolved in DCM (1 mL), and were added to a solution of G1 (10 mg, 0.122 mmol) in DCM (1 mL). This was stirred for 24 h, and meanwhile the mixture turned from purple to orange. After this, ethyl vinyl ether (5 mg) was added to the mixture and stirred for a further 10 min. Then this was added dropwise to vigorously stirring, dry ice cooled hexane (20 mL), forming a greyish precipitate which was isolated by filtration, dried under reduced pressure (<1 mbar, 50 °C, 48 h), and weighed (292 mg, 85.9 %). SEC:  $M_n = 1.0 \times 10^5 \text{ g mol}^{-1}$ ,  $M_w = 1.5 \times 10^5 \text{ g mol}^{-1}$ ,  $\bar{D} = 1.5$ .

**5.2.4.2 Random ROM copolymerisation of MFM and EHNBEDC with MG2**

EHNBEDC (156 mg, 0.566 mmol) and MFM (160 mg, 0.566 mmol) were dissolved in DCM (1 mL), and were added to a solution of MG2 (10 mg, 0.113 mmol) in DCM (1 mL). This was stirred for 24 h, and meanwhile the mixture turned from green to orange. After this, ethyl vinyl ether (5 mg) was added to the mixture and stirred for a further 10 min. Then this was added dropwise to vigorously stirring, dry ice cooled hexane (20 mL), forming a greyish precipitate which was isolated by filtration, dried under reduced pressure (<1 mbar, 50 °C, 48 h), and weighed (282 mg, 89.2 %). SEC:  $M_n = 5.1 \times 10^4 \text{ g mol}^{-1}$ ,  $M_w = 8.0 \times 10^4 \text{ g mol}^{-1}$ ,  $\bar{D} = 1.6$ .

**5.2.4.3 Block ROM copolymerisations of MFM and EHNBEDC with G1**

EHNBEDC (168 mg, 0.608 mmol) was dissolved in  $\text{CDCl}_3$  (0.5 mL). This was added to G1 (10 mg, 0.122 mmol) in  $\text{CDCl}_3$  (1 mL), and after 6 h was analysed by  $^1\text{H}$  NMR spectroscopy to check the absence of norbornene protons – after which MFM (172 mg, 0.608 mmol) in chloroform (0.5 mL) was added and the mixture was stirred for a further 18 h, at which point ethyl vinyl ether (5 mg) was added and stirred for a further 10 min. This mixture was then added dropwise to dry ice cooled, vigorously stirring hexane (20 mL) forming a greyish precipitate which was isolated by filtration, dried under reduced pressure (<1 mbar, 50 °C, 48 h), and weighed (288 mg, 84.7 %). SEC:  $M_{n\text{-high}} = 3.3 \times 10^4 \text{ g mol}^{-1}$ ,  $M_{w\text{-high}} = 5.8 \times 10^4 \text{ g mol}^{-1}$ ,  $\bar{D} = 1.7$ ;  $M_{n\text{-low}} = 2.3 \times 10^3 \text{ g mol}^{-1}$ ,  $M_{w\text{-low}} = 9.8 \times 10^3 \text{ g mol}^{-1}$ ,  $\bar{D} = 4.4$ . This was then repeated with the MFM block added in first, followed by EHNBEDC. Yield: (324 mg, 95.3 %). SEC:  $M_n = 2.3 \times 10^4 \text{ g mol}^{-1}$ ,  $M_w = 3.4 \times 10^4 \text{ g mol}^{-1}$ ,  $\bar{D} = 1.5$ .

**5.2.4.4 Block ROM copolymerisations of MFM and EHNBEDC with MG2**

EHNBEDC (156 mg, 0.566 mmol) was dissolved in  $\text{CDCl}_3$  (0.5 mL). This was added to MG2 (10 mg, 0.113 mmol) in  $\text{CDCl}_3$  (1 mL), and after 6 h was analysed by  $^1\text{H}$  NMR to check the absence of norbornene protons – after which MFM (160 mg, 0.566 mmol) in chloroform (0.5 mL) was added and the mixture was stirred for a further 18 h, at which point ethyl vinyl ether (5 mg) was added and stirred for a further 10 min. This mixture was then added dropwise to dry ice cooled, vigorously stirring hexane (20 mL) forming a greyish precipitate which was isolated by filtration, dried under reduced pressure (<1 mbar, 50 °C, 48 h), and weighed (272 mg, 86.1 %). SEC:  $M_{n\text{-high}} = 1.2 \times 10^5 \text{ g mol}^{-1}$ ,  $M_{w\text{-high}} = 4.1 \times 10^5 \text{ g mol}^{-1}$ ,  $\bar{D} = 3.5$ ;  $M_{n\text{-low}} = 1.7 \times 10^4 \text{ g mol}^{-1}$ ,  $M_{w\text{-low}} = 2.3 \times 10^4 \text{ g mol}^{-1}$ ,  $\bar{D} = 1.4$ . This was then repeated with the MFM block added in first, followed by EHNBEDC. Yield: (271 mg, 85.9 %). SEC:  $M_{n\text{-high}} = 1.0 \times 10^5 \text{ g mol}^{-1}$ ,  $M_{w\text{-high}} = 1.4 \times 10^5 \text{ g mol}^{-1}$ ,  $\bar{D} = 1.3$ ;  $M_{n\text{-low}} = 1.3 \times 10^4 \text{ g mol}^{-1}$ ,  $M_{w\text{-low}} = 1.6 \times 10^4 \text{ g mol}^{-1}$ ,  $\bar{D} = 1.3$ .

**5.2.5 ROM copolymerisations of 2-hydroxyethyl-5-norbornene-2-carboxylate (HE-NBE-CO<sub>2</sub>) and 2-hydroxyethyl-5-norbornene-2-carboxylate butyl carbamate (MFM)****5.2.5.1 Random ROM copolymerisation of HE-NBE-CO<sub>2</sub> and MFM with G1**

HE-NBE-CO<sub>2</sub> (56 – 222 mg, 0.305 – 1.22 mmol) and 2-hydroxyethyl-5-norbornene-2-carboxylate butyl carbamate (257 – 0 mg, 0.915 – 0.00 mmol) were dissolved in DCM (2 mL), then added to G1 (10 mg, 0.0122 mmol) dissolved in DCM (2 mL). After 24 h, ethyl vinyl ether (5 mg) was added, and stirred for a further 10 min. Any precipitate formed at this point was removed by filtration. The DCM

soluble fraction was then added dropwise to dry ice cooled hexane and the precipitated polymer was then filtered and dried under reduced pressure (<1 mbar, 50 °C, 48 h) and weighed (0.0 – 88.0 %).

The DCM insoluble fraction which had previously been separated was stirred under reflux at 40 °C in DCM (20 mL) for 3 h. After this, the solid was isolated by filtration, and dried under reduced pressure (<1 mbar, 50 °C, 72 h). The insoluble solid was weighed – and the gel content was calculated (0 – 78 %).

#### 5.2.5.2 Random ROM copolymerisation of HE-NBE-CO<sub>2</sub> and MFM with MG2

HE-NBE-CO<sub>2</sub> (52 – 206 mg, 0.283 – 1.13 mmol) and MFM (239 – 0 mg, 0.848 – 0.00 mmol) were dissolved in DCM (2 mL), then added to MG2 (10 mg, 0.0113 mmol) dissolved in DCM (2 mL). After 24 h, ethyl vinyl ether (5 mg) was added, and stirred for a further 10 min. Any precipitate formed at this point was removed by filtration. The DCM soluble fraction was then added dropwise to dry ice cooled hexane and the precipitated polymer was then filtered and dried under reduced pressure (<1 mbar, 50 °C, 48 h) and weighed (0.9 – 93.1 %).

The DCM insoluble fraction which had previously been separated was stirred under reflux at 40 °C in DCM (20 mL) for 3 h. After this, the solid was isolated by filtration, and dried under reduced pressure (<1 mbar, 50 °C, 72 h). The insoluble solid was weighed – and the gel content was calculated (0 – 73 %).

#### 5.2.5.3 Block ROM copolymerisation of MFM then HE-NBE-CO<sub>2</sub> with MG2

MFM (80 – 239 mg, 0.283 – 0.848 mmol) was dissolved in CDCl<sub>3</sub> (1 mL). This was added to MG2 (10 mg, 0.113 mmol) in CDCl<sub>3</sub> (1 mL), and after 6 h was analysed by <sup>1</sup>H NMR spectroscopy to check the absence of norbornene protons – after which HE-NBE-CO<sub>2</sub> (155 – 52 mg, 0.848 – 0.283 mmol) in chloroform (1 mL) was added and the mixture was stirred for a further 18 h, at which point ethyl vinyl ether (5 mg) was added and stirred for a further 10 min. Any precipitate formed at this point was removed by filtration. The chloroform soluble fraction was then added dropwise to dry ice cooled hexane and the precipitated polymer was then filtered and dried under reduced pressure (<1 mbar, 50 °C, 48 h) and weighed (40.8 – 79.4 %).

The chloroform insoluble fraction which had previously been separated was stirred under reflux at 40 °C in DCM (20 mL) for 3 h. After this, the solid was isolated by filtration, and dried under reduced pressure (<1 mbar, 50 °C, 72 h). The insoluble solid was weighed – and the gel content was calculated (0 – 1 %).

#### 5.2.5.4 Block ROM copolymerisation of HE-NBE-CO<sub>2</sub> then MFM with MG2

HE-NBE-CO<sub>2</sub> (52 – 155 mg, 0.283 – 0.848 mmol) was dissolved in CDCl<sub>3</sub> (1 mL). This was added to MG2 (10 mg, 0.113 mmol) in CDCl<sub>3</sub> (1 mL), and after 6 h was analysed by <sup>1</sup>H NMR spectroscopy to check the absence of norbornene protons – after which MFM (239 – 80 mg, 0.848 – 0.283 mmol) in chloroform (1 mL) was added and the mixture was stirred for a further 18 h, at which point ethyl vinyl ether (5 mg) was added and stirred for a further 10 min. Any precipitate formed at this point was removed by filtration. The chloroform soluble fraction was then added dropwise to dry ice cooled



hexane and the precipitated polymer was then filtered and dried under reduced pressure (<1 mbar, 50 °C, 48 h) and weighed (17.9 – 89.3 %).

The chloroform insoluble fraction which had previously been separated was stirred under reflux at 40 °C in DCM (20 mL) for 3 h. After this, the solid was isolated by filtration, and dried under reduced pressure (<1 mbar, 50 °C, 72 h). The insoluble solid was weighed – and the gel content was calculated (0 – 47 %).

### **5.2.6 In-bulk ROM copolymerisation of 2-hydroxyethyl-5-norbornene-2-carboxylate butyl carbamate (MFM) and hexamethylene-1,6-bis(5-norbornene-2-carboxylate-2-ethoxy carbamate) (DFM2)**

Hexamethylene-1,6-bis(5-norbornene-2-carboxylate-2-ethoxy carbamate) (DFM2) (121 mg, 0.226 mmol) was dissolved in 2-hydroxyethyl-5-norbornene-2-carboxylate butyl carbamate (MFM) (572 mg, 2.034 mmol), overnight. To this, MG2 (10 mg, 0.0113 mmol) was added. The mixture was stirred, but quickly became very viscous – unable to be stirred within 1 h. After 24 h, a DCM extraction was performed using the following method: DCM (30 mL) was added and the mixture was stirred under reflux at 40 °C for 3 h. The solid was isolated by filtration, dried under reduced pressure (<1 mbar, 50 °C, 72 h), and weighed (534 mg, 76 %).

### **5.2.7 In-mould bulk ROM copolymerisation of 2-hydroxyethyl-5-norbornene-2-carboxylate butyl carbamate (MFM) and hexamethylene-1,6-bis(5-norbornene-2-carboxylate-2-ethoxy carbamate) (DFM2) for DMTA testing**

#### **5.2.7.1 In-mould bulk ROM copolymerisation of MFM and DFM2 with G1**

DFM2 (0 – 194 mg, 0.00 – 0.366 mmol) was dissolved in MFM (582 – 687 mg, 2.07 – 2.44 mmol) in a vial, overnight. To this, G1 (10 mg, 0.122 mmol) was added, vigorously stirred for 5 s, and transferred to a rectangular mould (20 × 10 × 0.5 mm). The mould was transferred to the thermal press and pressed for 40 min (40 °C, 6 – 8 tonnes). The sample was placed in the DMTA clamp and subjected to an amplitude of 1 µm at 1 Hz. The temperature was raised from -120 °C to 200 °C at a rate of 2 ° per min. The storage and loss moduli, and tan(δ), were monitored, and the T<sub>g</sub> was calculated (29.5 – 46.0 °C).

#### **5.2.7.2 In-mould bulk ROM copolymerisation of MFM and DFM2 with MG2**

DFM2 (0 – 180 mg, 0.00 – 0.339 mmol) was dissolved in MFM (540 – 636 mg, 1.92 – 2.26 mmol) in a vial, overnight. To this, MG2 (10 mg, 0.113 mmol) was added, vigorously stirred for 5 s, and transferred to a rectangular mould (20 × 10 × 0.5 mm). The mould was transferred to the thermal press and pressed for 40 min (60 °C, 6 – 8 tonnes). The sample was placed in the DMTA clamp and subjected to an amplitude of 1 µm at 1 Hz. The temperature was raised from -120 °C to 200 °C at a rate of 2 ° per min. The storage and loss moduli, and tan(δ), were monitored, and the T<sub>g</sub> was calculated (36.9 – 49.9 °C).

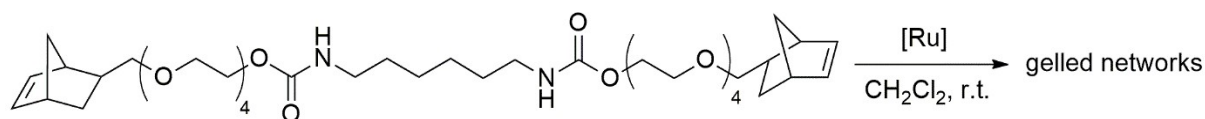
### 5.2.8 In-mould bulk ROM copolymerisation of 2-hydroxyethyl-5-norbornene-2-carboxylate butyl carbamate (MFM) and 2-hydroxyethyl-5-norbornene-2-carboxylate (HE-NBE-CO<sub>2</sub>) for DMTA testing

2-Hydroxyethyl-5-norbornene-2-carboxylate (HE-NBE-CO<sub>2</sub>) (0 – 412 mg, 0.00 – 2.26 mmol) was dissolved in MFM (0 – 636 mg, 0.00 – 2.26 mmol) in a vial, overnight. To this, MG2 (10 mg, 0.113 mmol) was added, vigorously stirred for 5 s, and transferred to a rectangular mould (20 × 10 × 0.5 mm). The sample was transferred to the thermal press and pressed for 40 min (85 °C, 6 – 8 tonnes). The sample was placed in the DMTA clamp and subjected to an amplitude of 1 µm at 1 Hz. The temperature was then raised from -120 °C to 200 °C at a rate of 2 ° per min. The storage and loss moduli, and tan(δ), were monitored, and the T<sub>g</sub> was calculated (36.9 – 68.8 °C).

## 5.3 Results and Discussion

### 5.3.1 ROMP of hexamethylene-1,6-bis(5-norbornene-2-methoxy tetraethylene glycol carbamate) (DFM1)

Hexamethylene-1,6-bis(5-norbornene-2-methoxy tetraethylene glycol carbamate) (DFM1) was polymerised by ROMP with Grubbs initiators G1, G2 and MG2 (Equation 5.1).



**Equation 5.1:** ROMP of DFM1 with G1, G2 or MG2

Firstly, all three ROMP reactions successfully form gelled networks – suggesting the presence of two norbornene moieties in DFM1. As seen in previous chapters, modified Grubbs 2<sup>nd</sup> generation is much quicker to form the gel than the other two initiators due to its high rates of initiation and propagation. Grubbs 1<sup>st</sup> generation initiator is again the slowest of the three – 225 times slower to gelation – believed to be due to its much lower rate of propagation.

All three initiators generate low gel contents – between 13 and 47 %. Rather surprisingly, the ROMP with MG2 results in the lowest gel content (13 %). The reason for this could possibly be due to the rapid polymerisation facilitated by this initiator – forcing the reaction to gel quickly and not all of the norbornene functionality is able to undergo ROMP before the initiator end is trapped in the cross-linked network. G1 yields a cross-linked network with a gel content of 23 %. Since this initiator causes gelation to be much slower, it could possibly afford it the opportunity to increase to a higher level of cross-linking. Finally, G2 is slow to initiate and rapid to propagate, therefore ROMP can continue to a much greater level (47 %) before gelation.

DFM1 was synthesised from 5-norbornene-2-methoxy tetraethylene glycol (Figure 5.7) and 1,6-hexamethylene diisocyanate. 5-Norbornene-2-methoxy tetraethylene glycol was synthesised from the reaction of 5-norbornene-2-methanol and tetraethylene glycol. If unreacted tetraethylene glycol had

not been completely removed, it would remain as an impurity in the final product. This glycol would also react with the isocyanate to form the carbamate, but due to their lack of norbornene ring functionality, would not undergo ROMP. Thus, they would form part of the soluble fraction during the DCM extractions. To test for this, all the soluble fractions were studied using NMR spectroscopy.

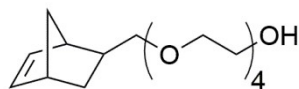


**Figure 5.7:** Structure of 5-norbornene-2-methoxy tetraethylene glycol

In Figure 5.8, it can be seen that H<sup>1</sup> and H<sup>2</sup> – highlighted in red between 5.96 and 6.09 ppm – have decreased in intensity despite H<sup>7</sup> (peaks appearing at 4.11 – 4.33 and 3.52 – 3.71 ppm) staying mainly unchanged. NH at 4.78 – 5.00 ppm also decreases slightly (highlighted blue) though not as markedly, as does H<sup>9</sup> (green) between 1.39 and 1.41 ppm. NH and H<sup>9</sup> should always be the same ratio since they come from the same starting material. These, along with the fact that H<sup>6</sup> (at 3.34 and 3.49 ppm) still appears suggests the DCM fraction contains DFM1 which has not undergone ROMP, and tetraethylene glycol impurity – perhaps in carbamate form. The spectra from G2 and MG2 seem to agree with this though they appear to only contain tetraethylene glycol with some form of carbamate functionality showing the indicative peaks again at 4.11 – 4.33 ppm. In these fractions there is no norbornene functionality observed, shown by the absence of peaks at 5.96 – 6.09 ppm. There are also no peaks in the spectra which would correlate to the olefinic protons of ring-opened polymer between 5 and 6 ppm. This infers that the monomer does not contain 100 % norbornene functionality.

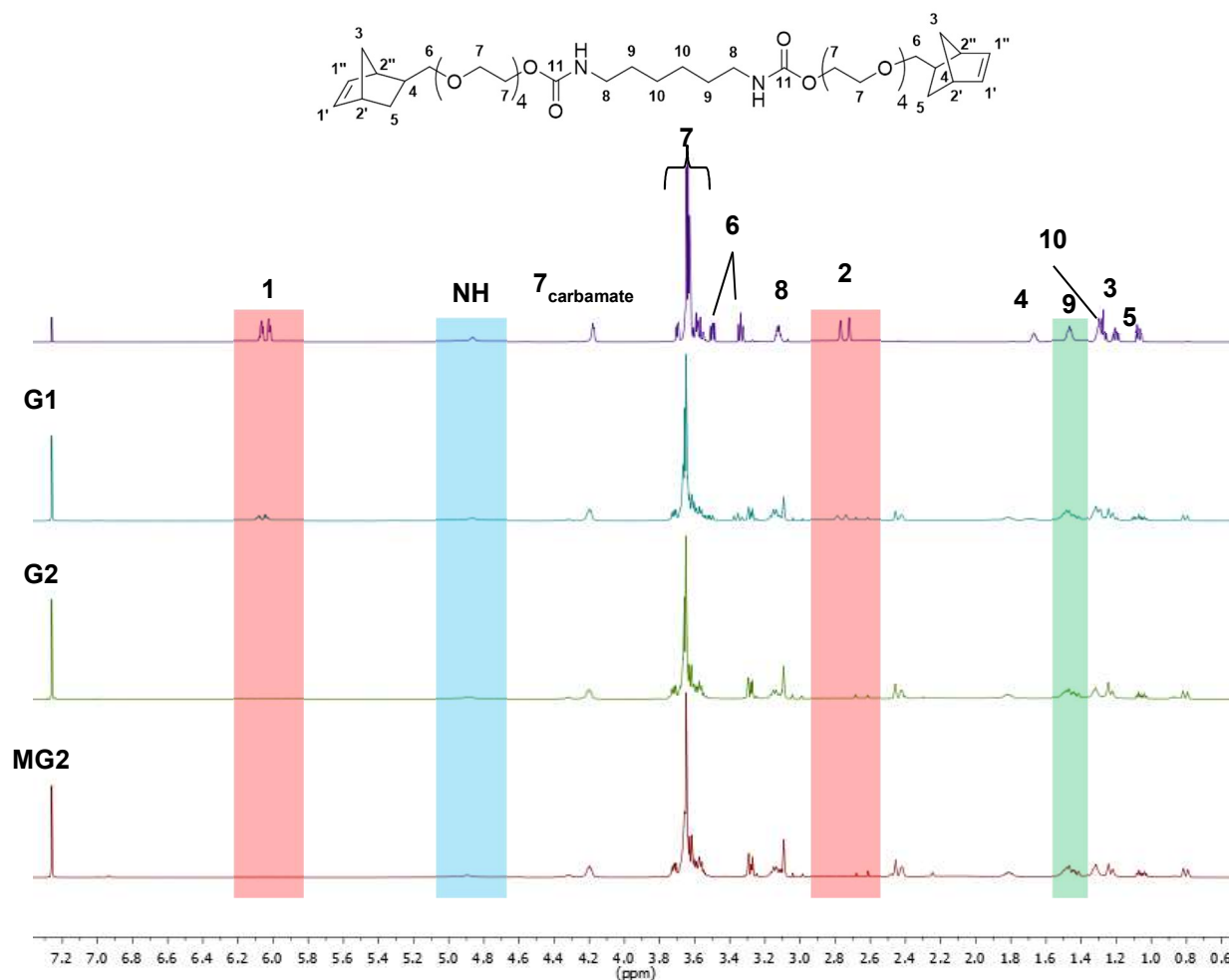


**Figure 5.8:**  $^1\text{H}$  NMR (400 MHz,  $\text{CDCl}_3$ ) spectra of poly(DFM1) and DCM soluble fractions with all three initiators, important parts of the spectra are highlighted

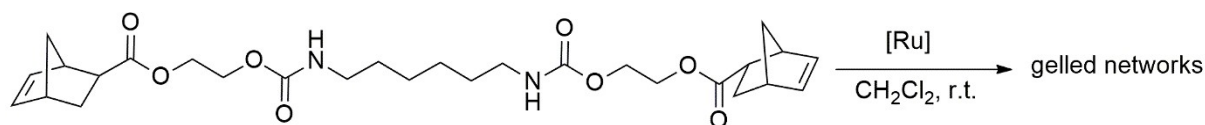
The data in Table 5.1 shows that the gel extracts of poly(DFM1) using G2 and MG2 both contain no norbornene containing compounds which is confirmed by looking at the integrations with respect to  $\text{H}^7$  (glycol protons between 4.11 – 4.33 and 3.52 – 3.71 ppm), appearing in all the spectra. As well as a decrease in the integration of both  $\text{H}^1$  and  $\text{H}^2$  (at 5.96 – 6.09 ppm) – both on the norbornene ring – it can be seen that  $\text{H}^9$  at 1.40 ppm increases. This is perhaps due to any leftover glycol reacting during synthesis with HDI to form oligomeric, linear carbamates. These, due to containing no norbornene species, will not undergo ROMP – and thus will stay in the DCM solution. This also results in very little change in the concentration of NH protons at 4.78 – 5.00 ppm.

**Table 5.1:** Integrations of selected protons in the starting material and the three DCM extracts, relative to H<sub>7</sub>

Initiator	Integration				
	H <sup>7</sup> (inc. carbamate)	H <sup>1</sup>	H <sup>2</sup>	H <sup>9</sup>	NH
<b>DFM1</b>	32.0	4.1	1.9	3.9	1.9
<b>G1</b>	32.0	1.2	1.3	4.2	1.2
<b>G2</b>	32.0	0.0	0.0	5.0	1.1
<b>MG2</b>	32.0	0.0	0.0	5.1	1.4

### 5.3.2 ROMP of hexamethylene-1,6-bis(5-norbornene-2-carboxylate-2-ethoxy carbamate) (DFM2)

Hexamethylene-1,6-bis(5-norbornene-2-carboxylate-2-ethoxy carbamate) (DFM2) was polymerised by ROMP using Grubbs ruthenium initiators G1, G2 and MG2 (Equation 5.2).

**Equation 5.2:** ROMP of DFM2 with G1, G2 or MG2

The ROMP of DFM2 generated polymers with high gel contents (97 – 100 %). The first reason for this could be due to the higher purity of DFM2 compared to the polyesters or DFM1. Firstly, the hydroxyethyl acrylate starting material is purified, which removes any contaminants that will not undergo ROMP, or may affect it adversely. This is not done for the polyesters – which start off containing maleic anhydride which could interfere with Grubbs initiators due to its unsaturation.

The data in Table 5.2 shows that the gel times of DFM1 and DFM2 are – when polymerised with G2 or MG2 – shorter than the ROMP of Polyester 1 or Polyester 2. A possible reason for this could be that DFM1 and DFM2 are much more well-defined molecules with known structures, whereas the polyester pre-polymers are both disperse materials with much more random structures.

**Table 5.2:** Table showing the gel times of all the multifunctional pre-polymers studied

Pre-polymer	Norbornene content (mmol g <sup>-1</sup> )	Gel time (s)		
		G1	G2	MG2
<b>Polyester 1</b>	2.4	1260	540	15
<b>Polyester 2</b>	4.0	1860	720	17
<b>DFM1</b>	2.6	1500	480	4
<b>DFM2</b>	3.8	480	60	<1

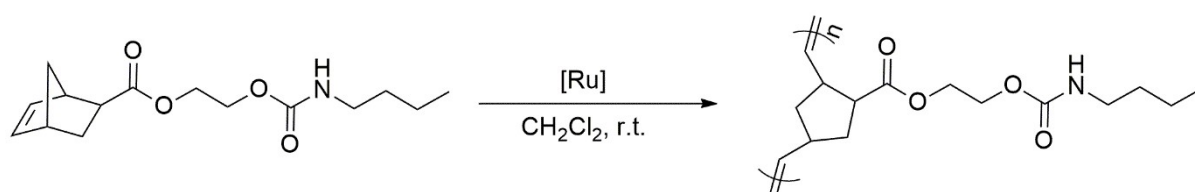
The data in Table 5.2 also shows how much the faster activation of MG2 (than G2) has on the time taken until gelation. What is perhaps a little surprising is that DFM2 manages to undergo ROMP to such a high degree to yield a polymer with a gel content of 100 % within 1 s.

The other possible reason why DFM2 gels so quickly and to a high degree of cross-linking is that the norbornene content is the second highest of the four multifunctional pre-polymers despite it being one of the least viscous. This could be another reason why DFM1 produces polymers with low gel contents due to its much lower norbornene content.

Due to the high gel contents, the DCM soluble fraction was very small and so unable to be analysed by NMR spectroscopy.

### 5.3.3 ROMP of 2-hydroxyethyl-5-norbornene-2-carboxylate butyl carbamate (MFM)

2-Hydroxyethyl-5-norbornene-2-carboxylate butyl carbamate (MFM) was polymerised by ROMP with Grubbs ruthenium initiators G1, G2 or MG2 (Equation 5.3).

**Equation 5.3:** ROMP of MFM using G1, G2 or MG2

Poly(MFM) was analysed utilising NMR spectroscopy, though due to its polymeric nature, the peaks are much broader than seen previously, and correlations were much weaker. The structure was, however, able to be resolved first by looking at the protons derived from the *N*-alkyl carbamate (Figure 5.10).

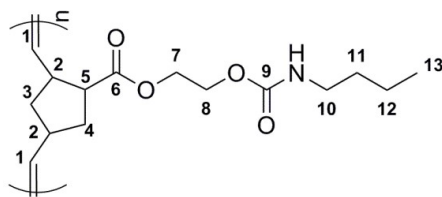


**Figure 5.9:** Numbered structure of poly(MFM)

For ease of discussion the carbon atoms in poly(MFM) have been numbered as shown in Figure 5.9.  $H^{13}$  is easy to identify at 0.89 ppm as it has the lowest shift of any of the peaks and appears almost unshifted from the monomer. This couples only to  $H^{12}$ , at 1.27 – 1.40 ppm, which in turn shows correlation to  $H^{13}$  and  $H^{11}$  at 1.40 – 1.50 ppm – thus  $H^{11}$  can be identified as the peak next to  $H^{12}$ .  $H^{10}$  is then identified at 3.04 – 3.21 ppm due to its coupling to the neighbouring  $H^{11}$ . These correlations are all highlighted in blue.  $H^7$  and  $H^8$  only correlate to one another and appear in the same region (3.97 – 4.46 ppm) as the respective protons in the monomer. There is a correlation shown to two, smaller peaks from  $H^7$  and  $H^8$  (3.56 – 3.78 ppm, red lines). This has been assigned as a minor isomer, since there is a ring structure in poly(MFM) – the ester group attached could be *endo* or *exo*, thus creating more peaks.

Since the correlations between these protons are all strong, they mask the weaker couplings of  $H^{1-5}$ . These can only be viewed when the spectra have been zoomed in (Figure 5.11).  $H^1$  can instantly be identified at 4.88 – 5.52 ppm due to the peaks' high shifts in the olefinic region, although lower than the norbornene double bond is found (typically around 6 ppm), which provides further evidence that the norbornene-containing starting material is no longer present and instead is replaced with this unsaturated polymer. The multiple peaks due to  $H^1$  are seen due to *cis/trans* at  $C^1$  and head-tail isomerism at  $C^4$  or  $C^5$  in the polymer. It also appears to have an integration of 3 H, though this is likely due to its overlapping with the peak due to NH, which also appears in this region.  $H^1$  is shown to correlate to  $H^2$  at 2.37 – 2.82 ppm, emphasised with blue lines, which appears as multiple peaks. This is most likely due again to the multitude of isomers which are possible in this polymeric system. These show correlation to  $H^3$  at 1.81 – 2.12 ppm (black line),  $H^4$  at 1.58 – 1.81 ppm (red line), and  $H^5$  at 2.92 ppm, although there are many overlapping peaks. The assignment of these is proved by the fact that  $H^4$  also correlates with  $H^5$  – shown by the green lines; but  $H^3$  correlates with neither of these.

One way of further confirming the proton spectrum is to correlate with the carbon spectrum. Here, in Figure 5.12 and Figure 5.13, blue spots to the right of red spots on the HSQC refer to CH or  $CH_3$  environments; and the opposite indicates  $CH_2$ ; and quaternary carbons have no correlation whatsoever as there are no protons to couple to. As seen in Figure 5.12, all the proton environments associated with  $H^1$  are CH as expected, proving this assignment. These correlate to multiple weak  $C^1$  environments between 129.5 and 134.7 ppm due to *cis* and *trans* isomers as well as *endo/exo* isomers in the ring. There will also be a slight difference in the shifts depending whether the ester group is on  $C^4$  or  $C^5$  on this repeating unit as well as neighbouring entities. As expected,  $C^6$  and  $C^9$  do not show up on the HSQC because both are quaternary carbons with no attached protons. Both

appear in the carbonyl range of the spectrum, with one in the ester region at 174.6 ppm and the other in the carbamate area at 156.3 ppm. These were therefore assigned to C<sup>6</sup> and C<sup>9</sup>, respectively.

The most highly shifted protons in Figure 5.13 are H<sup>7</sup> and H<sup>8</sup> and clearly correspond (blue lines) to several carbon environments depending on whether it is C<sup>7</sup> or C<sup>8</sup>, *exo* or *endo*, or *cis* or *trans*. This leads to several weak, broad peaks barely visible above the baseline between 61.0 and 62.6 ppm, even though this <sup>13</sup>C NMR was done with a concentrated sample over a long requisition time. All the carbons are also clearly shown to be CH<sub>2</sub>, which agrees with the structure. The red lines show correlation to C<sup>10</sup> at 40.6 and 40.8 ppm; C<sup>11</sup> at 32.1 and 32.4 ppm; C<sup>12</sup> at 20.0 and 20.1 ppm; and C<sup>13</sup> at 13.8 ppm. The appearance of two distinct carbon environments for each is due again to the different isomers. These peaks confirm that the DEPT experiment was successful in resolving CH<sub>2</sub> from CH<sub>3</sub> as C<sup>13</sup> is the only carbon to have three protons attached and the DEPT is in agreement.

C<sup>3</sup> is shown by the orange lines in Figure 5.13, and this also shows that H<sup>3</sup> overlaps with H<sup>12</sup> which can be observed by a slight shoulder on this peak. H<sup>4</sup> also overlaps with H<sup>3</sup>, but these can be separated by looking at the HSQC which shows two peaks which correlate to C<sup>4</sup> at about 36.0 ppm (green line), whereas the other overlapped peak corresponds to the previous assigned C<sup>3</sup> at 40.0 ppm. C<sup>2</sup> shows at least two distinct environments at 42.7 and 45.6 ppm (both shown to be CH, black lines) which is as expected since there are the different isomers as previously discussed, as well as there are two different C<sup>2</sup> even ignoring these. There is C<sup>2</sup> neighbouring C<sup>4</sup>, and one neighbouring C<sup>5</sup>. The peak at 45.6 ppm is sufficiently broad to say that it could arguably be more than one carbon environment, but these environments have very similar chemical shifts. Finally – using the purple lines – C<sup>5</sup> can be identified at 48.2 ppm, and the DEPT once more correctly shows this as CH. Since it is more deshielded, C<sup>5</sup> occurs at a higher chemical shift than C<sup>4</sup> due to the neighbouring ester group, which also helps to confirm the identity of C<sup>5</sup>.



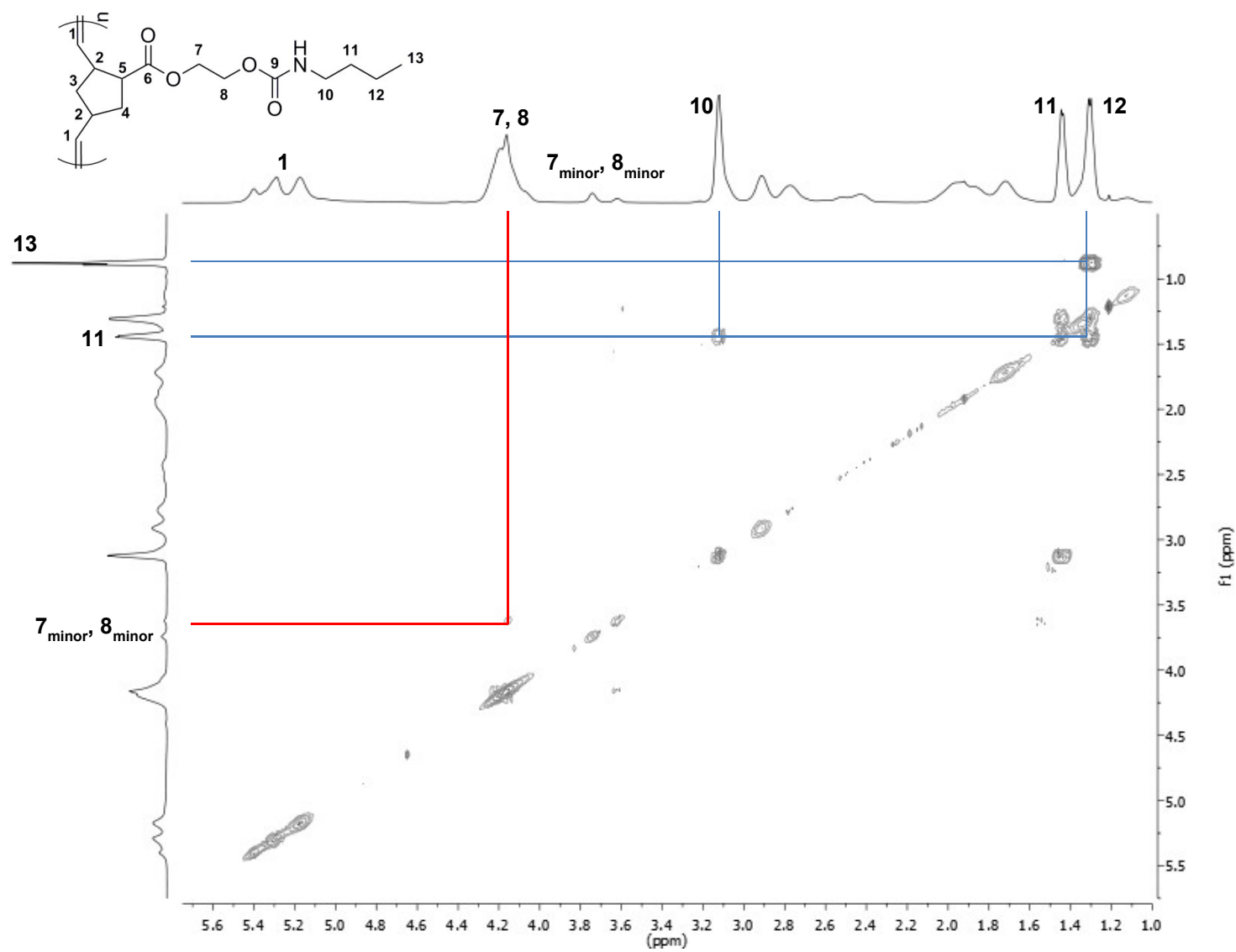


**Figure 5.10:**  $^1\text{H}$ - $^1\text{H}$  COSY (700 MHz,  $\text{CDCl}_3$ ) spectrum of poly(MFM) for  $\delta_{\text{H}} = 0.5\text{--}5.6$  ppm

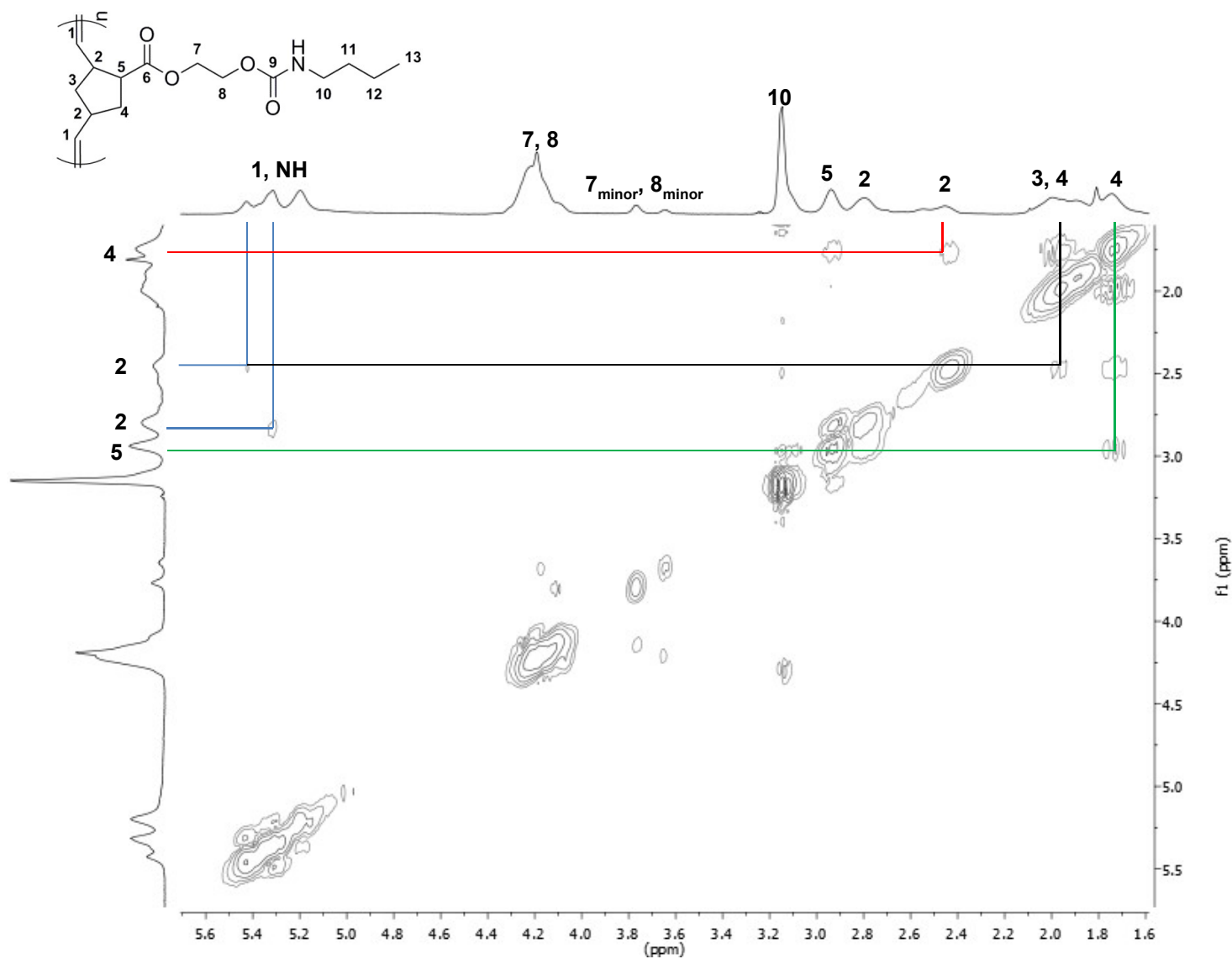


**Figure 5.11:**  $^1\text{H}$ - $^1\text{H}$  COSY (700 MHz,  $\text{CDCl}_3$ ) spectrum of poly(MFM), zoomed in to eradicate alkane carbamate tail

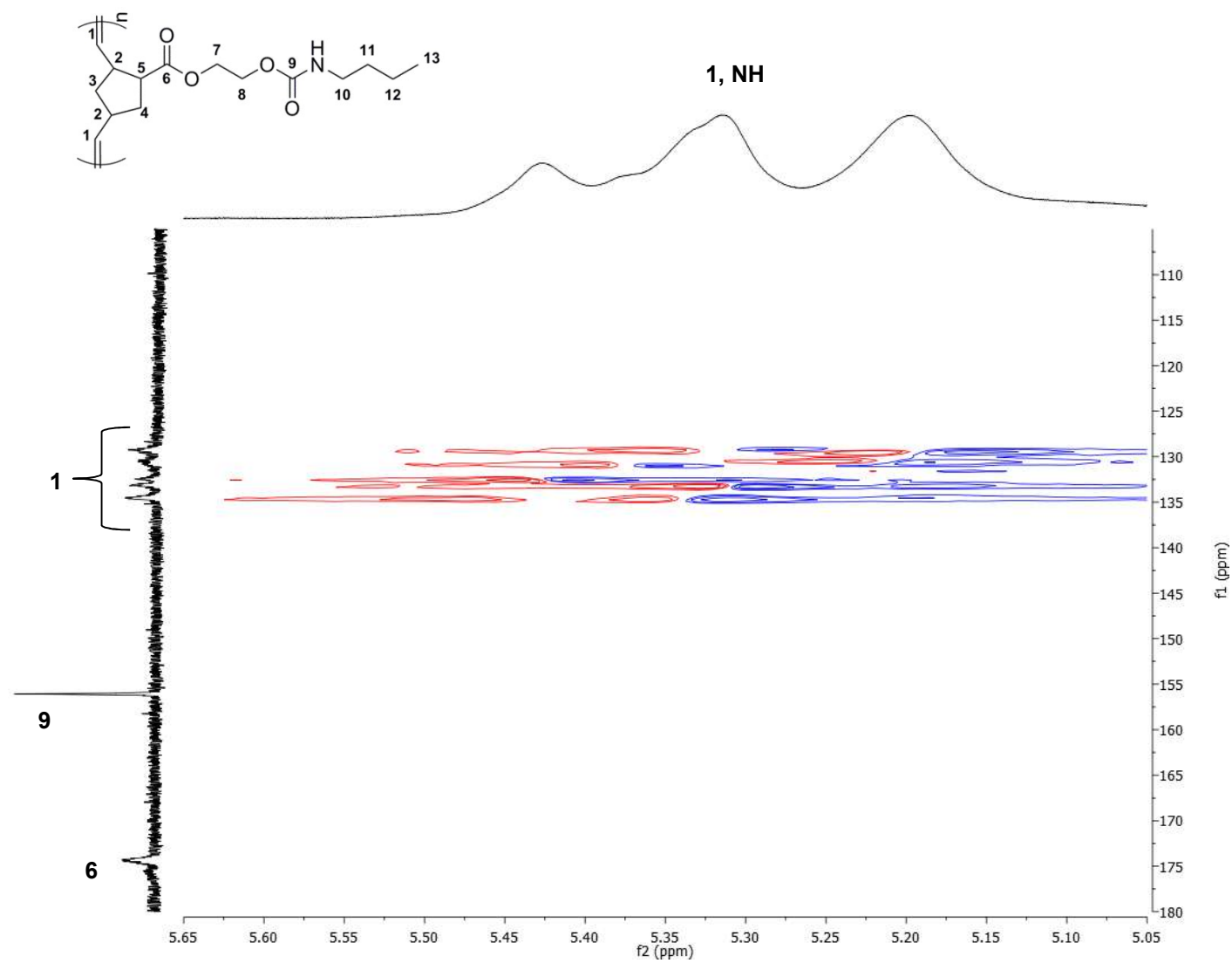


**Figure 5.12:**  $^1\text{H}$ - $^{13}\text{C}$  HSQC (700 MHz ( $^1\text{H}$ ) and 176 MHz ( $^{13}\text{C}$ ),  $\text{CDCl}_3$ ) spectrum of poly(MFM), zoomed in to view olefinic and carbonyl regions

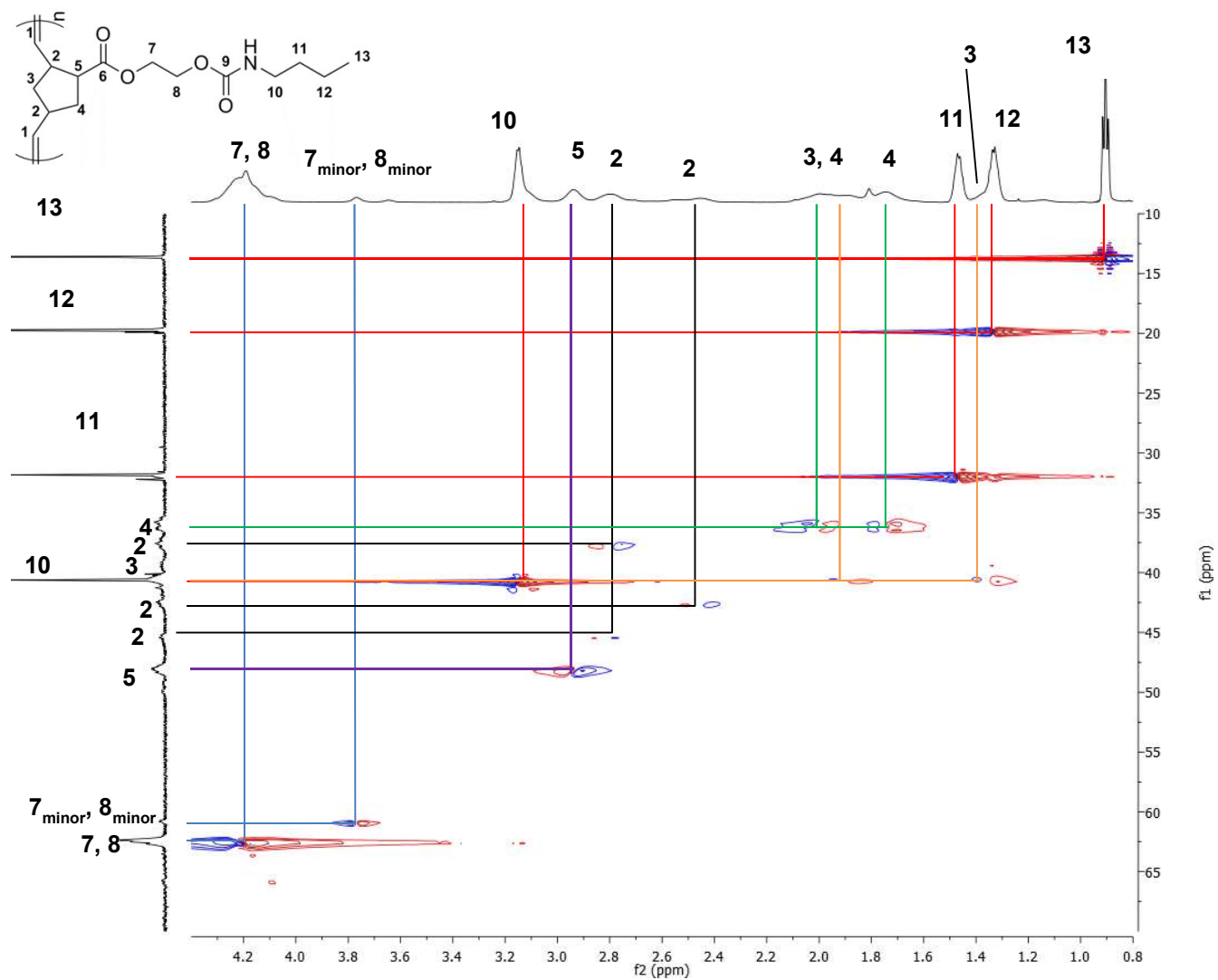


**Figure 5.13:**  $^1\text{H}$ - $^{13}\text{C}$  HSQC (700 MHz ( $^1\text{H}$ ) and 176 MHz ( $^{13}\text{C}$ ),  $\text{CDCl}_3$ ) spectrum of poly(MFM) for  $\delta_{\text{H}} = 0.8\text{--}4.4$  ppm and  $\delta_{\text{C}} = 10\text{--}70$  ppm

Poly(MFM) is soluble in chloroform and THF, and therefore must be a linear polymer. Thus indicating that the excess DCPD used for the synthesis of MFM and its precursor, 2-hydroxyethyl-5-norbornene-2-carboxylate (HE-NBE-CO<sub>2</sub>), was successfully removed.

The yields summarised in Table 5.3 suggest that MFM is fairly active with respect to ROMP. This also suggests that the hexane utilised for precipitating the polymer was a good choice of non-solvent for poly(MFM). The one surprising result is that the yield of this polymer (89.1 – 91.6 %) is higher than poly(EHNBEDC) (63.7 – 87.7 %) despite the fact that MFM has both *exo* and the unfavourable (for ROMP) *endo* isomers. This may be due to MFM being intrinsically more active for ROMP or perhaps that methanol is not as good a non-solvent for poly(EHNBEDC).

**Table 5.3:** A summary of poly(MFM) produced using G1, G2 and MG2

Polymer	Initiator	[M]:[I]	Yield (%)	$M_n^{th}$ ( $\times 10^3$ g mol <sup>-1</sup> )	$M_n^{SEC}$ ( $\times 10^3$ g mol <sup>-1</sup> )	$M_w^{SEC}$ ( $\times 10^3$ g mol <sup>-1</sup> )	$\bar{D}$
<b>N</b>	G1	100:1	90.6	28	11	15	1.4
<b>O</b>	G2	100:1	91.6	28	61	110	1.8
<b>P</b>	MG2	100:1	89.1	28	50	79	1.5

The  $M_n$  and  $M_w$  of **N** are lower than both **O** and **P**, due to the use of the less active initiator, G1. This means that the degree of polymerisation in **N** is lower than **O** and **P** – leading to the lower  $M_n$  and  $M_w$  values.  $\bar{D}$  is still fairly high however, due to the presence of the mixture of *exo* and *endo* isomers which will polymerise at different rates. **O** has a much broader dispersity due to the slow initiation characteristic of G2 and its rapid propagation rate which also leads to a much higher molecular weight than expected. **P** is somewhere in between **N** and **O** in terms of molecular weight due to MG2's much quicker initiation – lowering the  $M_n$  and  $M_w$  from **O** but due to its high activity, this makes the molecular weight higher than **N**. **P** also shows a narrower dispersity than **O** due to the rate of initiation being greater than G2.

Again, there is a large disparity between the theoretical and measured  $M_n$ . The SEC is calibrated using polystyrene standards, which has a different hydrodynamic volume to polynorbornene; therefore, the exact values of  $M_n$  and  $M_w$  found by SEC are not accurate. This could be overcome in future by finding standards based on polynorbornene, or by using all three detectors on the SEC instead of only the refractive index.

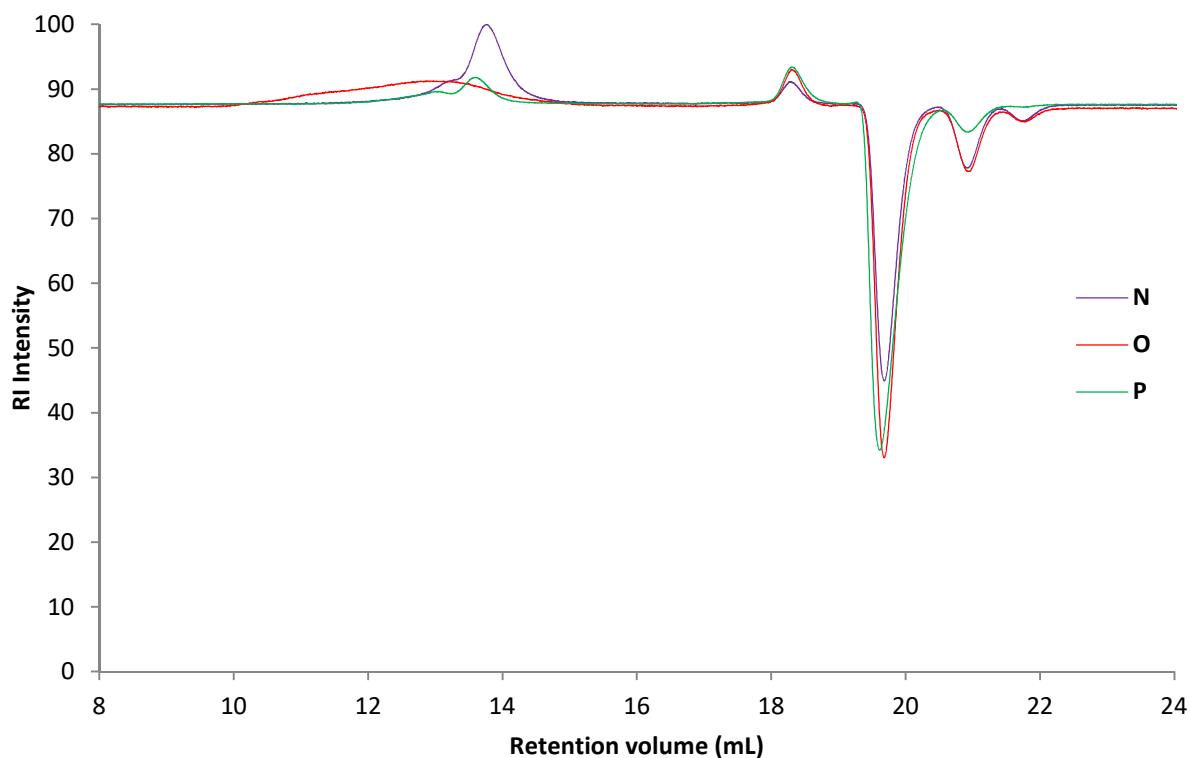


**Figure 5.14:** SEC traces for **N**, **O** and **P**

The SEC traces of poly(MFM), Figure 5.14, show clearly how broad the dispersity of **O** is. What can also be seen is that **O** has a much higher molecular weight (lower retention volume) than either of the other two polymers. Surprisingly, both **N** and **P** appear to be slightly bimodal with a smaller, higher molecular weight shoulder appearing in both traces. All three have a similar solvent trace (18 mL onwards) though with differing intensities. The differences in intensity shown could suggest that perhaps less solvent is passing the detector in **N**, which may mean that the concentration could have been different.

### 5.3.4 Random ROM copolymerisation of MFM and EHNBEDC

For the random copolymerisation of MFM with EHNBEDC, only Grubbs 1<sup>st</sup> generation and modified 2<sup>nd</sup> generation initiators were used. Grubbs 2<sup>nd</sup> generation initiator was not used due to its slow rate of initiation and high rate of propagation.

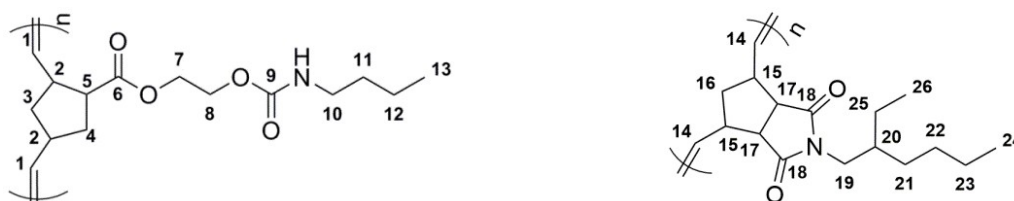


**Figure 5.15:** Numbered structures of (from left to right) poly(MFM) and poly(EHNBEDC)

The NMR spectra, shown in Figure 5.16, of the polymers **Q** (random copolymer made with G1) and **R** (random copolymer made with MG2) were analysed and compared with the homopolymers of MFM. The peaks highlighted in blue show that incorporation of MFM into the polymer was successful and the red highlighted peaks show the incorporation of EHNBEDC. This shows, in union with the reasonably monomodal SEC traces, that the random copolymerisation of these two monomers was fairly successful with both initiators. H<sup>1</sup> and NH (at 4.88 – 5.32 ppm) and H<sup>14</sup> (two multiplets at 5.45 – 5.54 ppm and 5.68 – 5.79 ppm), and H<sup>7</sup> and H<sup>8</sup> (3.55 – 4.46 ppm), are shifted from the rest of the spectrum so that they do not overlap with any other peaks than themselves.

H<sup>7</sup> and H<sup>8</sup> only appear in poly(MFM) at 3.55 – 4.46 ppm, so the integration of these with respect to the total integration of H<sup>1</sup> + NH + H<sup>14</sup> (4.88 – 5.79 ppm) can be utilised to compare the relative contents of the two monomer units incorporated into the copolymer as shown in Table 5.4. This table shows that both **Q** and **R** copolymers contain a higher poly(MFM) content, which is surprising since the EHNBEDC contains only the reactive *exo* isomer, whereas MFM is a mixture of both *endo* and *exo*.

**Table 5.4:** Table detailing the relative contents of the monomers in the two attempted copolymers

Polymer	Integration		Content (%)		Possible copolymer?
	H <sup>1</sup> , NH & H <sup>14</sup>	H <sup>7</sup> & H <sup>8</sup>	EHNBEDC	MFM	
Poly(EHNBEDC)	2.0	0.0	100	0.0	✗
Poly(MFM)	2.0	2.7	0.0	100	✗
Copolymer <b>Q</b>	2.0	1.9	30	70	✓
Copolymer <b>R</b>	2.0	1.8	33	67	✓

Again, as mentioned previously in Chapter 1, the true ‘random-ness’ of the polymer formed will depend on the two monomers’ reactivity ratios.<sup>4</sup> Here, both monomers are quite similar (norbornene-functionalised) and so perhaps would be likely to form a random copolymer. To prove this however, further kinetic studies would need to be undertaken.

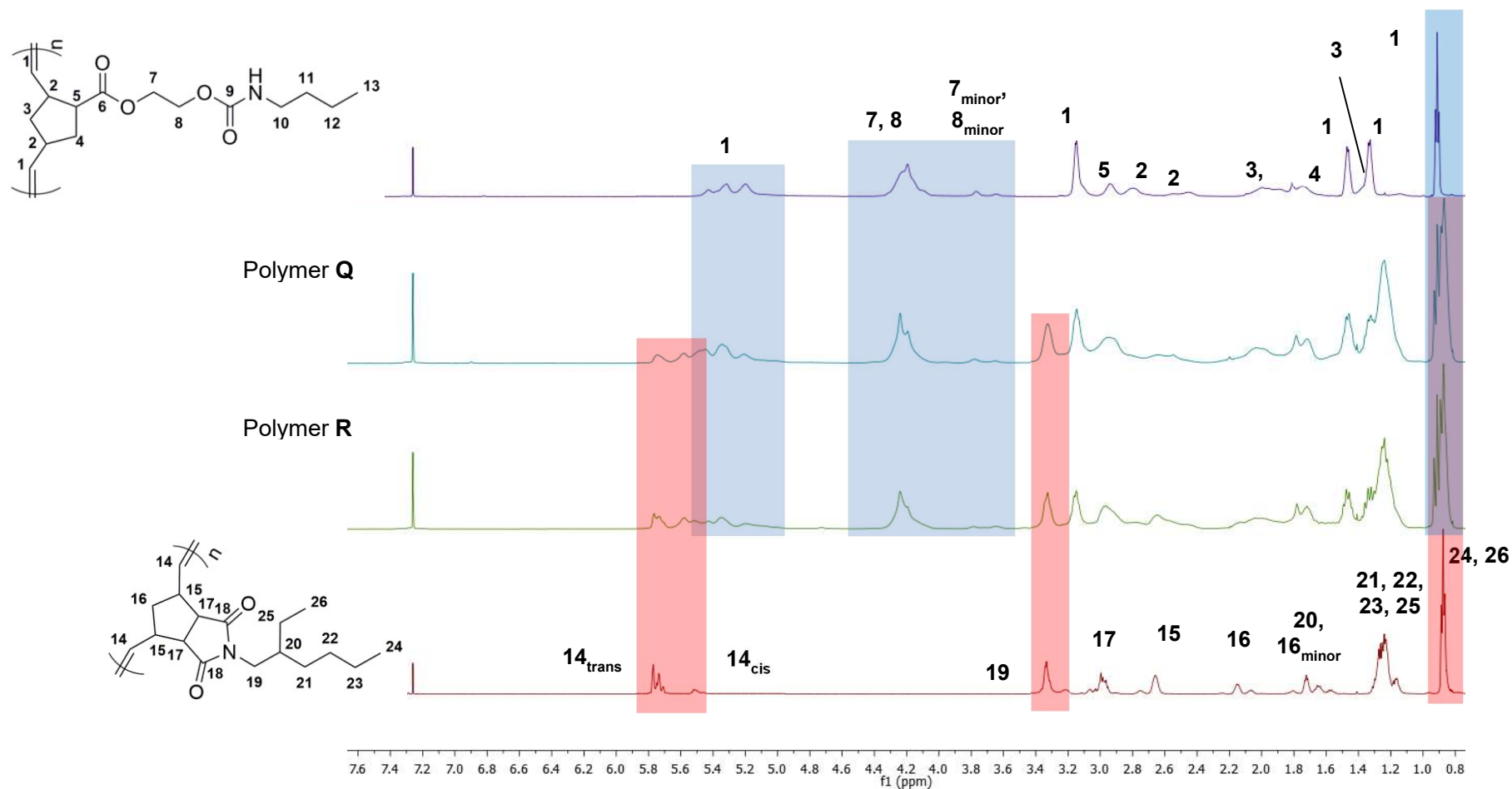


**Figure 5.16:**  $^1\text{H}$  NMR spectra (700 MHz,  $\text{CDCl}_3$ ) of poly(MFM) (purple), Copolymer **Q** (blue), Copolymer **R** (green), and poly(EHNBEDC) (red)



The first observation from the data in Table 5.5 is that both produce fairly high yields.

**Table 5.5:** A table showing the SEC data of random copolymers **Q** and **R**

Copolymer	Initiator	Yield (%)	$M_n^{\text{th}}$ ( $\times 10^3 \text{ g mol}^{-1}$ )	$M_n^{\text{SEC}}$ ( $\times 10^3 \text{ g mol}^{-1}$ )	$M_w^{\text{SEC}}$ ( $\times 10^3 \text{ g mol}^{-1}$ )	$\bar{D}$
<b>Q</b>	G1	85.9	28	100	150	1.5
<b>R</b>	MG2	89.2	28	51	80	1.6

The molecular weights (Table 5.5) show that, similar to the homopolymers, the theoretical molecular weights are much lower than the SEC measured values. This would suggest that the  $dn/dc$  values used for these polymers are not valid. The  $dn/dc$  values for similar species (although these were poly(oxa)norbornenes) found in the literature<sup>5</sup> gave values with an even greater disparity from the theoretical. The other noticeable oddity from the molecular weights is that **Q** has a greater  $M_n$  (and  $M_w$ ) than **R** which would be unexpected due to the higher activity of MG2, though perhaps the initiation of G1 was not as quick, and thus longer chains were formed. This would, however, broaden the dispersity, and as can clearly be seen **Q** has a very slightly narrower dispersity. However, these dispersities tend to suggest that copolymerisation here is reasonably well controlled, though ROMP can achieve much narrower dispersities, for example the polymerisation of EHNBEDC shown previously. The SEC trace of the copolymer **R** (Figure 5.17) presents a sizeable higher molecular weight shoulder, at lower elution volume, but **Q** shows one broad peak. The nature of the shoulder is not understood. One explanation is that it could be due to slight premature termination of the active ends. Another is that the lower molecular weight part is homopolymer, and the higher molecular weight is copolymer.

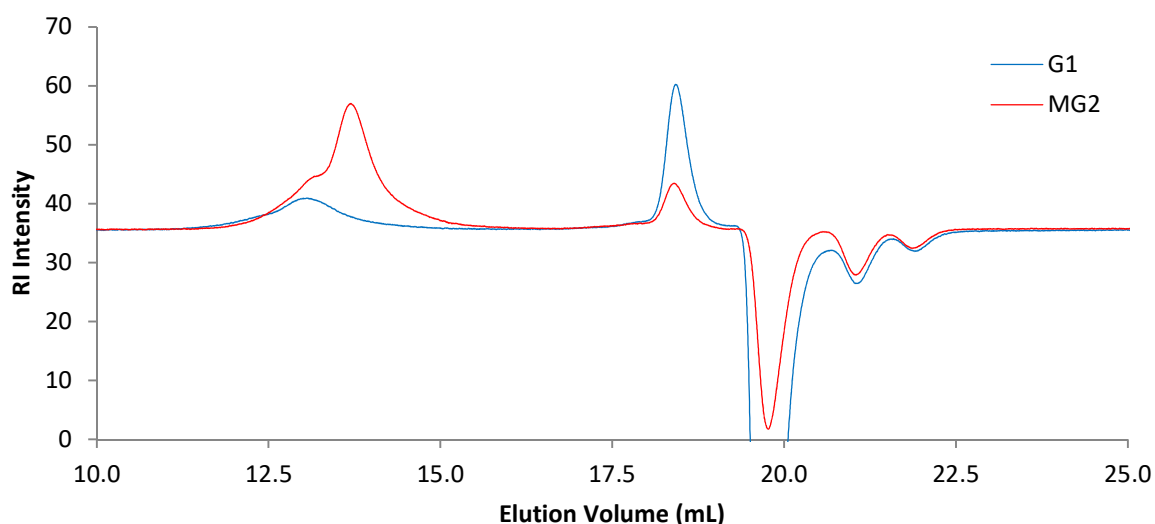


**Figure 5.17:** The SEC traces of the random copolymers produced using G1 (blue) and MG2 (red)

### 5.3.5 Block ROM copolymerisation of EHNBEDC and MFM

The syntheses of block copolymers **S** and **U** were performed by the addition of 50 equivalents (with respect to the initiator) of EHNBEDC, followed by 50 equivalents of MFM. The block copolymers **T** and **V** were made the other way around. The details of these four block copolymers are detailed in Table 5.6.

**Table 5.6:** Table detailing copolymers **S** – **V** and their monomer contents

Polymer	Initiator	[M <sub>total</sub> ]:[I]	[MFM]:[EHNBEDC] <sup>th</sup>	[MFM]:[EHNBEDC] <sup>NMR</sup>
<b>S</b>	G1	100 : 1	0.50 : 0.50	0.13 : 0.87
<b>T</b>	G1	100 : 1	0.50 : 0.50	0.62 : 0.38
<b>U</b>	MG2	100 : 1	0.50 : 0.50	0.46 : 0.54
<b>V</b>	MG2	100 : 1	0.50 : 0.50	0.08 : 0.92

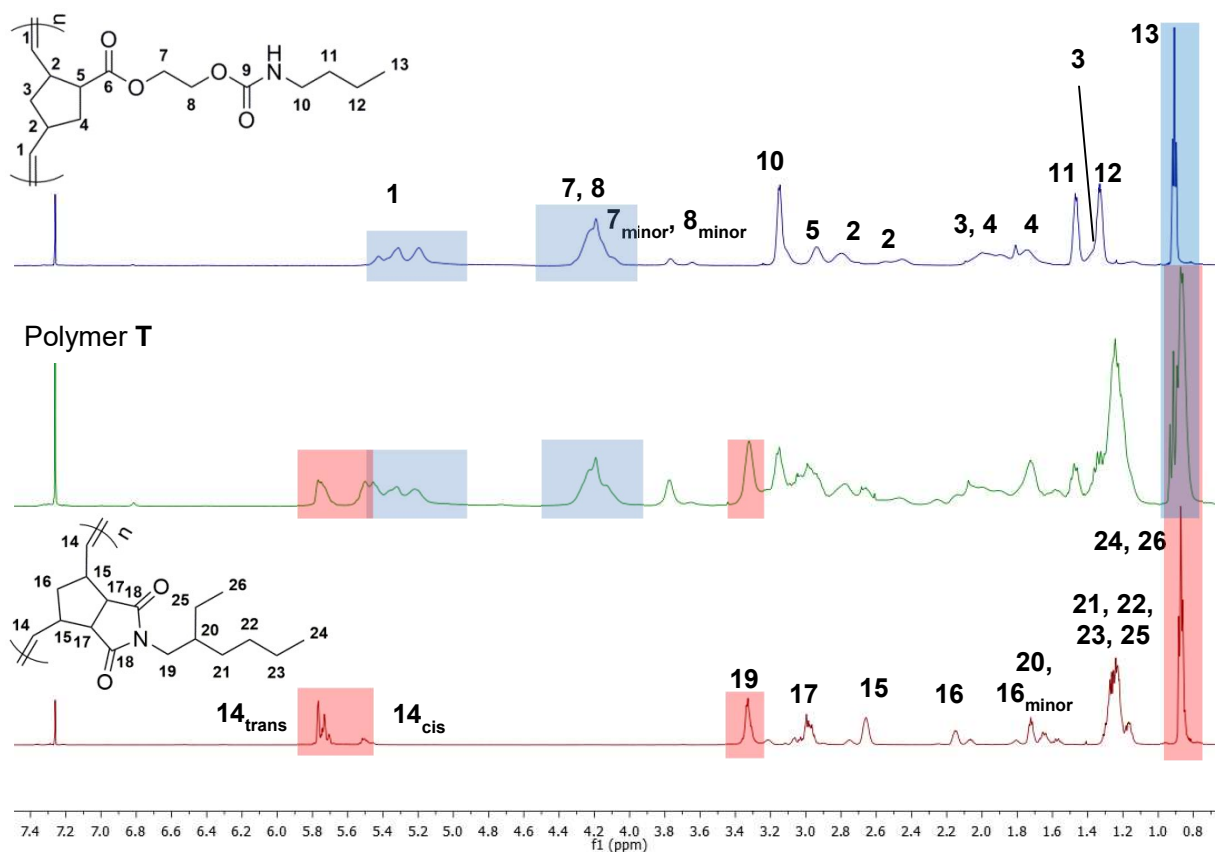


**Figure 5.18:** <sup>1</sup>H NMR (700 MHz, CDCl<sub>3</sub>) spectra of poly(MFM) (blue), **T** (green), and poly(EHNBEDC) (red)

The <sup>1</sup>H NMR spectrum and the structure of **T** are shown in Figure 5.18 and Figure 5.19, respectively. The peaks highlighted in blue show that the incorporation of poly(MFM) has taken place, and the

peaks highlighted in red show that the incorporation of poly(EHNBEDC) has also taken place. These two blocks have already been discussed in terms of their  $^1\text{H}$  NMR resonances in Sections 5.3.3 and 3.3.2, respectively.

Integrating  $\text{H}^1$  and  $\text{NH}$  (4.88-5.32 ppm), and  $\text{H}^{14}$  (5.45-5.54 and 5.58-5.79 ppm) in the copolymer against the peaks associated with  $\text{H}^7$  and  $\text{H}^8$  (3.55-4.46 ppm) from the poly(MFM) block should give the ratio of the two blocks to one another using Equation 5.4, and these values are shown in Table 5.6.

$$3 (\text{MFM}) + 2 (\text{EHNBEDC}) = \text{Integration} (\text{H}^1 + \text{NH} + \text{H}^{14})$$

$$4 (\text{MFM}) = \text{Integration} (\text{H}^7 + \text{H}^8)$$

**Equation 5.4:** Simultaneous equations used to solve the relative ratios of MFM and EHNBEDC

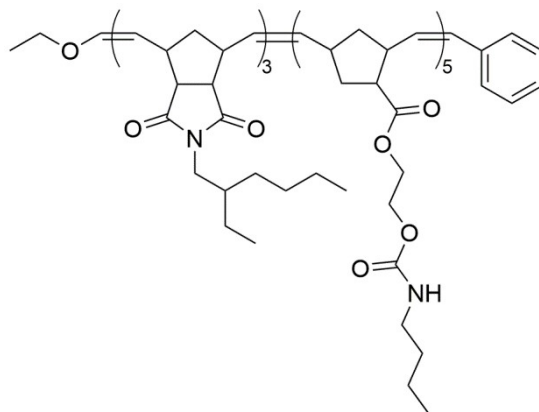


**Figure 5.19:** Structure of Polymer **T** after reaction with ethyl vinyl ether

The yields achieved in this experiment, Table 5.7, are similar to their random copolymer counterparts. This suggests that both G1 and MG2 stay active long enough to polymerise a second block.

**Table 5.7:** Table detailing SEC data of attempted block copolymers – rows with two values for  $M_n$  and  $M_w$  are bimodal

Polymer	Initiator	Yield (%)	$M_n^{th}$ ( $\times 10^3$ g mol $^{-1}$ )	$M_n^{SEC}$ ( $\times 10^3$ g mol $^{-1}$ )	$M_w^{SEC}$ ( $\times 10^3$ g mol $^{-1}$ )	$\bar{D}$
<b>S</b>	G1	84.7	28	33	58	1.7
				2.3	9.8	4.4
<b>T</b>	G1	95.3	28	23	34	1.5
<b>U</b>	MG2	86.1	28	120	410	3.5
				17	23	1.4
<b>V</b>	MG2	85.9	28	100	140	1.4
				13	16	1.3

The SEC traces are shown in Figure 5.20. It is easy to see that both **S** and **V** are bimodal. **U** also has a significant higher molecular weight peak next to the main polymer signal. This suggests that these three systems have not successfully formed a block copolymer, but possibly a mix of homopolymers and copolymers. **S** and **V** are also not polymerised in a controlled manner as can be seen by the broadness of the peaks, and also their broad dispersity ( $\bar{D}$ ).

The lower molecular weight peak of **V** appears at around 2300 Da. This would approximate to a chain length of around 8 repeat units. The larger peak however would be 400 monomer units. The reason for this is unclear; however, it could be due to premature termination of the active ends or backbiting.

The SEC trace for **T** is monomodal, noting the single peak between 13.8 and 14.5 mL on Figure 5.20, and therefore indicating the formation of block copolymer. However, **T** contains a slightly higher proportion of MFM (62 %) than the theoretical 50:50 with respect to EHNBEDC in its structure. The reason for this could possibly be that the ROMP of MFM is more facile than the ROMP of EHNBEDC as the structure of MFM is smaller than EHNBEDC and therefore there will be less steric interaction between the monomer and the propagating alkylidene site.

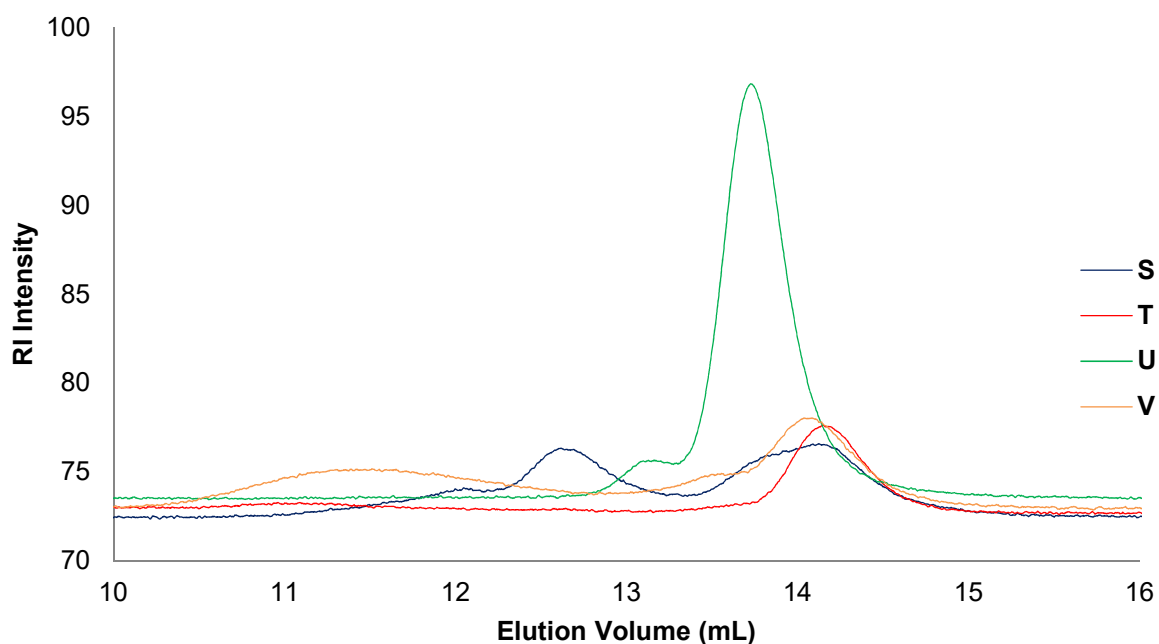
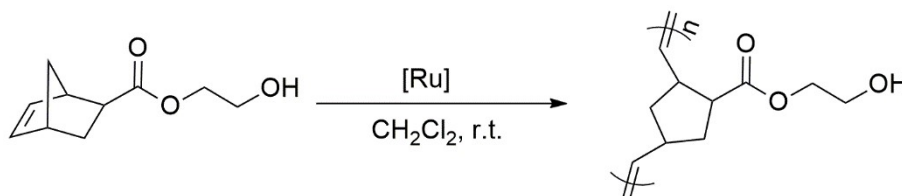


Figure 5.20: SEC traces of polymers S-V

### 5.3.6 ROMP of 2-hydroxyethyl-5-norbornene-2-carboxylate (HE-NBE-CO<sub>2</sub>)

2-Hydroxyethyl-5-norbornene-2-carboxylate, HE-NBE-CO<sub>2</sub>, was polymerised by ROMP with Grubbs ruthenium initiators G1, G2 and MG2 (Scheme 5.2).



Scheme 5.2: ROMP of 2-hydroxyethyl-5-norbornene-2-carboxylate with G1, G2 or MG2

Rather surprisingly when 2-hydroxyethyl-5-norbornene-2-carboxylate undergoes ROMP, an insoluble precipitate is formed, which is not soluble in any common solvent even when heated. Upon addition to G1, HE-NBE-CO<sub>2</sub> also turns the reaction mixture blue, which might suggest some sort of oxidation state change on the ruthenium.

### 5.3.7 Random ROM copolymerisations of HE-NBE-CO<sub>2</sub> and MFM

Since ROMP of HE-NBE-CO<sub>2</sub> formed insoluble gelled material, its copolymerisation with MFM was investigated. At lower concentrations it was hoped that there would be enough MFM character to take the polymer into the solvent. Any soluble polymer was then precipitated, and gel extraction was undertaken on the insoluble fraction.

Table 5.8 shows that increasing the level of HE-NBE-CO<sub>2</sub> increases the gel content, though it does not seem to form much of a gel until HE-NBE-CO<sub>2</sub> is over 50 equivalents with respect to the initiator.

Conversely, the soluble polymer yield decreases, which seems logical as more of the reaction mixture is going into the gelled material. Surprisingly there seems to be very little difference between the gel contents achieved when using G1 or MG2, and similar numbers are achieved for the yield of polymer precipitated. This may be because both monomers are equally active with respect to ROMP and are therefore not affected by choice of initiator.

Unfortunately, all the attempted random copolymers of HENBEDC and MFM showed poor solubility in THF and DMF which meant SEC analysis to estimate their molecular weights was not possible. Though some of the polymers were slightly soluble in chloroform which meant some NMR spectroscopic analysis was available.

**Table 5.8:** Table showing details of MFM / HE-NBE-CO<sub>2</sub> containing copolymers

Initiator	HE-NBE-CO <sub>2</sub> (eq.)	MFM (eq.)	Gel Content (%)	Linear polymer yield (%)
<b>G1</b>	0	100	0	90.6
	25	75	0	71.2
	50	50	0	88.0
	75	25	72	8.7
	100	0	78	0.0
<b>MG2</b>	0	100	0	89.1
	25	75	0	93.1
	50	50	0	87.4
	75	25	55	0.9
	100	0	73	1.0

Figure 5.22 shows a comparison of the chloroform soluble copolymers produced using Grubbs 1<sup>st</sup> generation initiator. What these <sup>1</sup>H NMR spectra show is, at first glance, H<sup>1</sup> at 4.88-5.52 ppm (highlighted in blue) increases in intensity with respect to the green highlighted H<sup>13</sup> at 0.89 ppm. This is due to the lower content of MFM in the polymer.

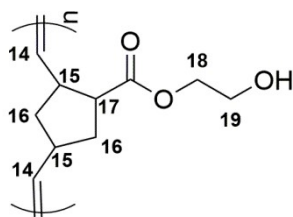


**Figure 5.21:** Numbered structure of the ring-opened product of HE-NBE-CO<sub>2</sub>

Another peak which clearly increases in intensity is the one highlighted in purple at 3.55 – 4.66 ppm, which is likely attributable to the protons next to the hydroxyl group (H<sup>19</sup> in Figure 5.21) as the polymer increases in HE-NBE-CO<sub>2</sub> character. All the protons H<sup>1-8</sup> appear to increase in intensity with respect to H<sup>10-13</sup>. This is because H<sup>1-8</sup> will mostly overlap with H<sup>14-19</sup> which will appear in both moieties. However, H<sup>10-13</sup> only appear in the butyl carbamate part of MFM. Of course, H<sup>1</sup> and H<sup>14</sup> overlap with NH so this will slightly counteract the change in the blue highlighted region.

This is not easily quantifiable however since, in all regions of the spectra, there are many overlapping peaks. Although keeping the total integration of the red and purple regions constant, one can see the integration of H<sup>13</sup> decrease as the polymers have a lower MFM content. This was repeated with Grubbs modified 2<sup>nd</sup> generation initiator, and very similar results were observed. The NMR spectra were identical, and the same conclusions could be drawn.

Unfortunately, what cannot be seen from any of this data is whether this is a true copolymer, or a mixture of homopolymers. SEC analysis could not be performed, as these polymers showed poor solubility in the two available SEC solvents, THF and DMF.

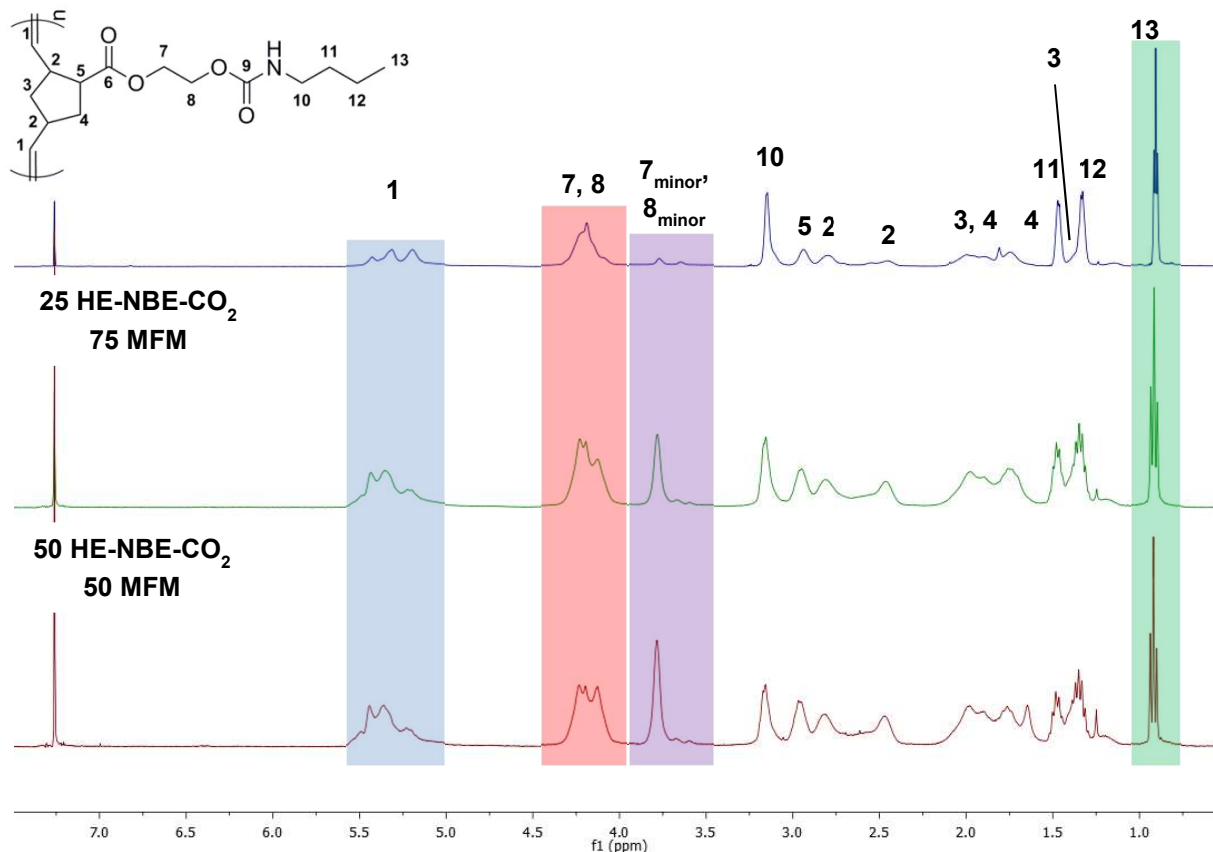


**Figure 5.22:**  $^1\text{H}$  NMR (700 MHz,  $\text{CDCl}_3$ ) spectra of poly(MFM) and copolymers of HE-NBE- $\text{CO}_2$  and MFM produced using G1

### 5.3.8 Block ROM copolymerisations of HE-NBE- $\text{CO}_2$ and MFM

As discussed earlier, ROMP of MFM (Section 5.3.3) and HE-NBE- $\text{CO}_2$  (Section 5.3.6) resulted in the formation of soluble and insoluble materials, respectively. Block copolymerisation of MFM and HE-NBE- $\text{CO}_2$  was carried out using MG2 as the initiator. It was anticipated that ROMP of MFM followed by the sequential addition of HE-NBE- $\text{CO}_2$  would result in a soluble block copolymer.

As the data in Table 5.9 show, when MFM is added first, there is no gelled network formed. However, the polymer yield decreases with increasing HE-NBE- $\text{CO}_2$ , suggesting that this monomer is not all becoming part of the polymer. This could perhaps be due to co-ordination of some of the oxygen atoms (most likely of the carbonyl group) of the monomer to the ruthenium centre, making it less active towards metathesis. A similar phenomenon is seen with solvents, for example although acetone is 'tolerated', it is advised that DMF, a highly polar solvent, should be avoided.<sup>6</sup>



**Table 5.9:** Table showing the gel contents and linear polymer yields of attempted MFM / HE-NBE-CO<sub>2</sub> block copolymers when MFM is added first, using MG2 as the initiator

Monomer added first	HE-NBE-CO <sub>2</sub> (eq.)	MFM (eq.)	Gel Content (%)	Linear polymer yield (%)
<b>MFM</b>	25	75	0	79.4
	50	50	0	70.2
	75	25	0	40.8

The data in Table 5.10 shows that at 25 equivalents of HE-NBE-CO<sub>2</sub>, there is no formation of a gelled material – possibly due to the shorter polymer length not being able to form many hydrogen bonds between chains. The gel content at 50 equivalents is low (1 %) suggesting that this polymer is only just starting to form the gelled network – or perhaps even within error of no gelation whatsoever. However, considerable amount of gel formation is observed at 75 equivalents of HE-NBE-CO<sub>2</sub>.

**Table 5.10:** Table showing the gel contents and linear polymer yields of attempted MFM / HE-NBE-CO<sub>2</sub> block copolymers when HE-NBE-CO<sub>2</sub> is added first, using MG2 as the initiator

Monomer added first	HE-NBE-CO <sub>2</sub> (eq.)	MFM (eq.)	Gel Content (%)	Linear polymer yield (%)
<b>HE-NBE-CO<sub>2</sub></b>	25	75	0	89.3
	50	50	1	76.0
	75	25	47	17.9

The data in Table 5.10 also shows that with increasing concentration of HE-NBE-CO<sub>2</sub>, the linear polymer yield drops – due to the formation of gel and the presence of unreacted monomers. The linear polymer yield is measured by taking the soluble fraction of the reaction and precipitate into ice-cold hexane.

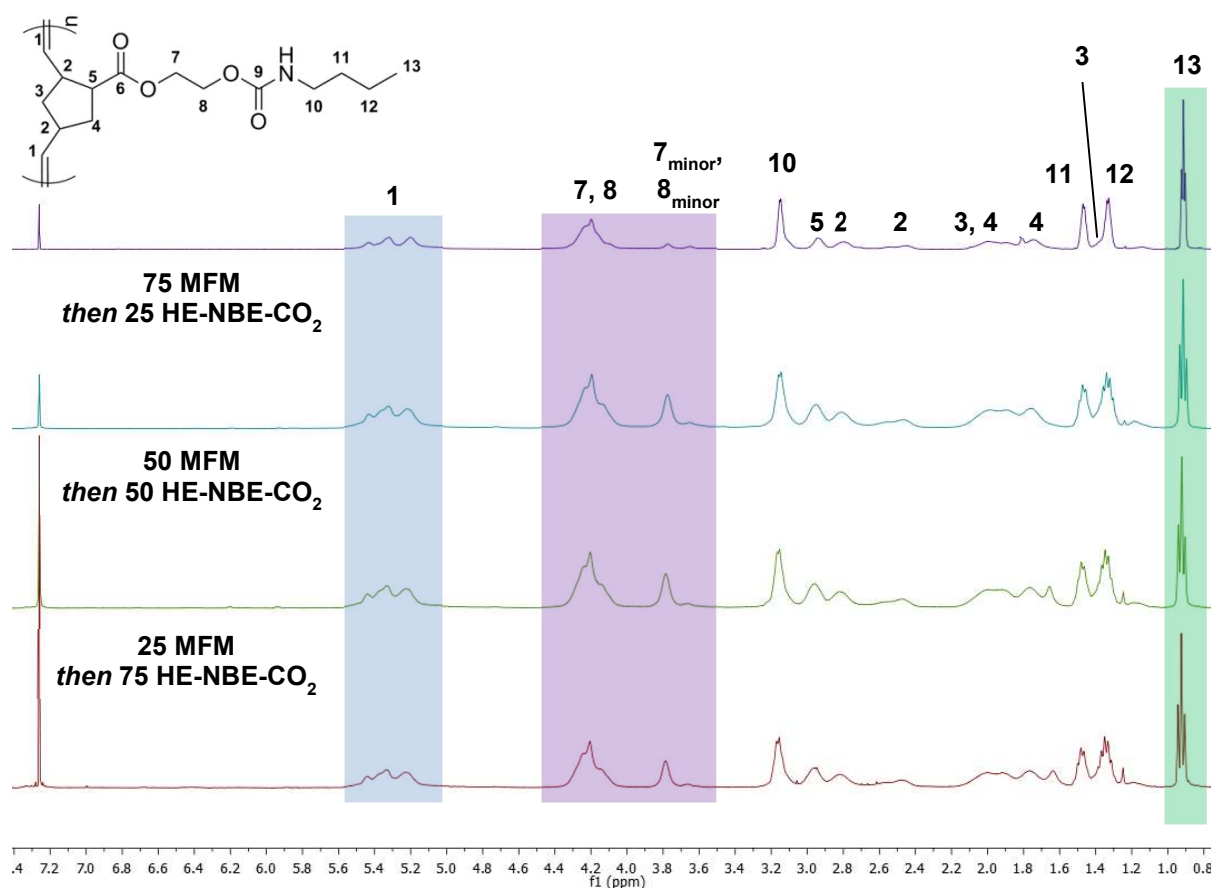


**Figure 5.23:**  $^1\text{H}$  NMR (700 MHz,  $\text{CDCl}_3$ ) spectra for attempted block copolymers with MFM added first, in DCM

Figure 5.23 shows, that the increasing the number of equivalents of HE-NBE- $\text{CO}_2$  does not seem to increase its incorporation into the attempted block copolymer. This can be seen by the fact that the peaks highlighted in purple between 3.44 and 4.46 ppm do not seem to increase in intensity as the level of HE-NBE- $\text{CO}_2$  is increased threefold. The intensities of the unsaturated backbone and the NH peak (blue, 4.88-5.52 ppm) and  $\text{H}^{13}$  (green, 0.89 ppm) also seem to stay reasonably constant. Combining this with the decline in linear polymer yield suggests that not all the HE-NBE- $\text{CO}_2$  is undergoing ROMP – even though the initiator should be still active. In fact, the activity of the initiator after 6 h was checked by adding a little 5-ethylidene-2-norbornene (an extremely reactive liquid monomer) and this immediately underwent ROMP – seen by a large increase in the reaction mixture's viscosity.

SEC analysis could not be performed on any of the above polymers, as none were soluble in either THF or DMF.

### 5.3.9 In-bulk ROM copolymerisation of 2-hydroxyethyl-5-norbornene-2-carboxylate butyl carbamate and hexamethylene-1,6-bis(5-norbornene-2-carboxylate-2-ethoxy carbamate)

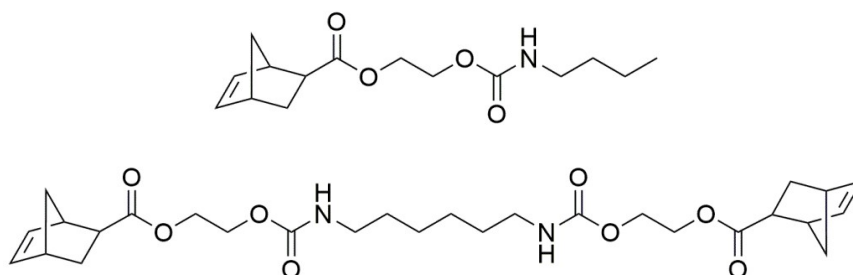


**Figure 5.24:** Structures of MFM (top) and DFM2 (bottom)

The ROM copolymerisation of MFM and DFM2, shown in Figure 5.24, was attempted in-bulk to prove the monomers were miscible and that copolymerisations could occur in the heat press at elevated temperatures. Due to limited supply of both monomers, this experiment was only carried out using MG2. A gel content of 76 % at 20 equivalents of DFM2 suggests that the copolymerisation was achieved to a reasonably high degree.

In solution, the ROMP of DFM2 yielded polymers with gel contents greater than 97 %. The fact that the gel content in bulk is slightly lower is no surprise due to poorer mixing and that the viscosity of the reaction mixture increases rapidly, preventing further polymerisation. The NMR spectra of the soluble fraction of this reaction was analysed (Figure 5.25).

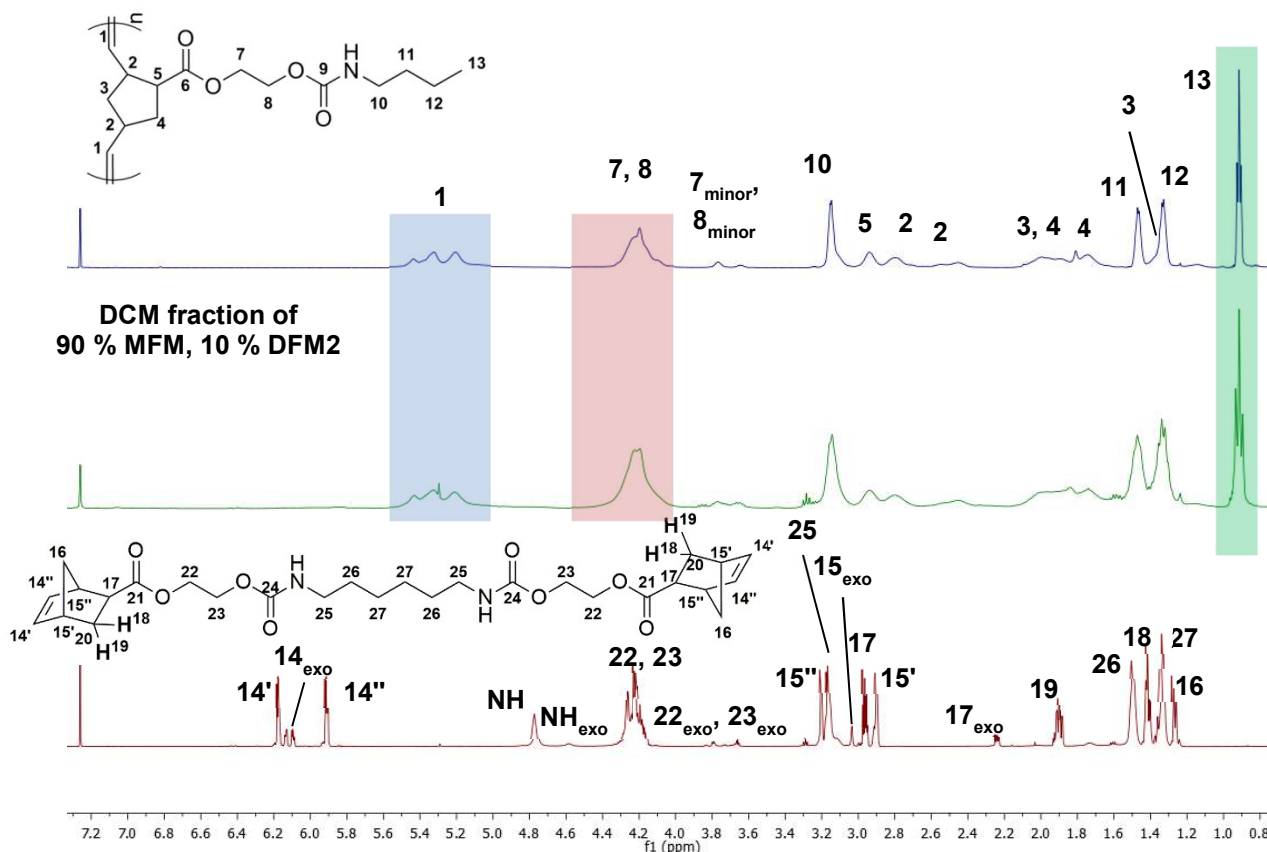


**Figure 5.25:**  $^1\text{H}$  NMR (700 MHz,  $\text{CDCl}_3$ ) spectra of poly(MFM) (top, blue), DCM fraction of copolymer (middle, green), and DFM2 (bottom, red)

As can be seen in the spectra in Figure 5.25, the non-gel fraction of this experiment appears to be composed of poly(MFM), highlighted in blue, red and green. The resonance in the green area at 0.89 ppm represents the  $\text{CH}_3$  group in the linear polymer. This resonance does not appear in DFM2. The blue area shows the unsaturated backbone of the poly(MFM), between 4.88 and 5.52 ppm, which would not appear in the monomer. The monomer would show a resonance due to the norbornene olefinic protons at around 6 ppm which is absent here. Finally, the red highlighted area represents the resonance due to the protons between the ester and carbamate groups between 3.55 and 4.46 ppm. The only peak which is clearly different to poly(MFM) is the sharp peak around 5.3 ppm which is attributable to residual DCM.

It is expected that poly(MFM) has a lower  $T_g$  than poly(DFM2) then its presence will lower the  $T_g$ , though nowhere near as much as if MFM had to been left in its monomeric state. The presence of poly(MFM) may also make the sample less brittle, so may also achieve better properties if this is required.

### 5.3.10 Mechanical Testing

#### 5.3.10.1 In-mould bulk ROM copolymerisation of MFM and DFM2 for DMTA testing

It was shown in 5.3.9 that MFM and DFM2 could be copolymerised, and so they could be tested mechanically. For this system, G1 showed the ability to form polymer even at the elevated temperatures of the heat press environment. 15 % difunctional monomer was chosen as the upper limit as this is approximately the saturation point of DFM2 in MFM.

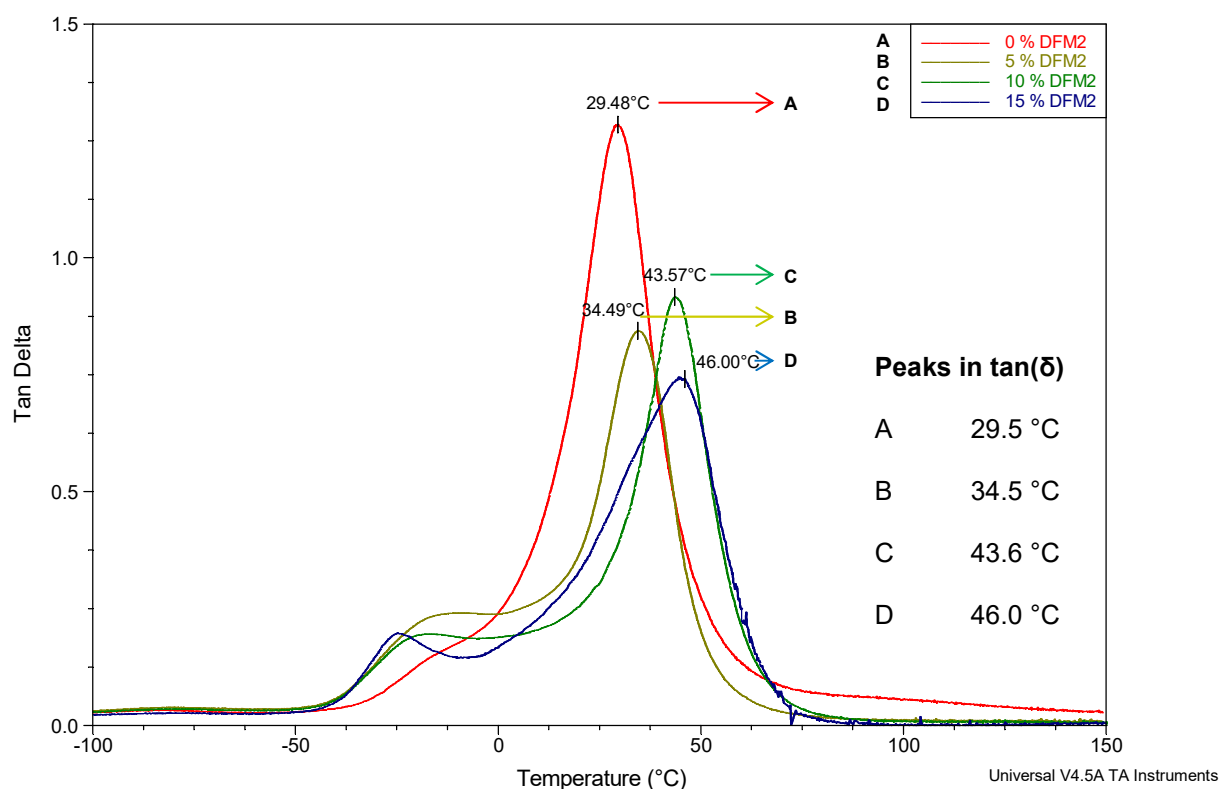


**Figure 5.26:** DMTA trace (-100 to 150 °C) of MFM/DFM2 copolymers initiated with G1, showing  $\tan(\delta)$  – a peak in which shows the  $T_g$  of the material

From Figure 5.26, a clear trend can be seen in  $T_g$  (the large peak in  $\tan(\delta)$ ) with it gradually increasing with increasing DFM2 content from 29.5 °C at 0 % DFM2 to 46.0 °C at 15 %. This is as expected since DFM2 will promote cross-linking, which should indeed raise the  $T_g$ .

There is significant plasticisation of the polymers here as seen previously in Chapter 3. This is due to residual monomer, and the effect of plasticisation on  $\tan(\delta)$  can be observed between -50 and 0 °C in Figure 5.26. This plasticisation again lowers the  $T_g$ .

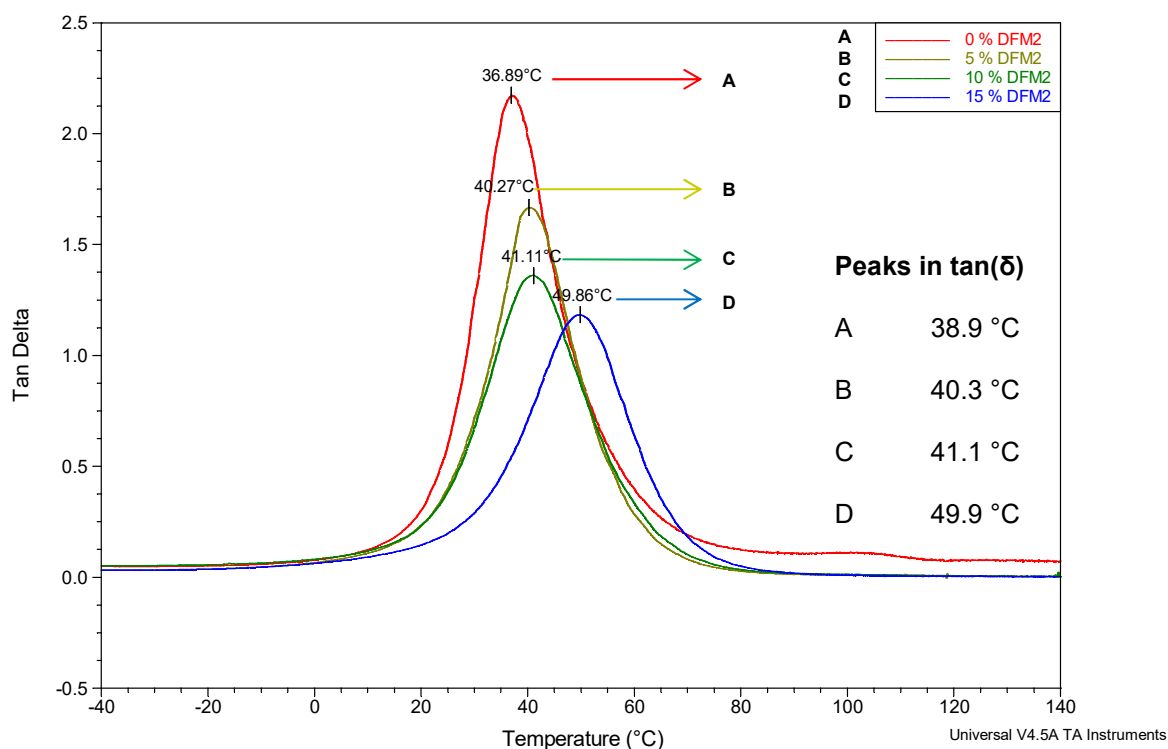


**Figure 5.27:** DMTA trace (-40 to 140 °C) of MFM/DFM2 copolymers initiated with MG2, showing  $\tan(\delta)$  – a peak in which shows the  $T_g$  of the material

Comparison of data in Figure 5.26 and Figure 5.27 shows, using MG2 rather than G1 increases the  $T_g$ . At 0 % DFM2 an increase from 29.5 to 36.9 °C is seen; at 5 % the increase is from 34.5 °C to 40.3 °C; and at 15 % there is an increase from 43.6 to 49.9 °C. The only exception is at 10 % DFM2 concentration, where the  $T_g$  decreases slightly to 41.1 °C from 43.6 °C when the copolymer is formed with G1. Reasons for this could include poorer mixing achieved with the MG2 initiator.

There is no extra peak, or shoulder, seen at lower temperature due to plasticisation by residual monomer. This is backed up by examination of the NMR spectrum presented in Figure 5.25, where only poly(MFM) could be seen in the DCM soluble portion. What can be seen again is that increasing cross-linking, by increasing the level of DFM2, increases the  $T_g$ .

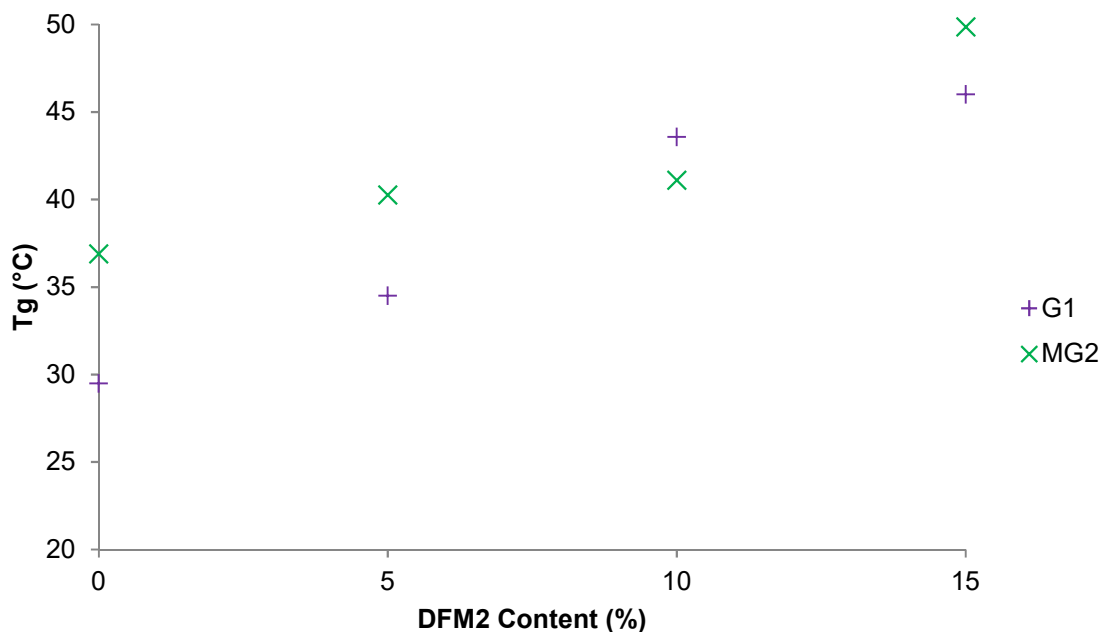


**Figure 5.28:** T<sub>g</sub>'s of MFM/DFM2 copolymers formed with G1 and MG2

Data in Figure 5.28 also suggest the trend between the difunctional content (DFM2) and T<sub>g</sub> exists and also highlights an anomaly – arguably in both sets of results – at 10 % level of DFM2. This is because it was expected that MG2 initiator would always produce polymers with higher T<sub>g</sub> due to the higher level of cross-linking achievable with lower residual monomer content. Unfortunately, due to low quantities of monomers and initiators, these experiments were not repeated enough to calculate errors so only suggestions can be made at this point.

For poly(MFM), there is no peak seen in tan( $\delta$ ) and nor do the storage and loss moduli cross below 200 °C. This suggests this linear polymer does not melt below this temperature, although when removed from the DMTA apparatus the appearance was much darker – probably due to the decomposition of the propagating alkylidene at these elevated temperatures.

Figure 5.29 highlights how much the storage modulus (same as Young's modulus under ideal conditions) changes when passing through the T<sub>g</sub> from 20 °C to 60 °C. Below the T<sub>g</sub>, the copolymers have storage moduli around 1500 MPa which is similar to polypropylene,<sup>7</sup> which decreases to around 5 – 40 MPa above it (similar to rubber or low density polyethylene). The drop off in E' can also be seen to follow the trend previously shown in tan( $\delta$ ), where the modulus decreases at a higher temperature with increasing DFM2. This again shows the trend of increasing T<sub>g</sub> since this is another method of measuring it – though it is more accepted to quote the peak in tan( $\delta$ ). Looking at poly(MFM) (0 % DFM2) as an example, below the T<sub>g</sub> (20 °C) the E' is 1690 MPa and reduces to 5.90 MPa when heated to 60 °C – which is above the T<sub>g</sub> of poly(MFM), 36.9 °C.

Finally, the order of E' is rather surprising. Around the T<sub>g</sub>, the system with 10 % DFM2 has the highest modulus (8880 MPa), which could possibly be due to better mixing in this system than 15 % (1620 MPa) which may have been expected to be the stiffer material but perhaps has reached the limit of

miscibility of the two monomers. Below the  $T_g$  the other three systems all have similar values of  $E'$ : 1690 MPa for 0 % DFM2; 1270 MPa for 5 % DFM2 concentration; and 1620 MPa for 15 %. However, above the  $T_g$ , the linear polymer has the lowest  $E'$  (5.90 MPa) – suggesting that this has become the most flexible. This is expected since there is no cross-linking in this system.

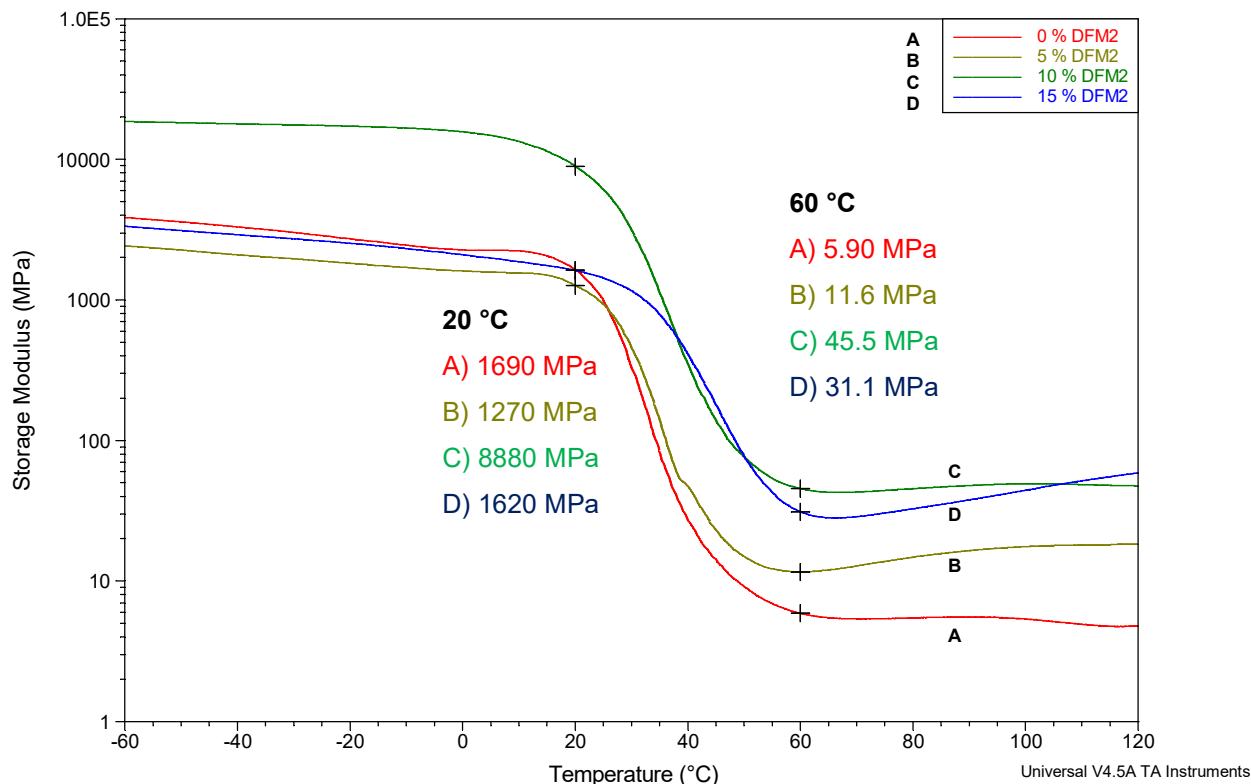


Figure 5.29: Storage moduli traces of MFM/DFM2 copolymers

### 5.3.10.2 In-mould bulk ROM copolymerisation of HE-NBE-CO<sub>2</sub> and MFM for DMTA testing

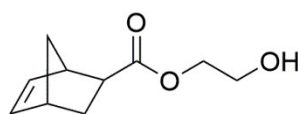


Figure 5.30: Structure of HE-NBE-CO<sub>2</sub>

HE-NBE-CO<sub>2</sub>, Figure 5.30, was shown to form gels when polymerised possibly due to strong hydrogen bonding. It was thought therefore copolymerising this with MFM may affect the  $T_g$  of the system. Both contain only one norbornene functional group and are low viscosity liquids. They were also found to be miscible at room temperature.

Data in Figure 5.31 shows that as HE-NBE-CO<sub>2</sub> is incorporated into the copolymer, the extra hydrogen bonding increases the  $T_g$  markedly. Having a 75 % HE-NBE-CO<sub>2</sub> content yields a polymer with a higher  $T_g$  (52.5 °C) than one with 15 % DFM2 (49.9 °C) from the previous experiment (Figure



5.27), and a 50 % HE-NBE-CO<sub>2</sub> content yields a polymer with a  $T_g$  slightly below (43.6 °C). This result means that the properties of this copolymer could be tailored quite easily with respect to  $T_g$ .

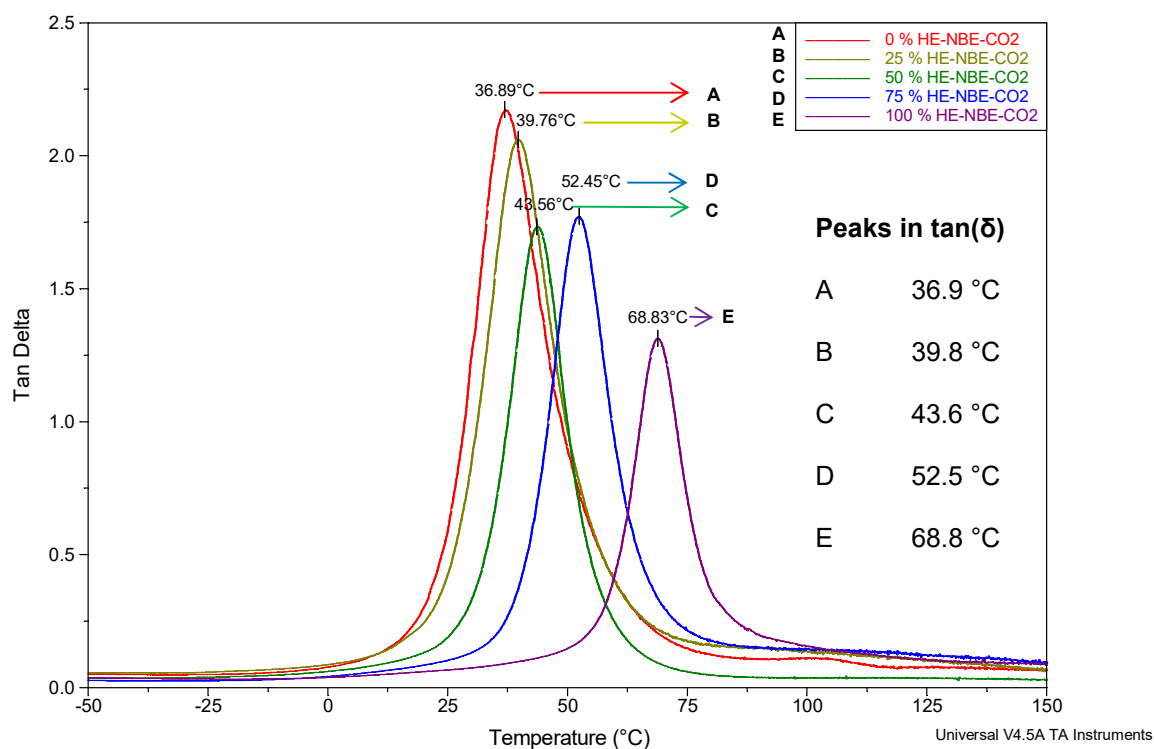


**Figure 5.31:** DMTA trace (-50 to 150 °C) of MFM/HE-NBE-CO<sub>2</sub> copolymers initiated with MG2, showing  $\tan(\delta)$  – a peak in which shows the  $T_g$  of the material

Figure 5.32 shows a clear trend of increasing  $T_g$  with increasing HE-NBE-CO<sub>2</sub> content, from 36.9 °C to 68.8 °C. The fact that as the content of HE-NBE-CO<sub>2</sub> increases above 50 %, the  $T_g$  increases faster is most likely caused by increased hydrogen bonding. For example, from 0 to 50 % HE-NBE-CO<sub>2</sub> content, the  $T_g$  rises by 6.7 °C; increasing this content to 100 % results in a further rise in the  $T_g$  of 15.2 °C. Again, unfortunately, due to limited quantities of monomers and initiator, the error was not calculated.

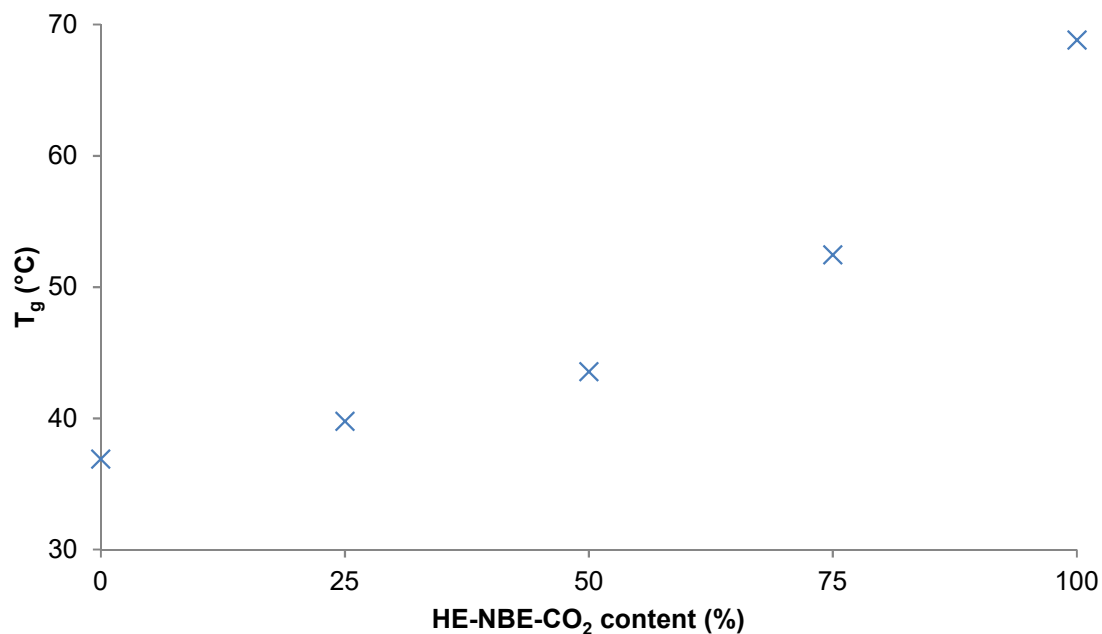


Figure 5.32: T<sub>g</sub>'s of MFM/HE-NBE-CO<sub>2</sub> copolymers

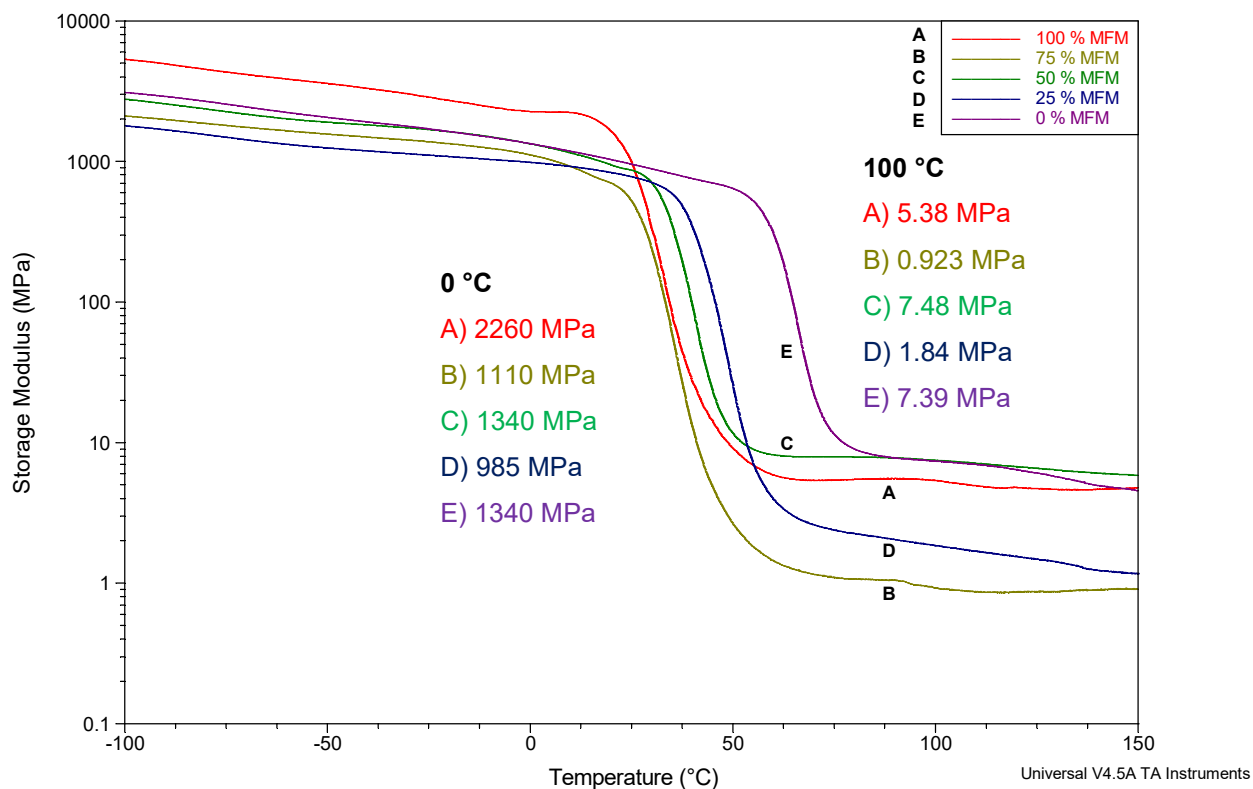


Figure 5.33: Storage moduli traces of MFM/HE-NBE-CO<sub>2</sub> copolymers

The structure of MFM and HE-NBE-CO<sub>2</sub> monomers are quite similar except that the hydroxyl group on HE-NBE-CO<sub>2</sub> is replaced with a carbamate group and a small alkyl group. Therefore, any change in E' would likely be due to increased hydrogen bonding with increasing equivalents of HE-NBE-CO<sub>2</sub>.

The change in  $T_g$  was much greater in this system (36.9 – 68.8 °C) than seen previously in Chapter 3 or this chapter, the value of  $E'$  had to be measured at two temperatures, decided as 0 °C and 100 °C, which were much further apart in order to measure it above and below the  $T_g$ 's of each copolymer.

As the data in Figure 5.33 shows, there is a difference in  $E'$  between the copolymers, with a range between 985 MPa and 2260 MPa at 0 °C, however they do not appear to follow any trend. Any change in  $E'$  could be due to better mixing between the initiators and monomers, or general quality of the samples formed. There is a far smaller range in the values of  $E'$  of the copolymers above their  $T_g$ 's (0.923 – 7.48 MPa) at 100 °C. At both 0 °C and 100 °C, the homopolymers of MFM (2260 MPa and 5.38 MPa, respectively) and HE-NBE-CO<sub>2</sub> (1340 MPa and 7.39 MPa, respectively) are two of the stiffest polymers produced – *i.e.* have amongst the highest  $E'$ .

The decrease in  $E'$  occurs at a much lower temperature in **A** (100 % MFM) from 2260 MPa to 5.38 MPa, trace than **E** (100 % HE-NBE-CO<sub>2</sub>) from 1340 MPa to 7.39 MPa, this shows the increasing temperature of the  $T_g$  with increasing proportions of HE-NBE-CO<sub>2</sub>. There is, however, no  $T_m$  observed in any of these copolymers below 200 °C – which would be expected to be seen since all the copolymers formed here are amorphous. This would be shown by a rapid decrease in the  $E'$  (showing a much less stiff polymer), and a corresponding peak in  $\tan(\delta)$  due to this change in the ratio of  $E'$  and  $E''$ . All the polymers came out of the DMTA blackened, suggesting thermal decomposition of the propagating alkylidene species.

## 5.4 Conclusions

The ROMP of DFM1 was successful, and it proved that carbamates were compatible with Grubbs initiators, *i.e.* they could undergo polymerisation without deactivating the initiators. The negative aspect of this monomer is that the low gel contents were a surprise, although this could be explained as a combination of rapid ROMP and the fact that DFM1 is not 100 % norbornene-functionalised. The much higher gel content when undertaking ROMP with DFM2 proves that with high norbornene contents, high levels of cross-linking can be achieved when using these carbamate-containing monomers.

Poly(MFM) – which was characterised using NMR spectroscopy – also achieves a high yield, and the SEC analysis shows that the polymerisation – with G1 and MG2 – can proceed in a reasonably well-controlled manner with  $\bar{D}$  of 1.4 and 1.5, respectively. The molecular weights deviated significantly from the theoretical, although this is due to the calibration of the SEC detector which uses polystyrene (PS) standards having different hydrodynamic volumes to that of these polymers. This means that they can only be compared with one another.

The random copolymerisation of MFM and EHNBEDC was shown to be possible, although both traces (with each initiator) showed high molecular weight shoulders in the SEC traces – suggesting that the polymerisation is not well controlled. The block copolymerisation of MFM and EHNBEDC, however, was only achievable using G1. One reason for this could be that G1 was more stable in the reaction mixture than MG2. This is because the ROMP of the first monomer was left for about 6 h

prior to the addition of the second monomer. The initiator needed to remain active over this duration to polymerise the second block.

ROMP of 2-hydroxyethyl-5-norbornene-2-carboxylate was possible, although it resulted in the production of insoluble gelled products when initiated by both G1 and MG2, with gel contents of 78 % and 73 %, respectively.

Random copolymers of HE-NBE-CO<sub>2</sub> with MFM were also investigated using G1 and MG2. The gel content is decreased with increasing MFM equivalents (from 72 % to 0 % for G1, and from 55 % to 0 % for MG2). There is also a general increase seen in the linear polymer yield (calculated by precipitating the soluble fraction of the gel extraction into ice-cold hexane) with increasing MFM.

The outcome of the block copolymerisation reaction of HE-NBE-CO<sub>2</sub> and MFM appears to be dependent on which monomer was added first to the initiator. The addition of MFM first produces polymers with no gel content. However, the yield of linear polymer decreases with increasing number of equivalents of HE-NBE-CO<sub>2</sub> monomer. If HE-NBE-CO<sub>2</sub> is added first, the gel content of the copolymer increases with increasing number of equivalents of HE-NBE-CO<sub>2</sub> from 0 to 47 %. Moreover, the linear polymer yield also decreases with increasing number of equivalents of HE-NBE-CO<sub>2</sub> monomer from 89.3 % at 25 equivalents, to 17.9 % at 75 equivalents.

It was also shown that the bulk ROM copolymerisation reactions of DFM2, HE-NBE-CO<sub>2</sub>, MFM, EHNBEDC, and Polyesters 1 and 2 were possible at elevated temperature and pressure, in mould. The addition of solvent would have been problematic as it would have acted as a plasticiser, lowering  $T_g$  and reducing the stiffness. The mechanical properties, including the  $T_g$ , were successfully measured over a wide temperature range and, where appropriate, agreed broadly with literature values, e.g. the  $T_g$  of poly(EHNBEDC). Comparison with Differential Scanning Calorimetry (DSC) was not, however, possible since no reliable  $T_g$  could be obtained.

Trends in  $T_g$  and  $E'$  were seen and rationalised for most of the copolymer systems here, although there were a few anomalies, for example the DFM2/MFM copolymers with 10 % DFM2 content. These DMTA experiments would ideally have been repeated if plentiful supply of monomers and initiators were available. The storage moduli values measured here could not be compared directly with those in the literature, as the reported values found in literature are usually Young's moduli.

Adding DFM2 to MFM can change the  $T_g$  of the resulting copolymer significantly. In this example the  $T_g$  is increased from 29.5 °C to 46.0 °C when initiated using G1; and from 36.9 °C to 49.9 °C when using MG2 as the initiator. This table also shows that there is a large difference in storage moduli between the different copolymers below the  $T_g$  (at 30 °C), however there is not any obvious pattern. This is highlighted by the fact that the copolymers with 5 %, 10 % and 15 % DFM2 contents have storage moduli of 1270, 8880 and 1620 MPa, respectively.

All the copolymers become much more elastic when heated above their  $T_g$  (to 60 °C), shown by the reduction in storage modulus by almost a factor of 100, for example at 5 % DFM2 the storage modulus reduces from 1270 MPa to 11.6 MPa.

It was shown that adding HE-NBE-CO<sub>2</sub>, an oxygen-rich monomer, to MFM increased the  $T_g$  of the polymer produced. Increasing the levels of HE-NBE-CO<sub>2</sub> with respect to MFM increased the  $T_g$ . For example, increasing the HE-NBE-CO<sub>2</sub> content from 0 % to 50 % to 100 % increased the  $T_g$  from 36.9 °C to 43.6 °C to 68.8 °C, respectively. There was little variation in the storage modulus between the polymers formed (from 1110 MPa at 25 % HE-NBE-CO<sub>2</sub> to 2260 MPa for 0 % HE-NBE-CO<sub>2</sub>), except at 75 % HE-NBE-CO<sub>2</sub>, which is much higher than expected (9850 MPa). This, however, could be attributed to much better mixing of HE-NBE-CO<sub>2</sub>, MFM, and MG2 during this test. There was an approximate 100 times decrease in storage modulus once more between 0 °C (below  $T_g$ ) and 100 °C (above the  $T_g$ ) from. For example, when the ratio of HE-NBE-CO<sub>2</sub> : MFM was 50:50, the reduction in storage modulus seen was from 1340 MPa to 7.48 MPa.

## 5.5 References

1. Angeletakis, C. Polyether-based composition curable by metathesis reaction. EP1820813 A1, **2007**.
2. Bielawski, C. W.; Grubbs, R. H., Living ring-opening metathesis polymerization. *Prog. Polym. Sci.* **2007**, 32 (1), 1-29.
3. Riegler, S.; Slugovc, C.; Trimmel, G.; Stelzer, F., Block Copolymers via ROMP – Awakening the Sleeping Beauty. *Macromol. Symp.* **2004**, 217 (1), 231-246.
4. Mayo, F. R.; Lewis, F. M., Copolymerization. I. A Basis for Comparing the Behavior of Monomers in Copolymerization; The Copolymerization of Styrene and Methyl Methacrylate. *J. Am. Chem. Soc.* **1944**, 66 (9), 1594-1601.
5. Matson, J. B.; Grubbs, R. H., Monotelechelic Poly(oxa)norbornenes by Ring-Opening Metathesis Polymerization using Direct End-Capping and Cross Metathesis. *Macromolecules* **2010**, 43 (1), 213-221.
6. Sanford, M. S.; Love, J. A.; Grubbs, R. H., Mechanism and Activity of Ruthenium Olefin Metathesis Catalysts. *J. Am. Chem. Soc.* **2001**, 123 (27), 6543-6554.
7. Scholl, M.; Ding, S.; Lee, C. W.; Grubbs, R. H., Synthesis and Activity of a New Generation of Ruthenium-Based Olefin Metathesis Catalysts Coordinated with 1,3-Dimesityl-4,5-dihydroimidazol-2-ylidene Ligands. *Org. Lett.* **1999**, 1 (6), 953-956.

## **Chapter 6. Conclusions and Future Work**

## 6.1 Conclusions

The work discussed in this thesis describes the synthesis of norbornene-functionalised polyesters and polyurethanes. There were several aims of this project, including developing a system which: incorporated one or more norbornene rings in the pre-polymer; could be polymerised using ROMP to yield linear or cross-linked polymers; utilised little, or no, styrene; produced products with comparable properties (e.g. high  $T_g$ , low water uptake, etc.) to current unsaturated polyester resins; can be polymerised in solvent, or in the presence of a reactive diluent; is as environmentally friendly as possible; and is as cost-effective as possible.

Norbornene-functionalised polyesters and polyurethanes were chosen due to their ease of synthesis, as the only by-product of polyester synthesis is water – which can be removed by distillation. Synthesis of polyurethanes should not produce any by-products unless the conditions are too forcing, in which case the isocyanates can react with any previously formed carbamates as shown previously in Chapter 2.<sup>1</sup> Norbornene moieties were targeted since these are amongst the most strained rings achievable.<sup>2</sup> These are also ideal due to their ease of formation, from the Diels-Alder reaction of cyclopentadiene and an electron deficient C=C double bond. Finally Grubbs ruthenium initiators were chosen as the catalysts due to their high tolerances of functional groups, including water and oxygen.<sup>3</sup> This reduces the cost of the reactions as efforts to keep the reactions anhydrous and anaerobic are unnecessary; and therefore increases the feasibility due to the ability to carry out ROMP under ambient conditions.

This project was based upon replacing the industry standard maleate-functionalised unsaturated polyester resins. Styrene would usually react with this maleate functionality in the pre-polymer backbone *via* free radical polymerisation.<sup>4</sup> Maleate functionalised pre-polymers were used as the basis of the norbornene-functionalised polyesters synthesised in Chapter 2, since maleate double bonds are extremely electron poor and therefore make ideal targets for the Diels-Alder reaction with cyclopentadiene, in order to yield norbornene functionality. Analysis by  $^1\text{H}$  and  $^{13}\text{C}$  NMR spectroscopy, size-exclusion chromatography, and acid value calculations all combined to confirm the successful syntheses of *N*-(2-ethylhexyl)-5-norbornene-2,3-dicarboximide, Polyester 1 and Polyester 2. 2-hydroxyethyl acrylate was used as an electron deficient double bond for the formation of polyurethanes since it contains a free hydroxyl group which can be reacted with a variety of isocyanates; both mono- and di-functionalised were used in this work.  $^1\text{H}$  and  $^{13}\text{C}$  NMR spectroscopy, Atmospheric Solids Analysis Probe – Mass Spectrometry (ASAP-MS), Thermogravimetric Analysis (TGA), and CHN Analysis confirmed the successful syntheses of DFM1, DFM2 and MFM.

In Chapter 3, it was shown that Grubbs 2<sup>nd</sup> generation initiator was successfully modified with pyridine, although this was already a well-known reaction.<sup>5</sup> The synthesised *N*-(2-ethylhexyl)-5-norbornene-2,3-dicarboximide (EHNBEDC) was successfully polymerised using all three Grubbs ruthenium initiators available (G1, G2 and MG2), and was characterised. Both multifunctional polyesters were successfully polymerised, and gel contents and gel times were determined. The DCM soluble fractions of these polymers were visualised using  $^1\text{H}$  NMR spectroscopy. Additionally, ROMP was also performed on both polyesters in bulk using EHNBEDC as a reactive diluent. Trends in gel

content were demonstrated with varying concentrations in the bulk reactions, for example dissolving varying amounts of Polyester 1 in EHNBEDC could change the gel content from 11 % (5 % Polyester 1), up to a gel content of 64 % (15 % Polyester 1). Similarly, dissolving 5 % Polyester 2 in EHNBEDC gave a polymer with a gel content of 30 %, which increased to 74 % when the amount of Polyester 2 used was increased threefold.

Polyesters 1 and 2 were ROM copolymerised separately with EHNBEDC in-mould for Dynamic and Thermal Analysis (DMTA). The products showed a decrease in the  $T_g$  with an increasing amount of either polyester. The stiffness of the materials showed no overall trend with respect to the level of polyester.

Adding small amounts of styrene (<5 %) was shown, in Chapter 4, to slow the ROMP of Polyester 1 and Polyester 2 when using Grubbs 1<sup>st</sup> or 2<sup>nd</sup> generation initiators, though did not seem to affect the modified 2<sup>nd</sup> generation's ability to polymerise. Increasing the level of styrene up to 2 equivalents with respect to the initiator continued to slow the ROMP of both polyesters using G1 and G2. There was no effect seen on the gel content with any level of styrene used, and the DCM soluble fraction showed no differences between each reaction. Styrene was shown, however, to inhibit the ROMP reaction when used as the reaction solvent.

Chapter 5 showed that DFM1 and DFM2 could effectively form gels – although DFM1 was shown to have a very low gel content. Both difunctional polyurethanes had their gel contents and gel times calculated, and the DCM soluble fraction of DFM1 was visualised using <sup>1</sup>H NMR. DFM2 produced no DCM soluble fraction when polymerised as the gel content was nearly 100 %. The norbornene-functionalised carbamate, MFM, was successfully polymerised and precipitated into hexane using all three ruthenium initiators. Random copolymers were shown to be accessible with MFM and EHNBEDC, and MFM and 2-hydroxyethyl-5-norbornene-2-carboxylate (HE-NBE-CO<sub>2</sub>). SEC was not available for the products of the copolymerisations with HE-NBE-CO<sub>2</sub> as these copolymers showed poor solubility. Block copolymers of both systems were more problematic with many of the systems showing bimodal distributions – suggesting homopolymers or, at least, uncontrolled copolymerisation.

Several polymers in Chapter 5 were tested using DMTA by carrying out in-mould ROMP reactions. Firstly, it was shown that DFM2 could successfully dissolve in MFM, and then could undergo ROMP in bulk. This allowed copolymer systems of these to be tested up to 15 % DFM2 – showing that increasing the level of DFM2 in the mixture increases the glass transition temperature ( $T_g$ ), using either G1 or MG2 as the initiator. Any polymers produced using G1 always showed a lower  $T_g$  peak due to plasticisation by residual monomer – and so MG2 was only used in future polymerisations. Increasing the level of the difunctional monomer showed no overall trend in stiffness of the materials produced. Mixing MFM and HE-NBE-CO<sub>2</sub> showed that greater concentrations of HE-NBE-CO<sub>2</sub> greatly increased the  $T_g$  as was predicted, likely due to the presence of strong hydrogen bonding. Again, however, there was not much difference seen in stiffness in the materials

These summaries of each chapter show that most of the aims of the project were achieved, with perhaps the exceptions of environmental and economic concerns. Although, as previously mentioned, ethyl vinyl ether can be added to any of the systems at the end of a reaction to remove as much



ruthenium from the polymer as possible. This is much easier with linear polymers, however, as the ruthenium can then be removed by re-precipitation several times, rather than an extraction which is more likely to change the properties of any gelled network produced. Economically speaking, ruthenium is expensive. In this project, ratios of 100:1 and 200:1 (monomer to initiator) have generally been used, although Grubbs catalysts have been shown to be active at much lower concentrations.<sup>6</sup> This would lower the cost of each reaction significantly.

## 6.2 Future Work

### 6.2.1 Use of latent initiators

Many of the monomers in this work have shown rapid ROMP upon mixing with modified Grubbs 2<sup>nd</sup> generation initiator. This can be problematic since the material must be pressed quickly, before it cross-links, which would prevent the polymer being heat-pressed into shape. Transferring the material into the vial can also be difficult as the reaction mixture quickly thickens and perhaps can become increasingly inhomogeneous. One solution to this could be the use of latent initiators, which are only active when heat is applied to the system similar to those used in the work of Thomas *et al.*<sup>7</sup> Here, mixing the catalyst with norbornene functionalised monomers at room temperature produced no polymer, although heating the mixture to 85 °C promoted rapid polymerisation. This would be ideal as this is around the temperature of the heat press utilised. One issue with these latent initiators is that they are not all commercially available and may have to be synthesised, and ones that are available<sup>8</sup> (Figure 6.1) are expensive.

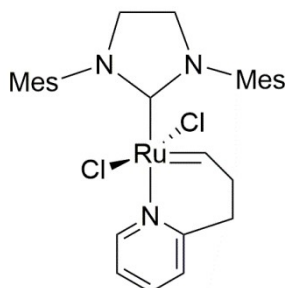


**Figure 6.1:** An example of a commercially-available latent initiator with an activity similar to MG2 when activated

### 6.2.2 Use of different polyesters

In this thesis, only diethylene glycol and propylene glycol were used to create the polyesters. There are many other choices of diol or polyol available which could produce a library of polyesters and their gel contents, gel times *etc.* could be investigated. The effect of styrene on the gel times (with G1) could also be explored and confirm if this is a phenomenon common to all polyesters created in this manner.

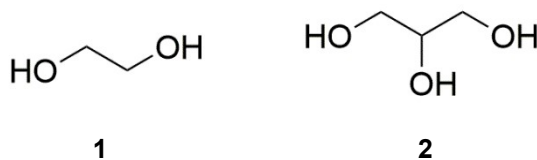
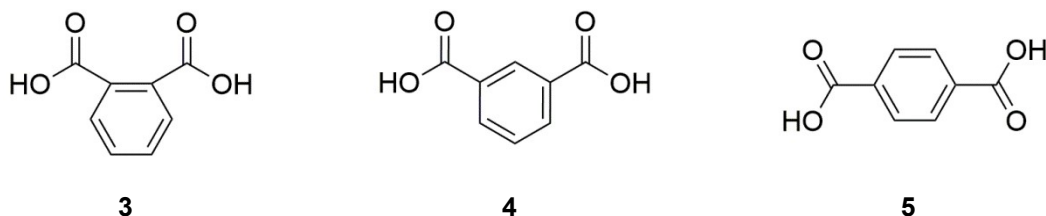
**Figure 6.2:** Ethylene glycol and glycerol

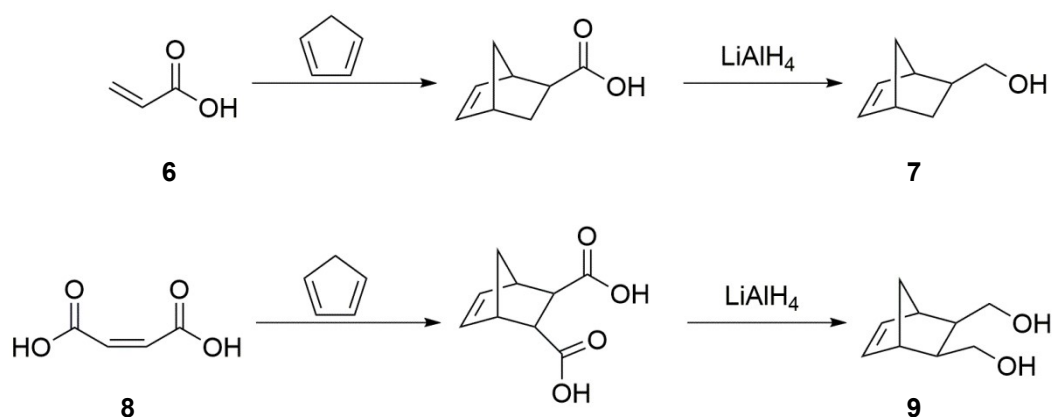
Figure 6.2 shows two example glycols which could be reacted into polyesters to give very different pre-polymers to Polyester 1 and 2. Ethylene glycol (**1**) is a very rigid diol and so may cause any norbornene containing polyester to undergo ROMP very slowly, as the viscosity of the reaction will be increased much quicker. Using glycerol (**2**) may produce more norbornene functionality per chain, and so could increase the gel content and decrease the gel time.

Adding in different acids (alongside maleic acid) may also alter properties. For example, Polyester 1 contained phthalic acid, but this has three isomers (**3**, **4** and **5**, Figure 6.3). The effect of these in ROMP and polymer products could also be examined.

**Figure 6.3:** phthalic acid, isophthalic acid, and terephthalic acid

### 6.2.3 Use of different polyurethanes

Like the polyester examples, there are two parts of the polyurethanes that can be altered: the hydroxyl functionalised, and the isocyanate. Commercially sourced norbornene-functionalised isocyanates could not be found, so the norbornene moiety must come from the hydroxyl functionalised starting material. Possible other examples of this starting materials could be hydroxypropyl acrylate (or any length of carbon chain), which can then undergo Diels-Alder with cyclopentadiene. Acrylic acid (**6**) could also be reacted with cyclopentadiene in the same manner and then reduced using lithium aluminium hydride to form norbornene methanol (**7**). Maleic acid (**8**) may also work similarly to provide a norbornene functionalised diol (**9**), Scheme 6.1. This diol could then react with diisocyanates to form oligomers, or isocyanates to form a monofunctional monomer which could undergo ROMP.



**Scheme 6.1:** Proposed production of 5-norbornene-2-methanol and 5-norbornene-2,3-dimethanol from acrylic acid and maleic acid, respectively

Norbornene methanol and norbornene dimethanol are both also commercially available.<sup>9-10</sup>

Butyl isocyanate was used in this thesis – but there are also varying lengths of the carbon chain available (*i.e.* ethyl isocyanate, hexyl isocyanate) which could be used. It is anticipated that use of longer chains would change the chemical properties of any monomer or polymer produced. Also, as well as hexamethylene-1,6-diisocyanate (HDI): toluene-2,4-diisocyanate (TDI) and 4,4'-Methylenebis(phenyl isocyanate) (MDI) are also readily available, as well as many others,<sup>11</sup> which could lead to an extensive library of polyurethanes.

#### 6.2.4 Different methods of mechanical testing

As mentioned previously in Chapter 3 and Chapter 5, only the glass transition temperature and storage moduli of the materials produced were measured using DMA. There is plenty more scope for this technique including measuring the Young's moduli by plotting the stress and strain of each sample against one another – the initial slope indicating the modulus. This would allow direct comparison against many other resin materials, since usually this is the modulus which is quoted (not storage).

It was noted that poly(2-hydroxyethyl-5-norbornene-2-carboxylate) had a similar structure to poly(hydroxyethyl methacrylate), a well-studied hydrogel.<sup>12</sup> Therefore, water absorption studies could be carried out on poly(2-hydroxyethyl-5-norbornene-2-carboxylate) and its copolymers to see if any of them had similar properties. The backbone of this polymer could also be hydrogenated to allow more flexibility of the pendant groups – which may also afford better hydrogen bonding and, perhaps, greater water uptake.

There are also numerous other mechanical analysis techniques available – although these usually require the production of much larger samples.

### 6.2.5 Green Chemistry

Currently, the E-factors calculated in Chapter 2 and Chapter 3 are quite high. There could be work carried out to reduce these down to more acceptable factors – for example, perhaps by using less solvent. Repeating some of these experiments using different conditions may also increase the yields of some reactions – thereby increasing the mass of the product and reducing the mass of waste produced. This would therefore decrease the E-factor of the reaction.

In Chapter 3, the idea of compostable polymers was also suggested. This could also be tested for the monomers and polymers produced in this thesis using the standardised method described by Song *et al.*<sup>13</sup> If the monomers and polymers in this work are shown to be compostable, once a library of suitable monomers is formed, the starting materials could be tailored to suit whether or not composting is a desirable property of the material.

### 6.3 References

1. Ulrich, H.; Tucker, B.; Sayigh, A. A. R., Base-catalyzed reactions of isocyanates. Synthesis of 2,4-dialkylallophanates. *J. Org. Chem.* **1967**, 32 (12), 3938-3941.
2. North, M., ROMP of Norbornene Derivatives of Amino-Esters and Amino-Acids. In *Ring Opening Metathesis Polymerisation and Related Chemistry: State of the Art and Visions for the New Century*, Khosravi, E.; Szymanska-Buzar, T., Eds. Springer Netherlands: Dordrecht, **2002**; pp 157-166.
3. Nguyen, S. T.; Johnson, L. K.; Grubbs, R. H.; Ziller, J. W., Ring-opening metathesis polymerization (ROMP) of norbornene by a Group VIII carbene complex in protic media. *J. Am. Chem. Soc.* **1992**, 114 (10), 3974-3975.
4. Church, J. M.; Berenson, C., Properties of Styrene-Polyester Copolymers. *Industrial & Engineering Chemistry* **1955**, 47 (12), 2456-2462.
5. Love, J. A.; Morgan, J. P.; Trnka, T. M.; Grubbs, R. H., A Practical and Highly Active Ruthenium-Based Catalyst that Effects the Cross Metathesis of Acrylonitrile. *Angew. Chem., Int. Ed.* **2002**, 41 (21), 4035-4037.
6. Martinez, H.; Ren, N.; Matta, M. E.; Hillmyer, M. A., Ring-opening metathesis polymerization of 8-membered cyclic olefins. *Polymer Chemistry* **2014**, 5 (11), 3507-3532.
7. Thomas, R. M.; Fedorov, A.; Keitz, B. K.; Grubbs, R. H., Thermally Stable, Latent Olefin Metathesis Catalysts. *Organometallics* **2011**, 30 (24), 6713-6717.
8. Straus, D. A.; Grubbs, R. H., Titanacyclobutanes: substitution pattern and stability. *Organometallics* **1982**, 1 (12), 1658-1661.
9. Casey, C. P.; Burkhardt, T. J., (Diphenylcarbene)pentacarbonyltungsten(0). *J. Am. Chem. Soc.* **1973**, 95 (17), 5833-5834.
10. Ludwig, J. R.; Zimmerman, P. M.; Gianino, J. B.; Schindler, C. S., Iron(III)-catalysed carbonyl-olefin metathesis. *Nature* **2016**, 533, 374.
11. Atkins, P.; Overton, T.; Rourke, J.; Weller, M.; Armstrong, F., *Inorganic Chemistry*. 4th ed.; Oxford University Press: Oxford, **2006**.

12. Liu, F.; Zhou, X.; Cui, F.; Jia, D., [Synthesis and properties of poly(hydroxyethyl methacrylate) hydrogel for IOL materials]. *Journal of Biomedical Engineering* **2007**, 24 (3), 595-8.
13. Song, J. H.; Murphy, R. J.; Narayan, R.; Davies, G. B. H., Biodegradable and compostable alternatives to conventional plastics. *Philos. Trans. R. Soc. London, Ser. B* **2009**, 364 (1526), 2127-2139.